In vitro Transport Profile of Antiepileptic Drugs by Human P-glycoprotein and Functional Evaluation of Human *MDR1* Polymorphisms on Transport Activity

ZHANG, Chunbo

A Thesis Submitted in Partial Fulfillment

of the Requirement for the Degree of

Doctor of Philosophy

in

Pharmacy

The Chinese University of Hong Kong

August 2011

Thesis/Assessment Committee

Professor Vincent Hon Leung Lee (Chair)

Professor Lawrence William Baum (Supervisor)

Professor Zhong Zuo (Co-Supervisor)

Professor Patrick Kwok Leung Kwan (Co-Supervisor)

Professor Yiu Loon Chui (Committee member)

Table of contents

Abstract

Purpose: Epilepsy is a major neurological disorder, affecting more than 50 million people worldwide. Antiepileptic drugs (AEDs) do not effectively treat 30-40% of patients. Export of AEDs by P-glycoprotein (Pgp, *ABCB1*, or *MDR1*), which is overexpressed in the blood-brain barrier in drug-resistant patients, may be a mechanism for resistance to AEDs. Single nucleotide polymorphisms (SNPs) 1236C>T, 2677G>T and 3435C>T have been associated with drug-resistant epilepsy and were sometimes found to have effects on Pgp activities. But whether (or which) AEDs are transported by Pgp remains unclear, and there is no direct evidence showing that polymorphisms affect the transport of AEDs by Pgp. Therefore, we propose to use monolayers of cells transfected with the *MDR1* variants to investigate 1) which AEDs are substrates for Pgp; and 2) the effect of *MDR1* polymorphisms (1236C>T, 2677G>T, and 3435C>T) on AED transport.

Methods: Stable transfected clones of human *MDR1* haplotypes combining 1236C>T, 2677G>T/A, and 3435C>T in LLC-PK1 cells were established and validated. The expression level and localization of Pgp were measured. Bi-directional transport assays or concentration equilibrium transport assays (CETA) were performed by using *MDR1*-transfected and non-transfected cells to determine the substrate status of the following AEDs: phenytoin (PHT), phenobarbital (PB), ethosuximide (ESM), carbamazepine (CBZ), eslicarbazepine acetate (ESL), oxcarbazepine (OXC), (S)-licarbazepine (S-LC), carbamazepine-10,11-epoxide (CBZ-E), rufinamide (RFM), lacosamide (LCM), zonisamide (ZNS), and pregabalin (PGB). LLC-PK1 cells transfected with *MDR1* variants were used to evaluate the effects of *MDR1* polymorphisms on transport activity of AEDs in CETA.

Results: In CETA, PHT, PB, and LCM were transported by *MDR1*-transfected cells from basolateral to apical sides, while RFM, ZNS, PGB and ESM were not transported. Pgp did not transport CBZ, but did transport its active metabolite CBZ-E. Pgp also pumped ESL, OXC, and their active metabolite S-LC. The transport of these drugs can be completely blocked by Pgp inhibitor verapamil or tariquidar. In bi-directional transport assays, the P_{app} for the basolateral to apical direction in *MDR1*-transfected cells was significantly higher than in non-transfected cells for PHT, OXC, ESL, and S-LC, and not for PB, CBZ-E, CBZ, or ESM.

To compare the extent of basolateral-to-apical transport efficiency of different variants, we calculated the amount of the transported drugs divided by expression level of *MDR1* in the apical

chamber for each variant. In the G418 selection condition, compared with reference haplotype CGC, the CTC haplotype increased Pgp activity to transport OXC and ESL, while the CGT and CTT haplotypes did not significantly affect Pgp function. In the vincristine sulfate selection condition, compared with CGC, the haplotype CTT decreased Pgp activity, while other haplotypes, including CGC, CGT, CAC, CTC, TGC, TGT, TTT, and TTC, did not affect function. Selection by vincristine sulfate may raise expression of Pgp and eliminate differences among the variants.

Conclusions: CETA may be a more sensitive system than the bi-directional transport assay to detect transport of drugs with high passive diffusion across the BBB. We conclude that PHT, PB, OXC, ESL, CBZ-E, S-LC, and LCM, but not ESM, CBZ, RFM, ZNS, and PGB, are transported by human Pgp. These data suggest that resistance to PHT, PB, ESL, OXC and LCM might be attributed to increased efflux function of Pgp because they or their active metabolites are Pgp substrates. The CTC haplotype exhibited increased directional transport activity by Pgp. The effects of *MDR1* polymorphisms on AED transport may provide a molecular explanation of the association between the polymorphisms and pharmacoresistance. This knowledge may help guide the design of genetic-based individualized therapy of epilepsy.

摘要

目的：癲癇是一種常見的神經系統疾病。在全世界超過 5000 萬癲癇病人中，30-40 ％的患者对抗癲癇藥物具有耐藥性。因為 P-glycoptotein（Pgp、ABCB1 或 MDR1）在耐藥病人的血腦屏障中高表達，所以抗癲癇藥物被 Pgp 轉運出大腦可能是導致耐藥性的一個原因。單核苷酸多態性（SNPs）位點 1236C>T、2677G>T 和 3435C>T 被發現與耐藥性癲癇相關，可能影響 Pgp 的功能。但 Pgp 是否轉運抗癲癇藥物或者轉運哪種藥物依然不清楚。目前沒有直接證據表明 SNPs 能夠影響 Pgp 對抗癲癇藥物的轉運。因此，我們計劃使用轉染包含多態性位點的 MDR1 的細胞來研究：1）哪種抗癲癇藥物是 Pgp 的底物；2）SNPs（1236C>T、2677G>T 和 3435C>T）對 Pgp 運輸抗癲癇藥物的影響。

方法：包含 1236C>T、2677G>T/A 和 3435C>T 三個位點基因多態性的人類 MDR1 基因被穩定轉染到 LLC-PK1 細胞中并測定 Pgp 在細胞內的表達水平和表達位置。通過雙向轉輸實驗或濃度平衡轉運實驗（CETA），我們檢測了以下抗癲癇藥物是否為 Pgp 底物：苯妥英鈉（PHT）、苯巴比妥（PB）、乙琥胺（ESM）、卡馬西平（CBZ）、eslicarbazepine acetate（ESL）、奧卡西平（OXC）、（S）-licarbazepine（S-LC）、卡馬西平-10 ,11-環氧化物（CBZ-E）、rufinamide（RFM）、lacosamide（LCM）、唑尼沙胺（ZNS）和普瑞巴林（PGB）。在濃度平衡轉運實驗中，轉染 MDR1 及其多態性位點的 LLC-PK1 細胞被用來檢測 SNPs 對 Pgp 轉運抗癲癇藥物的影響。

結果：在濃度平衡轉運實驗中，PHT、PB 和 LCM 可以被轉染 MDR1 的細胞從其底側轉運到頂側，而 RFM、ZNS、PGB 和 ESM 則不能。Pgp 不能轉運 CBZ，但它可以轉運 CBZ 的活性代謝物 CBZ - E。Pgp 還可以轉運 ESL、OXC、及其活性代謝物 S - LC。Pgp 對這些藥物的轉運功能可以完全被其抑製劑 verapamil 和 tariquidar 抑制。在雙向轉運實驗中，PHT、OXC、ESL 和 S-LC 的 Papp 值（從基

底到頂側）在轉染 MDR1 的細胞中明顯高於未轉染的細胞，而 PB、CBZ-E、CBZ 和 ESM 沒有區別。

為了比較不同變種對 Pgp 轉運效率的影響，我們計算了不同變種中轉運到頂側的藥物的總量與 Pgp 表達水平的比值。在 G418 篩選條件下，相對於 CGC 單體型，CTC 增強了 Pgp 轉運 OXC 和 ESL 的功能，而 CGT 和 CTT 則沒有顯著影響。在硫酸長春新鹼篩選條件下，相對於 CGC，CTT 降低了 Pgp 的轉運功能，而其他單體型（CGT、CAC、CTC、TGC、TGT、TTT 和 TTC）則沒有影響 Pgp 的功能。硫酸長春新鹼可能過度誘導了 Pgp 的表達因而消除了不同變種之間的區別。

結論：對於高透過血腦屏障的藥物而言，CETA 比雙向轉運試驗更靈敏。PHT、PB、OXC、ESL、CBZ-E、S-LC 和 LCM 是 Pgp 的轉運底物，而 ESM、CBZ、RFM、ZNS 和 PGB 則不是。這些數據表明，由於 PHT、PB、ESL、OXC、LCM 及其活性代謝物是 Pgp 的底物，病人對他們的耐藥性可能是由於 Pgp 的轉運引起的。CTC 單體型增強了 Pgp 的轉運功能。 MDR1 基因多態性對 Pgp 功能的影響可為 MDR1 基因多態性和耐藥性之間的聯繫提供分子學上的解釋。這方面的知識可以指導設計基於基因的癲癇個體化治療。

Acknowledgement

I would like to greatly appreciate my parents and brother. They offered me so many spiritual and material supports. I can not find words to express my thanks to them for their love.

I would like to greatly thank my supervisors Prof. Larry Baum, Prof. Zhong Zuo, and Prof. Patrick Kwan. Their patience guidance, logical thinking, and thoughtful help make me to graduate smoothly. Their enthusiasm in research, nice character, and outstanding leadership gave me deep impression and will promote me in further career and life.

I would like to thank all the graduate students for their help in my study and life. They gave me so much happiness and made my life more meaningful in Hong Kong. I also would like to thank all the technicians, professors, and other staffs in School of Pharmacy for their supports in my experiments and study. I would like to thank my friends, who gave me support in my soul, encouraged me to face reality, and made my life more colorful.

X

Publications

Zhang Chunbo, Zuo Z, Kwan P, Baum L. In vitro transport profile of carbamazepine, oxcarbazepine, eslicarbazepine acetate and their active metabolites by human P-glycoprotein. *Epilepsia.* 2011 Jun 21. doi: 10.1111/j.1528-1167.2011.03140.x. [Epub ahead of print]

Zhang Chunbo, Wong V, Ng P, Lui C, Sin N, Wong K, Baum L, Kwan P. Failure to detect association between polymorphisms of the sodium channel gene SCN1A and febrile seizures in Chinese patients with epilepsy. *Epilepsia.* 2010 Sep; 51(9):1878-81.

Zhang Chunbo, Kwan P, Zuo Z, Baum L. In vitro concentration dependent transport of phenytoin and phenobarbital, but not ethosuximide, by human P-glycoprotein. *Life Sci.* 2010; 86(23-24):899-905.

Zhang Chunbo, Kwan P, Zuo Z, Baum L. P-glycoprotein transport of carbamazepine analogs and metabolites. Abstract. *AAPS Annual Meeting*, New Orleans, U.S.A, Nov 14-18, 2010.

Zhang Chunbo, Zuo Z, Baum L, Kwan P. In vitro transport profile of carbamazepine and its analogs by human P-glycoprotein. Abstract. *8th Asian & Oceanian Epilepsy Congress*, Melbourne, Australia, Oct 21-24, 2010.

Zhang Chunbo, Baum L, Zuo Z, Kwan P. Transport of antiepileptic drugs by P-glycoprotein in cell monolayer models. Abstract. *63rd Annual Meeting of American Epilepsy Society*, Boston, MA, U.S.A, Dec 4-8, 2009.

Zhang Chunbo, Baum L, Zuo Z, Kwan P. P-glycoprotein substrate status of antiepileptic drugs phenytoin, phenobarbital, ethosuximide, and carbamazepine in cell monolayer models. Abstract. *International Conference on Personalized Medicine*, Hong Kong, Sep19-20, 2009.

List of figures

XVI

List of tables

List of abbreviations

AEDs	antiepileptic drugs
Pgp	P-glycoprotein
BBB	blood-brain barrier
CBZ	carbamazepine
OXC	oxcarbazepine
ESL	eslicarbazepine acetate
CBZ-E	carbamazepine-10,11-epoxide
MHD	monohydroxylated derivative
S-LC	S-licarbazepine
PHT	phenytoin
PB	phenobarbital
ESM	ethosuximide
RFM	rufinamide
LCM	lacosamide
ZNS	zonisamide
PGB	pregabalin
SAR	structure-activity relationship
PET	positron emission tomography
TDQ	tarquidar
LTG	lamotrigine
CETA	concentration equilibrium transport assay
MTT	3-[4,5 dimethyl thiazolyl-2]-2,5-diphenyltetrazolium bromide
TEER	transepithelial electrical resistance
SNPs	Single nucleotide polymorphisms
CAM	calcein acetoxymethylester
BMECs	brain microvascular endothelial cells
CsA	cyclosporine A
PBS	phosphate buffered saline
P_{app}	apparent permeability coefficient

LOQ	limits of quantification
LOD	limit of detection
Rho123	Rhodamine-123
VPA	valproate
TPM	topiramate

Chapter One

Introduction

Epilepsy is the second most common major neurological disorder, affecting more than 50 million people worldwide (Aiken *et al.*, 2000). It is a chronic brain disorder characterized by recurrent seizures, and is classified into two types: focal or generalized epilepsy. Focal epilepsy causes seizures originating from a discrete cortical site; generalized epilepsies causes seizures originating from both cerebral hemispheres (Everitt *et al.*, 1999; Hauser *et al.*, 1993; Shorvon, 1990). Although it is a major public health issue, we still understand little on many aspects of this disease. More than 20 antiepileptic drugs (AEDs) are used clinically, and this number is still increasing. Despite the availability of so many AEDs, 30-40% of patients do not respond to pharmacotherapy (Kwan *et al.*, 2000b; Regesta *et al.*, 1999). Most non-responsive epilepsy patients are resistant to several, often all, AEDs, even though the drugs differ from each other in pharmacokinetics, mechanisms of action, and interaction potential. Epilepsy drug-resistance was defined as: "failure of adequate trials of two tolerated and appropriately chosen and used AED schedules (whether as monotherapies or in combination) to achieve sustained seizure freedom" (Kwan *et al.*, 2010). The mechanisms underlying drug resistance of epilepsy patients are still unclear but may include pathology at the epileptic focus or polymorphisms of drug transporters (Weiss *et al.*, 2003b).

The blood-brain barrier (BBB) is a diffusion barrier, composed of endothelial cells, astrocyte end-feet, and pericytes (PCs) (Ballabh *et al.*, 2004). It limits the brain penetration of small molecules and protects the CNS from xenobiotics. More than 98% of small molecules cannot penetrate the BBB. Thus, the entry of most drugs to the CNS is limited by the BBB (Ghose *et al.*, 1999; Pardridge, 2007). In recent years, one of the potential mechanisms of AED resistance interesting researchers is overexpression of multi-drug transporters in endothelial cells of the blood-brain barrier (BBB) in non-responsive epilepsy patients. Since AEDs must traverse the BBB to enter the brain band exert their desired effects, the overexpression of multidrug transporters and multidrug

resistance-associated protein (MRP) in the endothelial cells of the BBB may contribute to drug resistance (Loscher *et al.*, 2005; Loscher *et al.*, 2007). One of the most intensively studied multidrug transporters is P-glycoprotein (Pgp, also known as ABCB1 or MDR1), which plays a central role in drug absorption and distribution in many organisms. Pgp was found as an overexpressed gene in human tumor cells in 1976 by Juliano et al. (Juliano *et al.*, 1976). Pgp functions as an ATP-driven efflux pump of substrates ranging from approximately 300 to 4000 Da in mass, including some HIV protease inhibitors, antibiotics, immunosuppressive agents, and many other prescribed drugs (Gottesman *et al.*, 1988; Hennessy *et al.*, 2007; Juliano *et al.*, 1976).

Brain concentrations of many drugs increase in *MDR1*-null mice (Mizuno *et al.*, 2003). Similarly, Pgp inhibitors increase drug penetration into the brain (Kemper *et al.*, 2003; Kemper *et al.*, 2004). For example, the Pgp inhibitor PSC833 can increase paclitaxel accumulation in the mouse brain (Fellner *et al.*, 2002). These studies suggest that Pgp plays a remarkable role in restricting access of drugs to the CNS. The capillary endothelial cells of the BBB highly express Pgp, and this expression is increased in epilepsy patients (Loscher, 2007; Loscher *et al.*, 2005). In addition, the expression is higher in drug-resistant than in drug-responsive patients (Dombrowski *et al.*, 2001; Tishler *et al.*, 1995). Some studies indicated that several AEDs are substrates or inhibitors of Pgp, implying that Pgp plays an important role in refractory epilepsy, although other studies in various models provided conflicting evidence (Baltes *et al.*, 2007a; Baltes *et al.*, 2007b; Luna-Tortos *et al.*, 2008b; Weiss *et al.*, 2003b). In general, evidence is greater for lipophilic AEDs as Pgp substrates (Kwan *et al.*, 2005; Loscher, 2007; Luna-Tortos *et al.*, 2008b). However, there is still no consensus on whether (or which) AEDs are substrates of Pgp.

As evidenced in the literature, a wide spectrum as well as different classes of drugs were substrates of the Pgp efflux pump (Stouch *et al.*, 2002). Identifying the substrate status of compounds is important for new drug design. Study on the structure-activity relationship (SAR) may help explain association between the common structural features of compounds and the activity of Pgp. Some papers and reviews have used different models

to focus on the SAR of chemicals acting as substrates for Pgp (Raub, 2006; Seelig, 1998; Stouch *et al.*, 2002). However, there is still no study or review focusing on describing the SAR of AEDs acting as substrates for Pgp.

Single nucleotide polymorphisms (SNPs) at 62 sites have been reported in the human *MDR1* gene (Kerb *et al.*, 2001; Kim *et al.*, 2001; Kroetz *et al.*, 2003; Sakaeda *et al.*, 2003; Schwab *et al.*, 2003). Some of these variants may influence the expression or function of Pgp (Lepper *et al.*, 2005; Pauli-Magnus *et al.*, 2004). Researchers have focused their studies on three SNPs which are in linkage and whose minor allele frequencies are high: 1236C>T in exon 12, 2677G>T/A in exon 21 (resulting in an Ala893Ser/Thr amino acid change), and 3435C>T in exon 26 (Kim *et al.*, 2001). The expression level of Pgp influences the degree of drug resistance of cancer cells to chemotherapy and affects drug efficacy (Fung *et al.*, 2009; Gerlach *et al.*, 1986; Giavazzi *et al.*, 1984). Studies have examined whether the SNPs affect the expression of Pgp. The 3435 T allele was associated with lower expression of *MDR1* in the duodenum of Caucasians (Hoffmeyer *et al.*, 2000), but other results contradicted that finding (Hung *et al.*, 2008; Kim *et al.*, 2001; Sakaeda *et al.*, 2001; Salama *et al.*, 2006). The 2677 T allele (or 893 Ser) resulted in an enhancement of efflux and a decrease in the intracellular accumulation of digoxin *in vitro* in several studies (Hung *et al.*, 2008; Kim *et al.*, 2001; Salama *et al.*, 2006), but no change in other reports (Kim *et al.*, 2001; Kimchi-Sarfaty *et al.*, 2002). Combinations of SNPs at positions 2677 and 3435 may have additional effects on MDR1 activities *in vivo* (Kurata *et al.*, 2002; Tang *et al.*, 2002). Evidence suggests that combinations of genotypes, or haplotypes, may affect transport *in vitro* (Chowbay *et al.*, 2003; Hung *et al.*, 2008; Johne *et al.*, 2002; Kimchi-Sarfaty *et al.*, 2007; Salama *et al.*, 2006). Kimchi-Sarfaty et al. noted that the synonymous allele 3435T, combined with one or two of the 2677T and 1236T alleles, resulted in insensitivity to Pgp inhibitors. The 3435 SNP affects the rate of folding of the Pgp protein as it is translated, thus affecting the insertion of Pgp into the membrane, resulting in a change in the interaction site of substrate and inhibitor and altering Pgp function (Kimchi-Sarfaty *et al.*, 2007).

1.1   The hypothesis that AEDs act as substrates for Pgp

P-glycoprotein is one of the most intensively studied ABC family members. The ABC family is a large group of proteins comprised of membrane transporters, ion channels, and receptors. The transporters are conserved among species. In humans, two different 170 kDa proteins are called Pgp. They are encoded by the *MDR1* (*ABCB1*) and *MDR2* (*ABCB4*) genes, which are located near each other on chromosome 7q21.1 (Callen *et al.*, 1987). In rodents, Pgp proteins are encoded by three genes, *mdr1a*, *mdr1b*, and *mdr2* (Silverman, 1999). The *MDR* genes are classified into two groups. Human *MDR1* and rodent *mdr1a* and *mdr1b* encode the transporters involved in multidrug resistance. *MDR1* has the same functions as *mdr1a* and *mdr1b*. *MDR2* and *mdr2* encode phosphotidylcholine transporters in biliary canaliculi (Borst, 1997; Silverman, 1999). Most reports use the term Pgp to refer to the protein encoded by *MDR1*, *mdr1a* and *mdr1b*, and that convention will be followed here.

The human Pgp is composed of two homologous halves. Each of them consists of an N-terminal, one hydrophobic transmembrane domain (approximately 250 amino acid residues), one hydrophilic nucleotide binding domain (approximately 300 amino acid residues) and a C-terminal (Chen *et al.*, 1986; Gros *et al.*, 1986) (Fig 1.1). The exact function of each domain and the molecular model detailing how Pgp pumps substrates from the intracellular space to the extracellular space are all still unresolved. Pgp modulates drug distribution and disposition in many organisms. There are hundreds of transport substrates of Pgp, including natural products, chemotherapeutic drugs, steroids, fluorescent dyes, linear and cyclic peptides, and ionophores. Most of them are hydrophobic, weakly amphipathic, and contain a heterocycle. However, the mechanism by which Pgp recognizes substrates is unclear. Many drugs used in our daily life are substrates of Pgp. The bioavailability of these drugs can be reduced by Pgp. In Pgp null (*mdr1a*$^{-/-}$ or *mdr1b*$^{-/-}$) mice, plasma concentration of some drugs was increased compared with wild type mice (Kim *et al.*, 1998).
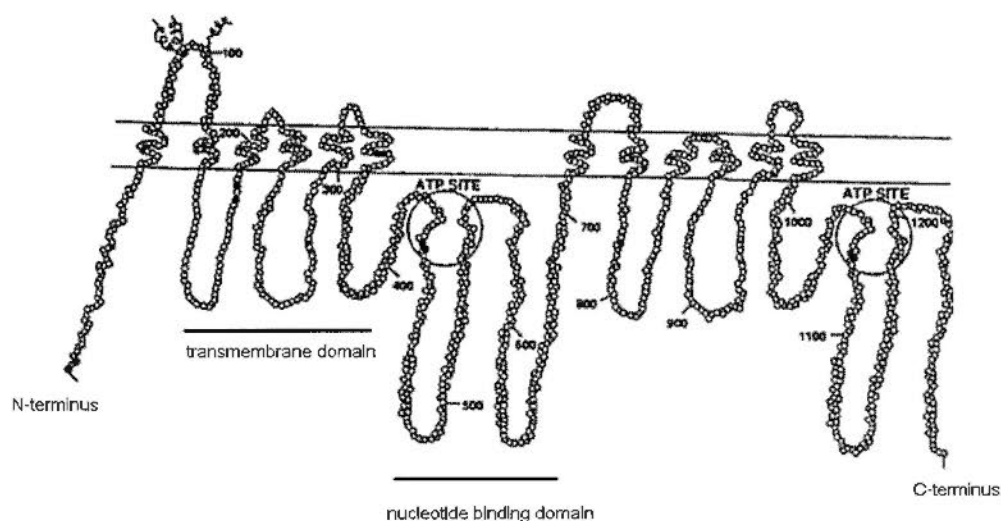
Fig 1.1 Model of human P-glycoprotein (modified from (Chen *et al.*, 1986))

P-glycoprotein is not only highly expressed in multidrug resistant tumor cells, but is also highly expressed in the barrier and excretory tissues, such as the epithelial cells of biliary hepatocytes, adrental cortex, pancreatic ductules, large intestine mucosal cells, proximal renal tutules, testis, placenta, and blood-tissue barriers (Beaulieu *et al.*, 1997; Cordon-Cardo *et al.*, 1990; Cordon-Cardo *et al.*, 1989; Fojo *et al.*, 1987; Kwan *et al.*, 2005; Sugawara *et al.*, 1988). The capillary endothelial cells in the blood brain barrier (BBB) express Pgp to high levels, as compared to other tissues. Pgp is located in the luminal plasma membrane (blood side) of brain capillary endothelial cells (Lee *et al.*, 2001) (Fig 1.2). The pattern of distribution of Pgp is ideal to limit drug entry to the brain or efflux of drugs from brain to blood, which suggests that Pgp plays an important role in protecting the brain against xenobiotics (Beaulieu *et al.*, 1997; Bendayan *et al.*, 2002; Demeule *et al.*, 2002; Kwan *et al.*, 2005; Lee *et al.*, 2001; Mizuno *et al.*, 2003; Pardridge *et al.*, 1997; Schinkel, 1997). In general, the more lipophilic drugs penetrate more readily into the brain. But there are many lipid-soluble drugs with lower brain permeability than would be predicted because they are pumped out of the brain by Pgp (Begley, 2004; Schmidt *et al.*, 2005). Most AEDs are very lipophilic, but about one-third of epilepsy patients do not respond to them. One of the possible explanations is that lipophilic AEDs are pumped out of the brain by Pgp in the BBB, which decreases the concentration of AEDs in the brain

and affects drug efficacy. In order to support the hypothesis, three criteria should be satisfied: first, the Pgp level in the BBB would be higher in drug-resistant than in drug-responsive epilepsy patients; second, the concentration of AEDs in the brain would be lower in drug-resistant than in drug-responsive epilepsy patients; third, the most important and direct evidence, AEDs would be substrates of Pgp, which would explain that the lower concentration of AEDs in brain may be caused by the overexpression of Pgp. The evidence from patients and animal models indicates that refractory epilepsy is associated with the overexpression of Pgp and lower concentration of AEDs in brain (Kimura *et al.*, 2007). *In vivo* and *in vitro* evidence also indicates that some AEDs act as substrates of Pgp, however there is some inconsistent evidence (Kwan *et al.*, 2005; Loscher *et al.*, 2005). These observations are consistent with the hypothesis that lipophilic AEDs are pumped out of the brain by Pgp in the BBB, which gives a reasonable explanation for drug refractory epilepsy.
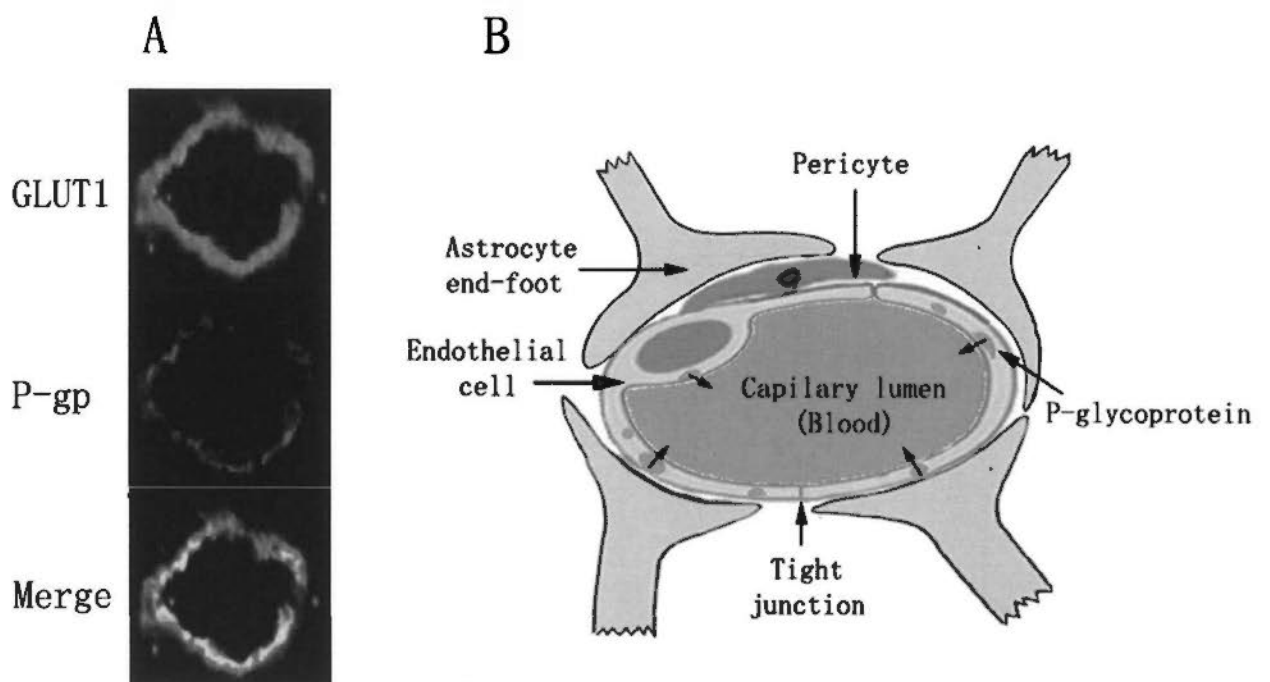
Fig 1.2 Pgp location and the blood-brain barrier.
A, Confocal micrographs showing immunohistochemical localization of Pgp (red and yellow).
Pgp is located on the luminal side of the microvessel. GLUT1 (green) shows the brain capillary
endothelial cells; B, Schematic illustration of blood brain barrier (cited and modified from
(Loscher *et al.*, 2005; Volk *et al.*, 2005a)).

1.2   Methods and criteria to identify substrate status of AEDs

Early studies of Pgp found that it was expressed in cancer cells and was a cause of drug resistance in cancer (Gottesman *et al.*, 1988; Hennessy *et al.*, 2007; Juliano *et al.*, 1976). Many compounds were shown to be substrates or inhibitors of Pgp (Avendano *et al.*, 2002; Ford *et al.*, 1993; Ford *et al.*, 1996; Kwan *et al.*, 2005). Evidence further indicated that Pgp is relevant to drug-resistant epilepsy, and that some AEDs are substrates or inhibitors for Pgp (Baltes *et al.*, 2007b; Hung *et al.*, 2008; Kwan *et al.*, 2007a; Luna-Tortos *et al.*, 2008b; Luna-Tortos *et al.*, 2009; Zhang *et al.*, 2010). Several methods have been established to detect whether AEDs are substrates for Pgp in *in vivo* and *in vitro*, including clinical research on patients, animal models, and cell based assays.

In clinical research, brain tissues isolated from drug-resistant epilepsy patients undergoing surgery to remove seizure foci are commonly used to detect the location and expression level of Pgp. This is a direct way to study the association between refractory epilepsy and the drug efflux function of Pgp. However, there is a limitation in using human brain to identify whether an AED is a substrate of Pgp, because, at present, there are not validated and readily feasible methods to detect the brain concentration of an AED and associate it with the Pgp level in live patients. Moreover, we lack correct controls to compare with drug-resistant epilepsy. Positron emission tomography (PET) will be a useful tool to directly detect the function of Pgp in human brains. In monkeys, the brain distribution of [^{11}C]-verapamil, a substrate of Pgp, increased in the presence of PSC833, an inhibitor of Pgp (Lazarowski *et al.*, 1999). PET was also used in human brains to detect effects of MDR1 SNPs (Brunner *et al.*, 2005; Takano *et al.*, 2006).

Animal models have played a key role in discovering and characterizing AEDs. They have advantages over clinical studies. First, animal models are used to detect associations among the expression level of Pgp in the BBB, the concentration of AEDs in the brain, and the drug responsiveness status of epilepsy (drug responsive or non-responsive). Using rat epilepsy models, we can select subgroups which either respond or do not respond to AED treatment. It is possible to detect the expression level of Pgp in different

brain regions and test the associated AED level. Then we can conclude whether drug non-responders differ from drug responders on Pgp expression in the BBB and whether the Pgp expression level affects AED concentration in the brain. For example, in PB-resistant rats, Pgp was overexpressed in the hippocampus and other limbic brain regions compared with PB-responsive rats, and the anticonvulsant activity of PB was restored by the Pgp inhibitor tarquidar (TQD) (Volk *et al.*, 2005b).

Second, animal models are used to detect the function of Pgp. Using *in vivo* microdialysis in rats, the concentration of AEDs, such as phenytoin (PHT), phenobarbital (PB), carbamazepine (CBZ), lamotrigine (LTG), and felbamate (FBM), in extracellular fluid of the cerebral cortex can be enhanced by Pgp inhibitors (Potschka *et al.*, 2002; Potschka *et al.*, 2001a; Potschka *et al.*, 2001b). In *mdr1a* knockout mice, which do not express the *mdr1a* isoform in the BBB, various drugs reached significantly higher brain concentrations than did wild type mice (Schinkel *et al.*, 1996). Animal models have the advantage that they are unbiased with respect to assumption about the specific nature of the target: any AEDs or Pgp expression levels could, in principle, be detected as a target, which may be restricted in human studies. These models can provide evidences on whether Pgp is involved in controlling the brain distribution of AEDs. However, they may have little resemblance to chronic epilepsy in humans.

However, *in vivo* studies with patients and animal systems may be too complex to prove that AEDs are substrates for Pgp and that a decrease of AED levels is caused by the overexpression of Pgp. *In vivo* methods are also not very practical for rapid and large-scale screening of compounds. Compared with *in vivo* systems, *in vitro* assays have advantages and are widely used. After detecting the activity of Pgp *in vivo*, *in vitro* systems can be used to optimize the discovery, or vice versa. Cell lines transfected with the *MDR1* gene, overexpressing the Pgp protein, are models to evaluate the potential of compounds to act as Pgp substrates/inhibitors. An advantage of *in vitro* methods is the potential to demonstrate the molecular mechanism of action between AEDs and Pgp. In cell lines overexpressing Pgp, we might obtain a direct result that an AED acts as a substrate for Pgp. We can confirm the result using Pgp inhibitors, which can reverse the

effect of Pgp overexpression on AED transport. Several AEDs, such as PHT, PB, and levetiracetam (LVT), were transported by Pgp in LLC and MDCK cell models. This directional transport of AEDs could be inhibited by selective Pgp inhibitors (Luna-Tortos *et al.*, 2008b). Moreover, through studying Pgp using genetics, bioinformatics, cell biology and biochemistry, its mechanisms of action are being revealed (Ambudkar *et al.*, 2006; Chang, 2007; Frelet *et al.*, 2006; Kimchi-Sarfaty *et al.*, 2007; Kimura *et al.*, 2007; Leschziner *et al.*, 2007). However, cell models also have disadvantages in screening for the substrate status of AEDs and only provide *in vitro* evidence whether AEDs are substrates of Pgp. *In vitro* screen can not replace screening in animal models, because *in vitro* systems cannot mimic physiological conditions. They cannot model the bioavailability, the brain accessibility, and the specific pharmacodynamic action in *in vivo* epileptic systems. We cannot deduce the conclusion that the same activity will occur *in vivo* just by the results in an *in vitro* system. Thus, it is necessary to validate the activity using *in vivo* systems. Further, animal models differ from humans; we also need to study the function in the human. Thus we need to find a more mature model to observe and demonstrate this complex phenomenon.

To evaluate the results of published studies, we need to establish the criteria to define whether an AED acts as a substrate for Pgp and whether this action is associated with refractory epilepsy. In order to define the substrate status of AEDs, we should satisfy criteria from *in vivo* and *in vitro* evidence: 1. In *in vitro*, or cell models, the AED is transported by Pgp, and this transport can be inhibited by Pgp selective inhibitors. Because different cell models may show inconsistent results, we should set up a standard to identify the reliability of evidence. Using more than one cell model to confirm that an AED acts as a Pgp substrate would increase the reliability. 2. In animal models, the brain concentration of an AED is decreased by overexpression of Pgp, and this decrease can be restored by Pgp inhibitors, or the brain concentration of an AED is increased by adding Pgp inhibitors or by decreasing Pgp expression. 3. Evidence from patients may also be considered. PET, intraoperative microdialysis, and tissue isolated from epilepsy patients by surgery are common methods which can be used to investigate the association between Pgp expression and AED brain concentration. But human samples are limited

and should be considered less in the contribution to substrate status. Combining these three types of evidence, we can define the substrate status of an AED: 1. If the AED is transported by Pgp *in vivo* (animal models or patients) and *in vitro* (cell models), we define that it is <u>likely</u> a substrate of Pgp. 2. If the AED is transported by Pgp *in vitro* or *in vivo*, we define that it is <u>probably</u> a substrate of Pgp. 3. If the AED is transported both *in vitro* and *in vivo*, but the results are inconsistent, we define it is <u>possibly</u> a substrate of Pgp. 4. If the AED is not transported *in vivo* or *in vitro*, we define that it is <u>unlikely</u> a substrate of Pgp. Because of the limited availability of human data, evidence from patients counts less in these criteria than does evidence from animal models. On the other end of the spectrum, cell models are sample and thus weigh more heavily than *in vivo* models in these criteria.

In order to define whether the Pgp substrate status of an AED is associated with refractory epilepsy, we must consider evidence from humans, animals, and cellular models. We may use these criteria: First, the AED is a Pgp substrate. Second, in clinical studies, the expression of Pgp is increased and the concentration of the AED is decreased in drug-resistant epilepsy brains compared with drug responsive brains, and the inhibition of Pgp is associated with clinical benefit. Third, the results in humans and animals are consistent. Combining the above criteria, we may be able to explain the relationship between Pgp and refractory epilepsy. However, the evidence reported to date is far from sufficient to give a definite conclusion now. More study of the relationship between AEDs and Pgp in epilepsy will be required.

1.3   The overexpression of Pgp in epilepsy patients and animal models

1.3.1 In epileptic patients

Pgp has the remarkable ability to restrict drug access to the CNS, which is demonstrated in the comparisons of Pgp gene knockout and wild type mice. Some evidence indicates that Pgp plays a role in the BBB of drug resistant epilepsy patients (Kwan *et al.*, 2005; Loscher, 2007; Robey *et al.*, 2008). Does the expression of Pgp differ between drug-

resistant and drug-responsive epilepsy patients? If the level of Pgp is higher in drug-resistant patients than in drug-responsive patients, the resulting lower concentration of AEDs in the parenchymal space may lead to the lack of drug response in such patients. Tishler et al. reported the enhancement of Pgp expression in the capillary endothelial cells of epileptic tissues compared with non-epileptic tissues. The brain mRNA level of *MDR1* was increased more than 10 times in these patients (Tishler *et al.*, 1995). Subsequent studies confirmed that the overexpression of Pgp was mainly located in the capillary endothelial cells (Dombrowski *et al.*, 2001). *In vitro*, the endothelial cells were isolated from refractory patient brain specimens. The overexpression of Pgp in refractory epileptic endothelial cells compared with non-epileptic endothelial cells was demonstrated at the mRNA and protein levels (Dombrowski *et al.*, 2001). Since the brain capillary endothelial cells form the blood-brain barrier (BBB), the overexpression of Pgp in these cells could export AEDs back to the vasculature and lead to low concentrations of AEDs around neurons, which may contribute to resistance to antiepileptic drugs which are substrates of Pgp.

Evidence exists that Pgp is overexpressed not only in endothelial cells but also in neurons and glial cells in drug resistant epilepsy patients (Table 1.1). Patients with mesial temporal lobe epilepsy (MTLE), tuberous sclerosis, malformations of cortical development (MCD) or focal cortical dysplasia (FCD) showed overexpression of Pgp in neurons and astrocytes (Jozwiak, 2007; Lazarowski *et al.*, 1999; Sisodiya *et al.*, 1999). The Pgp up-regulation in neurons and glial cells could lead to low concentrations of AEDs in the parenchymal space. The astrocytic foot processes around endothelial cells may pump drugs to endothelial cells. Neuroectodermal cells expressing *MDR1* had lower intracellular PHT concentrations than did *MDR1*-negative cells (Tishler *et al.*, 1995). Pgp mediated drug extrusion by astrocytes of epileptic tissues was greater than by control astrocytes (Marchi *et al.*, 2004). These results suggest that the upregulation of Pgp in astrocytes and neurons may also play a role in controlling the exchange of xenobiotics between brain and plasma at the BBB (Marchi *et al.*, 2004). The findings of overexpression of Pgp in the brain tissues of refractory epilepsy patients are not complete because most of them lack the adequate controls, tissues from drug responsive epilepsy

patients, since these patients are not normally subjected to brain surgery. Thus, we do not know whether Pgp overexpression in refractory epilepsy patients is associated with drug resistance or is just a general phenomenon of epilepsy irrespective of drug responsiveness.

Table 1.1 Overexpression of Pgp in human epileptic pathologies

Pathology	Pgp overexpression in cell types (Y/N)			References
	Endothelial cells	Neurons	Astrocytes	
Focal cortical dysplasia	Y	Y	Y	(Ak *et al.*, 2007; Aronica *et al.*, 2003; Sisodiya *et al.*, 2002; Sisodiya *et al.*, 2001)
Hippocampal sclerosis	Y	Y	Y	(Aronica *et al.*, 2004; Dombrowski *et al.*, 2001; Kubota *et al.*, 2006; Marchi *et al.*, 2004; Sisodiya *et al.*, 2002; Tishler *et al.*, 1995)
Tuberous sclerosis	Y	Y	Y	(Lazarowski *et al.*, 2004; Lazarowski *et al.*, 1999; Tishler *et al.*, 1995)
Temporal lobe epilepsy	Y	--	--	(Seegers *et al.*, 2002b)
Malformation of cortical development	--	--	Y	(Sisodiya *et al.*, 1999)

Y: Yes

N: No

--: Not available

1.3.2 In animal models

Animal models have provided evidence for Pgp overexpression in epileptogenic brain tissue from animals with refractory epilepsy (Table 1.2). Induced epileptic rat models were widely used in studying Pgp expression and AED distribution. Pgp was overexpressed in endothelial cells, neurons, and astrocytes in different kindled models (Liu *et al.*, 2007; Marchi *et al.*, 2006; Volk *et al.*, 2004). In some cases, the overexpression of Pgp was transient and reversible. Kainate-induced epileptic rats showed transient up-regulation of Pgp in different brain regions (Seegers *et al.*, 2002c). In electrically induced status epilepticus (SE) rats, Pgp up-regulated within 1 week after SE to levels greater than those in chronic epileptic rats, and this increase was reversible (van Vliet *et al.*, 2004).

In some reports, overexpression of Pgp was investigated by measuring immediately after kindling (Liu *et al.*, 2007; Marchi *et al.*, 2006; Volk *et al.*, 2004). But measuring the Pgp level two weeks after seizures revealed no overexpression, suggesting the transient nature of Pgp overexpression by seizures in the temporal lobe (Seegers *et al.*, 2002a). Overexpression of Pgp may thus be a result of uncontrolled seizures but not of the processes underlying epilepsy (Seegers *et al.*, 2002a; Seegers *et al.*, 2002c). However, a long-term increase of Pgp was reported in pentylenetetrazole kindled rats (Liu *et al.*, 2007; Marchi *et al.*, 2006; Volk *et al.*, 2004). The differences in extent of Pgp induction among the various models may be due to the different duration of seizures (Seegers *et al.*, 2002a; Seegers *et al.*, 2002c; van Vliet *et al.*, 2004).

The above studies did not demonstrate that the overexpression of Pgp was associated with drug-resistant epilepsy because they did not compare refractory animals with those that were responsive. Drug-resistant epilepsy rats were selected according to their response to PB. Pgp was overexpressed in the hippocampus and other limbic brain regions in the resistant rats compared with responsive rats, and Pgp was confined to the brain capillary endothelial cells (Volk *et al.*, 2005b; Xiao, 1999). Similarly, the Pgp level in capillary endothelial cells of PHT-resistant rats was twice that of PHT-responsive rats (Potschka *et*

al., 2004b). Pgp overexpression in the BBB resulted in decreases of brain levels of the Pgp substrates ondansetron, PHT, Rhodamine123 (Rho123) and PB (Liu *et al.*, 2007; Marchi *et al.*, 2006; Rizzi *et al.*, 2002). The reduced level of ondansetron in MAM induced seizure rats was reversed by adding a Pgp inhibitor (Marchi *et al.*, 2006). The brain levels of some drugs increased 10-50 fold in Pgp null (*mdr1a/b$^{-/-}$*) vs. wild type mice (Mizuno *et al.*, 2003; Schinkel *et al.*, 1994). The hippocampal PHT concentration of *mdr1a/b$^{-/-}$* mice was higher than that of wild type mice (Rizzi *et al.*, 2002). The above results suggest that the Pgp expression level plays an important role in the response to antiepileptic drugs.

Table 1.2 Overexpression of Pgp in rat epilepsy models

Rat model	Pgp overexpression in different regions (Y/N)					References
	Cerebral cortex	Hippocampus	Limbic regions	Amygdala	Dentate gyrus	
Pentylenetetrazole	Y	--	--	--	--	(Liu *et al.*, 2007)
Methylazoxymethanol (MAM)-rats	N	Y	--	--	--	(Marchi *et al.*, 2006)
Pilocarpine	--	Y	--	--	--	(Volk *et al.*, 2004)
Kainic acid	--	Y	Y	--	Y	(Jin *et al.*, 2005; Rizzi *et al.*, 2002; Seegers *et al.*, 2002c; Volk *et al.*, 2004)
Electrical	--	Y	Y	Y	Y	(Brandt *et al.*, 2006; Potschka *et al.*, 2004b; van Vliet *et al.*, 2004; Volk *et al.*, 2005b)

Y: Yes

N: No

--: Not available

1.4   AEDs act as substrates of Pgp

One of the hypotheses for the etiology of drug-resistant epilepsy is that overexpression of Pgp causes AEDs to be pumped out of the brain, decreasing the level of AEDs in refractory epileptic brains and thus contributing to the AED resistance of the epilepsy. One major element necessary to support this hypothesis is proof that AEDs are substrates of Pgp and can be transported out of the brain by Pgp, particularly by human Pgp. Most of the studies based on three systems: cell models, animal models, and patients. They have both advantages and disadvantages in identifying whether an AED acts as a substrate of Pgp.

1.4.1 *In vitro* cell models

In vitro cell models were used to study whether AEDs were substrates of Pgp (Table 1.3). There are three common detection methods based on cell lines: measure whether an AED affects the uptake of a substrate marker of Pgp, detect the permeability of an AED through polarized cell monolayers using transwells, or detect the uptake of an AED.

Weiss et al. (2003) used the calcein acetoxymethylester (CAM) uptake assay to test the ability of AEDs to inhibit Pgp in LLC-MDR1 cells (LLC-PK1 cells transfected with human *MDR1*) and primary porcine brain capillary endothelial cells. They found that CBZ, PHT, LTG, and valproate (VPA) inhibited the Pgp efflux function (Weiss *et al.*, 2003b). In OS2.4/Doxo cells (canine osteosarcoma cells induced by exposure to doxorubicin to highly express Pgp), gabapentin (GBP), LTG, LVT, and PB decreased Rho123 efflux, while CBZ, FBM, PHT, topiramate (TPM), and zonisamide (ZNS) did not affect the uptake of Rho123 (West *et al.*, 2007). This method is fast and reproducible, but it poorly distinguishes substrates and inhibitors of Pgp. The compounds acting as substrates or inhibitors of Pgp may have different binding sites (Ambudkar *et al.*, 2003). The relationships between AEDs and substrate markers may be competitive, noncompetitive, or cooperative. A decrease in the uptake of calcein or R123 by an AED indicates that they have a competitive relationship and that the AED can be a substrate or

inhibitor of Pgp. AEDs which do not inhibit the uptake may act as substrates of Pgp. Therefore, this is an indirect method to study the substrate status of AEDs, and a direct measurement is required for more reliable identification of substrate status.

The uptake of AEDs was also tested, which is a more direct method and avoids the confusion of multiple mechanisms. In LoVo/dx cells (derived from the LoVo human colon adenocarcinoma cell line and overexpressing Pgp), the 10-OH-CBZ concentration was equal to that in LoVo cells but could be increased by the Pgp inhibitor XR9576 (Marchi *et al.*, 2005). Yang et al. (2008) used cultured rat brain microvascular endothelial cells (rBMECs) to test the uptake of PB. The uptake occurred in a time-, concentration-, and temperature-dependent manner which could be increased by cyclosporine A (CsA), ketoconazole, or the metabolic inhibitor dinitrophenol, all of which also decreased the efflux of PB (Yang *et al.*, 2008).

Recently, more and more groups used monolayer systems to test AED bi-directional transport by Pgp. This method uses a simplified model of the blood-brain barrier. Cells expressing Pgp on the apical side are seeded on transwell membranes and grown to confluency. If the drug can be transported from the basolateral to the apical side of the monolayer, it is a substrate of Pgp. In a Caco-2 monolayer model, the transport rates of vigabatrin (VGB), GBP, PB, LTG, and CBZ were equivalent in both directions, while PHT, TPM, and ethosuximide (ESM) displayed apical to basal transport. But none of them were affected by Pgp inhibitors. Only acetazolamide (AZD) had an basolateral to apical P_{app} value much greater than apical to basolateral P_{app} value (3-fold greater), and the efflux was inhibited by a Pgp inhibitor (Crowe *et al.*, 2006; Owen *et al.*, 2001). In MDCKII or LLC cell monolayer models, VPA and CBZ did not exhibit directional transport (Baltes *et al.*, 2007a; Baltes *et al.*, 2007b). PHT and LVT were directionally transported by mouse Pgp but not human Pgp, while CsA (a substrate of Pgp) was transported by both types of Pgp (Baltes *et al.*, 2007b). However, using the concentration equilibrium transport assay (CETA) system in LLC and MDCKII monolayer models, Luna-Tortos et al. (2008) found that PHT, LVT, LTG and PB were substrates of human Pgp, but CBZ was not (Luna-Tortos *et al.*, 2008a).

In the above experiments, different cell lines were used, but transport was always compared between Pgp overexpressing cells and their control cells. The MDCK and LLC cell lines were transfected with the MDR1 gene and the higher level of Pgp were expressed than in other cell lines. The LLC and MDCK cell lines have the lower endogenous MDR1 gene compared with other cell lines. Cell monolayer models are more laborious than uptake assays and should thus be employed judiciously. However, they provide the best information to support the Pgp substrate status for AEDs. A potential difficulty could occur when the parent cell lines of Pgp induced cell lines express a background level of Pgp, which can affect the assay. But this problem can be removed by comparing transport by the Pgp overexpressing cell lines with transport by the wild type cell lines.

The cell lines used above are limited in their ability to reproduce the drug-resistance mechanisms of the BBB. To partially overcome this limitation, primary brain microvascular endothelial cells isolated from brain tissue have been used. Using co-cultures of brain capillary endothelial and glial cells, Dehouck et al. (1990) developed an easy and reproducible method to study the BBB *in vitro* (Dehouck *et al.*, 1990). In the rat microvascular endothelial cell (rBMEC) model, the transport of PB was significantly greater in the basal to apical direction than in the apical to basal direction, and CsA inhibited Pgp efflux (Yang *et al.*, 2008). In porcine brain capillary endothelial cells (pBCECs), CBZ significantly increased the intracellular calcein concentration (Weiss *et al.*, 2003b). Using human microvascular endothelial cells (HBMECs), researchers found that the permeability of PHT was 10-fold less in BBB models developed by cells isolated from drug-resistant epileptic patients than normal cells (Cucullo *et al.*, 2007).

Table 1.3 AEDs as substrates of Pgp in cell lines

Drug	Evidence for AEDs as substrates of Pgp in specific cell lines (Y/N)							References
	Caco-2	MDCK	LLC	BMEC	BREC	Daoy/ daoyar2	OS2.4/ Doxo	
Carbamzaepine	N	N	N	--	N	--	N	(Baltes et al., 2007b; Crowe et al., 2006; Mahar Doan et al., 2002; Maines et al., 2005; Owen et al., 2001; Weiss et al., 2003b; West et al., 2007)
Ethosuximide	N	--	--	--	--	--	--	(Crowe et al., 2006)
Phenytoin	N	Y	Y	Y	N	Y	N	(Baltes et al., 2007b; Crowe et al., 2006; Cucullo et al., 2007; Luna-Tortos et al., 2008b; Maines et al., 2005; Schinkel et al., 1996; Tishler et al., 1995; Weiss et al., 2003b; West et al., 2007)
Phenobarbital	N	--	Y	Y	--	--	Y	(Luna-Tortos et al., 2008b; Weiss et al., 2003b; West et al., 2007; Yang et al., 2008)
Sodium valproate	--	N	Y	--	--	--	--	(Baltes et al., 2007a; Weiss et al., 2003b)
Acetazolamide	Y	--	--	--	--	--	--	(Crowe et al., 2006)
Topiramate	N	--	N	--	--	--	N	(Crowe et al., 2006; Weiss et al., 2003b; West et al., 2007)
Levetiracetam	--	N	Y	--	--	--	Y	(Baltes et al., 2007b; Luna-Tortos et al., 2008b; West et al., 2007)
Vigabatrin	N	--	--	--	--	--	--	(Crowe et al., 2006)
Lamotrigine	N	--	Y	--	--	--	Y	(Crowe et al., 2006; Luna-Tortos et al., 2008b; Weiss et al., 2003b; West et al., 2007)
Gabapentin	N	--	N	--	--	--	Y	(Crowe et al., 2006; Weiss et al., 2003b; West et al., 2007)
Felbamate	--	--	--	--	--	--	N	(West et al., 2007)
Zonisamide	--	--	--	--	--	--	N	(West et al., 2007)

Y/N: Yes/No; --: Not available.
BREC: bovine retinal endothelial cells
rBMEC: rat brain microvessel endothelial cells

1.4.2 *In vivo* animal models

In vitro evaluations are usually followed by *in vivo* evaluations. *In vivo* experiments have more relation to the potential drug substrate status. And the *in vivo* results can be estimated from *in vitro* experiments. Potschka et al. (2001) used a microdialysis method to test drug concentrations in the extracellular fluid (ECF) of the cerebral cortex in rat brains. They found that the Pgp inhibitors, sodium cyanide, verapamil, and PSC 833, can increase the ECF concentration of PHT, indicating that Pgp is involved in the BBB efflux of PHT to the plasma (Potschka *et al.*, 2001b). Then the AEDs, PB, LTG, and FBM, were studied in the same model; all were increased in the ECF by verapamil (Potschka *et al.*, 2002). The concentration of CBZ in the ECF was also enhanced by verapamil and probenecid, the inhibitors of Pgp and MRP respectively, indicating that Pgp and MRP are involved in the regulation of brain concentrations of CBZ (Potschka *et al.*, 2001a). But *mdr1a/b(-/-)* and wild-type mice did not exhibit significantly different concentrations of CBZ in brain after administration (Owen *et al.*, 2001). The ECF concentration of LVT was not regulated by verapamil and probenecid (Potschka *et al.*, 2004a). This may explain good efficacy of LVT in AED-refractory epilepsy.

The above results in animal models implicate Pgp in the BBB as playing an important role in the efflux of AEDs from the brain. However, the animals were normal and thus do not represent the pathological conditions of epilepsy, especially refractory epilepsy. Animal epileptic models have the advantage of mimicking the pathological condition of epilepsy patients, and we can evaluate the association between the levels of Pgp and AEDs in brains. Brandt et al. (2006) used the TLE rat model to test the effect of Pgp inhibitor on the distribution of AEDs in brain. In PB-resistant rats, Pgp was overexpressed in the hippocampus and other limbic brain regions compared with PB-responsive rats (Volk *et al.*, 2005b). They found that the anticonvulsant activity of PB was restored by the Pgp inhibitor tarquidar (TQD). Thus, a Pgp inhibitor may counteract resistance to an AED in refractory epilepsy (Brandt *et al.*, 2006). In brains of electrically induced epileptic rats, refractory rats had more Pgp and lower PHT concentration than did responsive rats. TQD increased the PHT concentration and efficacy in refractory rats

(van Vliet *et al.*, 2006). Furthermore, the pharmacokinetic profile of PHT was tested in brain and liver. The PHT concentration decreased 20-30% in the brain regions with Pgp overexpression, and the decrease was ameliorated by TQD. TQD increased PHT level in brain regions without Pgp overexpression. But the brain concentration of PHT was not affected by the overexpression of Pgp in the liver, indicating that Pgp only plays an efflux role in the BBB (van Vliet *et al.*, 2007).

The Pgp knockout mice *mdr1a$^{-/-}$* and *mdr1a/1b(-/-)* were also used to analyze the substrate status of AEDs. In *mdr1a$^{-/-}$* mice, Schinkel et al. did not find a significant difference of [^{14}C]-PHT level in brain compared with wild type mice, which was inconsistent with *in vitro* data (Schinkel, 1997; Schinkel *et al.*, 1996; Sisodiya *et al.*, 1999; Sugawara *et al.*, 1988). Sills et al. measured the tissue distribution of eight drugs (PHT, PB, CBZ,VPA, LTG, VBG, GBP, and TPM) in *mdr1a$^{-/-}$* mice and found that the brain/serum concentration ratios of CBZ, TPM, LTG, and GBP were higher in the knockout mice than the wildtype mice, indicating that these four drugs may be substrates of Pgp (Sills *et al.*, 2002). However, administration of CBZ did not result in significantly different concentrations in brains of *mdr1a/b(-/-)* mice compared with wild type mice (Owen *et al.*, 2001). The results from knockout mice can be compared with those from Pgp transfected cells (LLC-MDR1 and MDCK-MDR1). Other transporters and enzymes may influence the pharmacological results, and the confusing results need more investigation to explain. *Mdr1a*-deficient CF-1 mice were also used for detection of compounds that entered the CNS compartment (Tang-Wai *et al.*, 1995; Yamazaki *et al.*, 2001). These mice provide another model to evaluate the Pgp substrate status of AEDs.

1.4.3 In epilspsy patients

Some researchers analyzed the AED distributions in the brains of epilepsy patients to test whether AED concentrations were decreased by the regional overexpression of Pgp. The ECF concentrations of several AEDs, such as CBZ, oxcarbazepine (OXC), LTG and LVT, were significantly lower than their CSF concentrations in patients with intractable epilepsy (Rambeck *et al.*, 2006). But it is not possible to judge whether these findings

relate to overexpression of multidrug transporters in the brain because data from non-epileptic tissues were not included. 10,11-dihydro-10-hydroxy-5H-dibenzo(b,f)azepine-5-carboxamide (10-OHCBZ) is one of the main metabolites of OXC. The 10-OHCBZ brain-plasma concentration ratio and the mRNA level of *MDR1* in brain are inversely linearly correlated in epilepsy patients (Marchi *et al.*, 2005). The distribution of [^{11}C]-verapamil was tested in epileptogenic and nonepileptogenic brain regions of patients with drug resistant unilateral TLE by using PET. But there was no significant difference between epileptogenic and nonepileptogenic regions (Langer *et al.*, 2007). PET has been used successfully in measurement of drug concentrations in the CNS (Takano *et al.*, 2006). PET may be widely used in the future to directly analyze the function of Pgp in transport of AEDs in humans. Nuclear magnetic resonance (NMR) could also be used as a tool to measure drug concentrations in humans. ^{11}C, ^{31}P, or ^{19}F radiolabeled drugs can be detected, and this method is suitable for head measurements (Aszalos, 2007). Although human studies have some disadvantages, including multiple transporters at many organs, the difficulty of getting suitable controls, and other unexpected influences, they are the most direct method to test the Pgp substrate status of AEDs in relation to pathology.

1.4.4 The substrate status of AEDs

The preponderance of the above evidence indicates that several AEDs are likely substrates of Pgp, while several are likely not (Table 1.3). However, the evidence is often inconsistent among the different models used, and the cell culture models do not fully represent the reality *in vivo*. In order to define the Pgp substrate status of AEDs, we need to consider the reliability of the evidence. Since *in vitro* cell models and *in vivo* animal models each have advantages—of simplicity and of mimicking pathological and physiological conditions, respectively—we give them the same weighting as evidence of substrate status. *In vitro*, different cell lines and detection methods have different reliability: transwell experiments > uptake of AEDs > influence of Pgp substrate markers by AEDs. Clinical evidence has the advantage that the samples are patients, not just models, but suffers from the disadvantages of lacking suitable controls and of lacking a

method to test Pgp transporter function in isolation from the function of other transporters. Therefore, we give clinical data less weight than cell and animal models.

We combined the evidence from humans, animal models (*in vivo*) and cell models (*in vitro*) to conclude whether each AED acts as a substrate for Pgp (Table 1.4). LTG, PB, and PHT are likely substrates of Pgp since they exhibited consistent results with both *in vivo* and *in vitro* experiments. LVT, AZD and OXC are probable substrates of Pgp. LVT was found to be a substrate in humans and cell models, but not in an animal model. Evidence for OXC as a substrate was found in humans, but there is no report in animal and cell models. AZD was found to be a substrate for Pgp in a cellular model (Crowe *et al.*, 2006). CBZ and FBM are possible substrates of Pgp because the *in vivo* evidence is positive although *in vitro* evidence is negative. Human data indicated that CBZ is a substrate, but rat models and most of the cellular evidence indicated that CBZ is not a substrate. Rat models supported FBM as a substrate, but cell models did not. TPM, EMS, VGB and ZNS are somewhat unlikely to be substrates of Pgp because all available evidence was negative; however, for some drugs, only one report has been published, thus the possibility remains that future studies may provide contradictory data. Pgp is not the only transporter involved in AED efflux. The multidrug resistance transporters (MRPs), such as MRP1 and MRP2, are also involved in the efflux of AEDs (Hoffmann *et al.*, 2007; Kwan *et al.*, 2005; Loscher *et al.*, 2005; Luna-Tortos *et al.*, 2008b). Thus, more studies are needed to determine which AEDs are substrates for Pgp and whether they also act as substrates of other transporters.

Table 1.4 AEDs as substrates of Pgp in research models

Drug	Evidence for AEDs as substrates of Pgp in categories of research models (Y/N)			References
	Patients	Animals	Cell lines	
Carbamzaepine	Y	?	N	(Baltes et al., 2007b; Crowe et al., 2006; Mahar Doan et al., 2002; Maines et al., 2005; Owen et al., 2001; Potschka et al., 2001a; Rambeck et al., 2006; Weiss et al., 2003b; West et al., 2007)
Ethosuximide	--	--	N	(Crowe et al., 2006)
Phenytoin	--	Y	Y	(Baltes et al., 2007b; Crowe et al., 2006; Cucullo et al., 2007; Luna-Tortos et al., 2008b; Maines et al., 2005; Schinkel et al., 1996; Tishler et al., 1995; Weiss et al., 2003b; West et al., 2007)
Phenobarbital	--	Y	Y	(Luna-Tortos et al., 2008b; Potschka et al., 2002; Weiss et al., 2003b; West et al., 2007; Yang et al., 2008)
Sodium valproate	--	--	?	(Baltes et al., 2007a; Weiss et al., 2003b)
Acetazolamide	--	--	Y	(Crowe et al., 2006)
Topiramate	--	--	N	(Crowe et al., 2006; Weiss et al., 2003b; West et al., 2007)
Levetiracetam	Y	N	Y	(Baltes et al., 2007b; Luna-Tortos et al., 2008b; Potschka et al., 2004a; Rambeck et al., 2006; West et al., 2007)
Vigabatrin	--	--	N	(Crowe et al., 2006)
Lamotrigine	Y	Y	Y	(Crowe et al., 2006; Luna-Tortos et al., 2008b; Potschka et al., 2002; Rambeck et al., 2006; Weiss et al., 2003b; West et al., 2007)
Gabapentin	--	--	?	(Crowe et al., 2006; Weiss et al., 2003b; West et al., 2007)
Felbamate	--	Y	N	(Potschka et al., 2002; West et al., 2007)
Zonisamide	--	--	N	(West et al., 2007)
Oxcarbazepine	Y	--	--	(Rambeck et al., 2006)

Y: Yes; N: No; --: Not available.?: Conflicting evidence.

25

1.5   Structure-activity relationship (SAR) between Pgp and AEDs

The goal of studying the structure-activity relationship (SAR) is to find a means of predicting the substrates of Pgp. In order to find the common set of structural and functional features required by the interaction between Pgp and its substrates, some attempts were made and many approaches have been used to achieve this goal. However, SAR for Pgp is complicated, and only a few published papers exist. There are limited reports on the SAR between the substrate action of Pgp and AEDs. This section will collate the current reports on the SAR of compounds as substrates for Pgp and attempt to analyze the SAR of AEDs required to act as the substrate for Pgp. With the common structural features required of substrates for Pgp, we analyzed the structures of AEDs using multiple models.

There are several models to predict Pgp substrates. Hundreds of compounds which have been tested as substrates of Pgp were analyzed using different models to find the potential common structures required as the substrates for Pgp. Most models give the same minimal requirements of molecules to act as the substrates of Pgp: one or two hydrophobic centers, including an aromatic ring, electron donor groups (>C=O, -OH, >N-), and/or H-bond donor (-OH, >N-, =NH, -NH-) (Raub, 2006). Seelig indicated that the carbonyl groups are the most efficient electron donor group, followed by alkoxy and tertiary amino groups. Most of the aromatic rings are phenyl groups (Seelig, 1998). The more H-bond donors and acceptors the compound contains, the more likely it acts as a substrate for Pgp. AEDs meeting these requirements include PHT, PB, CBZ, OXC, primidone (PRM), FBM, ZNS, LTG, and flunarzine (FNR) (Table 1.5). Evidence indicates that PHT, PB, and LTG are Pgp substrates (Table 1.4). TPM, VGB, and ESM, which do not meet the minimal requirements, were not found to act as Pgp substrates (Table 1.4). However, FBM, ZNS, and CBZ, which meet the requirements, were not found to be substrates of Pgp (Table 1.4). Meanwhile some AEDs, including AZD, TPM, VPA, LVT, and GBP, which could not meet the minimal requirements, acted as substrates for Pgp in *in vitro* experiments. Some of the predicted results and experimental results are inconsistent because the molecular models are still not accurate, and the

different models may give contradictory results, while the experimental evidence also used different models.

The minimal requirements of H-bond donors and accepters were not sufficient to identify the Pgp substrate status of compounds. Seelig analyzed the spatial relationship between the electron donor groups in substrates. There are two types of electron donor patterns in the substrate molecules: type I and type II. The type I unit contains two electron donors, and the distance between them is 2.5 ± 0.3 Å. The type II unit contains two or three electron donors, and the distance between the two outer groups is 4.6 ± 0.6 Å (Fig 1.3). Compounds containing at least one type I or type II unit could be predicted as substrates for Pgp (Seelig, 1998; Ueda *et al.*, 1997). The more type I and type II units, the stronger the substrate. PHT, PB, PRM, LTG, ESL, and LCM,satisfying the minimal requirements of H-bond donors, also contain at least one type I or type II unit (Table 1.5). PHT, PB, and LTG were tested and shown to be Pgp substrates (Table 1.4). AZD, TPM, and LVT contain type I units and act as Pgp substrates, although they do not satisfy the minimal requirements of being H-bond donors. OXC, CBZ-E, and S-LC do not contain any type I and type II units, although they do satisfy the minimal requirements of being H-bond donors. Only OXC was tested as a substrate for Pgp. GBP and VPA are in the opposite situation in that they do have type I or type II units but do not meet the minimal requirements of H-bind donors. They are Pgp substrates. By contrast, ZNS and CBZ are not substrates of Pgp although they satisfy the minimal requirements of being H-bond donors and not containing any type I or type II units.

A molecular scaffold was analyzed to determine the activity of chemicals acting as substrates of Pgp (Raub, 2006). Over 100 analogues were tested on MDCK-MDR1 cell monolayers by bidirectional transport assays to determine whether the scaffold increased or decreased Pgp transport efficiency. The scaffolds affecting Pgp transport efficiency is listed (Fig 1.4). AZD, TPM, and ZNS contain the Pgp transport enhancing scaffold, which may explain, in addition to its pattern of electron donors, why AZD and TPM act as Pgp substrates. Pgp pump efficiency is also affected by passive diffusion. An increase of passive diffusion can decrease pump efficiency (Raub, 2006).

The following groups appear in Pgp substrates from most to least frequently: $>C=O$, $-O-$, $-NR2$, $-NRH$, $-OH$, $-N=$, R-halide, $-S-$, $-NH2$, $>(Phe)2$. Among them, an ester group formed by alkoxy groups combined with a carbonyl group or a carboxy group is seen most often in functional units (Seelig, 1998). Among the currently available AEDs, PRM, PGB, TGB, and FNR have not been measured *in vitro* and *in vivo*. Considering the above elements required by substrates for P-gp, we predicted their P-gp substrate status. PRM and LCM contain aromatic rings and type I electron donor patterns, and may thus act as substrates for P-gp. FNR does not contain type I or type II electron donor patterns. The big LogP of FNR causes high passive diffusion, which may decrease the possibility for FNR to act as a substrate. There have been few published reports on the substrate status of ZNS, VGB, or AZD. We need further research to determine their substrate status and gain more information on the SAR of Pgp. More specific experimental assays and predictive approaches will be helpful in understanding SAR. Future success in predicting Pgp substrates and the SAR of AEDs will provide a more efficient, molecular approach for the design of new AEDs.

2.5±0.3Å	4.6±0.6Å
Type I	Type II
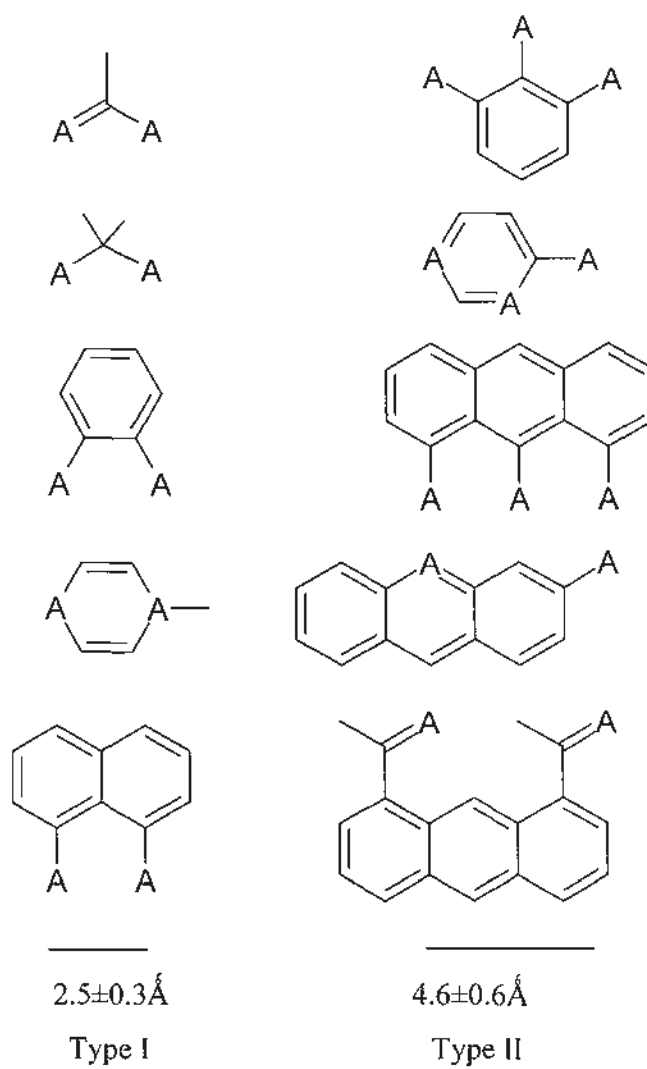
Fig 1.3   Type I and TypeII patterns of electron donors recognized by Pgp.
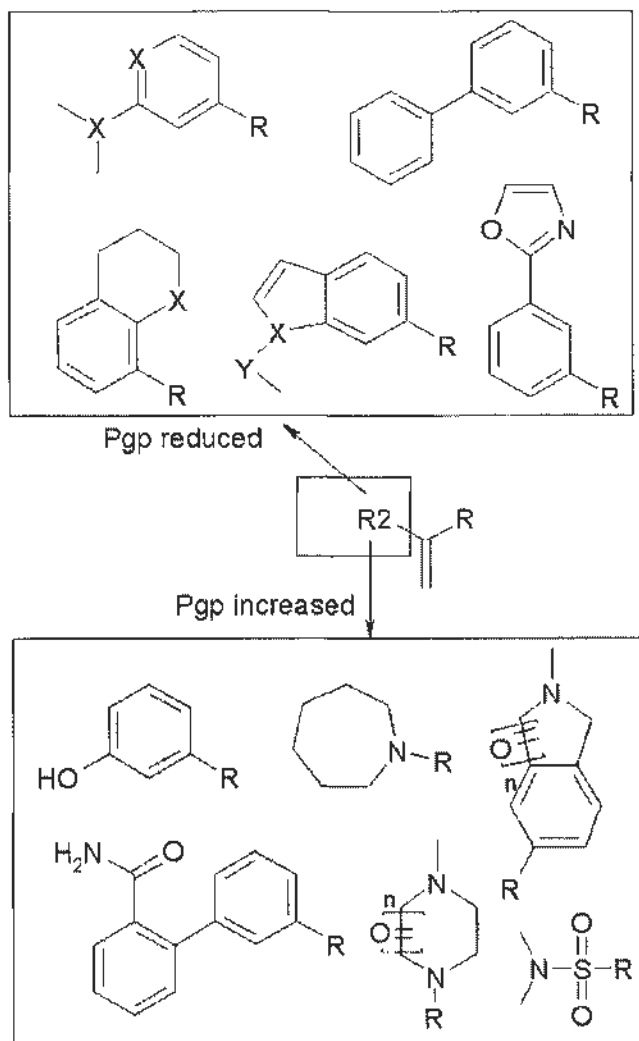
Fig 1.4   Scaffold affecting Pgp pumping efficiency.

Table 1.5 Structures and electron donor groups in AEDs.

Compound	Structure	Aromatic rings	H-bond donors (>N-, -OH, =NH, -NH-)	H-bond acceptors (>N-, -OH, =O)	Type I	Type II	Literature report as Pgp substrate/Model used
Phenytoin		2	2 –NH-	2 =O	1	--	Y: MDCK, LLC, BMEC, Daoy/daoyar2. N: Caco-2, BREC, OS2.4/Doxo
Primidone		1	2 –NH-	2 =O	2	--	N/A
Ethosuximide		0	1 –NH-	2 =O	2	--	N: Caco-2
Phenobarbital		1	2 –NH-	3 =O	1	1	Y: LLC, BMEC, OS2.4/Doxo N:Caco-2
Acetazolamide		0	1 –NH- 2 >N-	3 =O	1	--	Y: Caco-2
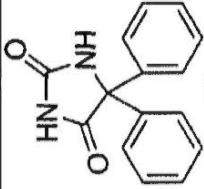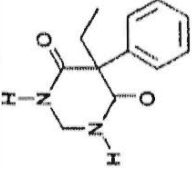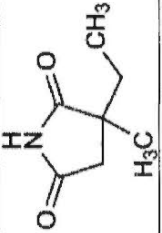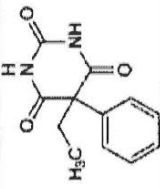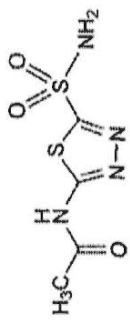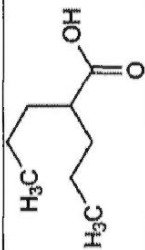
Valproic acid	0	0	1=O 1-OH	1	--	Y: LLC N: MDCK
Carbamazepine	2	1 >N-	1=O	--	--	N; Caco-2, MDCK, LLC, BREC, OS2.4/ Doxo
Oxcarbazepine	2	1 >N-	2=O	--	--	N/A
Felbamate	1	0	2=O	2	--	N: OS2.4/Doxo
Pregabalin	0	0	1=O 1-OH	1	--	N/A
Vigabatrin	0	0	1=O 1-OH	1	--	N: Caco-2
Tiagabine	0	1 >N-	1=O 1-OH 1 >N-	1	--	N/A
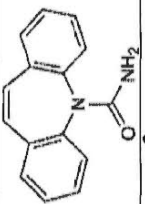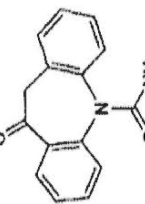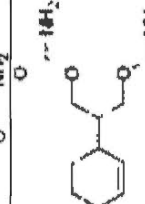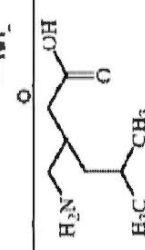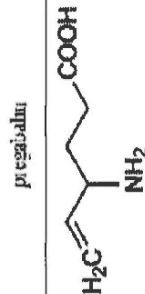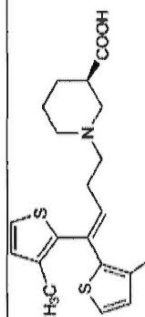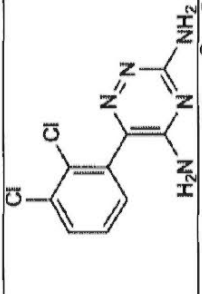
Lamotrigine		1	3 >N-	3 >N-	1	1	Y: LLC, OS2.4/Doxo N: Caco-2
Topiramate		0	0	2 =O	2	--	N: Caco-2, LLC, OS2.4/Doxo
Zonisamide		1	1 >N-	2 =O 1 >N-	--	--	N: OS2.4/Doxo
Levetiracetam		0	1 >N-	2 =O 1 >N-	1	--	Y: LLC, OS2.4/Doxo N: MDCK
Flunarizine		3	2 >N-	2 >N-	--	--	N/A
Gabapentin		0	0	1 =O 1 -OH	1	--	N: Caco-2, LLC Y: OS2.4/Doxo
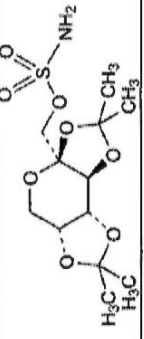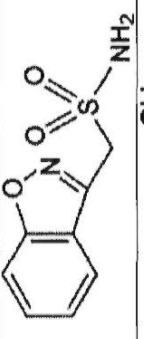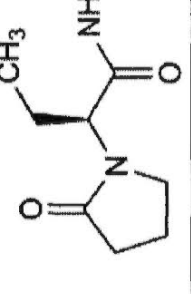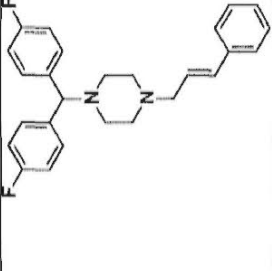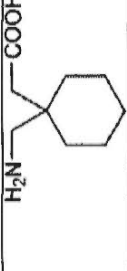
Compound	Structure						
Eslicarbazepine acetate		2	1 >N-	2=O	1	--	Y: LLC, MDCK
Lacosamide		1	2 –NH-	1=O	2	--	N/A
Carbamazepine 10,11-epoxide		1	1 >N-	1=O	--	--	Y: LLC, MDCK
S-licarbazepine		2	1 >N-	1=O 1-OH	--	--	Y: LLC, MDCK
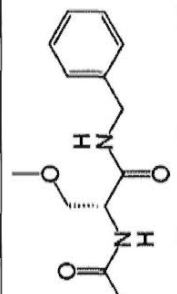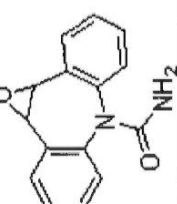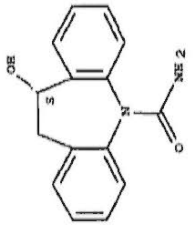
1.6   Single nucleotide polymorphisms affect the function of Pgp

Evidence indicates SNPs were associated with altered Pgp level and drug responsiveness (Eichelbaum *et al.*, 2004; Kwan *et al.*, 2009). SNPs at 62 sites have been reported in the human *MDR1* gene (Kerb *et al.*, 2001; Kim *et al.*, 2001; Kroetz *et al.*, 2003; Sakaeda *et al.*, 2003; Schwab *et al.*, 2003). Some of these variants may influence the expression or function of Pgp (Lepper *et al.*, 2005; Pauli-Magnus *et al.*, 2004). 1236C>T in exon 12, 2677G>T/A in exon 21 (resulting in an Ala893Ser/Thr amino acid change), and 3435C>T in exon 26 are exonic SNPs with high minor allele frequencies (Kim *et al.*, 2001) (Fig 1.5). Compared to the 3435C allele, the 3435T allele was associated with lower expression of *MDR1* in the duodenum of Caucasians (Hoffmeyer *et al.*, 2000), but other results contradicted that finding (Hung *et al.*, 2008; Kim *et al.*, 2001; Sakaeda *et al.*, 2001; Salama *et al.*, 2006). The 2677 T allele (or 893 Ser) resulted in an enhancement of efflux and a decrease in the intracellular accumulation of digoxin *in vitro* in several studies (Hung *et al.*, 2008; Kim *et al.*, 2001; Salama *et al.*, 2006), but no change in other reports (Kim *et al.*, 2001; Kimchi-Sarfaty *et al.*, 2002). A report indicated that neither 3435C>T nor 2677G>T, nor diplotypes (combinations of alleles at the two SNPs), associated with *MDR1* mRNA or Pgp protein expression levels in epileptogenic brain tissues (Mosyagin *et al.*, 2008). However, other studies found that diplotypes of SNPs at positions 2677 and 3435 may affect MDR1 activity *in vivo* (Kurata *et al.*, 2002; Tang *et al.*, 2002). Evidence suggested that haplotypes (combinations of alleles from multiple genotypes) may affect transport *in vitro* (Chowbay *et al.*, 2003; Hung *et al.*, 2008; Johne *et al.*, 2002; Kimchi-Sarfaty *et al.*, 2007; Salama *et al.*, 2006). Kimchi-Sarfaty et al. noted that the synonymous polymorphism 3435T allele, when combined with either the 2677T or 1236T alleles, or both, resulted in insensitivity to Pgp inhibitors. The 3435 SNP affects the rate of folding of the Pgp protein as it is translated, thus affecting the insertion of Pgp into the membrane, resulting in a change in the interaction site of substrate and inhibitor, and altering Pgp function (Kimchi-Sarfaty *et al.*, 2007).
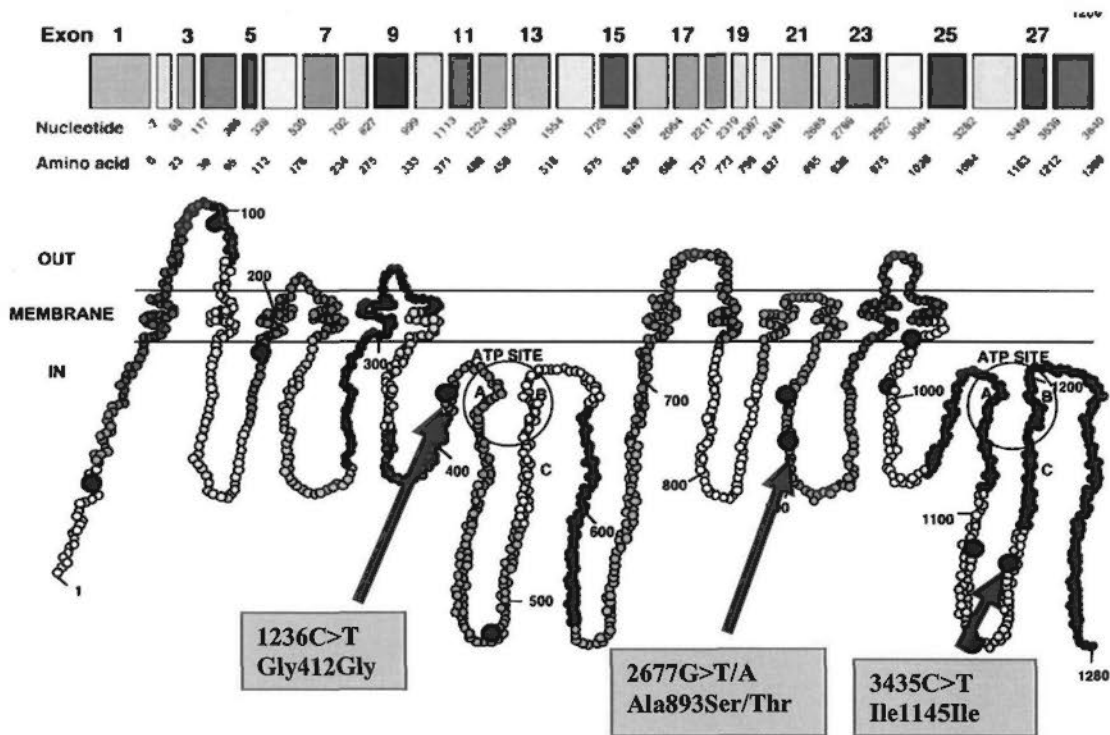
Fig 1.5   Illustration of MDR1 SNPs. 28 exons of MDR1 are shown as different colors at the top (modified from (Ambudkar et al., 2003)). The reported SNPs are shown as black-filed circles. The SNPs studied in our project are labeled by blue arrows.

Polymorphisms of *MDR1* have been associated with drug responsiveness (Basic *et al.*, 2008; Ebid *et al.*, 2007; Kwan *et al.*, 2007a; Siddiqui *et al.*, 2003). Siddiqui *et al.* first found that drug-resistant epilepsy patients were more likely than were drug-responsive patients to had the 3435 CC genotype (Siddiqui *et al.*, 2003). This result was confirmed in two other reports. The C allele at 3435 was more common in patients with drug-resistant epilepsy, compared with either those with drug-responsive epilepsy or control subjects, in Croatia (Basic *et al.*, 2008) and Egypt (Ebid *et al.*, 2007). On the other hand, Kwan et al. used more than 700 Han Chinese epilepsy patients and got the opposite result: a decreased frequency of CC in drug-resistant patients (Kwan *et al.*, 2007a). In Japanese, Seo et al. also found a decreased frequency of the C allele in drug-resistant patients (Seo *et al.*, 2006). The latter study also tested the 1236C>T and 2677G>T/A polymorphisms. The 2677 TT genotype was more common in drug-resistant patients. Among haplotypes of 1236C>T, 2677G>T/A, and 3435C>T SNPs, drug-resistant patients were more likely

36

to have the T-T-T haplotype and less likely to have the C-G-C haplotype (Seo *et al.*, 2006). In a gene-wide tagging study, 2677G/T/A genotypes significantly associated with drug resistance (Kwan *et al.*, 2009). In a study of international pharmacogenetic cohorts, 3435C>T did not associate with rate of recurrence of unprovoked seizures, and it did not play a major role in determining the efficacy of seizure control with initial treatment by AEDs (Szoeke *et al.*, 2009). 3435C>T also did not associate with drug resistance or carbamazepine plasma level/dose index (Ozgon *et al.*, 2008). Some studies in India reported that there was no significant difference in genotype and allele frequencies between drug responsive and drug resistant epilepsy patients at 1236C>T, 2677G>T/A, and 3435C>T (Lakhan *et al.*, 2009; Vahab *et al.*, 2009). Ethnicity, and associated differences in linkage disequilibrium among SNPs, may be one of the reasons for the discrepant results between Asians and Caucasians (Szoeke *et al.*, 2009).

In cells, there was no difference in Pgp surface expression between 3435T and 3435C alleles (Kimchi-Sarfaty *et al.*, 2007; Salama *et al.*, 2006). Haplotypes of 1236C>T/2677G>T/3435C>T altered the intracellular accumulation of calcein-AM and BODIPY-FL-paclitaxel in a substrate-dependent manner (Gow *et al.*, 2008). Wang *et al.* studied the three SNPs and found that 3435T may decrease the mRNA stability of *MDR1* and decrease the mRNA expression level in liver (Wang *et al.*, 2005).

1236C>T, 2677G>T/A, and 3435C>T significantly minimized Pgp function by decreasing the cell uptake of Rho123 compared with wild type MDR1 in LLC-PK1 cells (Salama *et al.*, 2006). 1236C>T and 3435C>T were associated with a decrease of Pgp expression and increase of Pgp transport activity in placenta (Hemauer *et al.*, 2010). But in another study, 2677G>T/A and 3435C>T did not affect the transport of verapamil, digoxin, vinblastine, or cyclosporine A by Pgp (Morita *et al.*, 2003).

Hung et al. used a cultured cell method to study whether the above polymorphisms affect the efflux of AEDs by Pgp. They found that the 1236T-3435T and 1236T-2677A/T-3435T haplotypes resulted in less effective inhibition of AEDs against substrates of Pgp and caused lower intracellular concentration of substrates when adding AEDs (Hung *et*

al., 2008). The data suggested that polymorphisms of MDR1 influence the interaction between AEDs and Pgp. All the published studies to determine the influence of SNPs in *MDR1* used cell uptake models, and there is no direct evidence showing that the polymorphisms affect the directional transport of AEDs by Pgp. Therefore, we propose to use monolayers of cells transfected with *MDR1* variants to investigate their effects on AED transport.

1.7   Proposed objectives to determine substrate status of AEDs and functional evaluation of human *MDR1* polymorphisms on their transport activities

The data collected so far generally support some AEDs as substrates for Pgp, but the evidence is mixed or missing for several AEDs. Thus, the status of AEDs as substrates for Pgp needs further study before firm conclusions can be drawn.

Polymorphisms of *MDR1* have been associated with drug responsiveness (Basic *et al.*, 2008; Ebid *et al.*, 2007; Kwan *et al.*, 2007a; Siddiqui *et al.*, 2003), and the *in vitro* data suggest that polymorphisms of *MDR1* influence the interaction between AEDs and Pgp. However, there is no direct evidence showing that the polymorphisms affect the directional transport of AEDs by Pgp. Therefore, we propose to use monolayers of cells transfected with the *MDR1* variants to investigate their effects on AED transport.

1.7.1 The aims of the proposed study:

A. To determine whether anti-epileptic drugs (AEDs) are substrates for the drug efflux transporter P-glycoprotein (Pgp).

B.   To investigate the effect of *ABCB1* (MDR1, Pgp) polymorphisms (1236C>T, 2677G>T/A, and 3435C>T) on AED transport.

1.7.2 Strategies to achieve our aims:

A. MDCKII and LLC-PK1 cell lines transfected with *MDR1* and grown in monolayers to study the transport of AEDs by Pgp *in vitro*.

B. *MDR1* mutated at 1236C>T, 2677G>T/A, and 3435C>T, then transfected into LLC-PK1 cells to study the effect of polymorphisms on the transport of AEDs by Pgp *in vitro*.

1.7.3 Choice of the studied drugs

The antiepileptic drugs were chosen by literature research based on the following criteria: first, the drugs are used widely in the clinic; second, the drugs are easily analyzed by HPLC/UV or LC-MS/MS methods; third, the literature on the substrate status of drugs is inconsistent or absent.

1.7.4 Significance of the study

The data obtained from the experiments will give direct evidence as to whether (and, if so, which) AEDs are substrates of human Pgp. This information may explain why some patients are refractory to AEDs, given the overexpression of Pgp in the drug-resistant epilepsy brain.

The frequencies of polymorphic alleles of *MDR1* in drug-resistant epilepsy patients may significantly differ from those in drug-responsive patients. The effects of *MDR1* polymorphisms on AED transport may provide a molecular explanation of the association between the polymorphisms and pharmacoresistance. This knowledge may help guide the design of genetic-based individualized therapy of epilepsy, and may lead to development of drugs to help treat the large number of patients who are refractory to all currently available AEDs.

1.8 Study scheme

The scheme of this study is illustrated in Fig 1.6:

```
                    ┌──────────────────────────────────────┐
                    │   Literature research to identify the │
                    │   antiepileptic drugs used in this project │
                    └──────────────────────────────────────┘
                                    │
                                    ▼
┌─────────────────┐      ┌─────────────────┐      ┌─────────────────┐      ┌─────────────────────────┐
│ Drug assay      │      │   Validation    │      │ Establishment of│      │ • Sequencing            │
│ development and  │ ◄──  │   of methods    │ ◄──  │  MDR1 variant   │ ──►  │ • Transfection          │
│ validation      │      │                 │      │   cell lines    │      │ • Real time PCR         │
│  • HPLC/UV      │      └─────────────────┘      └─────────────────┘      │ • Western blotting      │
│  • LC-          │               │                                         │ • Immunostaining        │
│    MS/MS        │               ▼                                         └─────────────────────────┘
└─────────────────┘      ┌─────────────────────────┐
                         │ Cell monolayer validation│
                         │  • TEER                 │
                         │  • Papp value           │
                         │  • Real time PCR        │
                         │  • Immunostaining       │
                         └─────────────────────────┘
```

- Drug assay development and validation
  - HPLC/UV
  - LC-MS/MS

Validation of methods

Establishment of *MDR1* variant cell lines

- Sequencing
- Transfection
- Real time PCR
- Western blotting
- Immunostaining

Cell monolayer validation

- TEER
- P_{app} value
- Real time PCR
- Immunostaining

Identify P-gp substrates

Measurement of the function of the *ABCB1* variants

- Bi-directional transport assay
- Concentration equilibrium transport assay
- Rho123 uptake assay

- Western blotting
- Real time PCR
- Immunostaining
- Concentration equilibrium transport assay

Fig 1.6 Proposed study scheme of this project

Solid boxes demonstrate objectives of this study. **Dotted boxes** demonstrate methods used in this study.

Chapter Two

Development of assay methods for determination of antiepileptic drugs and their metabolites

2.1   Introduction

It has been more than 100 years since the first chemical antiepileptic drug (potassium bromide) was found. First generation AEDs include phenobarbital (1918), phenytoin (1938), primidone (1952), ethosuximide (1960), carbamazepine (1963), valproic acid (1974), and vigabatrin (1989). Most of those were discovered by chance. Second generation AEDs were found for clinical use after 1992. They are felbamate, gabapentin, lamotrigine, topiramate, tigabine, oxcarbazepine, levetiracetam, pregabalin, zonisamide, lacosamide, and rufinamide (Aiken *et al.*, 2000; Chollet, 2002). There are some new drugs under development by pharmaceutical companies. The pharmacological mechanism differs among drugs. Altering ion channel activity is one important mechanism.

The quantification of AEDs and their metabolites in tissues and body fluids is important for investigations in different areas. Many papers describing the determination of specific antiepileptic drugs have been published. The AED quantification methods generally used were high-performance liquid chromatography with UV detector (HPLC/UV), GC-MS, and LC-MS/MS. We summarize below the suitable methods for determination of AEDs in our project.

Phenobarbital (PB)

The most common method for analysis of PB has been HPLC, which is rapid, effective, and inexpensive. HPLC/UV methods were published for measuring the concentration of PB in plasma or serum (Chollet, 2002). Some simultaneous determination methods of PB, other AEDs, and their metabolites were reported (Soldin *et al.*, 1976). In other tissues, such as hair, GC-MS was also used to determine the amount of PB (Goulle et al., 1995).

41

Phenytoin (PHT)

Methods for analysis of PHT in body fluid have included GC, GC-MS, and HPLC (Chollet, 2002). HPLC was the most commonly used method to determine the PHT concentration in plasma, urine, and some tissues (Bhatti et al., 1998). A GC-MS method was also reported for the detection of isotope-labeled PHT for PK study of epilepsy patients (Nelson et al., 1998).

Ethosuximide (EMS)

The current methods for determining EMS are limited because it is neither a strong chromophore nor a fluorophore. HPLC, GC, and immunoassay were reported (Chen et al., 1999; Chollet, 2002). Derivatization was used in HPLC to increase the sensitivity of quantification (Chen et al., 1999). A simultaneous determination method was also used to detect EMS without derivatization (Soldin et al., 1976).

Carbamazepine (CBZ) and carbamazepine-10,11-epoxide (CBZ-E)

CBZ is widely used clinically for treatment of epilepsy. CBZ-E is the active metabolite of CBZ, and its concentration is about 1/3 of CBZ in human plasma. The methods for determination of CBZ and CBZ-E include HPLC, LC-MS/MS and a few GC methods (Chollet, 2002). The simultaneous determination of CBZ and CBZ-E was reported by using HPLC/UV or LC-MS/MS in biological fluids (Oh et al., 2006; Stolker et al., 2004). The HPLC methods have the advantage of being inexpensive and rapid, but with less sensitivity and specificity.

Oxcarbazepine (OXC) and monohydroxylate derivative (MHD)

OXC was rapidly metabolized to its monohydroxylate derivative (MHD) after oral absorption. The MHD, a stereoselective structure, contains two forms: ~80% (S)-licarbazepine and ~20% (R)-licarbazepine (May et al., 2003). (S)-licarbazepine is the major active metabolite. Because OXC is rapidly converted to the MHD by enzymes, the plasma concentration of OXC is very low. HPLC methods were established to determine only OXC in plasma. The steroselective determination of (S)-licarbazepine and (R)-

licarbazepine in plasma was reported by using enantioselective high-performance liquid chromatography (Flesch et al., 1992; Volosov et al., 1999). Some methods were based on GC-MS to analyze OXC and its metabolites (von Unruh *et al.*, 1986), but most methods were HPLC.

Eslicarbazepine acetate (ESL)

ESL is a new antiepileptic drug having a structure similar to that of OXC and CBZ. It is the prodrug of (S)-licarbazepine, which acts on voltage-gated sodium channels (VGSC). ESL and its metabolites were determined by HPLC-MS and HPLC/UV (Almeida et al., 2005; Hainzl et al., 2001). LC-MS/MS was used to distinguish eslicarbazepine and R-licarbazepine (McCormack *et al.*, 2009). In recent years, HPLC/UV with improved sensitivity was widely used to determine ESL and metabolites (Alves et al., 2007a; Alves et al., 2007b).

Zonisamide (ZNS)

GC and HPLC/UV methods were reported for the analysis of ZNS (Berry, 1990; Matsumoto *et al.*, 1983). HPLC with different types of columns was commonly used to measure the concentration of ZNS in plasma or other body fluids. The simultaneous determination of ZNS and other AEDs was also reported by HPLC-diode array detector (DAD) (Vermeij *et al.*, 2007). A conventional HPLC method was also suitable for analyzing ZNS.

Rufinamide (RFM)

RFM is a new antiepileptic drug. It can treat partial seizures and drop attacks associated with the Lennox-Gastaut syndrome. HPLC methods were reported for measuring the concentration of RFM and its metabolites in human plasma and other body fluids (Rouan *et al.*, 1995). The simultaneous determination of RFM and other AEDs was also described (Contin *et al.*, 2010; Perucca *et al.*, 2008).

Pregabalin (PGB)

PGB is a structural analogue of γ-aminobutyric acid (GABA). It is used for neuropathic pain and for partial seizures and was recently approved by the European Union. There are several published LC-MS/MS methods for determining PGB in plasma (Nirogi *et al.*, 2009). HPLC with the derivatization of PGB was also used to analyze PGB in body fluids. Few reports have been published to detect PGB by using HPLC/UV (Berry *et al.*, 2005).

Lacosamide (LCM)

LCM is a functionalized amino acid, which was approved in Europe in 2008. HPLC and LC-MS/MS methods to determine LCM in plasma were reported (Cawello *et al.*, 2010; Gidal *et al.*, 1999).

Because the experiments in our project were conducted *in vitro*, HPLC/UV and LC-MS/MS methods with rapid and inexpensive sample treatment were used.

2.2 Materials and methods

2.2.1 Drugs

PHT, CBZ, CBZ-E, ESL and ESM were supplied by Sigma Aldrich (St. Louis, MO, USA). PB was purchased from Universal Chemicals, Inc (South Kearny, New Jersey, USA). OXC was obtained from the National Institute for the Control of Pharmaceutical and Biological Products (Beijing, China). S-LC was purchased from Toronto Research Chemicals Inc. (North York, Ontario, Canada). ZSN, PGB, LCM, and RFM were supplied by 3B Pharmachem International Co., Ltd (Wuhan, China). Acetonitrile (Labscan Asia, Thailand), ethanol (TEDIA Company, Inc., USA), and methanol (TEDIA Company, Inc., USA) were HPLC grade. All other reagents were at least analytical grade. The water was deionized by a Millipore water purification system (Millipore, Milford, USA).

2.2.2 Instrumentation and chromatographic conditions

2.2.2.1 HPLC/UV assay for the quantification of AEDs

The HPLC/UV system consisted of a Waters 2695 Separations Module and Waters 996 Photodiode Array detector. All the AEDs except PGB were separated using a C18 BDS Hypersil column (250 mm × 4.6 mm; 5 μm particle size, Thermo) with a guard column (Delta-Pak C18 Guard-Pak, Waters). Data were analyzed by Waters Millennium software (version 3).

The mobile phase consisted of eluent A (acetonitrile) and eluent B (20 mM sodium dihydrogen phosphate buffer, pH=4.6) at a special ratio for each drug. The flow rate was 1 ml/min, and the temperature of the auto-sampler was set at 8°C. The components of the mobile phase and the detection wavelength were determined by the particular drug to be detected (Table 2.1).

2.2.2.2 LC-MS/MS assay for the quantification of AEDs

The LC-MS/MS system consisted of an Agilent 1200 Series and ABI 2000 Q-Trap triple quadrupole mass spectrometer equipped with an electrospray ionization source (ESI). PGB was separated using a C18 BDS Hypersil column (250 mm × 4.6 mm; 5 μm particle size, Thermo) with a guard column (Delta-Pak C18 Guard-Pak, Waters).

The mobile phase of LC consisted of 0.1% formic acid (A) and acetonitrile (B). The mobile phase during the time interval from sample injection to 5 min was discarded in order to keep salt from entering the ESI. The gradient began with 15% eluent B for 4 min, changed linearly to 50% B over 4.5 min, and remained for 13 min before changing back to 15% B over 0.5 min and equilibrating at 15% B for 1.5 min prior to the next injection. The flow rate was 1 ml/min, and the temperature of the auto-sampler was set at 8°C. The sample injection volume was 20 μl. 60% of the LC mobile phase was split off, and only 40% was introduced to the ESI.

The instrumental condition was: positive ionization mode; nitrogen as nebulizer gas, auxiliary gas, curtain gas at 30, 70, 30 and collision gas at 3 psi, respectively; ion spray voltage at 3000 V; interface heater temper at 100ºC and auxiliary gas temperature at 350ºC. Other parameters were optimized for each drug prior to analysis. Analysis was conducted at multiple reaction monitoring (MRM): 160/55 amu for PGB and 309/281 amu for alprazolam.

2.2.3 Preparation of AED solutions

The stock of PHT was dissolved in ethanol at 2 mg/ml. Other AED stock solutions were prepared at 5 mg/ml in DMSO. The working solution of each drug was prepared by diluting the stock solution of each AED to various concentrations in methanol and H_2O (50:50, V/V). The standard curve was prepared at concentrations of 10, 5, 2.5, 1.25, 0.625, 0.3125, and 0.15625 µg/ml. An internal standard was chosen for each AED (Table 2.1). Concentrations of 9, 3, and 1 µg/ml were chosen as the high, medium, and low QC. Drugs were prepared for testing by diluting stock solutions to various concentrations in phosphate buffered saline (PBS) with 0.40 mM Mg^{2+} and 0.45 mM Ca^{2+}.

2.2.4 Validation of the developed assay method

2.2.4.1 Sensitivity

The specificity of each AED was evaluated by checking the chromatogram. The limit of quantification (LOQ) was defined as: the lowest concentration of the drug which results in a signal to noise ratio of 10:1 with accuracy below 20% and precision below 20%. The limit of detection (LOD) was defined as: the lowest concentration of the drug which results in a signal to noise ratio of 3:1. (FDA, 2001)

2.2.4.2 Calibration curve

The calibration curve was plotted by the peak-area ratio of each AED to internal standard versus the concentration of each AED. The $1/x^2$ weighted linear regression (r^2) was calculated for each AED.

2.2.5.4 Precision and accuracy

The inter-day and intra-day precision of each AED was detected by analysis of 3 replicates of QC samples in one day and on 3 separate days. The precision of each drug was calculated by relative standard deviation (R.S.D.), and accuracy of each AED was calculated by relative error (R.E.).

2.2.5.5 Stability

The stability of samples in transport buffer was evaluated by incubating the drugs in PBS buffer at 37°C for different durations. The stability of samples was measured by putting the drugs in the HPLC/UV auto-sampler at room temperature for 24 hours.

2.3   Results and discussions

2.3.1 Chromatography

The HPLC/UV methods were constructed under the conditions listed in Table 2.1. HPLC chromatography of each antiepileptic drug is illustrated in Figure 2.1. The established HPLC/UV methods can clearly resolve the drug and internal standard (IS). The LC-MS/MS method for PGB was constructed under the condition described in the materials and methods. The chromatography of PGB and IS, which can be separated well, is shown in Figure 2.2. The methods were suitable for the analysis of AEDs in our projects.
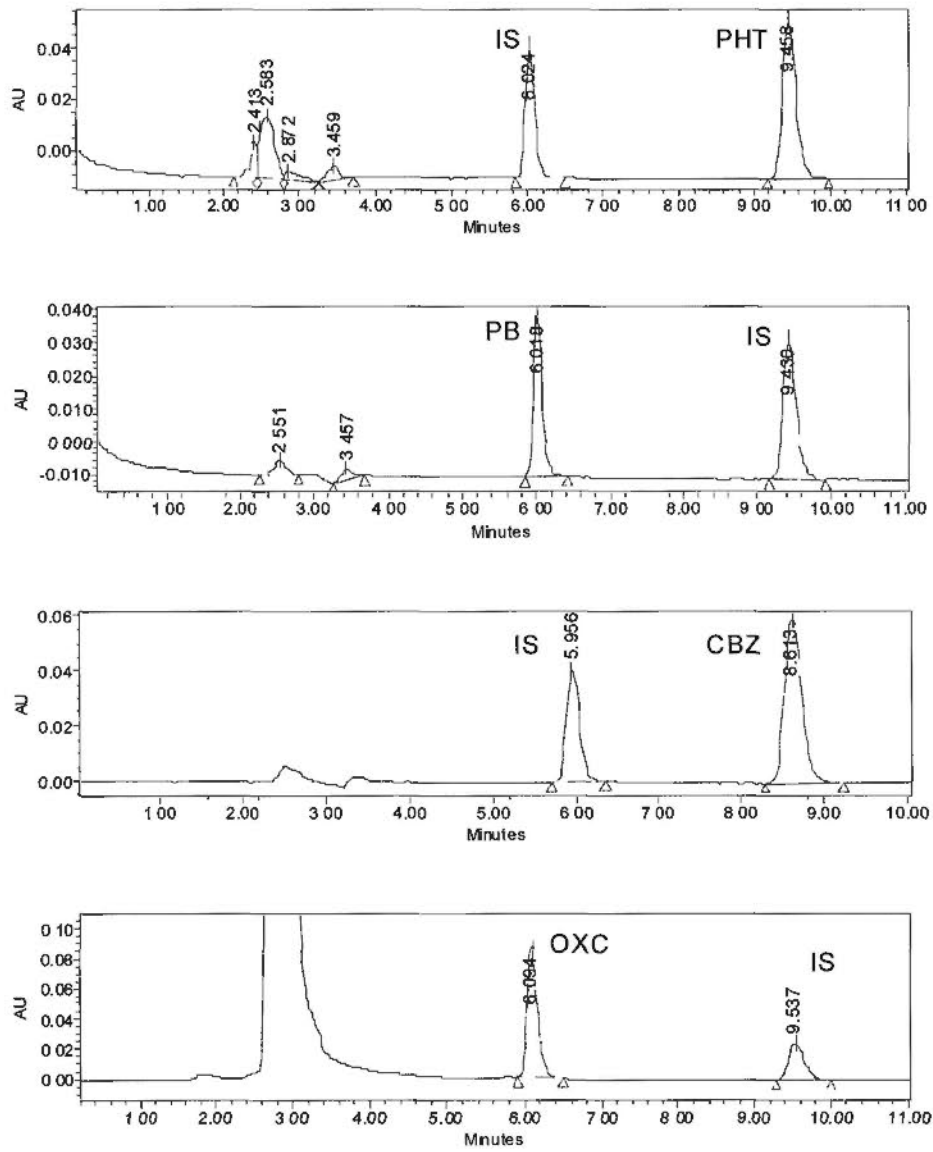
Fig 2.1a **HPLC chromatograms of standard solution at 2.5 µg/ml and IS at 1 µg/ml for PHT, PB, CBZ, and OXC.**
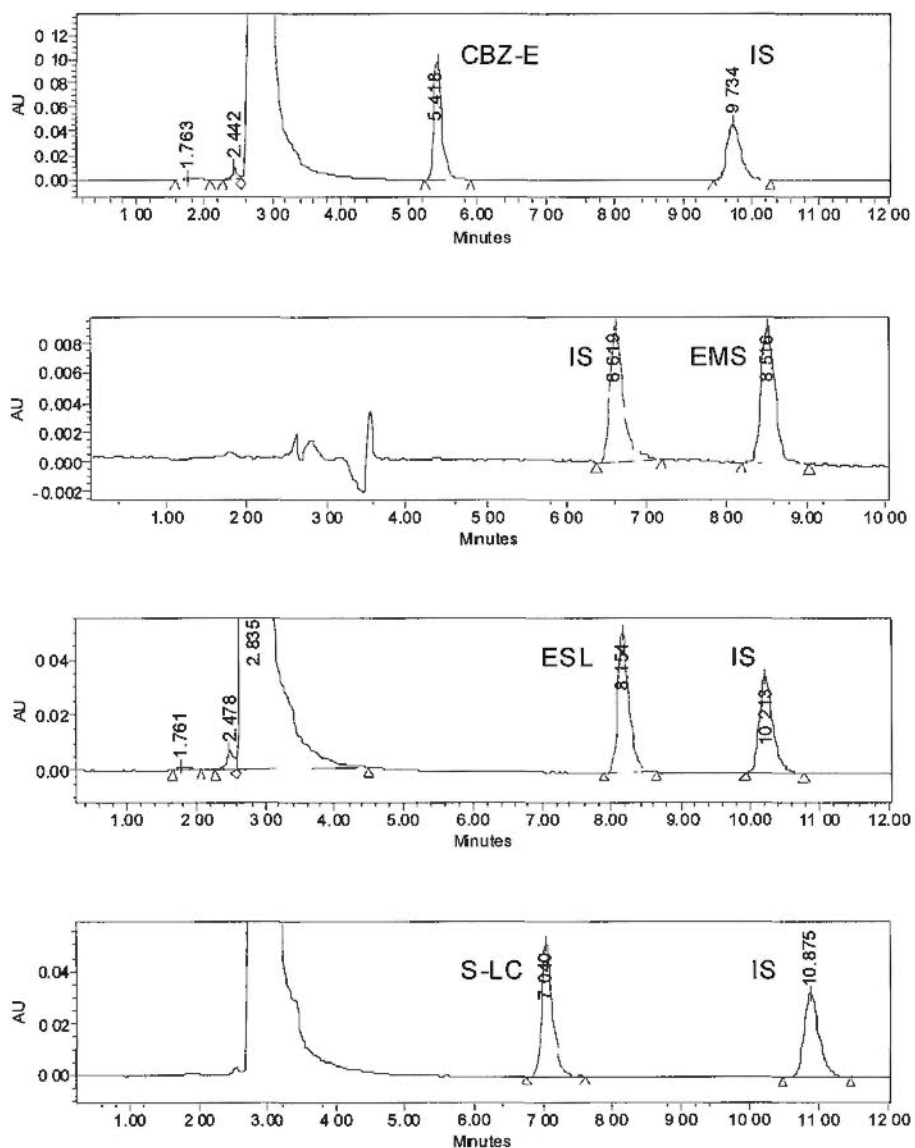
Fig 2.1b   HPLC chromatograms of standard solution at 2.5 µg/ml and IS at 1 µg/ml for CBZ-E, EMS, ESL, and S-LC.
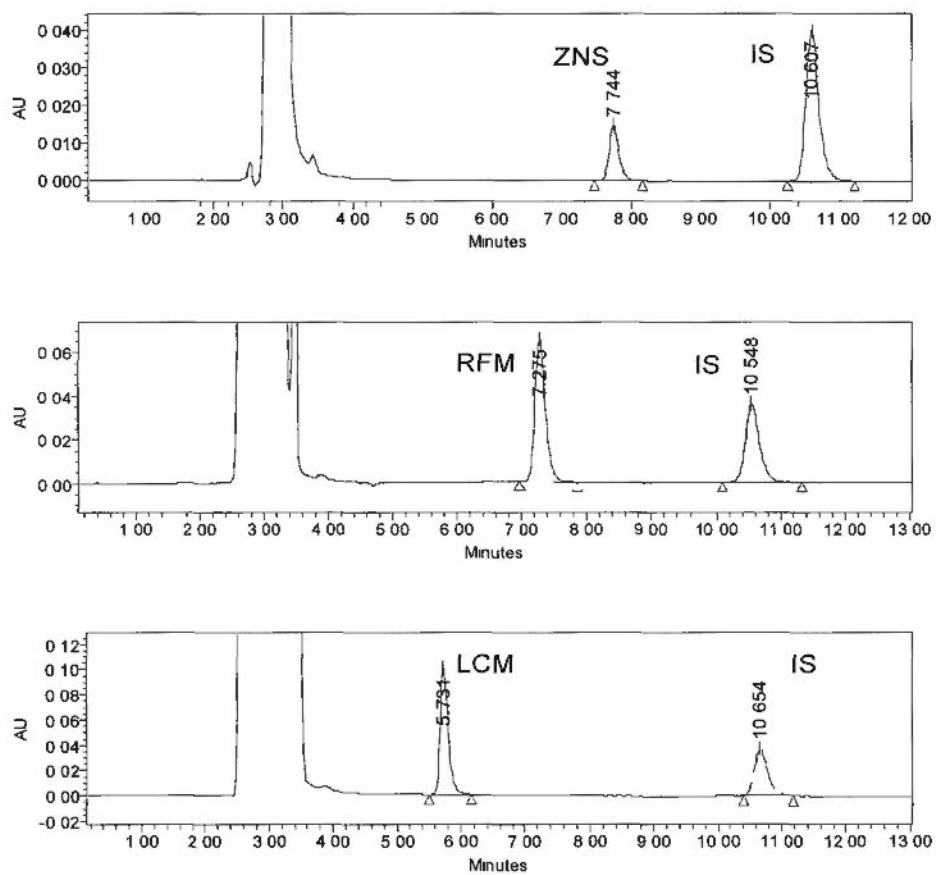
Fig 2.1c   HPLC chromatograms of standard solution at 2.5 µg/ml and IS at 1 µg/ml for ZNS, RFM, and LCM.
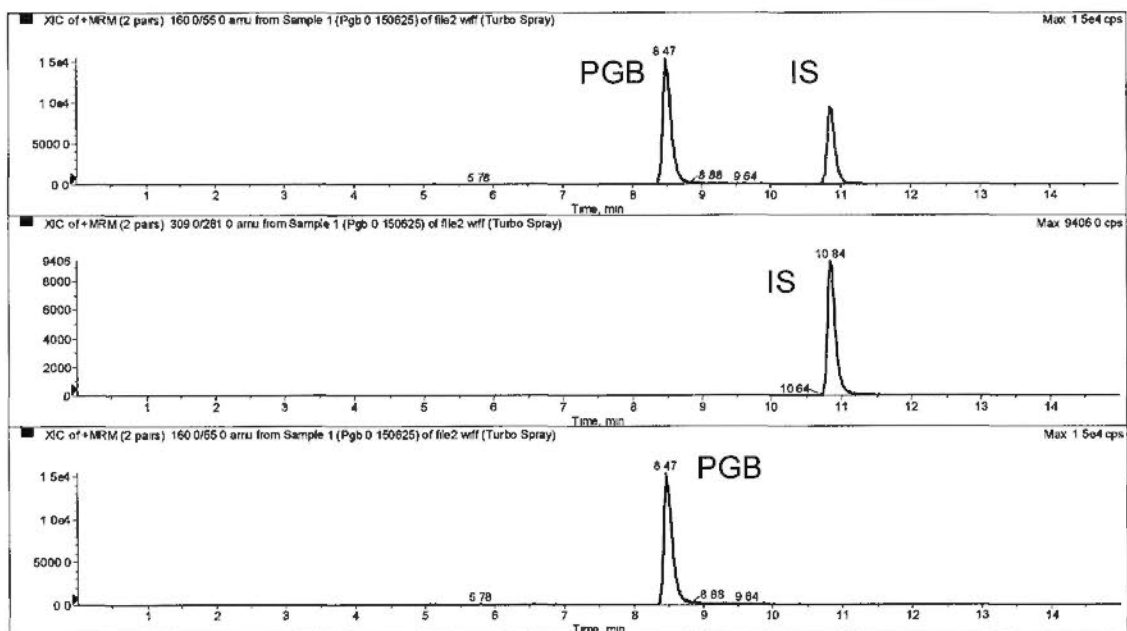
Fig 2.2 LC-MS/MS chromatograms of standard solution at 1.5 µg/ml and IS at 1 µg/ml for PGB.

Table 2.1 The condition of HPLC/UV methods for studied AEDs.

Compounds	Retention time (min)	Mobile phase	Internal standard (IS)	Flow rate (ml/min)	Wavelength of UV (nm)
Carbamazepine	8.613	35% acetonitrile in 20mM NaH$_2$PO$_4$ (PH4.6)	Phenobarbital	1	210
Carbamazepine-10,11-epoxide	5.418	35% acetonitrile in 20mM NaH$_2$PO$_4$ (PH4.6)	Phenytoin	1	210
Oxcarbazepine	6.094	35% acetonitrile in 20mM NaH$_2$PO$_4$ (PH4.6)	Phenytoin	1	210
S-licarbazepine	7.04	26% acetonitrile in 20mM NaH$_2$PO$_4$ (PH4.6)	Phenobarbital	1	210
Eslicarbazepine acetate	8.154	35% acetonitrile in 20mM NaH$_2$PO$_4$ (PH4.6)	Phenytoin	1	210
Ethosuximide	8.516	16% acetonitrile in 20mM NaH$_2$PO$_4$ (PH4.6)	Nadolol	1	204
Phenytoin	9.458	35% acetonitrile in 20mM NaH$_2$PO$_4$ (PH4.6)	Phenobarbital	1	204
Zonisamide	7.744	30% acetonitrile in 20mM NaH$_2$PO$_4$ (PH4.6)	Phenobarbital	1	210
Phenobarbital	6.018	35% acetonitrile in 20mM NaH$_2$PO$_4$ (PH4.6)	Phenytoin	1	204
Lacosamide	5.731	30% acetonitrile in 20mM NaH$_2$PO$_4$ (PH4.6)	Phenobarbital	1	210
Rufinamide	7.275	30%acetonitrile in 20mM NaH$_2$PO$_4$ (PH4.6)	Phenobarbital	1	210

2.3.2 Method validation

The calibration curve of each AED was determined over the concentration range of 0.15-10 μg/ml, and the $1/x^2$ weighted linear regression (r^2) for each curve was good (Table 2.2). The LOQ of each drug is listed in Table 2.2. The LOQ was much lower than the concentration of each drug tested in the subsequent studies.

Validation was performed for HPLC/UV and LC-MS/MS assay methods for AEDs. Low, medium, and high concentrations of QC were detected for all AEDs. The inter-day and intra-day accuracy and precision of each drug is listed in Table 2.2. For precision, the R.S.D. of each AED was below 10% in the LC-MS/MS and HPLC/UV methods. The intra-day and inter-day accuracy was also calculated; the R.E. of each AED was within the range of $\pm5\%$.

Table 2.2 Inter-day and intra-day precision, linear regression and accuracy of studied AEDs

Drugs	Linear range (µg/ml)	LOQ (µg/ml)	R^2	Nominal conc. (µg/ml)	Intra-day (n=3)			Inter-day (n=3)		
					Determined conc. (µg/ml)	Precision (%R.S.D.)	Accuracy (%R.E.)	Determined conc. (µg/ml)	Precision (%R.S.D.)	Accuracy (%R.E.)
OXC	0.15-10	0.05	0.9999	9.00	8.93	0.24	0.83	8.90	0.74	1.06
				3.00	3.03	1.30	-1.12	3.00	2.14	0.02
				1.00	1.02	3.23	-2.34	1.09	10.44	0.96
CBZ	0.15-10	0.05	0.9998	9.00	9.24	4.05	-2.66	9.36	5.08	-4.01
				3.00	3.11	0.55	-3.79	3.09	4.04	-2.89
				1.00	1.03	1.64	-3.35	1.03	2.35	-3.08
ZNS	0.15-10	0.03	0.9997	9.00	8.79	0.47	2.30	8.88	1.41	1.31
				3.00	3.00	4.14	0.15	2.97	2.66	0.95
				1.00	0.99	2.81	0.79	1.02	5.67	-2.46
ESL	0.15-10	0.03	0.9999	9.00	9.08	0.59	-0.85	9.17	1.94	-1.87
				3.00	3.05	0.18	-1.81	3.05	0.62	-1.59
				1.00	1.04	4.00	-4.48	1.05	2.60	-4.89
PHT	0.15-10	0.03	0.9999	9.00	8.95	3.74	0.52	9.13	3.18	-1.49
				3.00	3.02	0.34	-0.69	3.04	1.00	-1.22
				1.00	1.02	3.21	-2.35	1.02	2.35	-1.69
RFM	0.15-10	0.035	0.9999	9.00	8.89	0.74	1.22	8.90	0.69	1.07
				3.00	3.07	1.01	-2.35	3.01	2.32	-0.19
				1.00	1.05	3.93	-4.82	1.02	3.71	-2.26

Table 2.2 Inter-day and intra-day precision, linear regression, and accuracy of studied AEDs (continued)

Drugs	Linear range (μg/ml)	LOQ (μg/ml)	R^2	Nominal conc. (μg/ml)	Intra-day (n=3)			Inter-day (n=3)		
					Determined conc. (μg/ml)	Precision (%R.S.D.)	Accuracy (%R.E.)	Determined conc. (μg/ml)	Precision (%R.S.D.)	Accuracy (%R.E.)
CBZ-E	0.15-10	0.05	0.9999	9.00	8.90	0.88	1.11	8.83	1.14	1.85
				3.00	2.94	2.54	1.99	2.95	1.70	1.54
				1.00	0.99	3.76	1.29	0.99	3.37	1.46
S-LC	0.15-10	0.03	1.0000	9.00	8.97	0.69	0.38	8.99	0.74	0.07
				3.00	2.98	1.03	0.68	3.02	2.77	-0.75
				1.00	1.00	1.14	-0.27	1.03	4.74	-2.51
EMS	0.15-10	0.05	0.9998	9.00	9.01	0.41	-0.10	9.05	1.17	-0.54
				3.00	2.95	1.75	2.95	2.93	2.64	2.21
				1.00	0.96	4.51	3.93	0.98	6.87	1.64
PB	0.15-10	0.03	0.9999	9.00	9.05	0.45	-0.56	8.99	0.81	0.12
				3.00	3.06	1.07	-1.96	2.92	4.92	2.78
				1.00	1.02	2.68	-2.44	0.99	3.10	0.79
LCM	0.15-10	0.04	0.9999	9.00	9.01	0.36	-0.12	8.95	2.35	0.54
				3.00	3.04	1.67	-1.50	3.04	5.47	-1.26
				1.00	1.03	0.19	-2.71	0.99	3.88	1.21
PGB	0.15-10	0.01	0.9999	9.00	2.77	3.37	0.74	-0.75	1.46	0.07
				3.00	2.64	4.74	1.17	2.21	-2.51	-0.54
				1.00	4.92	6.87	0.81	2.78	1.64	0.12

The stability of AEDs was tested in transport buffer under the same conditions as the transport assay experiments. At 37°C, the AEDs were stable in PBS buffer with Mg^{2+} and Ca^{2+} for 4 hours (Table 2.3). The AEDs were also stable in the auto-sampler at room temperature for 48 hours. The stability test data are listed in Table 2.4.

Table 2.3 The stability of studied AEDs in transport buffer (PBS) at 37°C for 2 hours and 4 hours.

Drugs	0 hr			2 hr			4 hr		
	Concentration (µg/ml)	SD (µg/ml)	Percentage remained (%)	Concentration (µg/ml)	SD (µg/ml)	Percentage remained (%)	Concentration (µg/ml)	SD (µg/ml)	Percentage remained (%)
OXC	20.0	0.1	100.0	20.2	0.1	100.9	19.9	0.1	99.6
CBZ	20.0	0.3	100.0	19.9	0.1	99.6	19.6	0.2	98.1
ZNS	20.0	0.1	100.0	19.3	0.2	96.5	19.5	0.1	97.5
ESL	20.0	0.1	100.0	20.1	0.1	100.4	20.4	0.0	102.0
PHT	20.0	3.5	100.0	21.4	0.2	107.1	21.6	0.1	107.9
RFM	20.0	0.0	100.0	20.4	0.2	102.2	20.2	0.0	100.9
CBZ-E	20.0	0.0	100.0	19.9	0.0	99.5	20.3	0.0	101.5
S-LC	20.0	0.2	100.0	19.7	0.1	98.6	19.7	0.1	98.4
PB	20.0	0.0	100.0	19.8	0.0	99.2	20.1	0.0	100.5
LCM	20.0	0.1	100.0	19.3	0.2	96.5	19.4	0.2	97.2
EMS	20.0	0.2	100.0	20.5	0.2	102.5	20.4	0.1	101.9
PGB	19.8	0.2	100.0	19.3	0.1	97.3	20.0	0.1	100.7

Table 2.4 The stability of AEDs in auto sampler at room temperature for 24 hours and 48 hours.

Drugs	0 hr			24 hr			48 hr		
	Concentration (µg/ml)	SD (µg/ml)	Percentage remained (%)	Concentration (µg/ml)	SD (µg/ml)	Percentage remained (%)	Concentration (µg/ml)	SD (µg/ml)	Percentage remained (%)
OXC	8.9	0.0	100.0	8.9	0.1	100.1	8.8	0.1	99.1
CBZ	9.2	0.4	100.0	10.0	0.2	108.2	10.2	0.2	110.3
ZNS	8.8	0.0	100.0	8.9	0.2	101.5	8.9	0.1	101.5
ESL	9.1	0.1	100.0	9.0	0.1	99.5	9.4	0.1	103.5
PHT	9.0	0.3	100.0	9.3	0.0	104.0	9.1	0.3	102.0
RFM	8.9	0.1	100.0	8.9	0.0	99.6	9.0	0.0	100.8
CBZ-E	8.9	0.1	100.0	8.8	0.1	99.1	8.8	0.1	98.6
S-LC	9.0	0.1	100.0	9.0	0.1	100.8	9.0	0.1	100.2
PB	9.1	0.0	100.0	9.0	0.1	99.2	8.9	0.1	98.8
LCM	9.0	0.0	100.0	8.8	0.2	97.8	9.0	0.3	100.2
EMS	9.0	0.0	100.0	9.0	0.0	99.5	9.2	0.1	101.8
PGB	8.9	0.1	100.0	9.0	0.0	101.6	8.9	0.0	100.3

2.3.3 Discussion

According to the results of HPLC/UV and LC-MS/MS, the drug analysis methods established were qualified to separate the drugs from the IS and other compounds contained in the transport buffer (Figures 2.1 & 2.2). Validation of HPLC/UV and LC-MS/MS was performed. The linearity of the standard curves was good for all tested drug ($1 \geq R^2 > 0.999$). The inter-day and intra-day precision was lower than 10%, and the accuracy was good, indicating that the methods were valid (Table 2.2). Stability of the drugs was tested in transport buffer and the auto sampler for a longer duration than the time used in experiments. The drugs were stable during the experiments (Tables 2.3 & 2.4).

2.4 Conclusion

The established HPLC/UV and LC-MS/MS methods were qualified for further experiments. The methods produced good inter-day and intra-day precision, linearity, and accuracy. The drugs were stable in the transport buffer and auto sampler during the experiments, indicating the methods of drug analysis were suitable for our projects.

Chapter Three

In vitro concentration dependent transport of phenytoin and phenobarbital, but not ethosuximide, by human P-glycoprotein

3.1 Introduction

Although more than 20 antiepileptic drugs (AEDs) are used clinically, pharmacotherapy does not help 30-40% of epilepsy patients (Kwan *et al.*, 2000a). Mechanisms underlying drug resistance in epilepsy are unclear (Regesta *et al.*, 1999). AEDs traverse the blood-brain barrier (BBB) to exert their effects. Multidrug efflux transporters such as P-glycoprotein (Pgp, also called ABCB1 or MDR1) play an integral role in maintaining the functionality of the BBB via basolateral-to-apical transport of xenobiotics (Loscher *et al.*, 2005). Pgp overexpression contributes to cancer drug resistance (Gottesman *et al.*, 1988; Hennessy *et al.*, 2007; Juliano *et al.*, 1976). Subsequent observations that Pgp is overexpressed in epileptic foci support the hypothesis that Pgp may contribute to drug-resistant epilepsy (Kwan *et al.*, 2005; Loscher *et al.*, 2005), although which AEDs are transported by Pgp remains controversial.

Phenytoin (PHT), phenobarbital (PB), and ethosuximide (ESM) are common drugs for treatment of epilepsy. *In vivo*, Pgp inhibitors, such as verapamil, can increase the concentration of PHT and PB in rat brain (Potschka *et al.*, 2002; Potschka *et al.*, 2001b). Although whole brain level of PHT in *mdr1a*$^{-/-}$ mice did not differ from that of wild type mice (Schinkel, 1997; Schinkel *et al.*, 1996; Sills *et al.*, 2002), in *mdr1a/b*$^{-/-}$ mice PHT reached significantly higher level in the hippocampus (Rizzi et al. 2002), where *mdr1b* is abundantly expressed (Kwan et al. 2003). *In vitro*, PHT either did not affect human Pgp activity (Rivers *et al.*, 2008) or did so at concentrations exceeding therapeutic plasma concentrations (Weiss *et al.*, 2003b). In OS2.4/Doxo cells (canine osteosarcoma cells), PB decreased the efflux of Rhodamine-123 (Rho123), a substrate of Pgp, while PHT did not affect Rho123 uptake (West *et al.*, 2007). In MDR1-transfected HEK293 cells, both

PHT and PB inhibited Rho123 efflux (Hung *et al.*, 2008). These studies, however, did not directly measure drug transport by Pgp.

In Caco-2 monolayers, PB transport was equivalent in both directions, while PHT and ESM displayed apical to basal transportation, but Pgp inhibitors affected none of the drugs (Crowe *et al.*, 2006). Mouse but not human Pgp directionally transported PHT in Madin-Darby Canine Kidney II (MDCKII) or porcine kidney endothelial LLC-PK1 monolayer models (Baltes *et al.*, 2007b). However, using the concentration equilibrium transport assay (CETA) system, which is more suited for studying compounds of high BBB permeability, Luna-Tortós et al. demonstrated that human Pgp in LLC and MDCKII monolayers did transport PHT and PB. However, that study only examined one concentration of PB (50 µM) and two of PHT (5 µM and 50 µM), which may not represent the full range of concentrations experienced *in vivo* during AED treatment (Luna-Tortos *et al.*, 2008a).

We sought to help resolve the conflicting evidence on whether PHT, PB, and ESM are transported by Pgp using both cell monolayer bi-directional and concentration equilibrium transport assays (Luna-Tortos *et al.*, 2008b; Luna-Tortos *et al.*, 2009). With the latter assay, we tested ranges of clinically relevant drug concentrations to examine whether transport activity was concentration dependent.

3.2   Materials and methods

3.2.1 Drugs

PHT, ESM, and Rho123 were supplied by Sigma Aldrich (St. Louis, MO, USA). PB was purchased from Universal Chemicals, Inc (South Kearny, New Jersey, USA). PHT, PB and ESM were tested at concentrations covering the ranges of therapeutic plasma concentrations (Martin J Brodie, 2005). Verapamil was provided by Alexis Biochemicals (San Diego, CA, USA). All other materials were analytical grade.

3.2.2 LLC and MDCK cell monolayer models

3.2.2.1 Cell culture

Wildtype LLC-PK1 (LLC-WT) and MDCKII (MDCK-WT), and their human *MDR1* gene transfected cell lines (LLC-MDR1 and MDCK-MDR1), were kind gifts of Professor P. Borst (The Netherlands Cancer Institute, Amsterdam, Netherlands). They were handled as described previously (Bakos *et al.*, 1998; Zhang *et al.*, 2010). All the cell lines were used within 10 passages after receipt. Phosphate buffered saline (PBS) was from Sigma Aldrich (St. Louis, MO, USA). Dulbecco's Modified Eagle Medium (DMEM), Medium 199, and fetal bovine serum (FBS) were from Gibco (Grand Island, NY, USA).

Six-well transwells (Transwell®, 0.4 μm, polycarbonate membrane, 24 mm insert, Corning, NY, USA) coated with rat tail type I collagen (Sigma Aldrich, St. Louis, MO, USA) were used for the transport studies. The cells at densities of 2×10^6 (MDCK cells) or 1.5×10^6 (LLC cells) were seeded on the transwells as described previously (Luna-Tortos *et al.*, 2008a; Zhang *et al.*, 2007) followed by culturing in the relevant medium (MDCK: DMEM, 10% FBS, 100 U/ml penicillin-streptomycin; LLC: Medium 199, 10% FBS, 100 U/ml penicillin-streptomycin) at 37°C with 5% CO_2 for 5 days. The medium was changed every day.

3.2.2.2 Validation of cell monolayer in LLC and MDCK cell lines

The integrity of the monolayer was monitored by measuring the transepithelial electrical resistance (TEER) with an epithelial volt/ohm meter (World Precision instruments, Inc., FL, USA). Only the monolayers with TEER>100 Ω cm^2 (subtracting the background value of a transwell) before and after the experiment were used for the transport assay. The integrity of the monolayer was also verified by atenolol (paracellular marker) and propranolol (transcellular marker). Only the monolayers with integrity values comparable with published data were used (Crespi *et al.*, 2000; Thiel-Demby *et al.*, 2008; Wang *et al.*, 2008).

3.2.2.3 Cytotoxicities of PHT, PB and EMS to LLC and MDCK cells

Potential cytotoxicity of AEDs was tested by MTT (3-[4,5 dimethyl thiazolyl-2]-2,5-diphenyltetrazolium bromide) assay as described previously, with slight modification (Han *et al.*, 2008). Cells at a density of 1.5×10^4 cells/well were seeded in 96 well plates and cultured for 48 hr. After withdrawing the culture medium, 150 µl transport buffer with various concentrations of AEDs was added to each well and incubated for various times according to the periods of drug exposure in the transportation assays at $37^\circ C$ in 5% CO_2. Then 20 µl of 5 mg/ml MTT was loaded to each well followed by incubation for another 4 hr at $37^\circ C$ in 5% CO_2. The buffer was removed and replaced with 200 µl DMSO in each well. The absorbance of each well in the plate was recorded at a wavelength of 590 nm on a microplate reader (Benchmark, BioRad, USA).

3.2.2.4 Preparation of transport buffer

The transport study was carried out in phosphate buffer saline supplemented with 0.9 mM calcium chloride and 0.4 mM magnesium chloride (PBS⁺) with pH value 7.3.

3.2.2.5 Stabilities of PHT, PB and EMS in transport buffer

PHT, PB and EMS were dissolved in transport buffer at a concentration of 20 µg/ml, respectively. The prepared solution was incubated in shaking water bath at $37^\circ C$ for 4 hr. Samples were taken at 2 hr and 4 hr time points respectively and the drug concentrations was determined by HPLC/UV to calculate the percentage of drug remained.

These drugs were also put in auto-sampler for 48 hr to test the stability at room temperature. At 9 µg/ml, durg concentration was determined at 0 hr, 24 hr, and 48 hr by HPLC/UV to calculate the percentage of drug remained.

3.2.2.6 Concentration equilibrium transport assay (CETA) of PHT, PB and EMS in LLC and MDCK cell monolayer models

Both LLC and MDCK cells were used for CETA, in which the volumes on the apical and basolateral sides were 2 ml and 2.7 ml, respectively. Drugs were initially added to both sides of the monolayer at 5 μg/ml, 10 μg/ml, and 20 μg/ml for PHT and PB, and at 5.6 μg/ml and 56 μg/ml for ESM. Aliquots of 100 μl apical and 130 μl basolateral samples, which did not affect the hydrostatic pressure on the cell monolayers, were collected at various time points of drug exposure (30, 60, 90, 120, and 180 min). For ESM, the drug exposure time was extended to 240, 360, and 600 min. In order to test the effect of Pgp inhibition on AED transport, the above AED transport assays were conducted in the presence of verapamil (100 μM). The collected samples were stored at -20^{0}C until analysis (Zhang *et al.*, 2010).

3.2.2.7 Bi-directional transport assay of PHT, PB and EMS in LLC and MDCK cell monolayer models

MDCK cells were used for the bi-directional transport assays, in which the apical and basolateral volumes of transport buffer were 1.5 ml and 2.6 ml, respectively. Twenty minutes before the beginning of each transport assay, the growth medium was replaced with PBS^{+}. The AEDs were added to the basolateral (B) side of the monolayer at 10 μg/ml for PHT and PB and 5.6 μg/ml for ESM. Aliquots of 0.5 ml samples were taken from the apical side (A) at different time points (30, 60, 90, and 120 min), and the same volume of fresh PBS buffer was added to the apical side after each time point.

3.2.3 Identification of MDR1 in LLC and MDCK cells

3.2.3.1 Real time-PCR analysis

To quantify *MDR1* mRNA levels in the cell lines, RNA was isolated using Trizol (Invitrogen, CA, USA) as described by the manufacturer. 1 μg total RNA was treated

with 0.5 U of DNase I (Invitrogen, CA, USA) and used for RT-PCR. Reverse-transcription was performed using the SuperScript First-Strand Synthesis System (Invitrogen, CA, USA). Real time PCR was performed with KAPA SYBR® qPCR Master Mix (Kapa Biosystems, MA, USA) in a Roche LightCycler II (Mannheim, Germany). PCR amplification was carried out by using the following primer pairs: *MDR1*, 5'-CCCATCATTGCAATAGCAGG-3' and

5'-TGTTCAAACTTCTGCTCCTGA-3'; *β-Actin*,

5'-CCTCTATGCCAACACAGTGC-3' and 5'-ACATCTGCTGGAAGGTGGAC-3'.

3.2.3.2 Rhodamine-123 uptake assay and flow cytometry

To confirm the functional activity of Pgp, Rho123 uptake assays were performed as described previously, with minor modifications (Kimchi-Sarfaty *et al.*, 2007). Briefly, 3×10^5 cells were collected by trypsin and washed once with warm PBS. Then, cells were resuspended in 1 ml DMEM containing 5% FBS and Rho123 (1 μg/ml) followed by incubation at 37°C for 20 min. The cells were centrifuged and resuspended in 300 μl cold PBS. Flow cytometry analysis of Rho123 fluorescence at 585 nm was performed with the BD FACSAriaII (Becton Dickinson, San Jose, CA).

3.2.3.3 Immunofluorescent staining

To detect the location and protein level of Pgp in the cell lines, immunofluorescent staining was performed as described before, with some modifications (Zhang *et al.*, 2011). Briefly, cells were seeded on cover slips and cultured for 48 hr. The density of cells was about 80% when stained. After rinsing twice with cold PBS, the cells were fixed in 70% ethanol at -20°C for 15 min. The slips were washed with PBS 3 times for 5 minutes each. Then the cells were blocked by 10% FBS in PBS at room temperature for 30 minutes, followed by diluted Pgp antibody C219 (1:100, Abcam) in PBS with 0.5% BSA at 4°C overnight. Cells were rinsed with PBS twice and incubated in secondary antibody (1:300, Alex 488-conjugated IgG, Inivitrogen) in PBS with 0.5% BSA in the dark at room

temperature for 30 minutes. Finally, cells were washed by PBS twice, and slides were mounted for fluorescent microscopy.

3.2.4 Drug analysis

PB, PHT, and ESM were quantified by using high performance liquid chromatography with UV detection (HPLC/UV) as described before (Crowe *et al.*, 2006; Zhang *et al.*, 2010). A Thermo Hypersil BDS C_{18} column (5 µM pores, 250 mm × 4.6 mm inner diameter) was used. The HPLC methods were validated, and the inter-day and intra-day root mean square deviations were less than 5%. The limits of quantification for the drugs were 30 ng/ml for PHT, 30 ng/ml for PB, and 50 ng/ml for ESM.

3.2.5 Data analysis

For real time-PCR, relative expression levels of MDR1 mRNA in LLC, LLC-MDR1, MDCK, and MDCK-MDR1 cells were scaled to the mean relative expression level of the housekeeping gene *β-actin*.

For MTT assays, percentage survival was calculated according to the formula: (mean of drug treatment OD – mean of blank OD) / (mean of control OD – mean of blank OD) x 100%. 80% was considered to be safe for the drugs.

For the Rhodamine-123 uptake assay, fluorescence values for LLC-MDR1 and MDCK-MDR1 were scaled to the median fluorescence in wild type cells, which was regarded as 1. Significant differences between wild type cells and MDR1-transfected cells were calculated by student's t-test, with $p < 0.05$ considered as significant.

In the bi-directional transport assay, the permeability coefficient (Papp) of AEDs was calculated as described before (Zhang *et al.*, 2010; Zhang *et al.*, 2007). Papp = $(dQ/dt)/(A \times C)$, where dQ/dt is the rate of permeation; A is the area of the membrane surface (cm^2) and C is the initial concentration of drug in the donor chamber.

In the CETA, the data are presented as the percentage of the drug loading concentration in either apical or basolateral chamber vs. time, as described before (Luna-Tortos *et al.*, 2008a; Zhang *et al.*, 2010). Values were shown as means $\pm$ SEM. At various time intervals, differences of drug concentration between the two chambers of each well were compared, and differences of drug concentration between the two chambers in wildtype (WT) were compared with those from MDR1-transfected cells. Significant differences between two groups or more than two groups were calculated by student's t-test or one-way ANOVA, respectively, with $p<0.05$ considered as significant.

3.3 Results

3.3.1 Stabilities of PHT, PB and EMS in transport buffer

As shown in Fig 3.1 and Table 3.1, after incubation for 2 hr and 4 hr, the percentages of compound remaining of PHT, PB and EMS were around 100%, indicating that these compounds would be stable at 37 °C in the transport buffer for at least 4 hr. The drugs were also tested at room temperature in auto-sampler for 48 hr and they were also stable (Table 3.2).
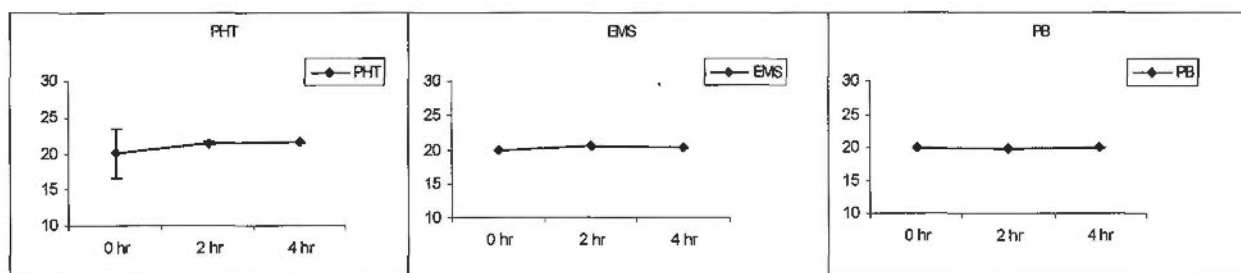
Fig 3.1 Stabilities of PHT, PB and EMS in transport buffer at 37 °C

Table 3.1 Stabilities of PHT, PB and EMS in PBS at 37 °C

Drugs	0 hr			2 hr			4 hr		
	Concentration (µg/ml)	SD (µg/ml)	Percentage (%)	Concentration (µg/ml)	SD (µg/ml)	Percentage (%)	Concentration (µg/ml)	SD (µg/ml)	Percentage (%)
PHT	20.0	3.5	100.0	21.4	0.2	107.1	21.6	0.1	107.9
PB	20.0	0.0	100.0	19.8	0.0	99.2	20.1	0.0	100.5
EMS	20.0	0.2	100.0	20.5	0.2	102.5	20.4	0.1	101.9

Table 3.2 Stabilities of PHT, PB and EMS in PBS in auto-sampler at room temperature.

Drugs	0 hr			24 hr			48 hr		
	Concentration (µg/ml)	SD (µg/ml)	Percentage (%)	Concentration (µg/ml)	SD (µg/ml)	Percentage (%)	Concentration (µg/ml)	SD (µg/ml)	Percentage (%)
PHT	9.0	0.3	100.0	9.3	0.0	104.0	9.1	0.3	102.0
PB	9.1	0.0	100.0	9.0	0.1	99.2	8.9	0.1	98.8
EMS	9.0	0.0	100.0	9.0	0.0	99.5	9.2	0.1	101.8

3.3.2 Cytotoxicities of PHT, PB and EMS to LLC and MDCK cells

MTT assays indicated that the concentrations of AEDs tested were not toxic to the four cell lines for at least 180 min in the case of PHT and PB and 600 min in the case of ESM (Fig 3.2), but cell damage occurred after 14 hours of exposure to ESM (data not shown).
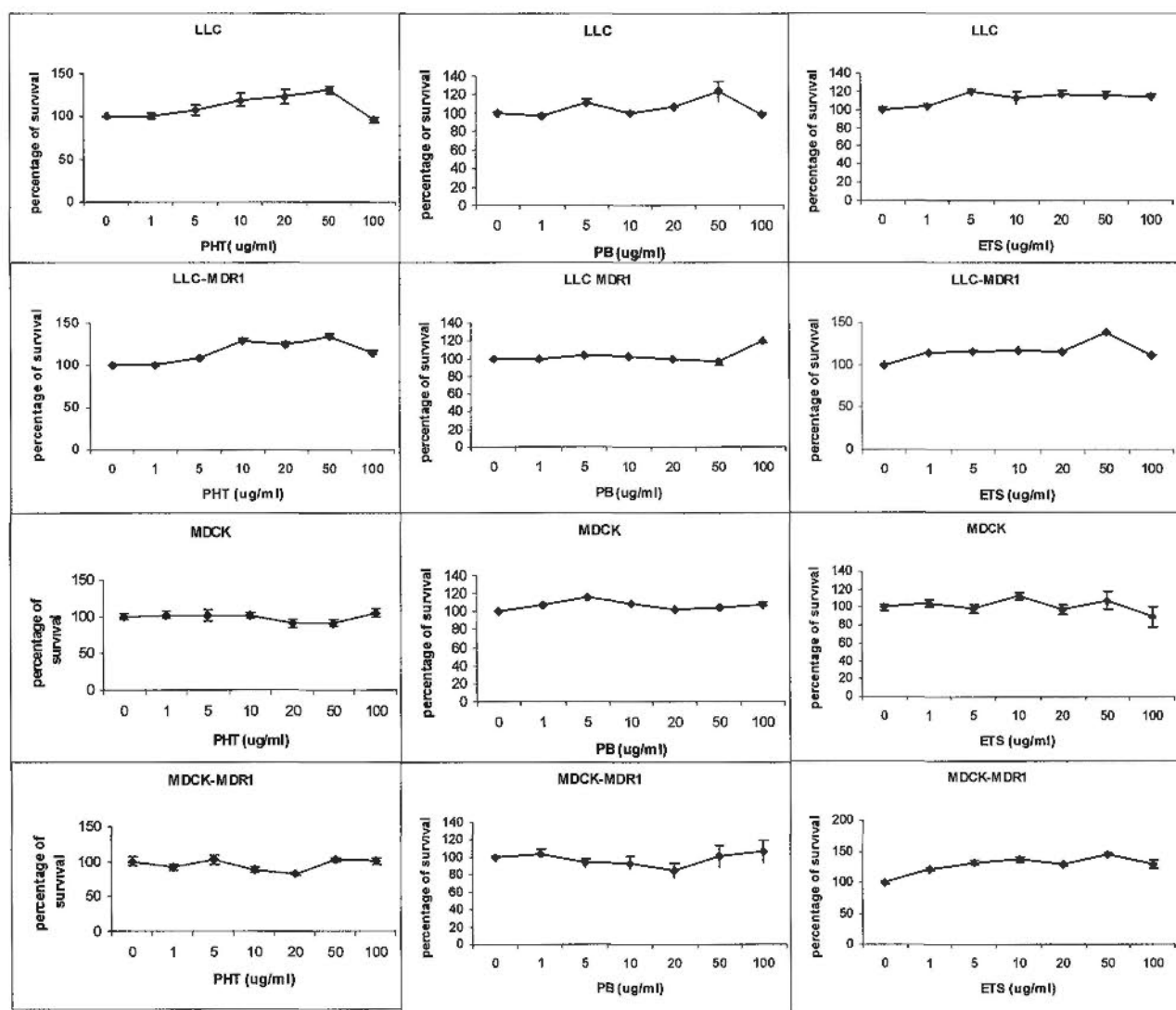
Fig 3.2   **Cytotoxicities of PHT, PB and EMS for LLC, LLC-MDR1, MDCK, and MDCK-MDR1 cells**

3.3.3 Identification of MDR1 in LLC and MDCK cells

3.3.3.1 Real time-PCR analysis

Real time PCR results demonstrated the expression level of human *MDR1* mRNA in the tested MDCK-MDR1 and LLC-MDR1 cells, which is shown in Fig 3.3. The expression of human Pgp in MDR1-transfected cell lines was significantly higher than in wild-type cells. The Pgp level in MDCK-MDR1 cells was similar to that in LLC-MDR1 cells (LLC-MDR1: *MDR1/β-actin*=0.20±0.06; MDCK-MDR1: *MDR1/β-actin*=0.16±0.06; *p*=0.27). The level of endogenous Pgp in wild-type cells was slight, and the level of canine Pgp in MDCKII cells was higher than the level of swine Pgp in LLC cells (LLC: *MDR1/β-actin*=5.1x10^{-5}±3.9x10^{-5}; MDCK: *MDR1/β-actin*=0.02±0.01; *p*<0.05) (Fig 3.3).
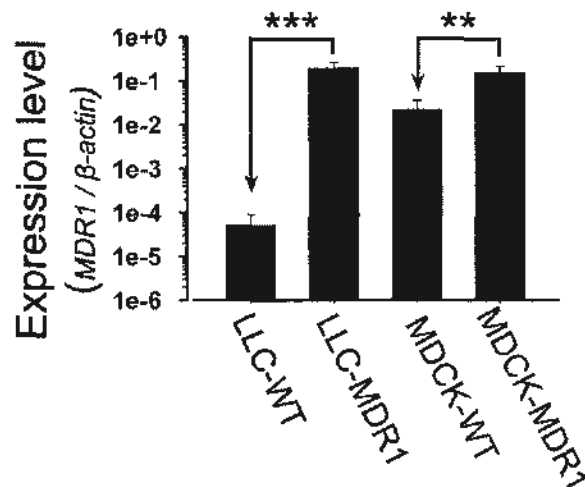
Fig 3.3   **Real time PCR of Pgp in LLC and MDCK wild type and MDR1-transfected cell lines.** Relative expression levels of MDR1 for LLC, LLC-MDR1, MDCK, and MDCK-MDR1 cells were calculated as the ratio of MDR1 to *β-actin* (n=3, ***p*<0.01, ****p*<0.001).

3.3.3.2 Immunofluorescent staining

The protein expression level of Pgp was detected by immunofluorescent staining, which confirmed that the MDR1-transfected cell lines expressed significantly more Pgp than non-transfected cells (Fig 3.4). LLC-MDR1 cells had a higher level of Pgp than MDCK-MDR1 cells. More Pgp protein appears to be located on the cell membrane than in the cytoplasm (Fig 3.4).
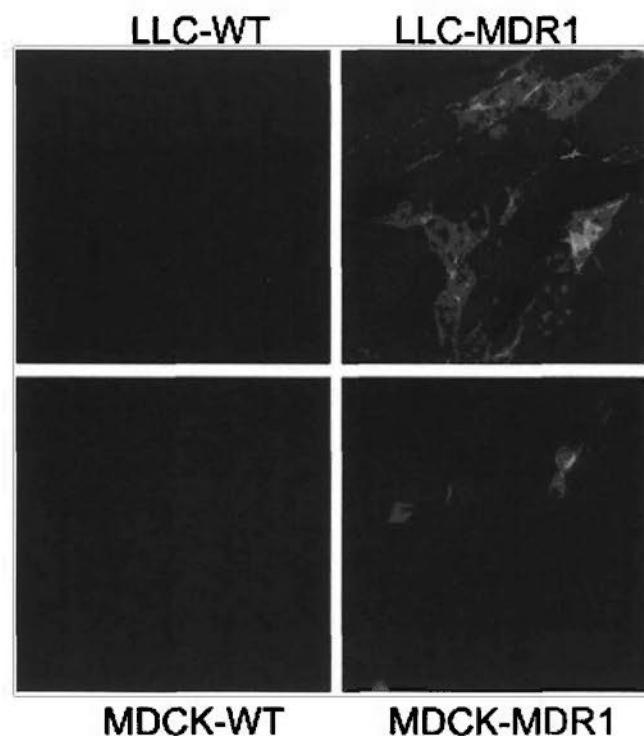
Fig 3.4 **Immunofluorescent staining of Pgp in LLC and MDCK wild type and MDR1-transfected cell lines to show the lcation and expression of Pgp**

3.3.3.3 Rhodamine-123 uptake of PHT, PB and EMS in cells

Densities of Rho123 in LLC-MDR1 and MDCK-MDR1 cells were 16% ($p<0.001$) and 41% ($p<0.001$) in LLC-WT and MDCK-WT cells respectively (Fig 3.5), confirming the presence of Pgp in the transfected cell lines.
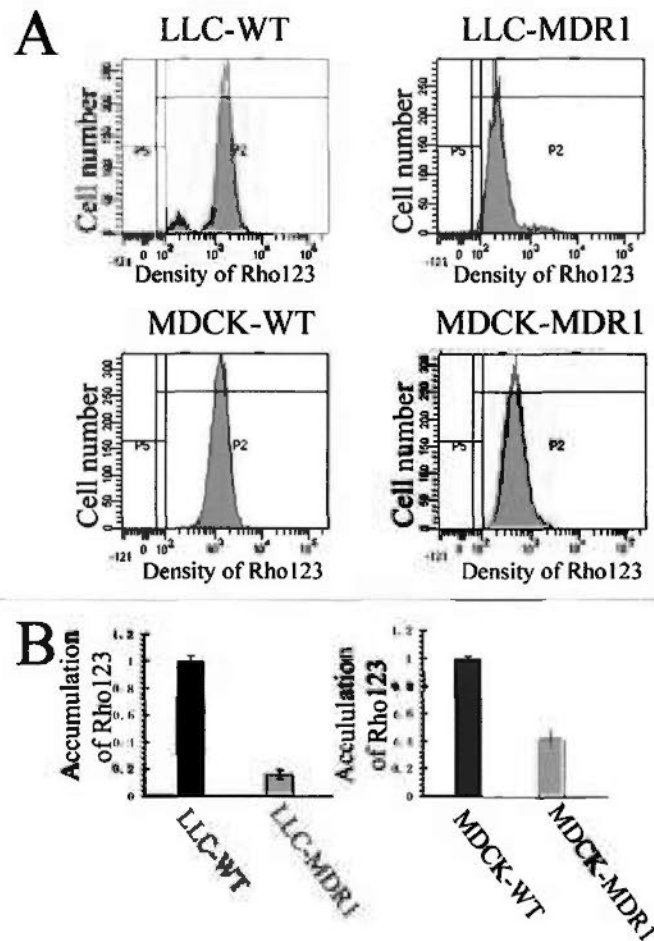
Fig 3.5   **Rhodamine-123 accumulation in LLC and MDCK wild type and MDR1-transfected cell lines.** (A) The density of Rho123 was detected by flow cytometry. (B) Relative fluorescence values (shown as mean ± SEM) in MDR1-transfected cells were compared with wildtype cells (whose median fluorescence levels were defined to be 1).

3.3.4 Transport profile of PHT

As expected, in the CETA of wildtype LLC and MDCK cells (not expressing MDR1), there was no significant difference in the concentrations of PHT between the apical and basolateral sides (Fig 3.6). When PHT was loaded at 10 µg/ml (40 µM) in the MDR1 expressing cells, the concentration of PHT on the apical side became significantly higher than on the basolateral side from 60 minutes of drug exposure onward for MDCK-MDR1 cells (Fig 3.6A) and from 90 minutes onward for LLC-MDR1 cells (Fig 3.6B). Addition

of the Pgp inhibitor verapamil eliminated the differences between apical and basolateral concentrations (Fig 3.6), indicating that PHT was transported by Pgp.

To examine whether the concentration of the drugs affected the transport of tested AEDs by Pgp in CETA, we tested other concentrations of PHT. Efflux transport by both MDCK-MDR1 and LLC-MDR1 cells was detected at 5 µg/ml (20 µM) and 10 µg/ml (40 µM). However, such transport disappeared when the loading concentration of PHT reached 20 µg/ml (79 µM) (Fig 3.6).

In bi-directional transport assays, the P_{app} value (basolateral to apical direction) of PHT (10 µg/ml, 40 µM) in MDCK-MDR1 cells was significantly higher than that of wildtype cells, but the difference was small (Fig 3.7A).
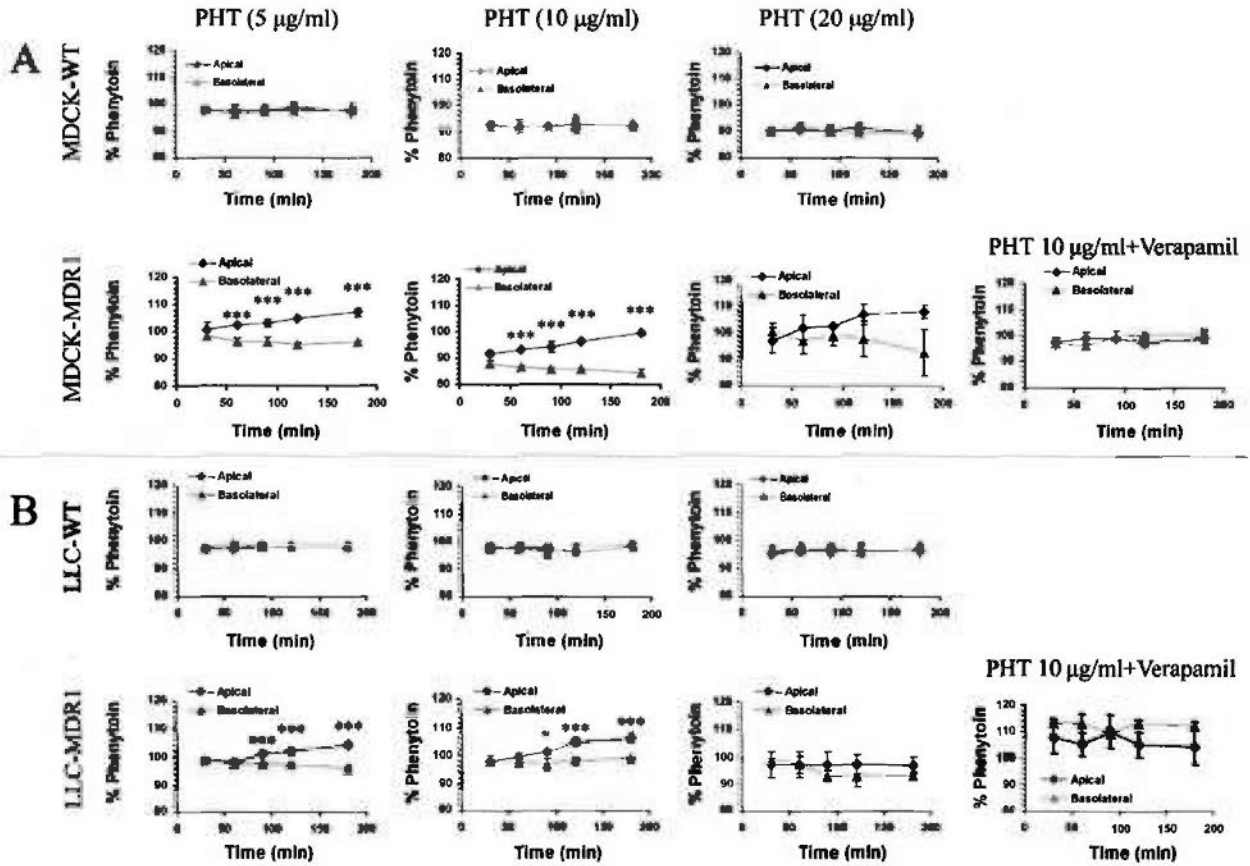
Fig 3.6   Concentration equilibrium transport assays of phenytoin in wildtype (WT) MDCKII and LLC-PK1 cells or cells transfected with the human MDR1 gene. PHT was transported by MDCK-MDR1 (A) and LLC-MDR1 (B) cells when the initial PHT concentration was 5 µg/ml or 10 µg/ml, but the difference between apical and basolateral concentrations did not reach significance when the initial PHT concentration was 20 µg/ml. The transport was inhibited by verapamil (100 µM). Data are given as the percentage of the initial drug concentration in either apical or basolateral chamber vs. time. Experiments were performed in triplicate, and values are shown as mean±SEM. Significant differences in drug concentrations between the two chambers are indicated by asterisks ([*]$p<0.05$, [**]$p<0.01$, [***]$p<0.001$).
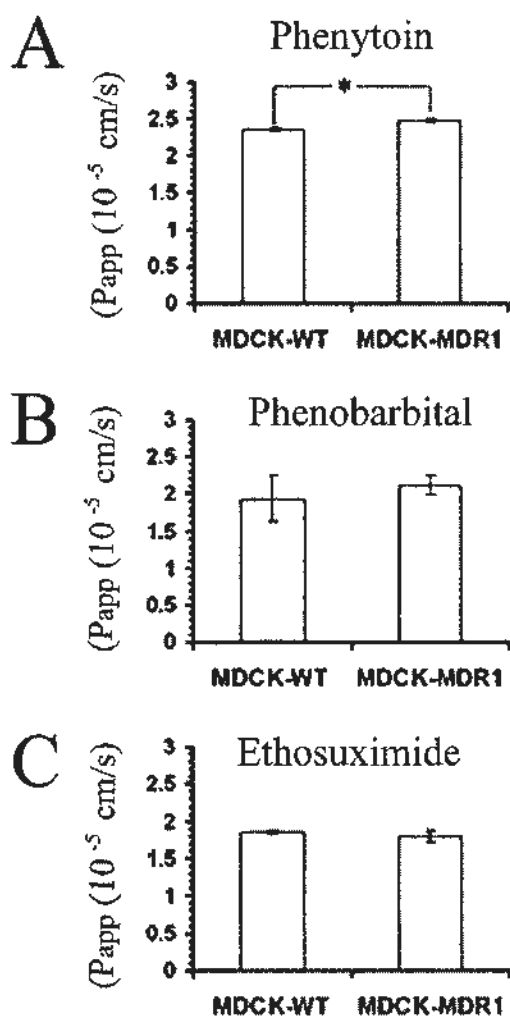
Fig 3.7   **Bi-directional transport assays (B to A direction) of (A) phenytoin (10 μg/ml, 40 μM), (B) phenobarbital (10 μg/ml, 43 μM) and (C) ethosuximide (5.6 μg/ml, 40 μM).** Apparent permeability (P_{app}) = $(dQ/dt)/(A \times C)$ where dQ/dt is the rate of permeation, C is the initial concentration, and A is the area of the monolayer. Experiments were performed in triplicate, and values are shown as mean±SEM and compared between wildtype (WT) and MDR1-transfected cells. *p=0.002.

3.3.5 Transport profile of PB

Similar to the CETA results for PHT, when PB was loaded at 10 μg/ml (43 μM), the concentration of PB on the apical side of MDCK-MDR1 cells became significantly higher than that on the basolateral side from 120 minutes of drug exposure onward, and such transport was inhibited by verapamil (Fig 3.8A). Compared with the findings for PHT, the difference in drug concentrations between apical and basolateral sides was much less for PB (Fig 3.6A and Fig 3.8A). In addition, PB at 10 μg/ml showed no transport by LLC-MDR1 cells (Fig 3.8B).

To examine whether the concentration of the drugs affected the transport of tested AEDs by Pgp in CETA, we tested other concentrations of PB. In contrast to the results of PHT, PB demonstrated efflux transport at 20 μg/ml (86 μM) but not at 5 μg/ml (22 μM) in MDCK-MDR1 cells (Fig 3.8A). In LLC-MDR1 cells, no significant efflux transport of PB was detected at any concentration (Fig 3.8B).

In bi-directional transport assays, the P_{app} values of PB (10 μg/ml, 43 μM) did not differ significantly between wildtype cells and MDR1-transfected cells (Fig 3.7B).
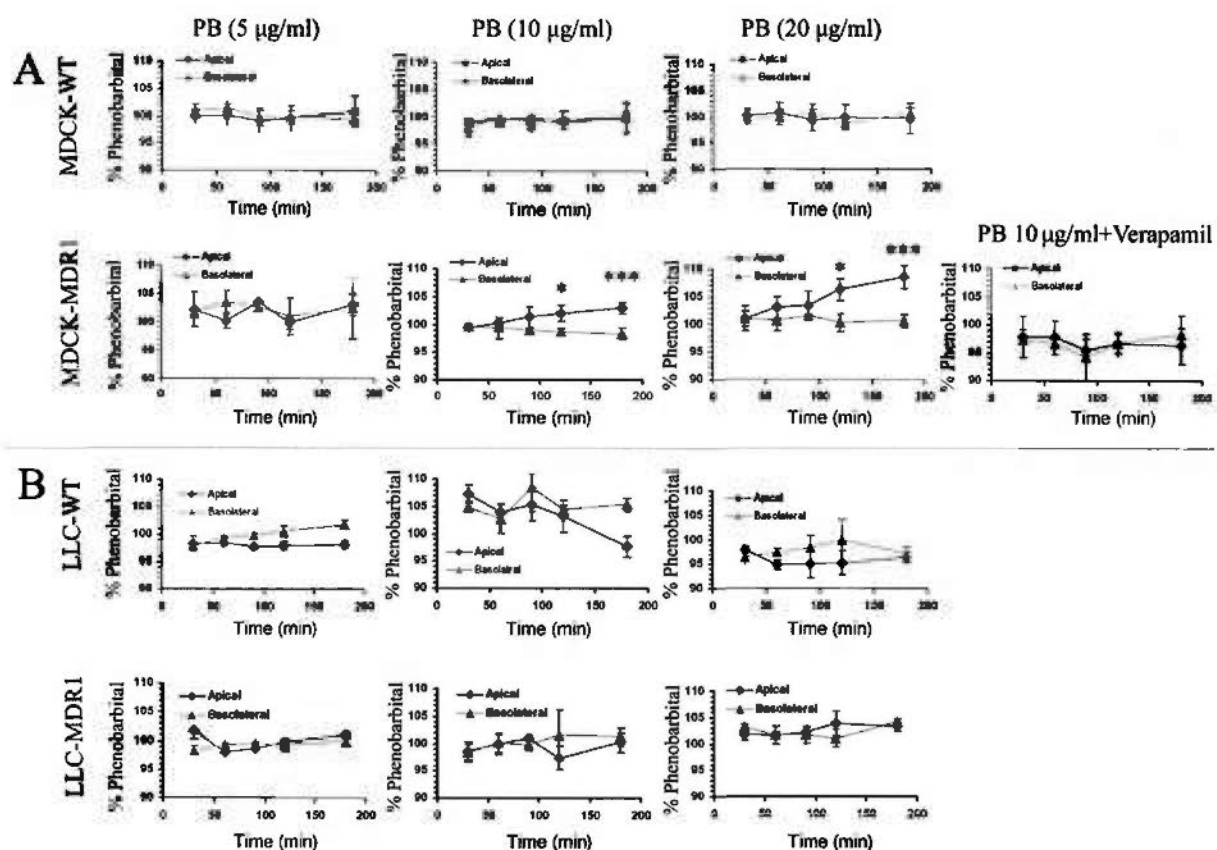
Fig 3.8   **Concentration equilibrium transport assays of phenobarbital in wildtype (WT) MDCKII and LLC-PK1 cells or cells transfected with the human MDR1 gene.** (A) PB was transported by MDCK-MDR1 cells when the initial PB concentration was 20 μg/ml or 10 μg/ml, but the difference between apical and basolateral concentrations did not reach significance when the initial PB concentration was 5 μg/ml. The transport was inhibited by verapamil (100 μM). (B) PB was not transported by LLC-MDR1 cells at any concentration tested. Data are given as the percentage of the initial drug concentration in either apical or basolateral chamber vs. time. Experiments were performed in triplicate, and values are shown as mean±SEM. Significant differences in drug concentrations between the two chambers are indicated by asterisks ($*p<0.05$, $**p<0.01$, $***p<0.001$).

3.3.6 Transport profile of EMS

For ESM, there was no significant difference between the apical and basolateral concentrations after drug exposure of 180 minutes at 5.6 μg/ml (40 μM) and 56 μg/ml (397 μM) in either MDCK-MDR1 or LLC-MDR1 cells (Fig 3.9). In order to confirm the

results, we extended the drug exposure periods to 4, 6, 10, and 24 hours to increase the sensitivity and found that there was also no significant difference between the apical and basolateral sides, suggesting that ESM may not be transported by Pgp at clinically relevant concentrations (Fig 3.10).

In bi-directional transport assays, the P_{app} values of ESM (5.6 μg/ml, 40 μM) did not differ significantly between wildtype cells and MDR1-transfected cells (Fig 3.7C).
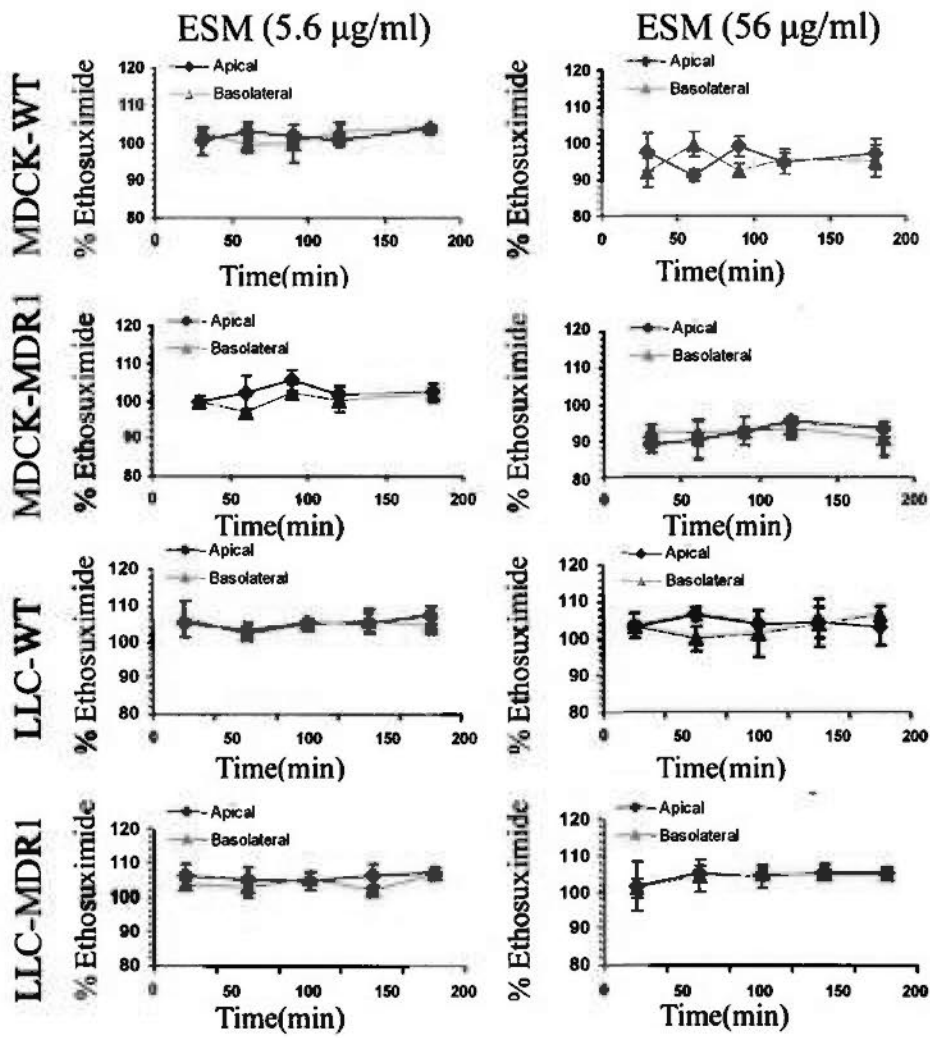
Fig 3.9   **Concentration equilibrium transport assays of ethosuximide in wildtype (WT) MDCKII and LLC-PK1 cells or cells transfected with the human MDR1 gene.** ESM was not significantly transported by either MDCK-MDR1 (A) or LLC-MDR1 (B) cells when the initial ESM concentration was either 5.6 µg/ml or 56 µg/ml. Data are given as the percentage of the initial drug concentration in either apical or basolateral chamber vs. time. Experiments were performed in triplicate, and values are shown as mean±SEM.
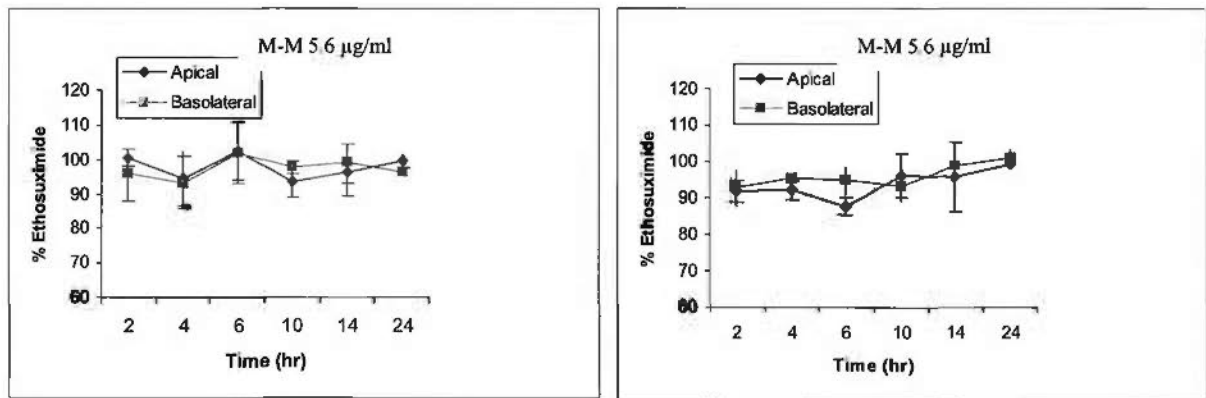
Fig 3.10   Concentration equilibrium transport assays of ethosuximide in MDCK-MDR1 cells for 24 hr. ESM was not significantly transported by MDCK-MDR1.

3.4   Discussion

Efflux transport of AEDs from the brain by Pgp is one of the potential mechanisms of drug resistance that are being actively investigated by researchers. The hypothesis is supported by evidence that Pgp expression is greatly increased at epileptic foci in brain tissues resected from patients with drug resistant epilepsy (Kwan *et al.*, 2005; Loscher *et al.*, 2005). However, the weak link in the hypothesis is definitive evidence that Pgp transports AEDs at therapeutic concentrations. The present data are therefore important because they provide further direct evidence, using polarized cell monolayers in two transport assay systems, on whether the commonly used AEDs, PHT, PB, and ESM are transported by Pgp at clinically relevant concentrations. Although little transport activity was demonstrated in the conventional bi-directional transport assay system, results from the CETA system suggested that PHT and PB were transported by human Pgp and that the transport was affected by the drug concentrations, whereas ESM was not transported by human Pgp.

In previous reports, PHT efflux was studied using Caco-2, LLC, and MDCK cell lines (Baltes *et al.*, 2007b; Crowe *et al.*, 2006; Luna-Tortos *et al.*, 2008b). In bi-directional transport assays, PHT was not transported by human Pgp (Baltes *et al.*, 2007b), although we found evidence of weak transport using this system. In CETAs, Luna-Tortós et al (2008) noted transport of PHT from basolateral to apical sides by human Pgp (Luna-Tortos *et al.*, 2008b). The concentrations used in these previous studies ranged from 5 to 50 µM (Baltes *et al.*, 2007b; Crowe *et al.*, 2006; Luna-Tortos *et al.*,

2008b). In this range of concentrations, we also demonstrated that PHT was transported by human Pgp, using both LLC-MDR1 and MDCK-MDR1 cells in CETA. But when we tested a higher concentration (20 µg/ml = 79 µM), we found that the transportation was not significant, though a trend was still evident (Fig 3.6). At this high dose, perhaps PHT saturates Pgp, thus reducing the proportion of PHT pumped per unit time below the sensitivity of the assay. In general, our observation of concentration dependence demonstrates the importance of examining a range of concentrations in transport assays.

PB was also previously reported to be efflux transported by LLC-MDR1 cells in CETAs, though not in Caco-2 cells in bi-directional transport assays (Crowe *et al.*, 2006; Luna-Tortos *et al.*, 2008b). The concentrations tested were 10 µM (Caco-2 cells) and 50 µM (LLC-MDR1 cells). In the present study, we found that PB was transported by human Pgp in MDCK-MDR1 cells in CETAs at 10 µg/ml (43 µM) and 20 µg/ml (86 µM). Its lack of detectable transport at 5 µg/ml (21.5 µM) suggested that it might have a relatively low affinity toward Pgp so that the small amount of PB transported might have been below the detection limit. However, PB was not transported by LLC-MDR1 cells at any tested concentrations in the present study. The reason for the discrepant results between the two cell lines needs further exploration. It is possible that the expression level of Pgp in the LLC-MDR1 cells was lower than in the MDCK-MDR1 cells, although Rho123 efflux from both cell lines was comparable, suggesting similar Pgp activity (though this was only tested after incubation for 25 minutes) (Fig 3.5). In addition, transport activity was measured for up to 3 hours of drug exposure, thus the possibility of significant transport of PB by the LLC-MDR1 cells at longer duration of drug exposure cannot be excluded. In the present study, extending the time of drug exposure is limited by the use of PBS as the transport buffer, which did not contain FBS and other chemicals, with the advantage of avoiding protein-drug binding but the disadvantage of lacking nutrition to keep cells alive for longer than about 12 hours.

To further confirm that PHT and PB were transported by Pgp, we used the Pgp substrate and inhibitor, verapamil, to block Pgp function (Pauli-Magnus *et al.*, 2000). The transportation of PHT and PB by MDR1-transfected cells was completely inhibited by verapamil (Fig 3.6 and Fig 3.7A). In addition, MDCKII and LLC-PK1

wild type cells expressed little Pgp protein compared with MDR1-transpected cells, and they did not transport PB or PHT, indicating that PB and PHT were transported by Pgp.

The possibility of concentration-dependent transport of AEDs by Pgp has not been well explored previously. We found that the concentrations of PHT and PB affected their transport by Pgp *in vitro*, which might account for some of the conflicting results in previous studies. This also implies that AED dosage might affect their transport by Pgp *in vivo*. There is a spatiotemporal range of drug concentrations *in vivo*, with variation occurring among tissues and over time after drug administration, therefore drug distribution may be affected by Pgp at some times and locations but not others. Further *in vitro* and *in vivo* studies are needed to clarify this complex picture.

ESM is effective against absence seizures (Gören and Onat 2007), yet they remain uncontrolled in a substantial proportion of treated patients (Glauser et al. 2010). In the present study, ESM at both high and low concentrations was not transported by LLC-MDR1 or MDCK-MDR1 cells. This finding was consistent with a previous study (Crowe *et al.*, 2006), indicating that ESM may not be a substrate of Pgp, and may therefore be employed as a "negative control" in future similar studies. Lack of transport of ESM by Pgp might help explain findings from a recent double-blind, randomized controlled trial (Glauser et al. 2010) that the medication was more effective than lamotrigine, a known Pgp substrate (Luna-Tortos et al. 2008), in the treatment of childhood absence epilepsy.

PHT and PB are common AEDs used widely in the clinic. PHT and PB are Pgp substrates, which suggests that these drugs may cause drug resistance in epileptic patients, and physicians should pick other drugs, those which are not Pgp substrates, or use multitherapy. EMS is not a Pgp substrate, and it may be more effective to treat patients with absence seizures.

In contrast to the finding of transport of PHT and PB by Pgp in CETAs, only minimal transport of PHT, and no transport of PB, was demonstrated in the conventional bi-directional transport assay system. This confirms that the CETA is more sensitive than the bi-directional transport assay in detecting Pgp transport of drugs with high

passive permeability, such as the AEDs (Luna-Tortos *et al.*, 2008b). This is because by applying equal drug concentrations to both sides of the monolayer at the beginning of the transport experiment, the chance that directional transport is concealed by passive diffusion is reduced. Our findings strengthen the suggestion that CETA should be used instead of the conventional bi-directional transport assay for study of compounds with high passive permeability across the BBB, particularly if they also have low transport efficiency (Luna-Tortos *et al.*, 2008b).

3.5   Conclusions

Using MDR1-transfected monolayer cell models, we demonstrated that PHT and PB, but not ESM, are substrates of human Pgp, and that the transport of PHT and PB was affected by drug concentration. Because of its superior sensitivity, CETA is the preferred transport assay system and should be extended to study Pgp transport of other commonly used AEDs. A range of clinically relevant concentrations should be tested when evaluating whether an AED is transported by Pgp. Results of *in vitro* studies will need to be confirmed in appropriate *in vivo* models. Determination of which AEDs are transported by Pgp will be vital in the appropriate design of clinical trials to overcome drug resistance in epilepsy.

Chapter Four

In vitro transport profile of carbamazepine, oxcarbazepine, eslicarbazepine acetate and their active metabolites by human P-glycoprotein

4.1   Introduction

Pharmacoresistance of antiepileptic drugs (AEDs) is a major public health problem. Although more than 20 AEDs are used clinically, epilepsy does not respond to pharmacotherapy in 30-40% of patients (Kwan *et al.*, 2000a). Resistance to these drugs is also a problem in treatment of schizophrenia, depression, and bipolar disorder (Gitlin, 2006; Mihaljevic Peles *et al.*, 2008; Morinigo *et al.*, 1989). The mechanisms underlying AED resistance are still not clear (Regesta *et al.*, 1999). The efflux multidrug transporters, notably P-glycoprotein (Pgp, also named ABCB1 or MDR1), are among the best studied candidates for contributing to drug resistance. Overexpression of Pgp in cancer cells contributes to cancer drug resistance (Gottesman *et al.*, 1988; Hennessy *et al.*, 2007; Juliano *et al.*, 1976). Pgp is physiologically expressed on the luminal membrane of capillary endothelium in the brain and plays an integral role in maintaining the functionality of the blood-brain barrier (BBB) via basolateral-to-apical transport of xenobiotics (Loscher *et al.*, 2005). Observations that Pgp is overexpressed in epileptic foci support the hypothesis that Pgp may contribute to drug-resistant epilepsy (Kwan *et al.*, 2005; Loscher *et al.*, 2005). The efflux function of Pgp in the BBB is also considered a possible reason for pharmacoresistance in the treatment of depression (Kato *et al.*, 2008; Kwan *et al.*, 2005; Weiss *et al.*, 2003a). If many AEDs are substrates of Pgp, the overexpression of Pgp could help to explain the drug resistance in epilepsy and in psychiatric disorders treated by AEDs. Therefore, it is important to study the Pgp substrate status of AEDs.

Carbamazepine (CBZ) and its structural analogs oxcarbazepine (OXC) and eslicarbazepine acetate (ESL) represent an important group of AEDs (Fig 4.1A), sharing a common mode of action by exerting voltage-dependent blockade of neuronal voltage-gated sodium channels (Kwan *et al.*, 2007b). Both CBZ and OXC

84

are widely used in the treatment of epilepsy, while ESL has been recently approved in Europe for this indication (Gil-Nagel *et al* , 2009). CBZ and OXC are also used to treat bipolar disorder, schizophrenia, and aggression (Hirschfeld *et al* , 2004; Hosak *et al* , 2002; Huband *et al*, 2010). OXC and ESL are 10-keto and 10-acetoxy-10,11-dihydro analogs of carbamazepine respectively. The major metabolic pathway for CBZ is the formation by CYP3A4 of the major stable active metabolite carbamazepine-10,11-epoxide (CBZ-E), which reaches a steady-state of about 10-20% of the plasma concentration of CBZ (Klotz, 2007; Kudriakova, 1992; Winnicka *et al* , 2002). OXC is a prodrug which is metabolized to its active monohydroxylated derivative (MHD), namely S-licarbazepine (S-LC, also known as S-MHD or S-OH-CBZ) (80%) and R-licarbazepine (20%), while ESL is predominantly reduced to S-LC (Bialer *et al* , 2010; McCormack *et al* , 2009).
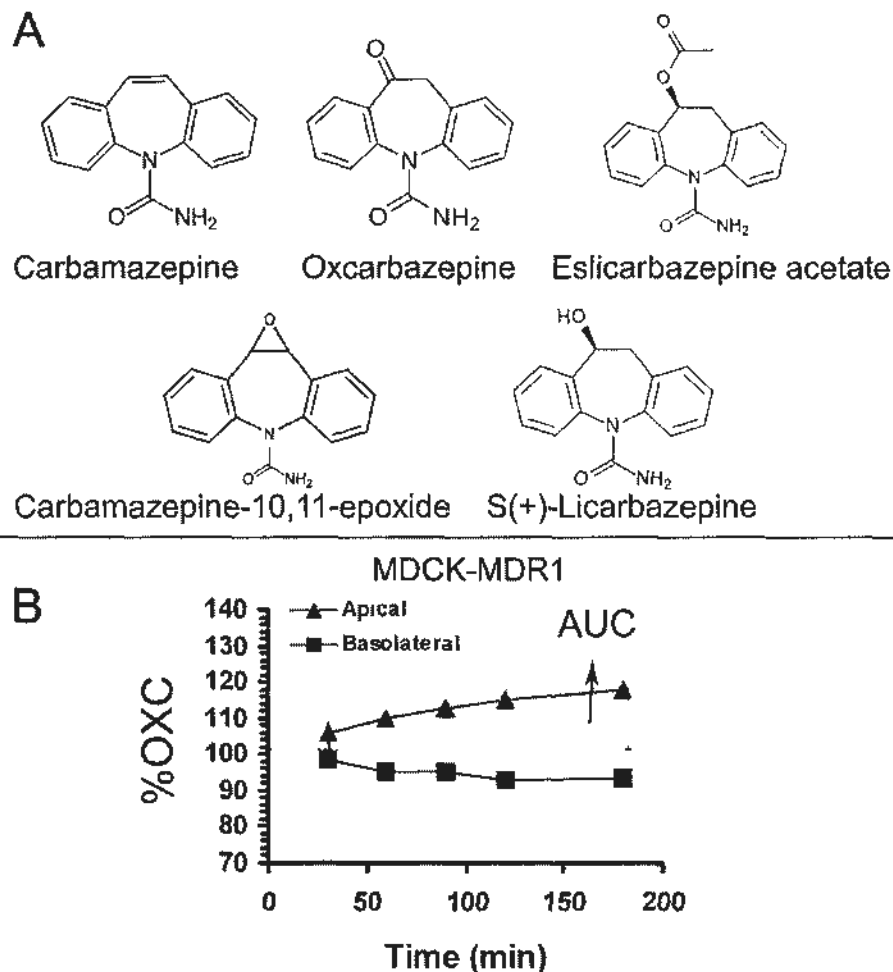
Fig 4.1 Chemical structures of studied AEDs and illustration of the method of calculation of the AUC of AEDs transported by Pgp

There is conflicting evidence whether CBZ and CBZ-E are transported by Pgp. In microdialysis rat models, the concentration of CBZ in the extracellular fluid of the cerebral cortex was enhanced by verapamil, an inhibitor of Pgp (Potschka *et al.*, 2001a), indicating that Pgp is involved in the regulation of brain concentrations of CBZ. However, the hippocampal concentration of CBZ was not affected by Pgp inhibition or overexpression of Pgp in the brains of rats refractory to phenytoin (Höcht *et al.*, 2009). There were no differences in whole brain CBZ levels in *mdr1ab(-/-)* or *mdr1a(-/-)* mice versus wild-type mice (Owen *et al.*, 2001; Sills *et al.*, 2002), although hippocampal concentrations of CBZ and CBZ-E in *mdr1ab(-/-)* mice were significantly higher (Rizzi *et al.*, 2002). Human *in vivo* studies showed that concentrations of CBZ in extracellular space of the epileptogenic temporal lobe were significantly lower than those in subarachnoid cerebrospinal fluid from patients with intractable epilepsy (Rambeck *et al.*, 2006), but whether this was related to Pgp transport was unknown. In *in vitro* interaction studies, CBZ has been found to inhibit Pgp efflux function inconsistently,[28-30] and no Pgp mediated transport of CBZ in various monolayer models was demonstrated (Baltes *et al.*, 2007b; Crowe *et al.*, 2006; Luna-Tortos *et al.*, 2008b; Owen *et al.*, 2001).

Relatively fewer studies have investigated whether OXC and its derivative are substrates of Pgp, although the findings were more consistent. OXC concentration in extracellular fluid in rat hippocampus was increased by verapamil (Clinckers *et al.*, 2005). Microdialysis study in humans showed that the 10-OH-CBZ brain-plasma concentration ratio and the mRNA level of *MDR1* in brain are inversely linearly correlated in patients with OXC-resistant epilepsy (Marchi *et al.*, 2005). In LoVo/dx cells (human colon adenocarcinoma cells), the 10-OH-CBZ concentration could be increased by the Pgp inhibitor XR9576 (Marchi *et al.*, 2005). Whether ESL and its active metabolites are transported by Pgp has not been studied.

It has been shown that Pgp substrate status may be species specific, and results from *in vitro* models may be affected by the high passive diffusion of the AEDs (Baltes *et al.*, 2007b; Marchi *et al.*, 2005). Using the concentration equilibrium transport assay (CETA), which is highly sensitive and can avoid the effect of high passive diffusion, we have previously shown that phenytoin and phenobarbital are transported by human

Pgp in a dose dependent fashion (Zhang *et al.*, 2010). In the present study, we employed both bi-directional and concentration equilibrium transport assays to determine whether CBZ, OXC, ESL, CBZ-E, and S-LC were transported by human Pgp.

4.2   Materials and methods

4.2.1 Drugs

CBZ, CBZ-E, ESL, MTT (3-[4,5 dimethyl thiazolyl-2]-2,5-diphenyltetrazolium bromide), and Rho123 were supplied by Sigma Aldrich (St. Louis, MO, USA). OXC was obtained from the National Institute for the Control of Pharmaceutical and Biological Products (Beijing, China). S-LC was purchased from Toronto Research Chemicals Inc. (North York, Ontario, Canada). Verapamil was provided by Alexis Biochemicals (San Diego, CA, USA). Tariquidar was kindly provided by Dr. Kenneth To (The Chinese University of Hong Kong, Hong Kong). Verapamil and MTT were dissolved in water, and other drugs were dissolved in DMSO (<0.1% DMSO in final solution). CBZ, CBZ-E and S-LC were tested at concentrations covering the ranges of therapeutic plasma concentrations (Marchi *et al.*, 2005; Martin J Brodie, 2005; McCormack *et al.*, 2009; Winnicka *et al.*, 2002). All other chemicals were analytical grade.

4.2.2 LLC and MDCK cell monolayer models

4.2.2.1 Cell culture

LLC (LLC-WT), MDCKII (MDCK-WT), and their human *MDR1* gene transfected cell lines (LLC-MDR1 and MDCK-MDR1) were kindly provided by Professor P. Borst (The Netherlands Cancer Institute, Amsterdam, Netherlands). Cell culture was performed as described previously (Bakos *et al.*, 1998; Zhang *et al.*, 2011).

4.2.2.2 Validation of cell monolayer in MDCK and LLC cell lines

Integrity of monolayers was verified by atenolol (paracellular marker) and propranolol (transcellular marker). The bi-directional transport assays of atenolol and propranolol were performed by measuring the apparent permeability (P_{app}) as described previously (Crespi *et al.*, 2000; Thiel-Demby *et al.*, 2008; Wang *et al.*, 2008; Zhang *et al.*, 2011).

4.2.2.3 Cytotoxicities of tested AEDs to LLC and MDCK cells

The potential cytotoxicities of the tested compounds on the cell lines were evaluated by MTT as described before (Han *et al.*, 2008; Zhang *et al.*, 2011). Briefly, 1.5×10^4 cells/well were seeded in 96 well plates and cultured for 48 hr. After withdrawing the culture medium, 200 μl PBS buffer with various concentrations of AEDs was added and incubated for 3 hr. Buffer was then replaced with 200 μl of 0.5 mg/ml MTT in PBS and incubated for another 3 hr. The solution was replaced with 200 μl DMSO, and the absorbance was determined at a wavelength of 590 nm on the microplate reader (Benchmark, BioRad, USA).

4.2.2.4 Transport assay of AEDs

The transport assays were conducted in two ways: the concentration equilibrium transport assay (CETA) and bi-directional transport assay described previously (Zhang *et al.*, 2010; Zhang *et al.*, 2011). Briefly, culture medium was replaced with warm PBS buffer for 10 minutes before transport assays. For CETA, drug was added to both sides of monolayers at equal concentrations. Volumes on apical and basolateral sides were 2 ml and 2.7 ml, respectively. Studied drug concentrations were 2 μg/ml and 10 μg/ml for CBZ-E; 5 μg/ml, 10 μg/ml, and 20 μg/ml for CBZ and OXC; and 10 μg/ml for ESL and S-LC. Aliquots of 100 μl and 130 μl from the apical and basolateral side, respectively, which did not affect the hydrostatic pressure on monolayers, were collected at various time points of drug exposure (30, 60, 90, 120, and 180 min). The above transport assays were repeated in the presence of the Pgp inhibitors tariquidar (2 μM) or verapamil (100 μM).

In bi-directional transport assays, drug was added to either the apical side (1.5 ml of transport buffer) or basolateral side (2.6 ml of transport buffer) of the monolayer at 10 μg/ml initially. Aliquots of 0.5 ml samples were taken from the other side (receiver chamber) at different time intervals (30, 60, 90, 120 min). The same volume of fresh PBS buffer was added to the receiver chamber after each sampling. The apparent permeability (P_{app}) of drug across the monolayer was calculated. All transport assays were performed in triplicate. The collected samples were stored at -20°C until analysis.

4.2.3 Rhodamine-123 uptake assay and flow cytometry

To confirm the functional activity of Pgp, Rho123 uptake assays were performed as described previously, with minor modifications (Kimchi-Sarfaty *et al.*, 2007; Zhang *et al.*, 2011). Briefly, 3×10^5 cells were collected by trypsin and washed once with warm PBS. Then, cells were resuspended in 1 ml DMEM containing 5% FBS and Rho123 (1 μg/ml) followed by incubation at 37°C for 20 min. The cells were centrifuged and resuspended in 300 μl cold PBS. Flow cytometry analysis of Rho123 fluorescence at 585 nm was performed with the BD FACSAriaII (Becton Dickinson, San Jose, CA).

4.2.4 Drug analysis

CBZ, CBZ-E, OXC, S-LC, and ESL were quantified by high performance liquid chromatography with UV detection (HPLC/UV) as described before (Marchi *et al.*, 2005; Zhang *et al.*, 2010; Zhang *et al.*, 2011). An HPLC system (Waters, Milford, MA, USA) equipped with a 2695 solvent delivery module, a Thermo Hypersil BDS C18 column (5 μM pores, 250 mm × 4.6 mm inner diameter), and a 996 photodiode-array (PDA) UV detector was used. The mobile phase consisted of 20 mM NaH_2PO_4 in water and acetonitrile (65:35 for CBZ, CBZ-E, OXC, and ESL; 74:26 for S-LC). The limits of quantification (LOQ) were 50 ng/ml for CBZ, CBZ-E, and OXC; and 30 ng/ml for ESL and S-LC. The relative standard deviation (R.S.D.) of both intra-day and inter-day precision for all the drugs were below 5%.

4.2.5 Data analysis

For Rhodamine-123 uptake, fluorescence values for LLC-MDR1, MDCKII, and MDCK-MDR1 cells were scaled to the median fluorescence value of LLC cells, which was defined as 100.

The apparent permeability value (P_{app}) was calculated as described previously using the following equations (Zhang *et al.*, 2010; Zhang *et al.*, 2011): $P_{app} = [(dC/dt \times V)]/(A \times C)$, dC/dt = change of the drug concentration in the receiver chambers over time; V = volume of the solution in the receiver chamber; A = membrane surface area; C = loading concentration in the donor chamber. The transport ratio (TR) was calculated as $P_{app\ b\text{-}A} / P_{app\ a\text{-}B}$. The corrected transport ratio (cTR) was calculated as TR (MDR1-transfected cells) / TR (non-transfected cells).

Results for individual transport assays in CETA are presented as the percentage of the drug loading concentration vs. time (Zhang *et al.*, 2010; Zhang *et al.*, 2011). Differences of drug concentration between the apical and basolateral chambers of each well were compared. An increase in drug concentration in the apical chamber compared with the basolateral chamber indicated the presence of basolateral-to-apical transport.

When the drug was transported to the apical chamber by Pgp, the concentration increased above the initial concentration (>100%) over time. To compare the extent of transport among drugs, area under the percentage increase of drug concentration vs. time curves (AUC) in the apical chamber were calculated (Fig 4.1B). The equation was: AUC = percentage above the initial concentration × time (min) (Luna-Tortos *et al.*, 2008b).

All the data were shown as means ± SD. Significant differences between two groups or more than two groups were evaluated by student's t-test or one-way ANOVA, respectively, with $p < 0.05$ considered significant.

4.3 Results

4.3.1 Validation of cell monolayer in LLC and MDCK cell lines

Integrity of the monolayer system of all four cell lines (LLC, LLC-MDR1, MDCKII, and MDCK-MDR1) was verified by testing that the apparent permeability values of atenolol and propranolol. The P_{app} values for atenolol and propranolol were within the range of 0.6×10^{-6} to 1.2×10^{-6} cm/s and 20×10^{-6} to 30×10^{-6} cm/s respectively, which were comparable to those previously published (Crespi et al., 2000; Thiel-Demby et al., 2008; Wang et al., 2008)

4.3.2 Cytotoxicities of AEDs to LLC and MDCK cells

MTT assays indicated that concentrations of AEDs tested were not toxic to the four cell lines (Fig 4.2).
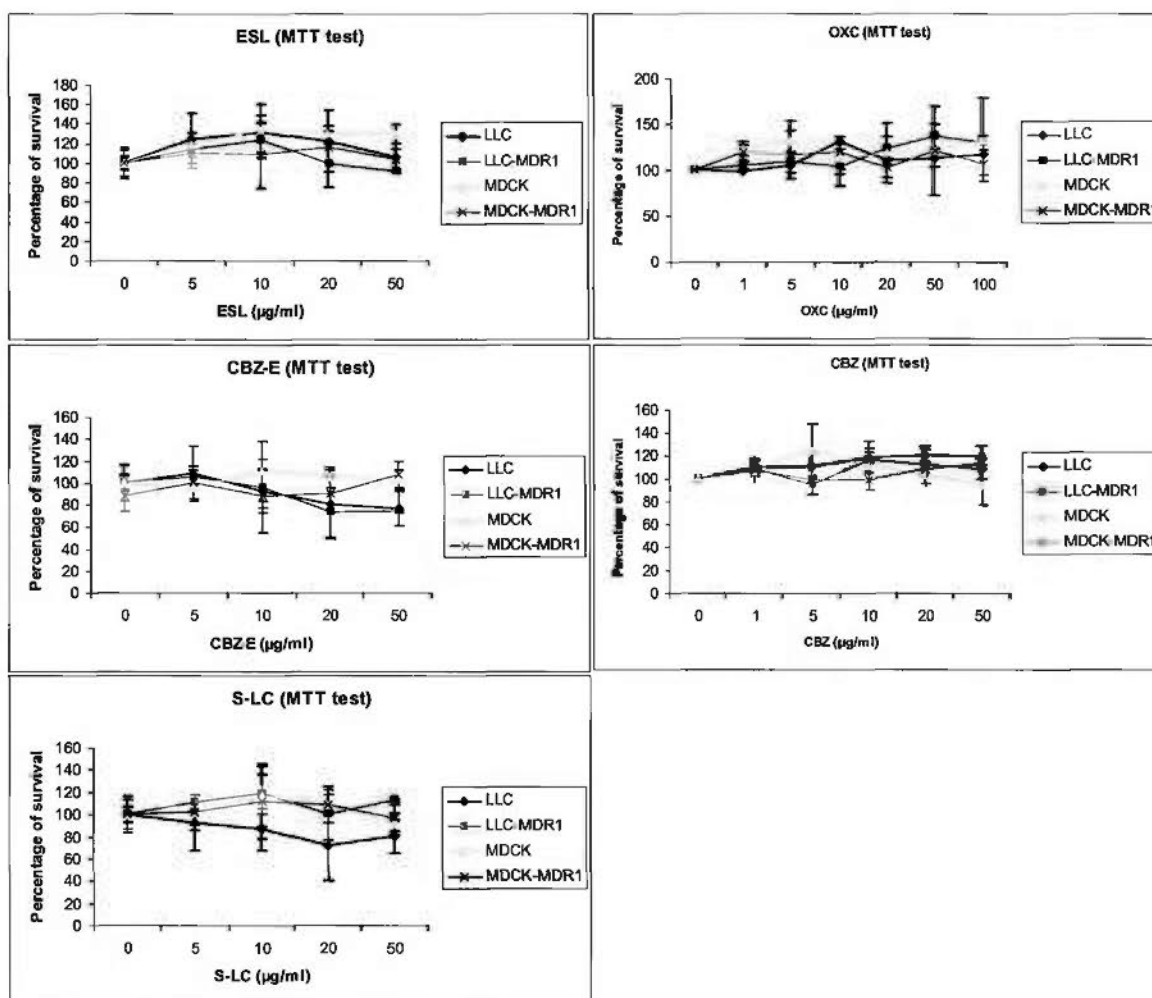
Fig 4.2   Cytotoxicities of CBZ, CBZ-E, OXC, ESL, and S-LC for LLC, LLC-MDR1, MDCK, and MDCK-MDR1 cells

4.3.3 Stabilities of tested AEDs in transport buffer

The stabilities of AEDs in transport buffer were performed and described in chapter two. As shown in Fig 4.3 and Table 2.3, after incubation for 2 hr and 4 hr, the percentages of tested AEDs remaining were around 100%, indicating that these compounds are stable at 37°C in the transport buffer for at least 4 hr. The drugs were also tested at room temperature in an auto-sampler for 48 hr, and they were also stable (Table 2.4).
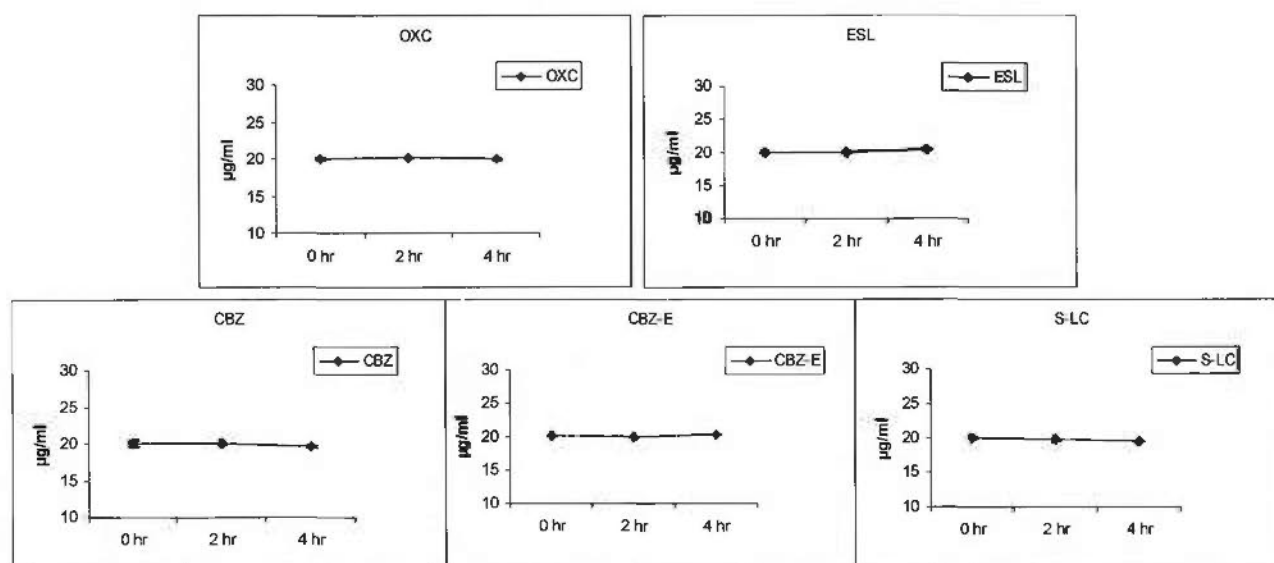
Fig 4.3 Stabilities of tested AEDs in transport buffer at 37°C

4.3.4 Rhodamine-123 uptake of AEDs in cells

The functional activity of MDR1 in the tested cell lines was detected by the Rho123 uptake assay. Rho123 is a substrate of Pgp. The decrease of fluorescent density in MDR1-transfected cells indicated the efflux function of Pgp. Densities of Rho123 in LLC-MDR1, MDCKII, and MDCK-MDR1 cells were 16%, 81%, and 26% of the values in LLC wildtype cells respectively (Fig 4.4A & B). Differences in Pgp level in these four cell lines were also confirmed by accumulation of Rho123 (Fig 4.4A & B). The differences between MDCK-MDR1 and LLC-MDR1, LLC-MDR1 and LLC, and MDCK-MDR1 and MDCK, were significant ($p < 0.05$).
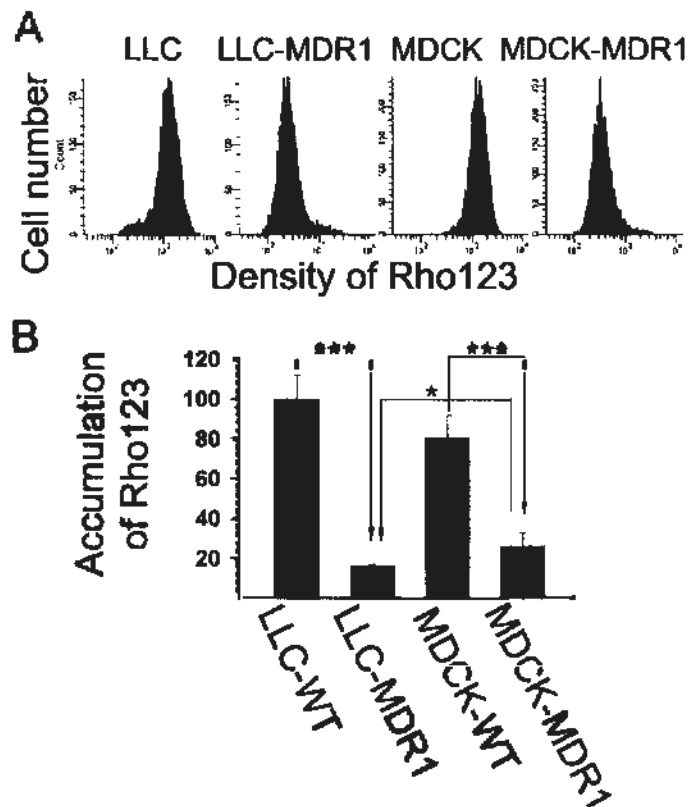
Fig 4.4 **Rhodamine-123 accumulation in LLC and MDCK wild type and MDR1-transfected cell lines.** (A) The density of Rho123 was detected by flow cytometry. (B) Relative fluorescence values (shown as mean ± SD) in LLC-MDR1, MDCKII, and MDCK-MDR1 cells were compared with LLC cells (whose median fluorescence levels were defined to be 100) (n=3, *$p<0.05$ ***$p<0.001$).

4.3.5 Results from transport assay of tested AEDs

In concentration equilibrium conditions for CBZ at 10 μg/ml, there was no significant difference between the apical and basolateral concentrations at any time point of drug exposure in both wildtype and MDR1-transfected cell lines (Fig 4.5A), indicating lack of transport by Pgp. CBZ at 5 and 20 μg/ml also exhibited no transport (data not shown). Interestingly, CBZ-E, the major active metabolite of CBZ, was found to be transported by Pgp in MDCK-MDR1 and LLC-MDR1 cells (Fig 4.5B & C). At 10 μg/ml, the concentration of CBZ-E in the apical side became significantly higher than that in the basolateral side from 60 minutes of drug exposure onward for MDR1-transfected cells. With addition of tariquidar and verapamil, typical Pgp inhibitors, such concentration differences between the apical and basolateral sides were

eliminated (Fig 4.5B). At 2 μg/ml, CBZ-E was still transported by LLC-MDR1 cells, while transport by MDCK-MDR1 cells was not significant (Fig 4.5C).
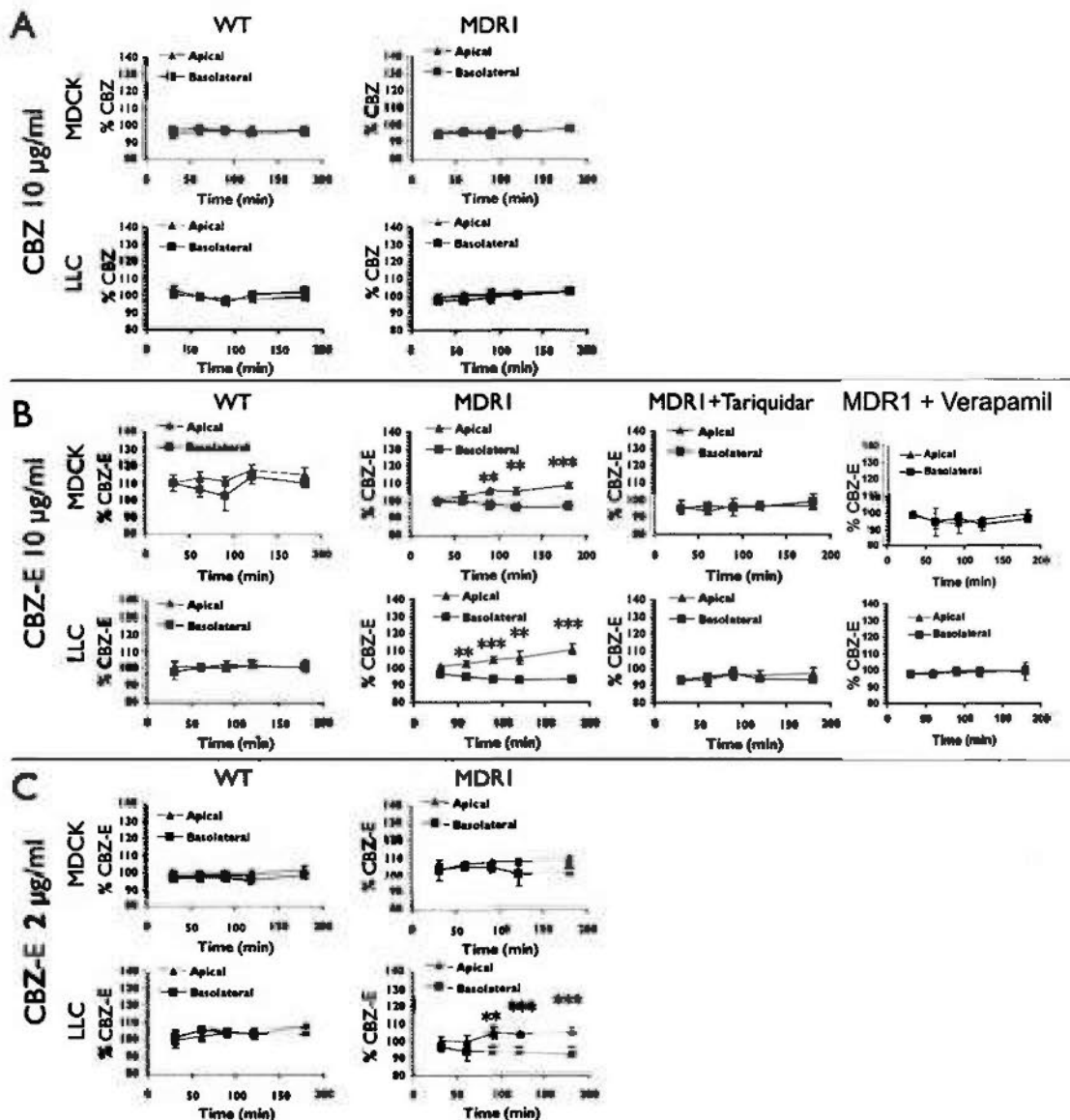
Fig 4.5   **Concentration equilibrium transport assays of carbamazepine (CBZ) and carbamazepine-10,11-epoxide (CBZ-E) for MDCKII and LLC cells transfected with the human MDR1 gene or for wildtype (WT) cells.** (A) CBZ was not significantly transported by either MDCK-MDR1 or LLC-MDR1 cells when the initial CBZ concentration was 10 μg/ml. (B) CBZ-E was transported by MDCK-MDR1 and LLC-MDR1 cells when the initial concentration was 10 μg/ml. The transport was inhibited by tariquidar (2 μM). (C) CBZ-E was transported by LLC-MDR1 cells when the initial concentration was 2 μg/ml, but the difference between apical and basolateral concentrations did not reach significance in MDCK-MDR1 cells. Data are given as the percentage of the initial drug concentration in either apical or basolateral chamber vs. time. Experiments were performed in

triplicate, and values are shown as mean ± SD. Significant differences in drug concentrations between the two chambers are indicated by asterisks (n=3, $^+p<0.05$, $^{**}p<0.01$, $^{***}p<0.001$).

OXC and ESL are analogs of CBZ, and S-LC is their major active metabolite (Kwan *et al.*, 2007b). We determined their substrate status for Pgp at/or around their typical plasma concentrations. Because OXC and ESL are rapidly reduced to their metabolites, their plasma concentrations are under the limit of quantification. We tested OXC and ESL at 10 μg/ml. The concentration of OXC in the apical side of MDR1-transfected cells became significantly higher than that in the basolateral side from 60 minutes of drug exposure onward, and such difference in concentration was almost completely inhibited by tariquidar and verapamil (Fig 4.6A). ESL was also transported by Pgp, which could also be inhibited by tariquidar and verapamil in MDR1-transfected cells (Fig 4.6B). Wildtype MDCK and LLC cell lines did not transport OXC or ESL, which further verified that they were transported by human Pgp (Fig 4.6A & B).

Similar to the parent drugs, S-LC at 10 μg/ml was significantly transported from basolateral to apical sides of LLC-MDR1 and MDCK-MDR1 cells. Such transport could also be inhibited by tariquidar and verapamil. No significant basolateral to apical transport of S-LC by wildtype cells was found (Fig 4.6C).
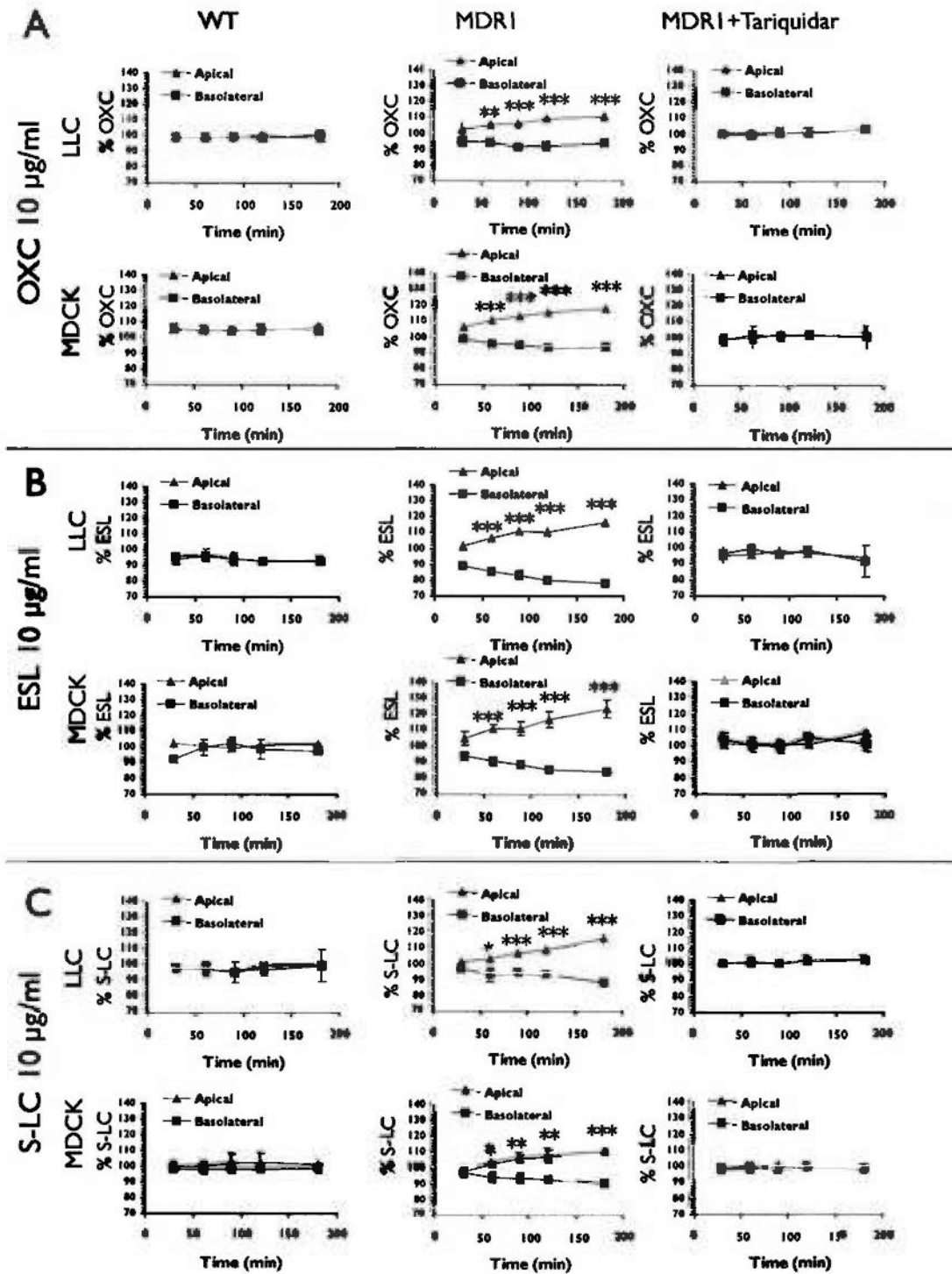
Fig 4.6   Concentration equilibrium transport assays of oxcarbazepine (OXC), eslicarbazepine acetate (ESL), and S-licarbazepine (S-LC) for wildtype (WT) MDCKII and LLC-PK1 cells or cells transfected with the human MDR1 gene. OXC (A), ESL (B), and S-LC (C) were transported by MDCK-MDR1 and LLC-MDR1 cells when the initial concentration was 10 μg/ml. The transport was inhibited by tariquidar (2 μM). Data are given as the percentage of the initial drug

concentration in either apical or basolateral chamber vs. time. Experiments were performed in triplicate, and values are shown as mean ± SD. Significant differences in drug concentrations between the two chambers are indicated by asterisks (*$p<0.05$, **$p<0.01$, ***$p<0.001$).

To compare the extent of basolateral-to-apical transportation of drugs in MDR1-transfected cells, we calculated the AUC of the percent increase vs. time in the apical chamber. It was demonstrated that the AUC for the drugs was in the order of ESL > OXC > S-LC > CBZ-E (Table 4.1 and Fig 4.7). The extent of inhibition of drugs by tariquidar and verapamil was determined (Table 4.1).
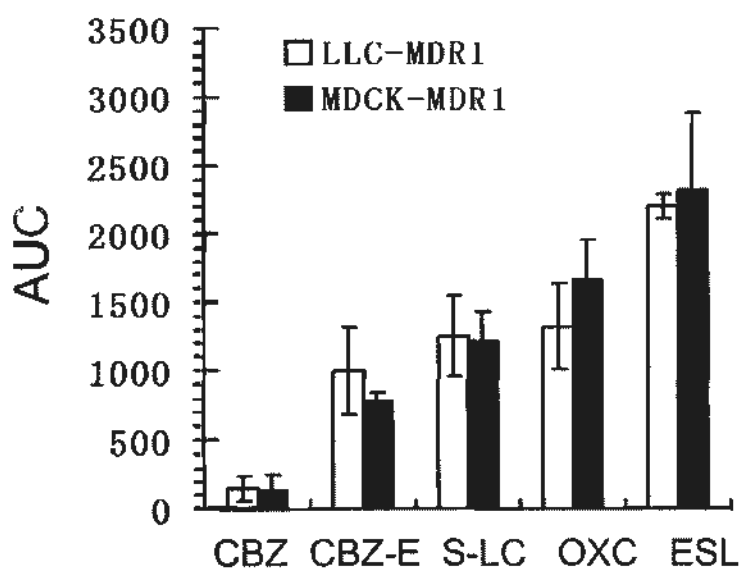
Fig 4.7   **Comparison of extent of transport of AEDs by LLC-MDR1 and MDCK-MDR1 cells.** The transport of drugs was estimated by the area under the excess drug concentration vs. time curves (AUC) in apical chambers. Excess drug concentration was calculated as the level above the initial concentration (as a percentage). Time was in units of minutes. Transport inhibition by tariquidar and verapamil was calculated based on AUC values. Experiments were performed in triplicate, and values are shown as mean ± SD.

Table 4.1   Comparison of the extent of transport by LLC-MDR1 and MDCK-MDR1 cells in concentration equilibrium transport assays

Drug/metabolite	LLC-MDR1 cells			MDCK-MDR1 cells		
	AUC	Inhibition by verapamil (%)	Inhibition by tariquidar (%)	AUC	Inhibition by verapamil (%)	Inhibition by tariquidar (%)
Carbamazepine-10, 11-epoxide	1004±312	88	80	779±61	95	100
(S)-licarbazepine	1260±297	74	90	1215±224	72	91
Oxcarbazepine	1324±316	94	92	1670±296	100	92
Eslicarbazepine acetate	2208±90	100	100	2327±555	96	99

The transport of drugs was estimated by the area under the excess drug concentration *vs.* time curves per hour (AUC) in apical chambers. Excess drug concentration was calculated as the level above the initial concentration (as a percentage). Transport inhibition by verapamil was calculated based on AUC values. Experiments were performed in triplicate, and values are shown as mean ± SD.

In the bi-directional transport assay, the above drugs were tested in LLC-WT and LLC-MDR1 cells. A drug was added to the apical or basolateral side at 10 μg/ml, and the P_{app} values of apical to basolateral (a-B) or basolateral to apical (b-A) were calculated, respectively. The data is shown in Table 4.2. Transport ratios of CBZ-E, OXC, ESL, and S-LC in LLC-MDR1 cells were significantly higher than in LLC-WT cells, confirming the results of the concentration equilibrium transport assay. As shown in Fig 4.8 and Table 4.2, corrected transport ratios were 1.35, 1.56, 1.66, and 2.02 respectively, while the cTR of CBZ was 1.03. As previously published, cTR>1.5 was considered as active asymmetrical transport (Schwab *et al.*, 2003). cTRs of OXC, ESL, and S-LC were larger than 1.5, indicating that they were transported from the basolateral to the apical side by Pgp in concentration gradient conditions. The cTR of CBZ-E was 1.35, but TRs significantly differed between MDR1-transfected and non-transfected cells, indicating that CBZ-E was a weak substrate of Pgp.
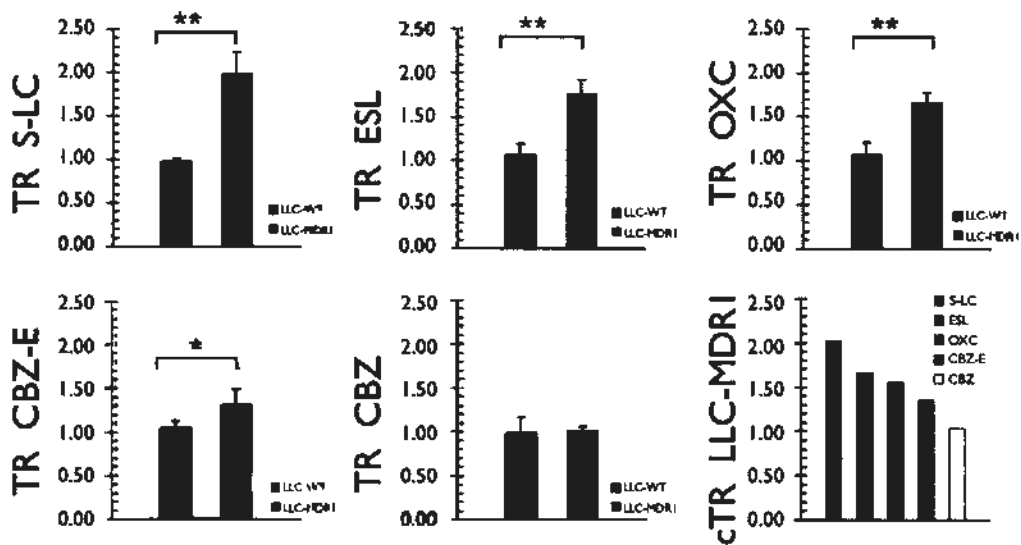
Fig 4.8   **Transport ratio (TR) and corrected transport ratio (cTR) of AEDs by LLC-WT and LLC-MDR1 cells.** For each drug, the TR was compared between LLC-WT and LLC-MDR1 cell lines. For each cell line, the cTRs of different drugs were compared. Experiments were performed in triplicate, and data are shown as mean ± SD (n=3, $*p<0.05$, $**p<0.01$).

Table 4.2 Summary of the transport of drugs by LLC-WT and LLC-MDR1 cells in bi-directional transport assays

Drug/metabolite		LLC-WT cells			LLC-MDR1 cells			
		P_{app} (cm/s)		TR	P_{app} (cm/s)		TR	cTR
		A-B	B-A		A-B	B-A		
(S)-licarbazepine	Mean	6.50E-06	6.36E-06	0.98	5.25E-06	1.03E-05	1.98	2.02
	SD	3.22E-07	3.13E-07	0.04	4.69E-07	4.46E-07	0.25	
Carbamazepine-10, 11-epoxide	Mean	1.47E-05	1.54E-05	1.05	1.20E-05	1.69E-05	1.41	1.35
	SD	6.54E-07	5.29E-07	0.08	1.22E-06	1.24E-06	0.17	
Carbamazepine	Mean	1.96E-05	1.91E-05	0.99	1.74E-05	1.85E-05	1.02	1.03
	SD	2.12E-06	1.85E-06	0.19	1.87E-06	1.98E-06	0.04	
Eslicarbazepine acetate	Mean	1.45E-05	1.53E-05	1.06	1.08E-05	1.89E-05	1.76	1.66
	SD	7.33E-07	1.57E-06	0.13	2.32E-07	1.31E-06	0.16	
Oxcarbazepine	Mean	1.70E-05	1.81E-05	1.07	1.28E-05	2.13E-05	1.67	1.56
	SD	1.64E-06	9.05E-07	0.13	7.06E-07	5.53E-07	0.11	

Bidirectional transport assays of drugs by LLC-WT and LLC-MDR1 cells. The P_{app} values of drugs in the apical to basolateral (A-B) and basolateral to apical (B-A) directions were calculated using the equation described in Materials and methods. The transport ratio (TR) was calculated as $P_{app\ B-A} / P_{app\ A-B}$, and the corrected transport ratio (cTR) was calculated as the TR of LLC-MDR1 cells divided by the TR of LLC wild type cells. Experiments were performed in triplicate (n=3).

4.4   Discussion

Efflux transport of AEDs from the brain by Pgp is one of the potential mechanisms of drug resistance. This hypothesis is supported by evidence that the brain expression of Pgp is markedly increased at epileptic foci in patients with refractory epilepsy (Kwan *et al.*, 2005; Loscher *et al.*, 2005; Tishler *et al.*, 1995). In addition, lack of Pgp expression increases the brain concentration of an antidepressant drug, and *MDR1* gene polymorphisms were associated with refractory depressive disorder (Kato *et al.*, 2008; Uhr *et al.*, 2000). However, the weak link in the hypothesis is definitive evidence that Pgp transports AEDs and their active metabolites at therapeutic concentrations. The present data provide further direct evidence on whether CBZ and other structurally related AEDs (OXC and ESL) and their major active metabolites (CBZ-E and S-LC) are transported by Pgp at clinically relevant concentrations. Using polarized cell monolayers in concentration equilibrium transport assays, results suggested that OXC, ESL, CBZ-E, and S-LC are transported by human Pgp, but CBZ is not.

In previous studies, CBZ inhibited Pgp efflux of CAM and Rho123 by MDR1 transfected LLC and 293 cells, respectively (Hung *et al.*, 2008; Weiss *et al.*, 2003b). But CBZ was not transported by Pgp in Caco-2, LLC-MDR1, or MDCK-MDR1 cells (Baltes *et al.*, 2007b; Crowe *et al.*, 2006; Luna-Tortos *et al.*, 2008b). In line with most previous *in vitro* and *in vivo* studies, we found that CBZ was not transported by LLC-MDR1 and MDCK-MDR1 cells when tested at a wide range of concentrations (5, 10, and 20 µg/ml), confirming that it is not a substrate of Pgp. Therefore, CBZ may be a weak, non-transported inhibitor of Pgp.

Interestingly, we found evidence that CBZ-E, the major active metabolite of CBZ, was transported by Pgp in the CETA. The transport of CBZ-E at 10 µg/ml was inhibited by tariquidar and verapamil, and there was no significant transport by wildtype cells, indicating that CBZ-E is a substrate of Pgp. In bi-directional transport, the TR of CBZ-E at 10 µg/ml by LLC-MDR1 cells was significantly higher than by LLC-WT cells (Fig 4.8 & Table 4.2). The cTR was 1.35, which was lower than 1.5, indicating that the substrate

status was weak (Table 4.2) (Schwab *et al.*, 2003). Post *et al.* reported that the CSF concentration of CBZ-E is positively correlated with the degree of clinical efficacy in acute antidepressant and antimanic treatment (Post *et al.*, 1983). Under steady state conditions, plasma CBZ-E concentrations range from 10% to 50% of those of the parent drug (Spina, 2002). Therefore transport of CBZ-E by Pgp might be relevant to CBZ drug resistance. When tested at the lower concentration of 2 μg/ml in the CETA, which is in the range of plasma concentrations found in patients (Winnicka *et al.*, 2002), CBZ-E demonstrated significant basolateral to apical transport by LLC-MDR1 cells, but transport by MDCK-MDR1 cells was not significant (Fig 4.5C). Compared with LLC-MDR1 cells, the protein level of Pgp in MDCK-MDR1 cells appeared to be lower (as shown in Fig 3.2), with a corresponding greater accumulation of Rho123 (Fig 4.4A & B), indicating that MDCK-MDR1 cells had lower Pgp activity. This might account for the failure to detect significant transport of low dose CBZ-E in MDCK-MDR1 cells.

There has been no report on whether the CBZ derivatives, ESL and OXC, are substrates of Pgp, except for indirect *in vivo* evidence from a study reporting increased OXC concentration in hippocampus of animals treated with verapamil (Clinckers *et al.*, 2005). We demonstrate *in vitro* that ESL and OXC are transported by Pgp (Fig 4.6A & B and Fig4.8). Pgp plays important roles not only in limiting entry of various drugs into the central nervous system but also in drug absorption and excretion in the intestinal, biliary, and urinary tracts (Giacomini *et al.* 2010). Pgp also increases drug metabolism by CYP3A in the intestine (Giacomini *et al.*, 2010; Lown *et al.*, 1997; Zhang *et al.*, 2001). Although ESL and OXC are rapidly metabolized by the liver, their Pgp substrate status may still be clinically important because it may affect intestinal absorption and thus the metabolic rate and efficacy. S-LC is the major active metabolite of OXC and ESL. We demonstrated that, at a clinically relevant concentration, S-LC was transported by MDCK-MDR1 and LLC-MDR1 cells (Fig 4.6C and Fig 4.8), consistent with previous *in vivo* and *in vitro* studies which tested the mixture of S- and R-licarbazepine (Marchi *et al.*, 2005; Rambeck *et al.*, 2006).

Based on the AUC values for the four substrates, CBZ-E had the least transport and ESL had the greatest transport by Pgp (Fig 4.7 and Table 4.1). Clinical studies demonstrated that, in treatment of the acute manic and depressive symptoms of bipolar disorder, CBZ and OXC have efficacy comparable to lithium and haloperidol (Hirschfeld *et al.*, 2004), although OXC is more effective and better tolerated than CBZ as adjunctive therapy to lithium in treatment of bipolar disorder patients (Juruena *et al.*, 2009). The differences in transport of CBZ, OXC, and S-LC by Pgp might account for the differences in add-on therapy efficacy found in the clinic. There is currently research on the potential use of ESL, S-LC, and other related compounds for treatment of schizoaffective disorder, bipolar disorder, and other neuropsychiatric disorders.

Despite the availability of animal *in vivo* models such as microdialysis, *in vitro* models have an important role to play in determining substrate status of a compound because it allows directly testing of human Pgp with relatively high throughput. MDCK or LLC cell monolayers are less hydrophobic, less rigid, and more fluid than the BBB in situ, which may cause lack of correlation in predicting the *in vivo* substrate status from *in vitro* results (Di *et al.*, 2009). Compared with the results of 31 CNS drugs between the transwell model of *MDR1* transfected MDCKII cells and *in vivo* data of *MDR1* knockout mice, Feng et.al. found that the transwell assay was more specific but slightly less sensitive (Feng *et al.*, 2008).

These data suggest that resistance to carbamazepine, oxcarbazepine, or eslicarbazepine acetate may be attributed to increased efflux function of Pgp because they or their active metabolites are Pgp substrates. Since CBZ is not a substrate itself, it might be more effective than OXC or ESL and can be used for monotherapy.

It is tempting to speculate whether the substrate status of the compounds tested can be predicted based on knowledge of their structure-activity relationships (SAR) (Hsiao *et al.*, 2008; Raub, 2006; Wang *et al.*, 2003). There are limited reports on the SAR between AEDs and their Pgp substrate status (Knight *et al.*, 1998). CBZ and its analogs tested here have the identical dibenzazepine nucleus but differ at the 10,11-position (Fig 4.1). Our

104

results showed that these compounds, with the exception of CBZ itself, are substrates for Pgp, which might imply that epoxide, acetate, hydroxyl, or ketone groups at the 10,11-position could affect the substrate status of dibenzazepine compounds. Thus, to avoid export from their targeted sites of action, new AEDs that lack such structures might be designed.

4.5 Conclusion

In conclusion, this study provided direct *in vitro* evidence that CBZ-E, ESL, OXC, and S-LC, but not CBZ, are substrates of human Pgp. Resistance to CBZ, OXC, or ESL may result from increased efflux function of Pgp because these drugs or their active metabolites are Pgp substrates.

Chapter Five

In vitro transport profile of new AEDs – lacosamide, rufinamide, pregabalin, and zonisamide – by human P-glycoprotein

5.1 Introduction

Epilepsy has been recognized for more than 3000 years. Even with modern pharmacotherapy, we still can not completely control this refractory disease. Although we have developed more than 20 antiepileptic drugs (AEDs) since the 1900s, the proportion of patients resistant to AEDs remains about 30-40% (Kwan *et al.*, 2000a), and the mechanism of pharmacoresistance to AEDs is still unclear. Overexpression of Pgp in cancer cells contributes to cancer drug resistance (Gottesman *et al.*, 1988; Hennessy *et al.*, 2007; Juliano *et al.*, 1976). P-glycoprotein (Pgp) is physiologically expressed on the lumenal membrane of capillary endothelium in the brain and plays an integral role in maintaining the functionality of the blood-brain barrier (BBB) via basolateral-to-apical transport of xenobiotics (Loscher *et al.*, 2005).

Previous data support the hypothesis that the efflux of antiepileptic drugs from the brain by P-glycoprotein is one of the mechanisms of drug resistance in epilepsy. Pgp is overexpressed in epileptic foci (Kwan *et al.*, 2005; Loscher *et al.*, 2005). Expression of Pgp is greater in drug-resistant than in drug-responsive patients (Dombrowski *et al.*, 2001; Tishler *et al.*, 1995). Some studies indicated that several AEDs are substrates or inhibitors of Pgp (Baltes *et al.*, 2007a; Baltes *et al.*, 2007b; Luna-Tortos *et al.*, 2008b; Weiss *et al.*, 2003b), implying that Pgp plays an important role in refractory epilepsy.

Researchers never give up the attempt to cure epilepsy, although it remains a big challenge. With many attempts to develop new drugs, several new generation antiepileptic drugs have been approved in recent years, including ESL (which was described in a previous chapter), zonisamide (ZNS), pregabalin (PGB), rufinamide (RFM), and lacosamide (LCM).

Zonisamide was first marketed in Japan and was later approved in the United States for treatment of partial seizures. It is a novel antiepileptic drug with a different structure than other AEDs (Table 1.5). ZNS blocks voltage-sensitive sodium channels and T-type calcium channels (Kothare *et al.*, 2008). It also may affect levels of neurotransmitters such as glutamate, GABA, acetylcholine, and dopamine (Kothare *et al.*, 2008).

ZNS is rapidly absorbed after oral administration, and the serum concentration reaches a maximum at 4-6 hours. The serum protein binding of ZNS is only 40-60%. The $t_{1/2}$ of ZNS is 50-70 hours (Johannessen *et al.*, 2006). ZNS exhibits linear pharmacokinetics and is extensively metabolized by acetylation, glucuronidation, and oxidation. ZNS is metabolized by CYP3A4 in the liver, and CYP inhibitors can significantly block the metabolism of ZNS (Johannessen *et al.*, 2006). The clinical data collected from Japan, European, and the United States show that it has efficacy in refractory partial and generalized epilepsy. The data also indicate that ZNS is more useful as monotherapy than polytherapy (Kothare *et al.*, 2008).

There have been only a few studies examining the substrate status of ZNS for Pgp *in vivo* or *in vitro*. In OS2.4/Doxo cells (canine osteosarcoma cells induced by exposure to doxorubicin to highly express Pgp), zonisamide (ZNS) did not affect the uptake of Rho123 (West *et al.*, 2007), suggesting that ZNS was not the substrate of Pgp. No evidence has been reported to indicate the relationship between the overexpression of Pgp and the concentration of ZNS in animal models or epileptic patients.

Pregabalin is a structural analogue of γ-amino butyric acid (GABA). PGB binds to voltage-gated calcium channel alpha (2)-delta subunits and reduces excitatory neurotransmitter release, and finally results in allosteric modulation of P/Q-type channels. It does not work by a GABAergic mechanism (Krasowski, 2010; Shneker *et al.*, 2005).

PGB is absorbed very rapidly and has excellent bioavailability. The concentration peaks in serum about 1 hour after oral administration. There is little protein binding and drug-

drug interaction in serum. Most of the PGB in the blood is not metabolized in the liver. Most of the unchanged PGB is excreted in urine. $T_{1/2}$ of PGB is 4.6-6.8 hours (Johannessen *et al.*, 2006). According to the clinical data, PGB is more effective than gabapentin and equally effective as lamotrigine at comparable doses (Baulac *et al.*, 2010; Delahoy *et al.*, 2010; Ryvlin *et al.*, 2008).

Lacosamide is a functionalized amino acid. It was approved in the United States and Europe. No precise mechanism of LCM has been established. It was found that LCM selectively enhanced slow inactivation of voltage-gated sodium channels with no effect on fast inactivation and may interact with collapsin response mediator protein-2 (Cross *et al.*, 2009).

The absorption of LCM is rapid and complete after oral administration, and the first-pass effect is limited. LCM reaches its maximum concentration in serum within 1-4 hours. The protein binding of LCM is about 15%, and $t_{1/2}$ is about 13 hours (Cross *et al.*, 2009). LCM has efficacy on partial seizures and is well tolerated (Kellinghaus, 2009).

Rufinamide is a novel AED with a triazole derivative structure. It prolongs the inactivated state of voltage-gated sodium channels. It does not bind to receptors of monoamine, acetylcholine, NMDA, histamine, or GABA (Hussar *et al.*, 2009).

85% of RMF is absorbed after oral administration, and the absorption can be increased by food. The maximum concentration of RFM can be increased 50% by taking together with food. The half-life of RFM is about 6-10 hours (Perucca *et al.*, 2008). It is extensively metabolized by carboxylesterases. RFM has efficacy in partial seizures and Lennnox-Gastaut syndrome in adults (Palhagen *et al.*, 2001; Perucca *et al.*, 2008).

We have determined that PHT, PB, OXC, ESL, and the drug metabolites S-LC and CBZ-E are the substrate of Pgp. There was little evidence on the substrate status of ZNS for Pgp (West *et al.*, 2007), and there were no reports studying LCM, RMF, or PGB.

Therefore, using the concentration equilibrium transport assay, we studied whether they are substrates of Pgp.

5.2 Materials and methods

5.2.1 Drugs

ZSN, PGB, LCM, and RFM were supplied by 3B Pharmachem International Co., Ltd (Wuhan, China). Verapamil was provided by Alexis Biochemicals (San Diego, CA, USA). Tariquidar was kindly provided by Dr. Kenneth To (The Chinese University of Hong Kong, Hong Kong). Verapamil and MTT were dissolved in water, and other drugs were dissolved in DMSO (<0.1% DMSO in final solution). ZSN, PGB, LCM, and RFM were tested at concentrations covering the ranges of therapeutic plasma concentrations. Acetonitrile (Labscan Asia, Thailand), ethanol (TEDIA company, Inc., USA), and methanol (TEDIA company, Inc., USA) were HPLC grade. All other reagents were at least analytical grade. The water was deionized by Millipore water purification system (Millipore, Milford, USA).

5.2.2 LLC and MDCK cell monolayer models

5.2.2.1 Cell culture

LLC-PK1 (LLC-WT), MDCKII (MDCK-WT), LLC-MDR1 and MDCK-MDR1 cells were cultured as described in previous chapters and previous publications (Zhang *et al.*, 2010; Zhang *et al.*, 2011). All the cell lines were used within 10 passages after receipt. Six-well transwells (Transwell®, 0.4 μm, polycarbonate membrane, 24 mm insert, Corning, NY, USA) were used for the transport studies. The cells at densities of 2×10^6 (MDCK cells) or 1.5×10^6 (LLC cells) were seeded on the transwells as described previously (Luna-Tortos *et al.*, 2008a; Zhang *et al.*, 2007) followed by culturing in the relevant medium (MDCK: DMEM, 10% FBS, 100 U/ml penicillin-streptomycin; LLC:

Medium 199, 10% FBS, 100 U/ml penicillin-streptomycin) at 37°C with 5% CO_2 for 5 days. The medium was changed every day.

5.2.2.2 Cytotoxicities of PGB, LCM, RFM and ZNS to LLC and MDCK cells

Potential cytotoxicity of AEDs was tested by MTT assay as described in a previous chapter (Zhang *et al.*, 2010; Zhang *et al.*, 2011). Cells at a density of 1.5×10^4 cells/well were seeded in 96 well plates and cultured for 48 hr. After withdrawing the culture medium, 150 µl transport buffer with various concentrations of AEDs was added to each well and incubated for various times according to the periods of drug exposure in the transportation assays at 37°C in 5% CO_2. Then 20 µl of 5 mg/ml MTT was loaded to each well, followed by incubation for another 4 hr at 37°C in 5% CO_2. The buffer was removed and replaced with 200 µl DMSO in each well. The absorbance of each well in the plate was recorded at a wavelength of 590 nm on a microplate reader (Benchmark, BioRad, USA).

5.2.2.3 Validation of cell monolayer in LLC and MDCK cell lines

The validation of cell monolayers of LLC and MDCK cells was performed as described in previous chapters (Zhang *et al.*, 2010; Zhang *et al.*, 2011). Briefly, the integrity of the monolayer was monitored by measuring the transepithelial electrical resistance (TEER) with an epithelial volt/ohm meter (World Precision instruments, Inc., FL, USA). Only the monolayers with TEER>100 Ω cm^2 (subtracting the background value of a transwell) before and after the experiment were used for the transport assay. The integrity of the monolayer was also verified by atenolol (paracellular marker) and propranolol (transcellular marker). Only the monolayers with integrity values comparable with published data were used (Crespi *et al.*, 2000; Thiel-Demby *et al.*, 2008; Wang *et al.*, 2008).

5.2.2.4 Concentration equilibrium transport assay of PGB, LCM, RFM and ZNS in LLC and MDCK cell monolayer models

The concentration equilibrium transport assay was performed as described in previous chapters (Zhang *et al.*, 2010; Zhang *et al.*, 2011). Briefly, the volumes on the apical and basolateral sides of cell monolayers were 2 ml and 2.7 ml, respectively. Drugs were initially added to both sides of the monolayer at 10 μg/ml for ZNS, and at 5 μg/ml for PGB, LCM, and RFM. Aliquots of 100 μl apical and 130 μl basolateral samples, which did not affect the hydrostatic pressure on the cell monolayers, were collected at various time points of drug exposure (30, 60, 90, 120, 180 and 240 min). In order to test the effect of Pgp inhibition on AED transport, the above AED transport assays were conducted in the presence of verapamil (100 μM) or tariquidar (10μM). The collected samples were stored at -20°C until analysis.

5.2.2.5 Drug analysis

LCM, RFM and ZNS were quantified by using high performance liquid chromatography with UV detection (HPLC/UV) as described in previous chapters (Zhang *et al.*, 2010; Zhang *et al.*, 2011). A Thermo Hypersil BDS C_{18} column (5 μM pores, 250 mm × 4.6 mm inner diameter) was used. PGB was quantified by using LC-MS/MS as described before. The HPLC/UV and LC-MS/MS methods were validated, and the inter-day and intra-day root mean square deviations were calculated. The lowest limits of quantification for the drugs were detected.

5.2.3 Data analysis

In the CETA, the data were presented as the percentage of the drug loading concentration in either apical or basolateral chamber vs. time, as described in previous chapters (Zhang *et al.*, 2010; Zhang *et al.*, 2011). Values were shown as means ± SEM. At various time intervals, differences of drug concentration between the two chambers of each well were compared, and differences of drug concentration between the two chambers in wildtype

(WT) cells were compared with those from MDR1-transfected cells. Significant differences between two groups or more than two groups were calculated by student's t-test or one-way ANOVA, respectively, with $p < 0.05$ considered as significant.

For MTT assays, percentage survival was calculated according to the formula: (mean of drug treatment OD – mean of blank OD) / (mean of control OD – mean of blank OD) x 100%. 80% was considered to be safe for the drugs.

5.3   Results

5.3.1 Stability of AEDs in transport buffer

The stability of PGB, LCM, RFM and ZNS in transport buffer was tested at 37°C. As shown in Fig 5.1 and Table 2.3, after incubation for 2 hr or 4 hr, the percentages of PGB, LCM, RFM and ZNS remaining were around 100%, indicating that these compounds are stable at 37°C in the transport buffer for at least 4 hr. The drugs were also tested at room temperature in an auto-sampler for 48 hr and were found to be stable (Table 2.4).
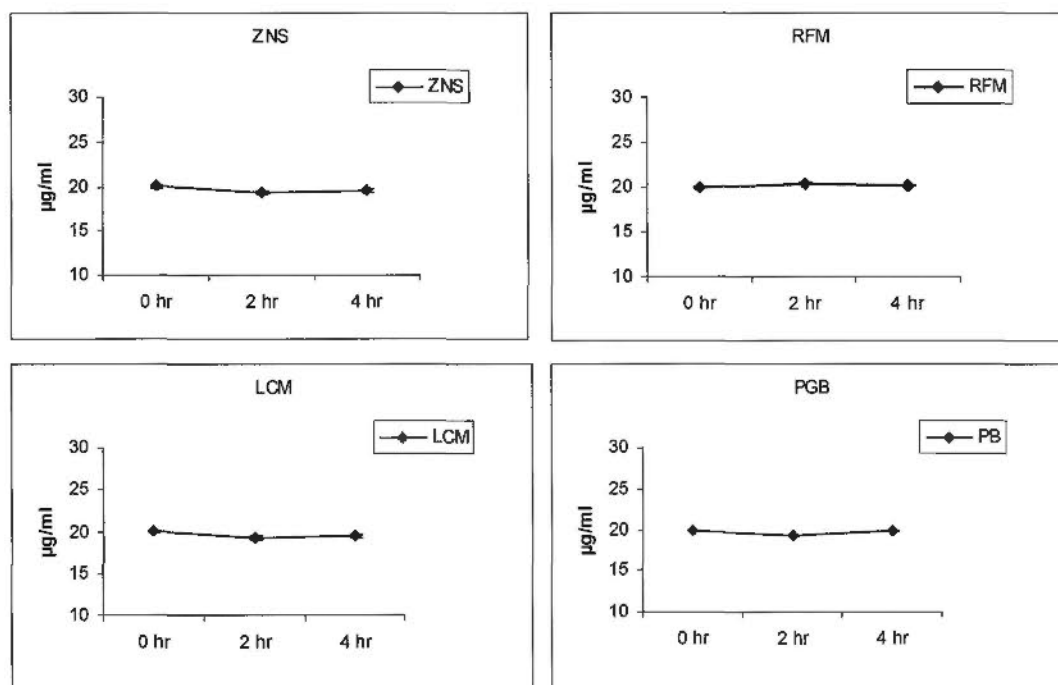
Fig 5.1 Stabilities of tested AEDs in transport buffer at 37°C.

5.3.2 Cytotoxicities of AEDs in cells

The cytotoxicities of PGB, LCM, RFM and ZNS were tested at concentrations of 1, 5, 10, 20, and 50 µg/ml using the MTT assay. The four drugs were not toxic to the four cell lines for at least 240 min (Fig5.2).
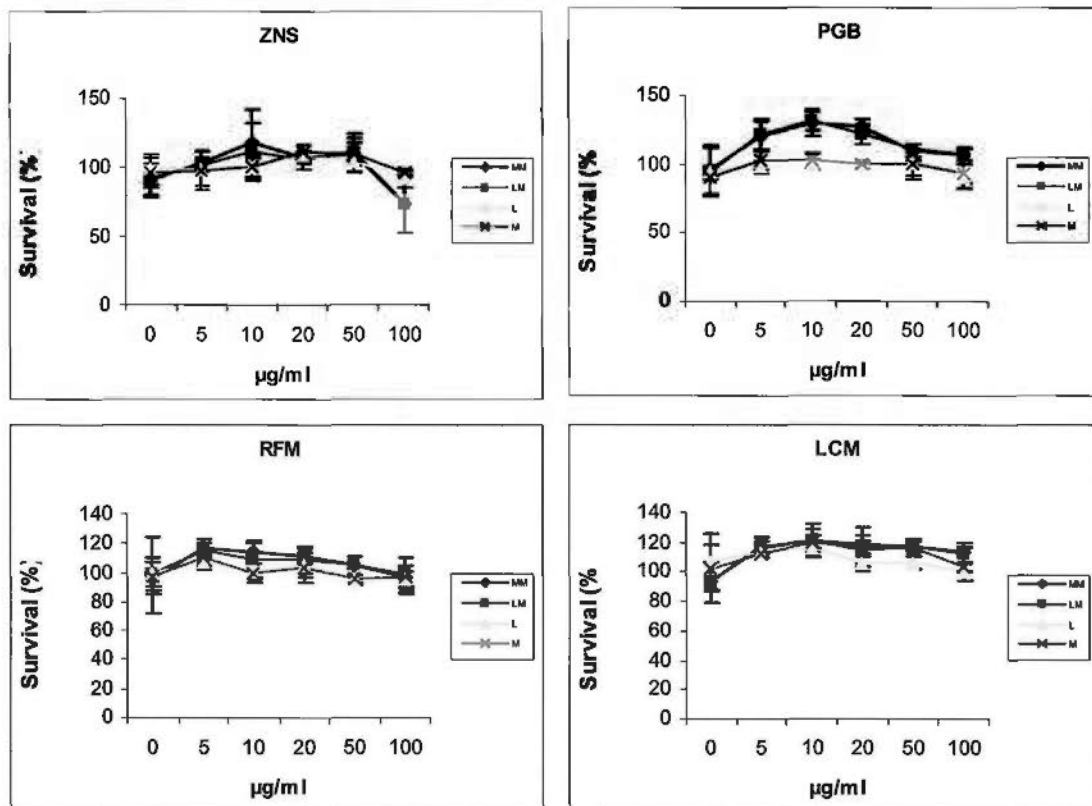
Fig 5.2   Cytotoxicities of ZNS, PGB, RFM, and LCM to LLC (L), LLC-MDR1 (LM), MDCK (M), and MDCK-MDR1 (MM) cells.

5.3.3 Transport profile of LCM

In the concentration equilibrium transport assay, 5 µg/ml LCM was applied to an LLC wildtype cell line (LLC-WT) and a cell line of LLC cells transfected with human Pgp (LLC-MDR1). This concentration is in the range of the clinical plasma concentration of

LCM (Cross *et al.*, 2009). For LLC-MDR1 cells, the concentration of LCM on the apical side was significantly higher than on the basolateral side from 90 min of drug exposure onward (Fig 5.3). For LLC wildtype cells, there was no significant difference between apical and basolateral sides (Fig 5.3). After adding the Pgp inhibitors verapamil (100 µM) or tariquidar (10 µM), the efflux of LCM from basilateral to apical sides was almost completely blocked, indicating that LCM was transported by Pgp.

In order to confirm the transport profile of LCM for Pgp, we performed the concentration equilibrium transport assay using 5 µg/ml LCM on MDCK-WT and MDCK-MDR1 cells. MDCK-MDR1 cells transported LCM to a similar degree as did LLC-MDR1 cells (Fig 5.4). A significant difference in LCM concentrations between apical and basolateral sides of monolayers was detected from 90 min of drug exposure onward for MDCK-MDR1 cells, but not for MDCK-WT cells. When the Pgp inhibitor tariquidar (2 µM) was added, the transport of LCM was almost completely inhibited (Fig 5.4), indicating that LCM is a substrate of Pgp.
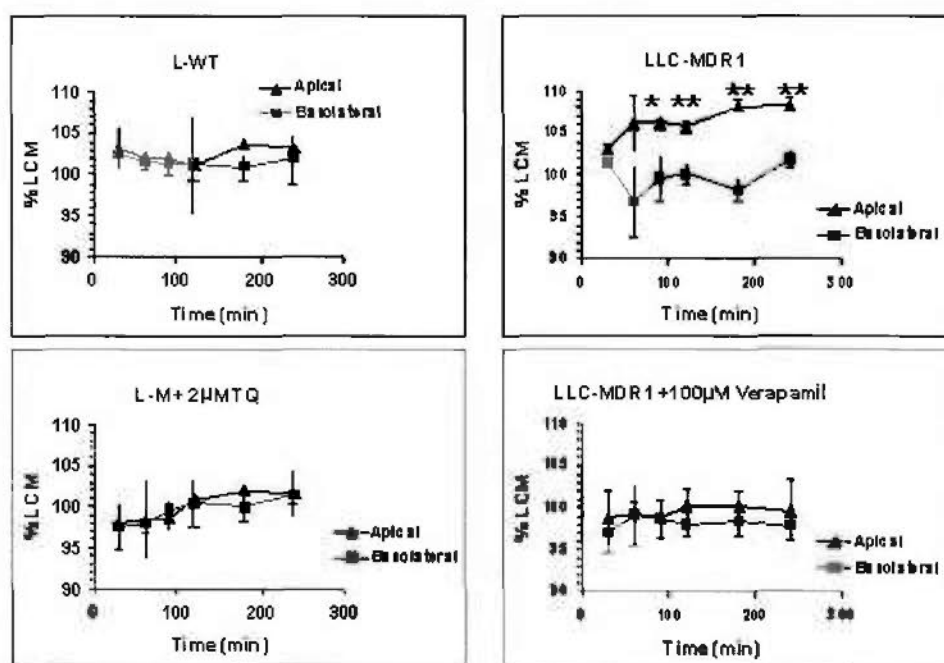
Fig 5.3 **Concentration equilibrium transport assays of lacosamide (LCM) for LLC wildtype (L-WT) cells and cells transfected with the human MDR1 gene (L-M).** Data are given

as the percentage of the initial drug concentration in either apical or basolateral chamber vs. time. Experiments were performed in triplicate, and values are shown as mean ± SD. Significant differences in drug concentrations between the two chambers are indicated by asterisks (n=3, *p<0.05, **p<0.01, ***p<0.001).
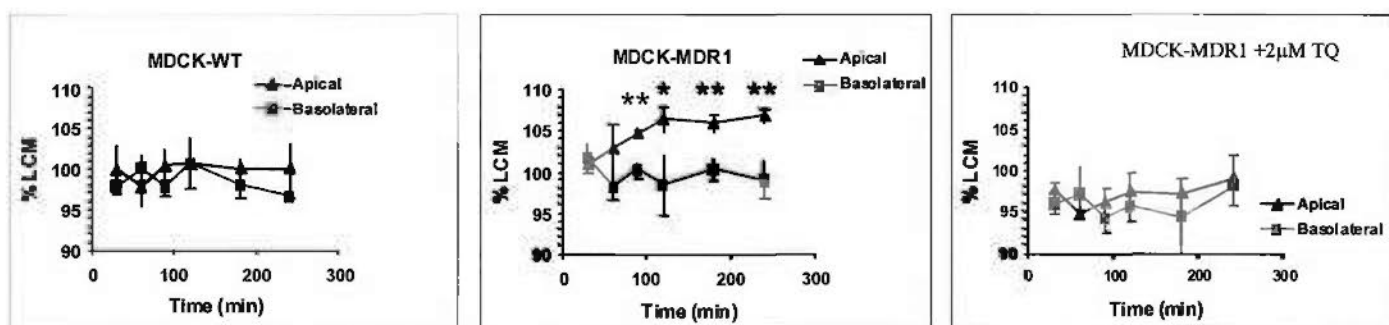
Fig 5.4 **Concentration equilibrium transport assays of lacosamide (LCM) for MDCK wildtype (MDCK-WT) cells and MDCK-MDR1 cells.** Data are given as the percentage of the initial drug concentration in either apical or basolateral chamber vs. time. Experiments were performed in triplicate, and values are shown as mean ± SD. Significant differences in drug concentrations between the two chambers are indicated by asterisks (n=3, *p<0.05, **p<0.01, ***p<0.001).

5.3.4 Transport profile of RFM

RFM was tested in concentration equilibrium transport assays at 5 µg/ml, which is in the range of clinical plasma concentrations (Perucca *et al.*, 2008). There was no significant different between apical and basolateral concentrations after exposing LLC-MDR1 cell monolayers to RFM for 4 hours (Fig 5.5). MDCK-MDR1 cells also displayed no transport (Fig 5.5). For both wildtype cell lines (LLC-WT and MDCK-WT), no significant differences between apical and basolateral concentrations of RFM were detected (Fig 5.5). These results indicated that RFM was not transported by Pgp.
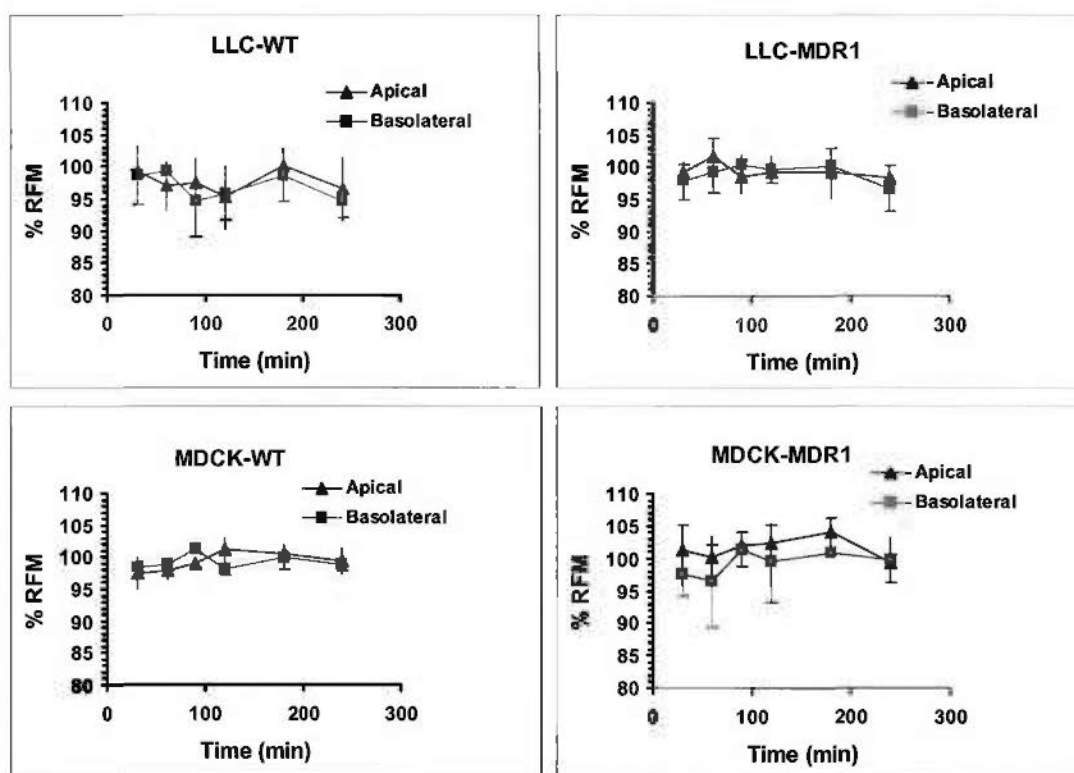
Fig 5.5 **Concentration equilibrium transport assays of rufinamide (RFM) for MDCKII and LLC cells transfected with the human MDR1 gene or for wildtype (WT) cells.** Data are given as the percentage of the initial drug concentration in either apical or basolateral chamber vs. time. Experiments were performed in triplicate, and values are shown as mean ± SD.

5.3.5 Transport profile of ZNS

ZNS was tested in concentration equilibrium transport assays. The plasma concentration of epileptic patients is 10-40 mg/L (Krasowski, 2010). ZNS, at 10 μg/ml, was added to apical and basolateral sides of monolayers for 4 hours, and samples were collected at different time points. No significant difference in ZNS concentrations was found between apical and basolateral sides for LLC-MDR1, MDCK-MDR, LLC-WT, and MDCK-MDR1, indicating that ZNS was not transported by Pgp (Fig 5.6).
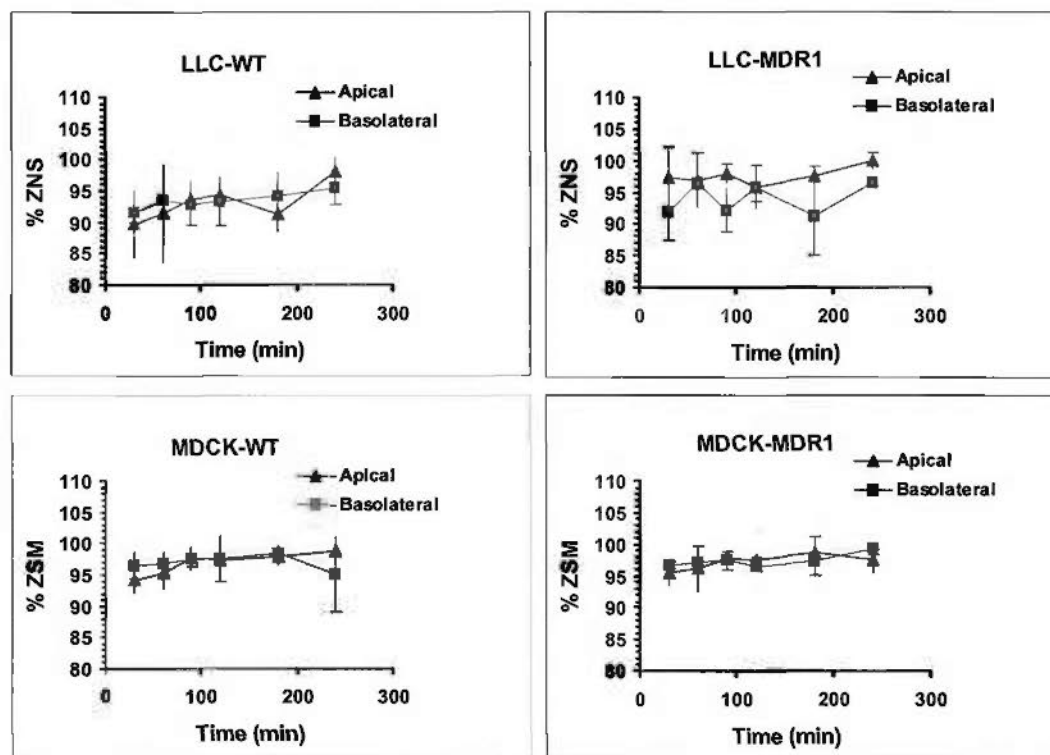
Fig 5.6 **Concentration equilibrium transport assays of zonisamide (ZNS) for MDCKII and LLC cells transfected with the human MDR1 gene or for wildtype (WT) cells.** Data are given as the percentage of the initial drug concentration in either apical or basolateral chamber vs. time. Experiments were performed in triplicate, and values are shown as mean ± SD.

5.3.6 Transport profile of PGB

In concentration equilibrium transport assays, PGB was tested within the range of clinical plasma concentrations (Krasowski, 2010). At 5 µg/ml, there were no significant differences between apical and basolateral concentrations for LLC-MDR1 and MDCK-MDR1 cells at any time point (Fig 5.7). In both wild type cell lines (LLC-WT and MDCK-MDR1), significant transport of PGB was not found (Fig 5.7). The above results indicated that PGB was not transported by Pgp.
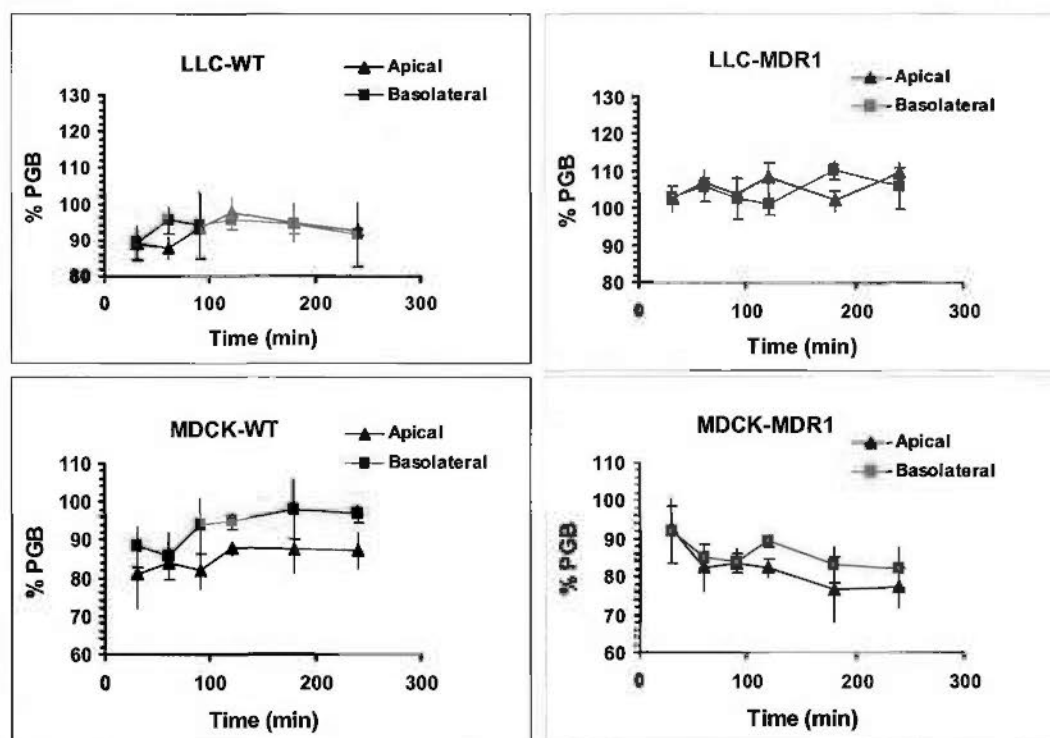
Fig 5.7 **Concentration equilibrium transport assays of pregabalin (PGB) for MDCKII and LLC cells transfected with the human MDR1 gene or for wildtype (WT) cells.** Data are given as the percentage of the initial drug concentration in either apical or basolateral chamber vs. time. Experiments were performed in triplicate, and values are shown as mean ± SD.

5.4   Discussion

Drug resistance in the treatment of epilepsy is a serious problem. The efflux transport of AEDs from the brain by Pgp might be involved. Several drugs have recently been developed and marketed, such as LCM, RFM, ZNS, and PGB. However, they did not greatly improve the cure rate of refractory epilepsy (Hamandi *et al.*, 2006; Kellinghaus, 2009; Kothare *et al.*, 2008; Perucca *et al.*, 2008; Ryvlin *et al.*, 2008). In previous chapters, we determined the substrate status of some AEDs. In this chapter, we set out to determine the substrate status of the above new AEDs.

The cytotoxicity test indicated that PGB, LCM, RFM, and ZNS were safe for cells in the concentrations tested for 4 hours. Stability testing indicated that all of the four drugs were stable during the experiments. The expression level of Pgp in MDR1 transfected cells was examined, and the function of Pgp in LLC-MDR1 and MDCK-MDR1 cells was also detected by the Rho123 uptake assay, as described in previous chapters. Cell monolayers were validated by an integrity assay, indicating that the cell monolayer models were suitable for experiments.

Few studies have examined the substrate status of ZNS for Pgp *in vitro*. ZNS did not affect the uptake of Rho123 by OS2.4/Doxo cells expressing high levels of Pgp (West *et al.*, 2007). In our experiment, ZNS was not transported by Pgp in LLC-MDR1 or MDCK-MDR1 cells, which is consistent with the published evidence (West *et al.*, 2007).

No published reported exist on the relationship between concentrations of PGB, LCM, ZNS, and FRM in brain and Pgp expression level *in vivo*. No evidence indicated the substrate status of PGB, LCM and RFM *in vitro*. In this study, LCM, starting at 5 μg/ml, was transported by Pgp in both LLC-MDR1 and MDCK-MDR1 cells, and the transport can be almost completely blocked by Pgp inhibitors (verapamil and tariquidar). There was no transport by wildtype cells, indicating that LCM is a substrate of human Pgp. RFM and PGB were not transported by Pgp in MDR1 transfected cells, indicating that they are not substrates of Pgp.

LCM is a Pgp substrate, while ZNS, PGB, and RFM are not. Therefore, the latter three drugs might be more likely to overcome Pgp-mediated drug resistance, and they may be chosen first to treat patients.

5.5   Conclusion

In concentration equilibrium transport assays, Pgp transported LCM but not PGB, RFM, or ZNS. Therefore, LCM is a substrate of Pgp, while PGB, RFM, and ZNS are not. The substrate status of these newly marketed drugs at clinically relevant concentrations

provides information to improve understanding of the function of Pgp in refractory epilepsy.

Chapter Six

Establishment of the cell lines of human *MDR1* polymorphisms

6.1   Introduction

As described in chapter one, evidences indicated that single nucleotide polymorphism (SNP) was associated with altered Pgp level and drug respond (Eichelbaum *et al.*, 2004; Kwan *et al.*, 2009). SNPs at 62 sites have been reported in the human *MDR1* (Kerb *et al.*, 2001; Kim *et al.*, 2001; Kroetz *et al.*, 2003; Sakaeda *et al.*, 2003; Schwab *et al.*, 2003). 1236C>T, 2677G>T/A, and 3435C>T are frequently studied exonic SNPs in *MDR1* (Kim *et al.*, 2001). Polymorphisms of *MDR1* have been associated with drug responsiveness (Basic *et al.*, 2008; Ebid *et al.*, 2007; Kwan *et al.*, 2007a; Siddiqui *et al.*, 2003).

In cells, there was not difference in Pgp surface expression between the 3435T and 3435C genotypes (Kimchi-Sarfaty *et al.*, 2007; Salama *et al.*, 2006). The 1236C>T/A893S/3435C>T altered the intracellular accumulation of calcein-AM and BODIPY-FL-paclitaxel in a substrate-dependent manner (Gow *et al.*, 2008). Wang *et al.* studied 1236C>T, 2677G>T, and 3435C>T, and indicated that the 3435C>T may be a main factor to change the mRNA stability of MDR1 and decrease the mRNA expression level in liver (Wang *et al.*, 2005). Kimchi-Sarfaty et al. noted that the synonymous polymorphism 3435T, combined with one or two of 2677T and 1236T, resulted in insensitivity to Pgp inhibitors. The 3435 SNP affects the rate of folding of the Pgp protein as it is translated, thus affecting the insertion of Pgp into the membrane, resulting in a change in the interaction site of substrate and inhibitor and altering Pgp function (Kimchi-Sarfaty *et al.*, 2007). C1236T, G2677T/A, and C3435T significantly minimized the Pgp function by decreasing the cell uptake of Rho123 compared with wild type MDR1 in LLC-PK1 cells (Salama *et al.*, 2006). C1236T and C3435T were associated with the decrease of Pgp expression level and increase of Pgp transport activity in placenta (Hemauer *et al.*, 2010). But in another study, G2677T/A, and C3435T did not

affect the transport of verapamil, digoxin, vinblastine, and cyclosporine A by Pgp (Morita *et al.*, 2003).

Hung et al. used a cultured cell method to study whether the above polymorphisms affect the efflux of AEDs by Pgp. They found that the 1236T-3435T and 1236T-2677A/T-3435T haplotypes resulted in less effective inhibition of AEDs against substrates of Pgp and caused lower intracellular concentration of substrates when adding AEDs (Hung *et al.*, 2008). The data suggest that polymorphisms of MDR1 influence the interaction between AEDs and Pgp. However, evidence showing that polymorphisms affect the directional transport of AEDs by Pgp is inconsistent. Therefore, we propose to use monolayers of cells transfected with *MDR1* variant haplotypes to investigate their effects on AED transport. In this study, we established the LLC cell lines transfected with the human MDR1 variants at 1236, 2677, and 3435 sites.

6.2   Materials and methods

6.2.1 Materials

Vincristine sulfate was bought from Tauto Biotech (Shanghai, Chian). LB medium, LB+agar medium, and 10×TBE buffer were supplied by USB Corporation (Cleveland, OH, USA). Geneticin was bought from Gibco (Invitrogen, Hong Kong). Albumin bovine serum and PBS tablet were supplied by Sigma. TRIzol reagent, DEPC treated water, and Lipofectamine 2000 were bought from Invitrogen. Acetonitrile (Labscan Asia, Thailand), ethanol (TEDIA company, Inc., USA), and methanol (TEDIA company, Inc., USA) were HPLC grade. Isopropyl alcohol and chloroform were supplied by Merck. All other reagents were at least analytical grade. The water was deionized by a Millipore water purification system (Millipore, Milford, USA).

6.2.2 Plasmids expressing human *MDR1* polymorphisms

6.2.2.1 Plasmids

pCl-neo plasmids containing MDR1 and its variants were kindly provided by Dr. Danxin Wang (Department of Pharmacology, Ohio State University, USA) and Dr. Deanna Kroetz (Department of Biopharmaceutical Science, University of California San Francisco, USA). Plasmids were MDR1-wt (1236C/2677G/3435C), MDR1-1236T (1236T/2677G/3435C), MDR1-2677T (1236C/2677T/3435C), MDR1-2677A (1236C/2677A/3435C), MDR1-3435T (1236C/2677G/3435T), MDR1-1236T/2677T (1236T/2677T/3435C), MDR1-2677T/3435T (1236C/2677T/3435T), MDR1-1236T/3435T (1236T/2677G/3435T), and MDR1-1236T/2677T/3435T (1236T/2677T/3435T). The plasmids only contained the coding region of MDR1 without untranslated regions (below figure).
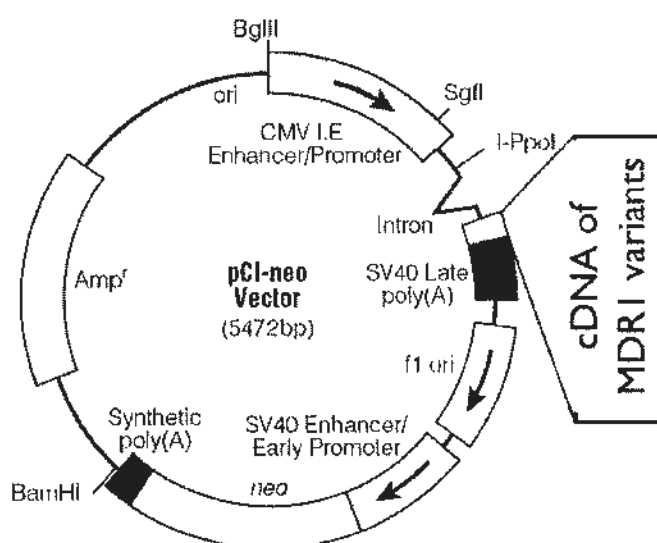
6.2.2.2 Transformation of plasmids

The plasmids were amplified by transformation into *E. coli* DH5α competent cells (Invitrogen) as described in the manual. Briefly, the competent cells were thawed on ice, and aliquots of 100 µl of competent cells were placed into chilled tubes. 10 ng plasmid DNA was added into the competent cells and mixed gently, followed by incubation on

ice for 30 minutes. After the incubation, the cells were heat-shocked at 42°C for 45 seconds in a water bath, then placed on ice for 2 minutes. 0.9 ml S.O.C. medium was added to the cells and shaken for 1 hour at 225 rpm at 37°C. Cells were diluted, spread on LB plates with 100 µg/ml ampicillin, and incubated overnight at 37°C.

6.2.2.3 Purification of plasmids

Single colonies were picked up from plates and incubated in 2.5 ml LB medium with 100 µg/ml ampicillin at 37°C overnight. Plasmids were purified by QiAprep Miniprep Kit (Qiagen). Briefly, *E.coli* cells containing plasmids were collected by centrifuge at 4°C. The pelleted bacterial cells were resuspended in 250 µl Buffer P1 and transfered to microcentrifuge tubes. Then 250 µl Buffer P2 was added into the tubes and mixed thoroughly by inverting 4-6 times. 350 µl Buffer N3 was added and mixed immediately by inverting the tube 4-6 times. After mixing, the tube was centrifuged at 13000 rpm for 10 minutes at room temperature. The supernatant to the QIArep spin column was centrifuged for 60 seconds and then washed by 0.75 ml Buffer PE. The plasmid DNA was eluted by 50 µl Buffer EB.

The size and purity of plasmids was checked by agarose electrophoresis (see blow). The concentration of plasmids was tested by UV spectrometer at A260 and A280 (NanoVue, GE Healthcare).
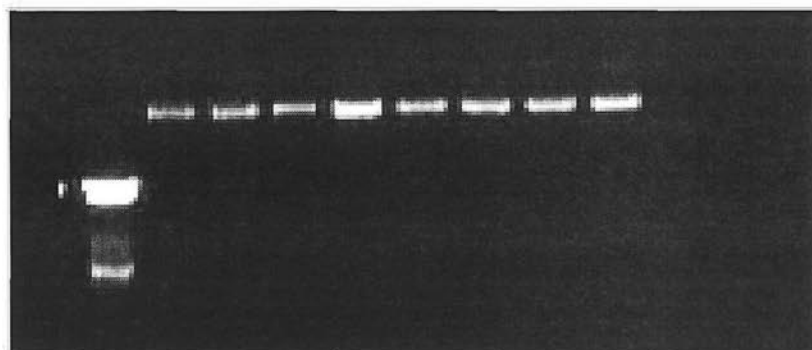
6.2.2.4 Sequencing of plasmids

In order to confirm the sequence of MDR1 variants, the plasmids containing MDR1 variants were checked by sequencing. The following primers were used: T7 universal primer, 5'-AGCTGATGCAGAGGCTCTAT-3', 5'-GCATGTATGTTGGCCTCCTT-3', 5'-GGCCGGTGGCATTCGAGTAG-3', 5'-TTACACGTGGTTGGAAGCTA-3', and 5'-TTGCTTCAGTAGCGATCTTC-3'.

6.2.3 Cell line establishment

Stable transfection of MDR1 variants was performed using Lipofectamine 2000 reagent (Invitrogen) as described in the manufacturer's handbook with modification. Briefly, 5×10^5 LLC cells were seeded in 6-well plates in Medium 199 without antibiotics and cultured for 24 hours to grow to about 80% confluence. The DNA-Lipofectamine 2000 mixture was prepared as follows for each transfection sample: A. 4 µg plasmid DNA was added to 200 µl Opti-MEM medium without serum (Gibco, Invitrogen), mixed gently, and incubated for 15 minutes at room temperature. B. 10 µl Lipofectamine 2000 was added to 200 µl Opti-MEM medium, mixed and incubated for 15 minutes at room temperature. C. The diluted Lipofectamine 2000 and diluted plasmid DNA were mixed gently and incubated for 20 minutes at room temperature. After incubation, the DNA-Lipofectamine 2000 mixture was added into 6-well plates which contain the LLC cells and mixed gently. The cells were incubated in a CO_2 incubator at 37°C for 4 hours, and the medium was replaced by fresh medium and incubated for 24 hours. For selection of stable clones, the cells were passaged at different densities and incubated for 24 hours. Medium containing 1.8-2.0 mg/ml Geneticin (G418, Invitrogen) was added to the plate, and cells were cultured for about 6 days. For the selection of clones expressing a high level of Pgp, the medium was replaced by medium with 1.5 µM vincristine sulfate and cultured for another 6 days. The separated stable clones containing MDR1 variants were picked up and seeded into 96-well plates and further identified by real-time PCR and immunoblotting.

6.2.4 RNA extraction

In order to measure the expression level of Pgp, the total RNA in stably-expressing clones was extracted by TRIzol reagent (Invitrogen) as described in the manufacturer's instructions. Cells were seeded in 24-well plates and cultured to about 90% confluence. 200 µl of TRIzol reagent was added to each well to lyse the cells. The cell lysate was homogenized by passing through a pipette about 10 times and was incubated for 5 minutes at room temperature. 40 µl chloroform was added to the cell lysate, which was then mixed gently and incubated for 3 minutes at room temperature. The sample was then centrifuged at 12000 g for 15 minutes at 4°C. The upper aqueous phase was transferred to a new tube, and 100 µl of isopropyl alcohol was added, mixed, and incubated for 10 minutes at room temperature. Then the sample was centrifuged at 12000 g for 10 minutes at 4°C to precipitate the RNA. The RNA was washed by 75% ethanol and air dried. Finally, the RNA was dissolved in DEPC treated water. The concentration of RNA was checked by UV spectrometry at A260 and A280 (NanoVue, GE Healthcare). The quality of the RNA was checked by agarose electrophoresis. RNA was stored at -80°C.

6.2.5 Reverse transcription PCR

Reverse transcription PCR was performed using a QuantiTect Reverse Transcription Kit (Qiagen) according to the manufacturer's protocol. Briefly, the template RNA was thawed on ice, and 1 µg template RNA, DEPC water, and 2 µl gDNA wipeout buffer were mixed to a volume of 14 µl, and incubated for 2 minutes at 42°C to eliminate the genomic DNA. Then the mixture was placed on ice and the reverse transcription master action system was prepared by adding 1 µl Quantiscript Reverse Transcriptase, 4 µl Quantiscript RT buffer, and 1 µl RT primer mix, and then mixing and incubating for 15 minutes at 42°C. The mixture was incubated for 3 minutes at 95°C to inactive the reaction. The cDNA was stored at -20°C.

6.2.6 Quantitative real-time PCR

To quantify *MDR1* mRNA levels in the cell lines, real time PCR was performed with FastStart Universal SYBR Green Master (Roche) in a Roche LightCycler 480 (Mannheim, Germany). PCR amplification was carried out by using the following primer pairs: *MDR1*, 5'-CCCATCATTGCAATAGCAGG-3' and 5'-TGTTCAAACTTCTGCTCCTGA-3'; *β-Actin*, 5'-CCTCTATGCCAACACAGTGC-3' and 5'-ACATCTGCTGGAAGGTGGAC-3'. The amplification program was pre-incubation at 50°C for 2 min and 95°C for 10 min; amplification at 95°C for 10 sec, 59°C for 20 sec, and 72°C for 10 sec; and repeating the amplification steps for 45 cycles.

6.2.7 Immunofluorescent staining

To detect the location and protein level of Pgp in the cell lines, immunofluorescent staining was performed as described before with some modification (Zhang *et al.*, 2011). Briefly, cells were seeded on cover slips and cultured for 48 hr. The density of cells was about 80% when stained. After rinsing twice by cold PBS, the cells were fixed in 4% PFA for 15 min. The slips were washed with PBS 3 times for 5 minutes each. Then the cells were blocked by 10% FBS in PBS at room temperature for 30 minutes, followed by diluted Pgp antibody JSB-1 (1:50, Enzo Life Science, USA) in PBS with 0.5% BSA at 4°C overnight. Cells were rinsed with PBS twice and incubated in secondary antibody (1:300, Alex 488-conjugated IgG, Inivitrogen) in PBS with 0.5% BSA in the dark at room temperature for 30 minutes. Finally, cells were washed by PBS twice, and slides were mounted to observe them on a fluorescent microscope.

6.2.8 Western blotting

6.2.8.1 Protein extraction

The western blotting was performed as described in the antibody handbook of abcam[®] with modifications. Cells on dishes were washed with cold PBS, followed by ice-cold lysis buffer (1 ml per 10^7 cells / 100 mm dish). Adherent cells were scraped off the dish

using a cell scraper, and then constant agitation was maintained for 30 minutes at 4°C. The cell suspension was centrifuged in at 4°C at 12,000 rpm for 10 min. The supernatant was aspirated and placed in a fresh tube. The protein concentration was measured by Bio-Rad Protein Assay Kit as described in the handbook.

6.2.8.2   Electrophoresis

For Pgp (170 kDa), a 7.5% gel was prepared as in the table below. Samples were boiled in SDS sample buffer (see 6.2.8.4), and 100 µg protein of each sample was loaded. The gel was run at constant voltage (50V as samples pass through the stacking gel and 100V as samples pass through the separating gel).

Materials	Resolving Gel	Stacking Gel
	7.5%	5%
40% Acrylamide	0.90 ml	0.27 ml
2% Bis-Acrylamide	0.5 ml	0.14 ml
0.5M Tris-HCl pH 6.8	0	0.63 ml
1.5M Tris- HCl pH 8.8	1.3 ml	0
10% SDS	50 µl	25 µl
dH2O	2.27 ml	1.4 ml
TEMED	2.5 µl	2.5 µl
10% Ammonium Persulfate	25 µl	12.5 µl

6.2.8.3 Transfer

The transfer buffer (listed in recipe) was cooled on ice and the sponge, PVDF membrane (soaked with methanol), and filter paper were soaked in transfer buffer for 5 min at 4°C. Transfer was performed at 100 V for 4 hr on ice.

6.2.8.4 Staining

The membrane was blocked in 5% milk for 30 min at room temperature. Primary antibody (C219 at a 1:1000 dilution; β-tubulin at a 1:300 dilution) was added and rotated

overnight at 4°C. Then the membrane was washed by TBST twice for 5 min each. Anti-mouse secondary antibody (1:2000) or anti-rabbit secondary antibody (1:1000) was added and incubated for 1 hr at room temperature. The membrane was washed 3 times for 5 min each.

Buffer Recipe

- Lysis buffer:

    1.21 g (50 mM) Tris

    1.75 g (150 mM) NaCl

    2 mL 10% SDS (0.1% SDS)

    149 mg (2 mM) EDTA

    (1%) Triton X-100

    (10%) Glycerol

    H_2O to 200 mL

- 4X Sample buffer:

    303 mg Tris pH 6.8

    0.5 g SDS

    3 mL glycerol

    2 mg bromophenol blue.

    1 mL β-mercaptoethanol

    5 mL water

- Transfer buffer: 1 L,

    3.03 g Tris

    14.2 g Glycine

    200 mL MeOH

    800 mL H_2O

- 10X Washing buffer: TBST

    58.4 g NaCl

    12.1 g Tris

    pH 7.5 and adding 1 mL Tween 20 and make up to 1L.

6.2.9 Data analysis

For real time-PCR, relative expression levels of *MDR1* mRNA in LLC variant cells were scaled to the mean relative expression level of the housekeeping gene *β-actin*. For western blotting, Pgp relative expression level was calculated by dividing the amount of Pgp by the amount of β-tubulin. The relative expression level of LLC-CGC (reference variant) was defined as 1 for both mRNA and protein.

All the data were shown as means ± SD. Significant differences between two groups or more than two groups were evaluated by student's t-test or one-way ANOVA, respectively, with $p<0.05$ considered significant.

6.3   Results

6.3.1 Selected clones

The plasmids containing *MDR1* variants were transfected into LLC-PK1 cells by Lipofectamine 2000 reagent and selected by G418 and/or vincristine sulfate. The stable clones resistant to G418 or both G418 and vincristine sulfate were collected. For each variant, about 25 clones were picked up for each selection condition.

6.3.2 mRNA expression level of *MDR1* by real-time PCR

The total RNA of LLC cells transfected with *MDR1* variants was extracted, and the RNA concentration was quantified by UV spectrometer. The quality of the RNA was checked by agarose electrophoresis. Figure 6.1 shows that the quality of total RNA extracted from the clones was good enough for RT-PCR.
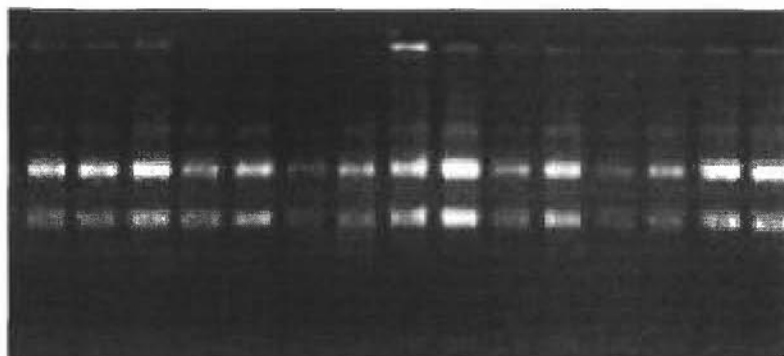
Fig 6.1 Agarose gel of total RNA extracted from *MDR1* variants

After transcribing the RNA to cDNA by RT-PCR, the mRNA levels of *MDR1* variants were quantified by real-time PCR. We used the mRNA level of *β-actin* as the internal standard to quantify the mRNA of *MDR1*. Figure 6.2 shows the amplification curves and melting peaks for *MDR1* and *β-actin*. The cycle threshold (Ct) values of *MDR1* and *β-actin* for each variant are listed in Table 6.1. For each variant, the level of *MDR1* adjusted for *β-actin* was also calculated (Table 6.1). The expression levels of *MDR1* were not high in the clones which were selected only by G418. We picked the clones with the highest levels of *MDR1* to perform the transport assay. For the selection using both G418 and vincristine sulfate, the expression level of *MDR1* was high. We chose the clones which expressed similar *MDR1* levels for further experiments.

Table 6.1 The mRNA expression level of *MDR1* in variants.

Variant name	MDR1 Ct (Mean)	β-actin Ct (Mean)	Adjusted MDR1 level*
LII-CTC-7	18.04	21.8	13.48
LII-CTC-9	18.77	21.92	8.857
LII-CGC-10	17.79	21.62	14.29
LII-CGC-11	19.05	22.33	9.726
LII-CTT-7	17.98	21.06	10.11
LII-CTT-8	16.53	20.5	15.67
LII-CGT-11	17.79	21.65	14.43
LII-CGT-16	19.46	22.37	7.486
LII-TTC-3	17.85	20.85	8.041
LII-TTC-4	21.15	23.27	4.372
LII-TTT-1	17.68	21.12	10.89
LII-TTT-2	16.63	20.71	16.92
LII-TGT-1	17.59	20.07	5.562
LII-TGT-3	17.58	20.3	6.602

LII-CAC-1	17.54	20.53	7.939
LII-CAC-2	18.00	21.01	8.039
LII-TGC-3	19.40	22.14	6.676
LII-TGC-9	22.91	26.19	9.718
L-CTC-5	19.95	20.38	1.344
L-CTC-6	22.64	21.6	0.487
L-CTT-10	17.73	19.37	3.125
L-CTT-2	18.56	19.44	1.849
L-CGC-5	24.30	25.91	3.067
L-CGC-9	24.77	18.71	0.015
L-CGT-5	16.62	18.42	3.473
L-CGT-6	18.67	19.1	1.348

*Adjusted *MDR1* level: $2^{Ct_{\beta\text{-actin}} - Ct_{MDR1}}$

Amplification Curves
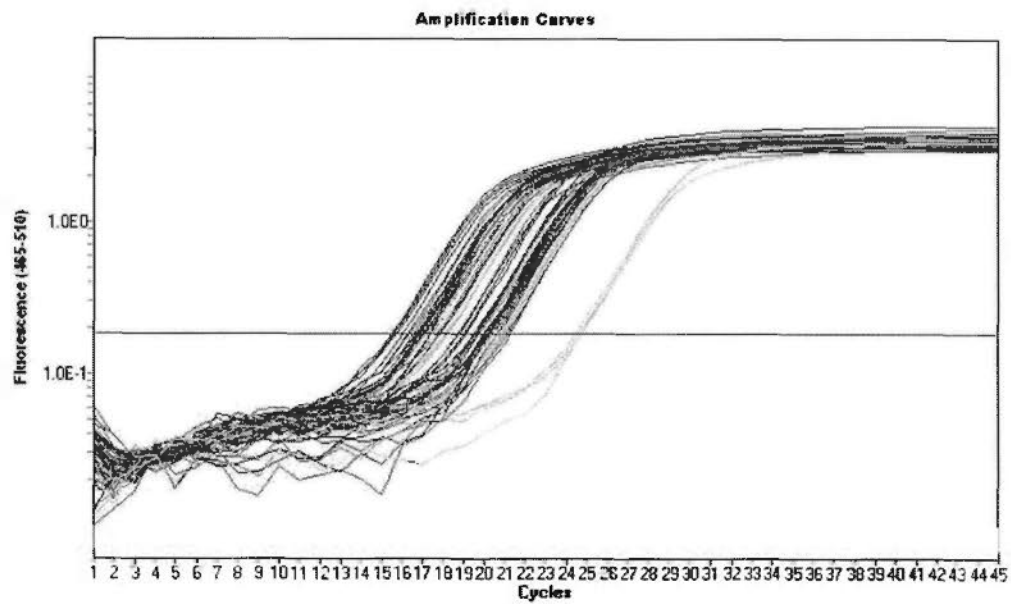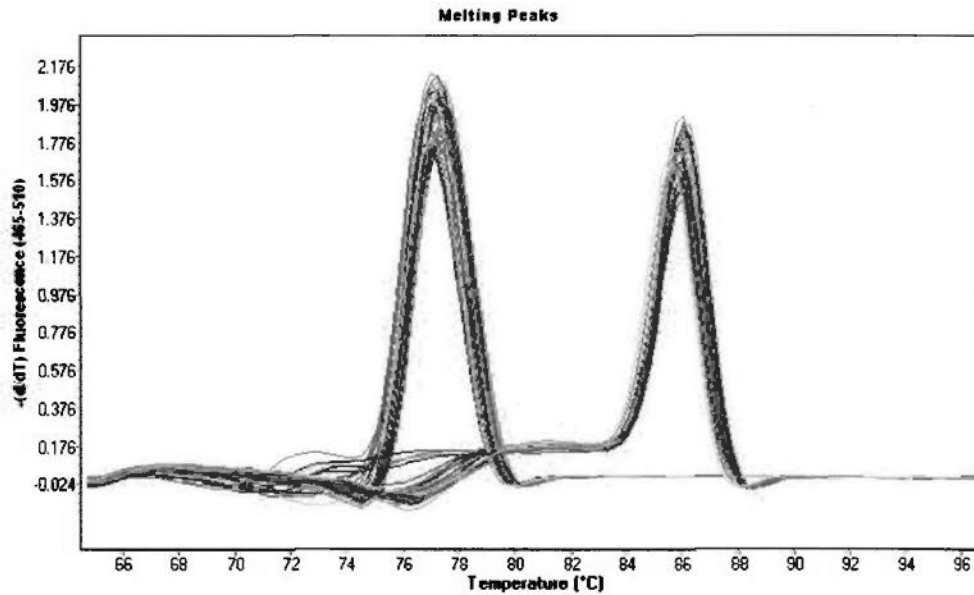
Fig 6.2 Amplification curves and melting peaks for *MDR1* and *β-actin* in real time PCR

6.3.3 Protein expression of Pgp

Western blotting was performed to measure the protein expression level of variants selected. The whole cell lysate was extracted, and Pgp and β-tubulin were detected. The relative protein expression level of Pgp was scaled to the relative expression level of housekeeping gene β-tubulin (Pgp / β-tubulin). There were two bands of Pgp detected, which were mature (upper band) and immature (lower band) Pgp. The mature Pgp was glycosylated, and the two bands were calculated to quantify the Pgp expression level (Figure 6.3 and Figure 6.4). Figure 6.3 shows the expression of Pgp in variants selected by G418. Figure 6.4 shows the expression level of variants selected by G418 and vincristine sulfate. The Pgp expression level of variants selected by G418 and vincristine sulfate was higher than those only selected by G418 (Figure 6.5).
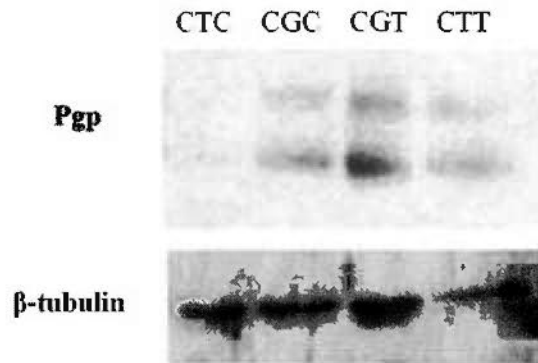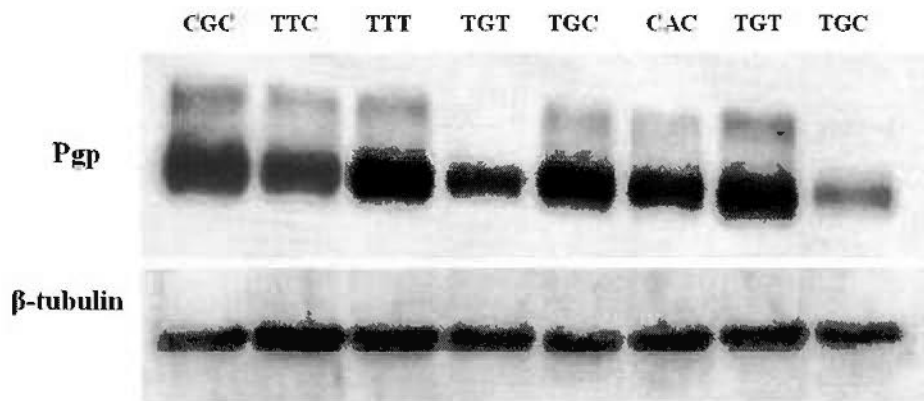
CTC CGC CGT CTT

Pgp

β-tubulin

Fig 6.3 Western blotting of variants selected by G418

CGC TTC TTT TGT TGC CAC TGT TGC

Pgp

β-tubulin

Fig 6.4 Western blotting of variants selected by G418 and vincristine sulfate

G418 and
vincristine sulfate   G418

Pgp

β-tubulin

CGC CTC CGT CTT CTC CGC CGT CTT
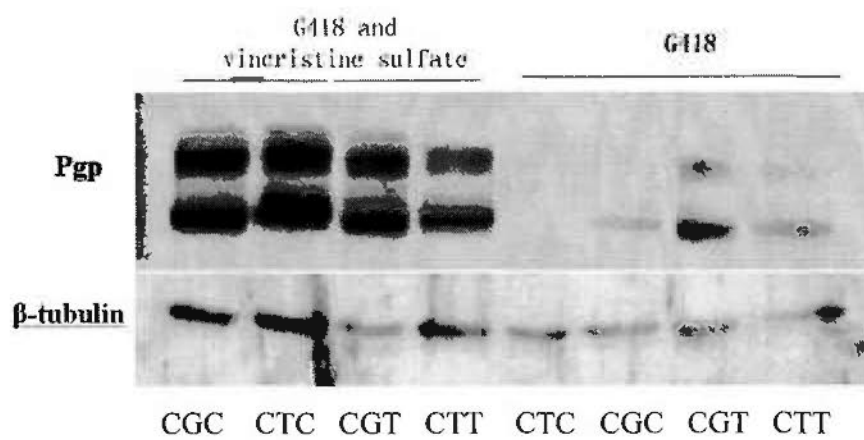
Fig 6.5   Pgp expression levels of variants selected by G418 and vincristine sulfate, or by only
G418

In each clone, the relative protein expression level was compared with the relative mRNA level. For both selection conditions, the mRNA expression levels were almost consistent with the protein levels (Figure 6.6 & 6.7), indicating that the variants do not greatly affect the translation of Pgp.
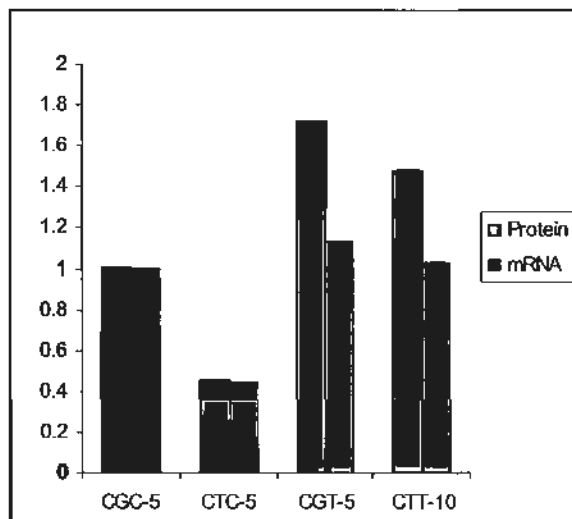
Fig 6.6   Comparing the mRNA and protein expression level in variants selected by G418. The protein level was calculated as Pgp/β-tubulin, in which the ratio in LII-CGC cells was defined as 1. The mRNA level was calculated as *MDR1/β-actin*, in which the ratio in LII-CGC cells was defined as 1.
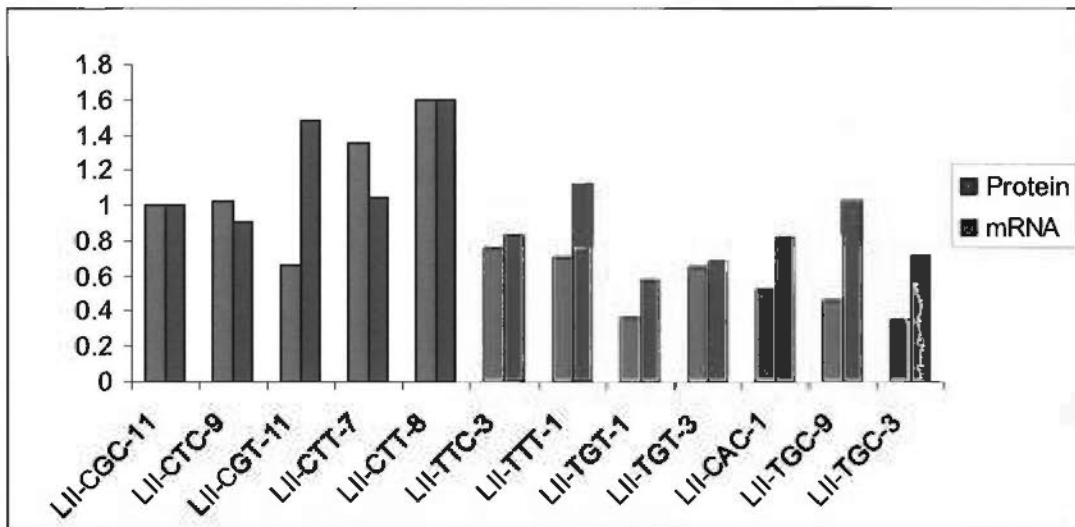
Fig 6.7 Comparing the mRNA and protein expression level in variants selected by G418 and vincristine sulfate. The protein level was calculated as Pgp/β-tubulin, in which the ratio in LII-CGC cells was defined as 1. The mRNA level was calculated as *MDR1/β-actin*, in which the ratio in LII-CGC cells was defined as 1.

The localization of Pgp in variants was detected by immunofluorescent staining. Pgp was generally localized at the cell membrane (Figure 6.8), indicating that the transfected *MDR1* gene was expressed at the correct location in variant cell lines.
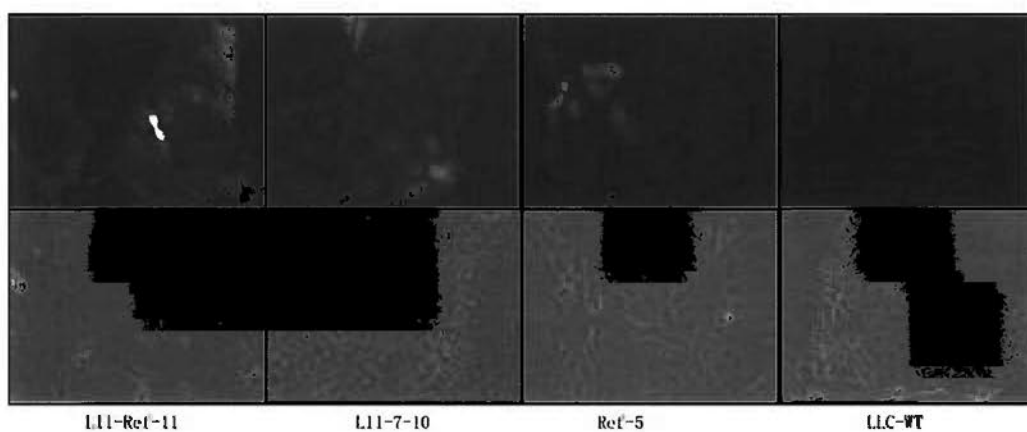
Fig 6.8 Localization of Pgp in variants. The first row is Pgp staining, shown as a fluorescent green signal, and the second row is the bright field images of cells.

6.4   Discussion

MDR1 encodes a 170 kDa protein, Pgp, which is a transmembrane transporter. Pgp is an ATP dependent transporter effluxing a wide spectrum of chemicals and drugs. SNPs in MDR1 were reported to affect Pgp function and expression level. In our current study, we used LLC-PK1 cells as the system to express Pgp variants and to detect their function.

Many publications have reported on the exonic SNPs 1236C>T, 2677G>T/A, and 3435C>T. They were associated with drug resistance in epilepsy (Basic *et al.*, 2008; Kwan *et al.*, 2007a; Kwan *et al.*, 2000a; Kwan *et al.*, 2009; Seo *et al.*, 2006; Siddiqui *et al.*, 2003). Several eukaryotic transient protein expression systems were used to study Pgp function *in vitro*, including recombinant baculovirus, vaccinia virus, and vaccinia-T7 systems (Miller, 1993; Moss, 1991; Ramachandra *et al.*, 1996). These systems express high levels of Pgp. However, the baculovirus system can disrupt the cell membrane, which affects the permeability of cells. The vaccinia virus and vaccinia-T7 systems have the advantage of keeping the cell membrane intact and the systems were easily modified. Transient expression systems have the advantage in being able to quickly and highly express Pgp. But transient expression systems do not offer consistent transfection efficiency, and the expression level of protein decreases quickly during cell culture, thus they are not suitable for the cell monolayer system.

Several stable systems have been established, including an Flp recombinase expression plasmid and a CMV plasmid system (Hung *et al.*, 2008; Schinkel *et al.*, 1995). In our project, we used the pCl-neo plasmid system, which used a neo selection marker and CMV promoter to establish stably expressing cell lines. The plasmids containing *MDR1* wild type or variant cDNA were transfected into LLC cells and selected by G418 or by G418 and vincristine sulfate. The expression level of Pgp in cell lines selected by G418 alone was low (Figure 6.5 and Table 6.1). A few clones had Pgp function when tested in the cell monolayer transport assay. That higher expression of Pgp has higher cytotoxicity may be the reason causing the low expression of Pgp. Vincristine sulfate is a substrate of Pgp and has high cytotoxcity. It can kill the cells with a low Pgp expression level, thus

selecting clones with high Pgp expression (Schinkel *et al.*, 1995). When 1.5 µM vincristine sulfate was added after selection by G418, we increased the number of clones expressing high Pgp levels and transport activity (Figure 6.5 and Table 6.1). Vincristine sulfate can induce other drug transporters, which may affect the transportation of drugs by Pgp (Schinkel *et al.*, 1995).

The LLC-PK1 cell line was used to do the transfections. The endogenous Pgp in LLC cells was less abundant than in MDCKII cells (data in previous chapter). The polarized LLC cell line transfected with *MDR1* variants can form a monolayer in transwells, allowing evaluation of the function of Pgp variants. The expression level of Pgp in selected clones was tested by real-time PCR and western blotting. *β-actin* and *β-tubulin* are housekeeping genes and were used as internal standards to quantify Pgp expression. The Pgp mRNA level of variants was calculated as *MDR1/β-actin*, and the protein level of Pgp was calculated as Pgp/β-tubulin. In each variant selected by G418 or by G418 and vincristine sulfate, comparing the mRNA level with the protein level showed that their variations were moderately consistent (Figure 6.6 and Figure 6.7). Since the primer pair for real-time PCR of the human MDR1 gene did not match perfectly to the porcine homologs, the real-time PCR may not indicate the expression level of the endogenous MDR1 gene very well in LLC cells. These data suggested that the variants do not strongly affect the translation from mRNA to protein. The human *MDR1* gene with SNPs at the 2677 and 3435 sites, which were transfected into LLC cells by the Flp recombinase system, demonstrated that 2677G>T/A and 3435C>T did not affect Pgp expression (Morita *et al.*, 2003). A transient expression system also indicated that the SNPs at 1236, 2677 and 3435 do not affect the expression level or cell surface expression (Kimchi-Sarfaty *et al.*, 2007).

The location of Pgp in variant clones was detected by immunostaining. More Pgp was located at the cell surface than in cytoplasm, indicating that the exogenous *MDR1* gene was expressed correctly in LLC cells (Figure 6.8).

6.5 Conclusion

pCI-neo plasmids containing *MDR1* SNPs at 1236, 2677, and 3435 sites were transfected into polarized LLC-PK1 cells. The stable clones were selected by two methods (by G418, or by G418 and vincristine sulfate). The mRNA and protein expression levels of Pgp were measured by real time PCR and western blotting, respectively. The expression level of Pgp in variants selected by G418 and vincristine sulfate was higher than by G418 alone. The relative expression level of mRNA and protein were consistent, indicating that SNPs do not affect the translation of the *MDR1* gene. Exogenous Pgp was localized at the cell surface, indicating that it was suitably placed to function in a transport assay.

Chapter Seven

Functional effects of human *MDR1* polymorphisms on transport activity

7.1   Introduction

As mentioned in chapter one, single nucleotide polymorphisms (SNPs) in *MDR1* may be associated with drug resistance in epileptic patients. Three SNPs in the cDNA (1236C>T, 2677G>T/A, and 3435C>T), which are in some degree of linkage disequilibrium, have been the target of investigation by researchers. At first, the effect of SNPs on Pgp function was studied in oncology. The SNPs may affect the expression of Pgp, which influences the degree of drug resistance of cancer cells to chemotherapy and affects drug efficacy (Fung *et al.*, 2009). The expression of Pgp was studied as one of the factors affecting the function of Pgp.

The effects of these three SNPs in humans were studied. The plasma level of digoxin, a substrate of Pgp, was significantly higher in individuals with 3435TT than in individuals with 3435CC (Hoffmeyer *et al.*, 2000; Johne *et al.*, 2002). The renal clearance of digoxin was lower in individuals with 3435T (Kurata *et al.*, 2002). CD56+ natural killer cells from people with the 3435CC genotype had more efflux of rhodamine than cells from people with 3435TT (Hitzl *et al.*, 2001). Europeans and Americans homozygous for the 3435C allele had a lower plasma level of fexofenadine (an antihistamine drug) than did people with the 3435T allele (Kim *et al.*, 2001). But a report indicated that there was no association between 3435 variants and fexofenadine disposition in German Caucasians. The 2677T genotype was associated with a lower AUC of fexofenadine than 2677G in plasma (Drescher *et al.*, 2002). Giloblastoma patients with the 1236CC genotype had a significantly higher rate of survival than patients with 1236C/T or 1236TT genotypes (Schaich *et al.*, 2009).

There was no difference in Pgp surface expression between cells expressing the 3435T or 3435C alleles (Kimchi-Sarfaty *et al.*, 2007; Salama *et al.*, 2006). Haplotypes of

1236/2677/3435 affected the intracellular accumulation of calcein-AM and BODIPY-FL-paclitaxel in a substrate-dependent manner (Gow *et al.*, 2008). Wang *et al.* studied 1236C>T, 2677G>T, and 3435C>T, and found that 3435C>T may be a key factor in changing the mRNA stability of *MDR1* and the *MDR1* mRNA expression level in liver (Wang *et al.*, 2005).

Kimchi-Sarfaty et al. noted that the synonymous allele 3435T, combined with the 2677T and/or 1236T allele, resulted in insensitivity to Pgp inhibitors. The 3435 SNP affects the rate of folding of the Pgp protein as it is translated, thus affecting the insertion of Pgp into the membrane, resulting in a change in the interaction site of substrate and inhibitor and altering Pgp function (Kimchi-Sarfaty *et al.*, 2007). The 1236T, 2677T/A, and 3435T alleles significantly reduced Pgp function, as shown by decreased cell uptake of Rho123 compared with wild type MDR1 in LLC-PK1 cells (Salama *et al.*, 2006). The 1236T and 3435T alleles were associated with decreased Pgp expression and increased Pgp transport activity in placenta (Hemauer *et al.*, 2010). But in another study, 2677 and 3435 alleles did not affect the transport of verapamil, digoxin, vinblastine, and cyclosporine A by Pgp (Morita *et al.*, 2003).

Hung et al. used a cultured cell method to study whether the above polymorphisms affect the efflux of AEDs by Pgp. They found that the 1236T-3435T and 1236T-2677A/T-3435T haplotypes resulted in less effective inhibition of AEDs against substrates of Pgp (Hung *et al.*, 2008). The data suggested that polymorphisms of *MDR1* influenced the interaction between AEDs and Pgp. All the published studies to determine the influence of SNPs in *MDR1* used the cell uptake model, and there was no direct evidence showing that the polymorphisms affect the directional transport of AEDs by Pgp. Therefore, we propose to use monolayers of cells transfected with the *MDR1* variants to investigate their effects on the transport of oxcarbazepine and eslicarbazepine acetate. We chose to use these drugs because they are stronger Pgp substrates than are other AEDs, which may show us more significant transportation difference among the variants.

7.2   Materials and methods

7.2.1 Materials

ESL, MTT (3-[4,5 dimethyl thiazolyl-2]-2,5-diphenyltetrazolium bromide), and Rho123 were supplied by Sigma Aldrich (St. Louis, MO, USA). OXC was obtained from the National Institute for the Control of Pharmaceutical and Biological Products (Beijing, China). Vincristine sulfate was bought from Tauto Biotech (Shanghai, Chian). Geneticin was bought from Gibco (Invitrogen, Hong Kong). Verapamil and MTT were dissolved in water, and other drugs were dissolved in DMSO (<0.1% DMSO in final solution). Acetonitrile (Labscan Asia, Thailand), ethanol (TEDIA Company, Inc., USA), and methanol (TEDIA Company, Inc., USA) were HPLC grade. All other chemicals were analytical grade.

7.2.2 Cell lines and cell culture

LLC (LLC-WT) cells were kindly provided by Professor P. Borst (The Netherlands Cancer Institute, Amsterdam, Netherlands). Cell lines for genetic variants were established in the previous chapter (Zhang *et al.*, 2010; Zhang *et al.*, 2011). Cell culture was performed as described previously. The stable clones transfected with *MDR1* variants were cultured with G418 (1 mg/ml) or vincristine sulfate (800 nM). Cell lines were used within 15 passages after transfection. Phosphate buffered saline (PBS), Dulbecco's Modified Eagle Medium (DMEM), Medium 199, and fetal bovine serum (FBS) were described in the previous chapter.

7.2.3 Real time-PCR analysis

To quantify *MDR1* mRNA levels in the cell lines, RNA was isolated using Trizol (Invitrogen, CA, USA) as described by the manufacturer (Zhang *et al.*, 2010; Zhang *et al.*, 2011). 1 μg total RNA was treated with 0.5 U of DNase I (Invitrogen, CA, USA) and used for RT-PCR. Reverse-transcription was performed using the SuperScript First-

Strand Synthesis System (Invitrogen, CA, USA). Real time PCR was performed with KAPA SYBR® qPCR Master Mix (Kapa Biosystems, MA, USA) in a Roche LightCycler II (Mannheim, Germany). PCR amplification was carried out by using the following primer pairs: *MDR1*, 5'-CCCATCATTGCAATAGCAGG-3' and 5'-TGTTCAAACTTCTGCTCCTGA-3'; *β-Actin*, 5'-CCTCTATGCCAACACAGTGC-3' and 5'-ACATCTGCTGGAAGGTGGAC-3'. For data analysis, relative expression levels of *MDR1* mRNA in LLC variant cells were scaled to the relative expression level of the housekeeping gene *β-actin* by the Roche cycler 480 software. The relative expression level of LLC-CGC (reference variant) was defined as 1.

7.2.4 Western blotting

The protein was extracted by RIPA buffer, and the protein concentration was tested by Bio-Rad protein Assay Kit as described previously. 100 μg protein of each sample was isolated by 7.5% SDS PAGE, and transfered to PVDF membrane at 100V for 4 hours at 4°C. Then, the membrane was blocked by 5% milk for 60 min at room temperature, and incubated with primary antibody (C219, 1:1000; Rabbit anti-tubulin, 1:500) overnight at 4°C. AP conjunct second antibody was incubated (1:2000) for 2 hours at room temperature. For data analysis, Pgp relative expression level was calculated as Pgp / β-tubulin. Each cell line was quantified three times. The relative expression level of LLC-CGC (reference variant) was defined as 1.

7.2.5 Validation of cell monolayer in *MDR1* variants

The validation of *MDR1* variant cell lines was performed as described previously (Zhang *et al.*, 2010; Zhang *et al.*, 2011). Briefly, first, integrity of monolayers was tested by measuring the transepithelial electrical resistance (TEER) with the epithelial volt/ohm meter (World Precision Instruments, Inc., FL, USA). Monolayers with TEER > 150 Ω cm^2 (subtracting the background value of a transwell) were used for assays. After each experiment, TEER was also tested, and monolayers with TEER decreased more than 15%

compared with the initial value were discarded. Second, integrity of monolayers was verified by atenolol and propranolol. The bi-directional transport assays of atenolol and propranolol were performed by measuring the apparent permeability (P_{app}) as described previously. Atenolol and propranolol were dissolved in PBS as working solutions at concentrations of 3 mM and 100 µM, respectively. Initially, 1.5 ml drug solutions were added to the apical side of the monolayer, and 2.6 ml fresh PBS was added to the basolateral side. Aliquots of 0.5 ml samples were taken from basolateral sides every 15 min for 2 hours, and the volume of PBS was replaced after each sampling. The P_{app} value from the apical to the basolateral side was calculated. Cell lines with integrity values which were comparable with published data were chosen for conducting further experiments (Crespi et al., 2000; Thiel-Demby et al., 2008; Wang et al., 2008).

7.2.6 Cytotoxicity test

The cytotoxicities of the tested compounds on *MDR1* variant cell lines were evaluated by MTT assay as described in the previous chapter (Zhang *et al.*, 2010; Zhang *et al.*, 2011). Briefly, 1.5×10^4 cells/well were seeded in 96 well plates and cultured for 48 hr. After withdrawing the culture medium, 200 µl PBS with various concentrations of AEDs was added and incubated for 4 hr. Buffer was then replaced with 200 µl of 0.5 mg/ml MTT in PBS. After 2 hr, the solution was replaced with 200 µl DMSO, and the absorbance was determined at a wavelength of 590 nm on a microplate reader (Benchmark, BioRad, USA).

7.2.7 Concentration equilibrium transport assay

MDR1 variant cell lines were used for concentration equilibrium transport assay (CETA) as described previously (Zhang *et al.*, 2010; Zhang *et al.*, 2011). Briefly, culture medium was replaced with warm PBS for 10 minutes before transport assays. Drugs were initially added to both sides of the monolayer at equal concentrations. Volumes on the apical and basolateral sides were 2 ml and 2.7 ml, respectively. Apical and basolateral samples were collected at various time points of drug exposure (30, 60, 90, 120, 180, and

240 min). Aliquots of 100 μl and 130 μl were collected from apical and basolateral sides, respectively, so as not to affect the hydrostatic pressure on the cell monolayers. The collected samples were stored at -20°C until analysis.

7.2.8 Drug analysis

OXC and ESL were quantified by high performance liquid chromatography with UV detection (HPLC/UV) as described before (Zhang *et al.*, 2010; Zhang *et al.*, 2011). The HPLC system (Waters, Milford, MA, USA) was equipped with a 2695 solvent delivery module, a Thermo Hypersil BDS C18 column (5 μM pores, 250 mm × 4.6 mm inner diameter), and a 996 photodiode-array (PDA) UV detector. The limits of quantification (LOQ) were 50 ng/ml for OXC and 30 ng/ml for ESL. The relative standard deviations (R.S.D.) of both intra-day and inter-day precision for all the drugs were below 5%.

7.2.9 Data analysis

For MTT assays, percentage survival was calculated according to the formula: (mean of drug treatment OD − mean of blank OD) / (mean of control OD − mean of blank OD) x 100%. 80% was considered to be safe for the drugs.

In CETA, the data are presented as the percentage of the drug loading concentration in either apical or basolateral chamber vs. time, as described before. Values are shown as mean ± SEM. At various time intervals, differences of drug concentration between the two chambers of each well were compared, and differences of drug concentration between the two chambers for wildtype (WT) cells were compared with those from MDR1-transfected cells. Significant differences between two groups or more than two groups were calculated by student's t-test or one-way ANOVA, respectively, with $p<0.05$ considered as significant.

7.3   Results and discussions

7.3.1 Selected clones

The stable clones were selected by two methods (G418 or G418 and vincristine sulfate). The mRNA and protein expression level of Pgp were measured by real time PCR and western blotting. The clones with suitable expression level of Pgp were chosen to perform further experiments.

7.3.2 AED cytotoxicity

The cytotoxicity test was performed on variant cell lines for ESL and OXC at concentrations of 5, 10, and 20 μg/ml. The MTT assay indicated that the concentrations of ESL and OXC tested were not toxic to the variant cell lines for at least 240 min (Fig 7.1).
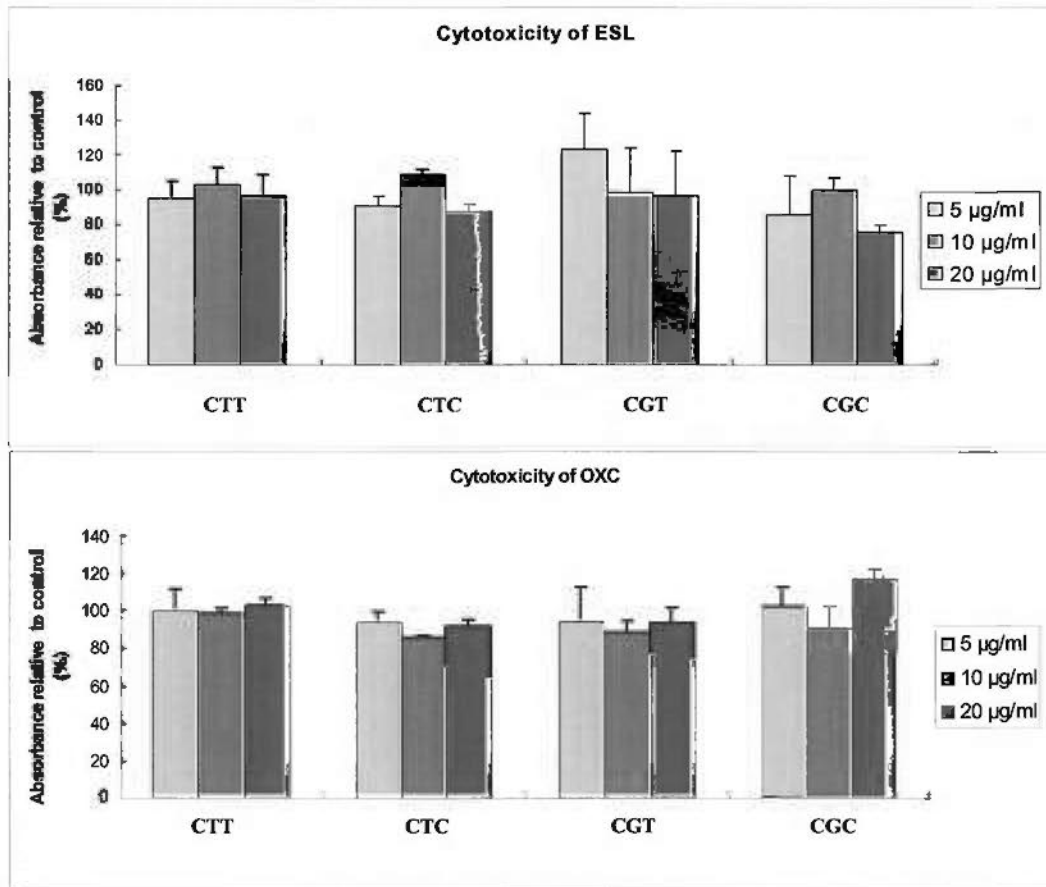
Fig 7.1 **Viability of cells exposed to ESL or OXC for MDR1-CTT (7-10), MDR1-CTC (CTC-5), MDR1-CGT (4-5), and MDR1-CGC (Ref-5) cell lines. Values are means ± SEM.**

7.3.3 Validation of cell monolayers of *MDR1* variants

Integrity of monolayers of the variants was verified by testing that the apparent permeability values (P_{app}) of atenolol and propranolol were within the range of 0.5×10^{-6} to 1.5×10^{-6} cm/s and 15×10^{-6} to 40×10^{-6} cm/s respectively, which were comparable to those previously published (Crespi *et al.*, 2000; Thiel-Demby *et al.*, 2008; Wang *et al.*, 2008; Zhang *et al.*, 2010; Zhang *et al.*, 2011).

7.3.4 Functional evaluation of *MDR1* polymorphisms

7.3.4.1 Functional evaluation of clones selected by G418

7.3.4.1.1 Transport assay of OXC

The clones selected by G418 were picked up, and the mRNA and protein level were measured. Wildtype cells and variant cells (2677G>T and 3435 C>T variants) were used in experiments. Pgp relative expression level was calculated by Pgp / β-tubulin for protein and *MDR1 / β-actin* for mRNA. The relative expression of *MDR1*-CGC (clone: L-REF-5) was defined as 1 for both mRNA and protein. The expression levels of Pgp mRNA and protein are shown (Fig 7.2, Table 7.1, and Table 7.2).
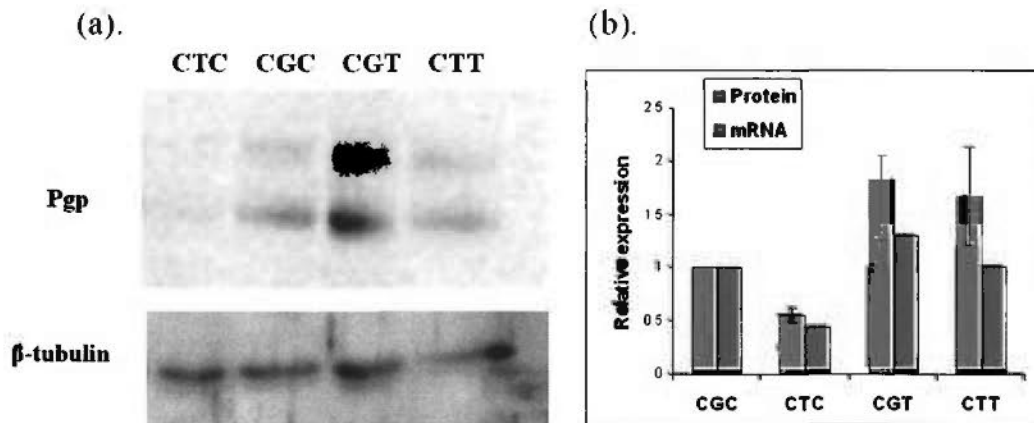
Fig 7.2   MDR1 protein and mRNA expression levels: (a) western blot of cell lines expressing genetic variants and (b) relative quantification of MDR1 protein and mRNA levels obtained by western blotting and real time PCR, respectively.

For the concentration equilibrium transport assay, cells were seeded into transwells, and OXC was added at a concentration of 5 µg/ml. Wildtype and variant cells all pumped OXC from the basolateral to the apical side (Fig 7.3). The concentration difference between apical and basolateral sides at 240 min (con. difference at 240 min) was calculated for each cell line. Because the expression level of Pgp was not the same among variant cell lines, the function of Pgp was evaluated by the concentration difference at

240 min divided by Pgp expression level (con. difference at 240 min / mRNA level or con. difference at 240 min / protein level) for each variant cell line. MDR1-CTC exhibited the biggest difference after correcting by the mRNA level of Pgp (Fig 7.4 & Table 7.1); the difference was significantly higher than that of MDR1-CGC (p=0.02). Differences for MDR1-CGT and MDR1-CTT were not significantly bigger than that of MDR1-CGC (p=0.19 and 0.087, respectively).

Table 7.1 The mRNA expression level and transport of OXC (at 5 µg/ml) by MDR1 variants.

		L-REF-5 (MDR1-CGC)	L-CTC-5 (MDR1-CTC)	L-4-5 (MDR1-CGT)	L-7-10 (MDR1-CTT)
mRNA level		1.0	0.4	1.1	1.0
Con. difference at 240 min (%)	Mean	15.4	20.1	27.8	20.9
	SD	4.2	6.2	8.2	5.1
Amount 0 to 240 min (µg)	Mean	1.9	2.4	2.8	2.5
	SD	1.1	0.7	0.7	0.6
Con. difference at 240 min / mRNA level	Mean	15.4	45.9	24.5	18.8
	SD	4.2	14.1	7.3	4.6
Amount 0 to 240 min / mRNA level	Mean	1.9	5.6	2.4	2.2
	SD	1.1	1.6	0.6	0.5
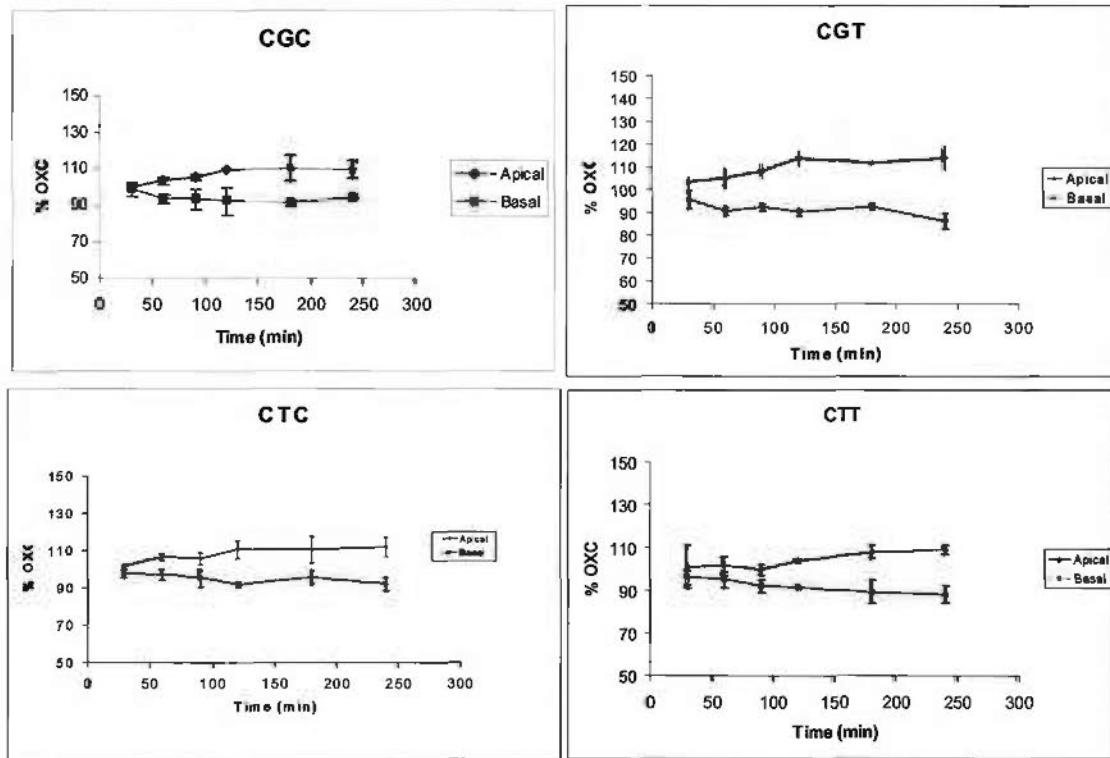
Fig 7.3   Concentration equilibrium transport assays of oxcarbazepine for MDR1-CGC (Ref-5), MDR1-CTC (CTC-5), MDR1-CGT (4-5), and MDR1-CTT (7-10). Data are given as the percentage of the initial drug concentration in either apical or basolateral chamber vs. time. Experiments were performed in triplicate, and values are shown as mean ± SD.

Con. difference at 240 min/mRNA level
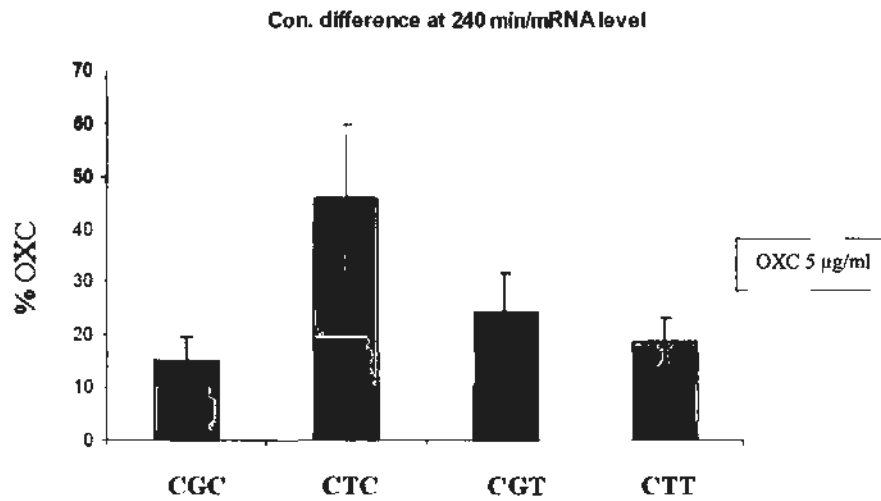
Fig 7.4 **The concentration difference between apical and basolateral sides at 240 min divided by the mRNA level of MDR1 for MDR1-CGC (Ref-5), MDR1-CTC (CTC-5), MDR1-CGT (4-5), and MDR1-CTT (7-10). Data are given as the percentage of the initial drug concentration in either apical or basolateral chambers. Experiments were performed in triplicate, and values are shown as mean ± SD.**

The amount of drug transported by Pgp during 240 min was also calculated and divided by Pgp expression level (amount 0-240 min / mRNA level or amount 0-240 min / protein level). This method of calculation gave results similar to those obtained using the concentration difference (Fig 7.5 & Table 7.1). For amount of drug transported, corrected by the mRNA expression level, the MDR1-CTC cell line transported more drug than MDR1-CGC (p=0.028) or MDR1-CGT (p=0.032). There were no significant differences among other variants.

Fig 7.5   The amount of drug transported by Pgp during 240 min divided by the mRNA level of Pgp for MDR1-CGC (Ref-5), MDR1-CTC (CTC-5), MDR1-CGT (4-5), and MDR1-CTT (7-10). Experiments were performed in triplicate, and values are shown as mean ± SD.

The concentration difference at 240 min and amount of drug transported by Pgp during 240 min were corrected by Pgp protein level. The values of amount 0-240 min / protein level and con. difference at 240 min / protein level for each variant were calculated (Table 7.2, Fig 7.6), exhibiting the same relative pattern in the comparison of variants as the data corrected by MDR1 mRNA level. The amount and con. difference of MDR1-CTC cells were significantly higher than those of MDR1-CGC ($p=0.031$ and 0.024, respectively), MDR1-CTT ($p=0.048$ and 0.040, respectively), and MDR1-CGT cells ($p=0.014$ and 0.028, respectively). There were no significant differences among MDR1-CGC, MDR1-CTT, and MDR1-CGT cell lines.

Table 7.2 Protein expression level and transport of OXC (at 5 µg/ml) by MDR1 variants.

		L-REF-5 (MDR1-CGC)	L-CTC-5 (MDR1-CTC)	L-4-5 (MDR1-CGT)	L-7-10 (MDR1-CTT)
Protein level	Mean	1.0	0.6	1.8	1.7
	SD	0.0	0.1	0.2	0.5
Con. difference at 240 min (%)	Mean	15.4	20.1	27.8	20.9
	SD	4.2	6.2	8.2	5.1
Amount 0-240 min (µg)	Mean	1.9	2.4	2.8	2.5
	SD	1.1	0.7	0.7	0.6
Con. difference at 240min/protein level	Mean	15.4	35.9	15.3	12.5
	SD	4.2	11.0	4.5	3.0
Amount 0-240min/ protein level	Mean	1.9	4.4	1.5	1.5
	SD	1.1	1.2	0.4	0.3
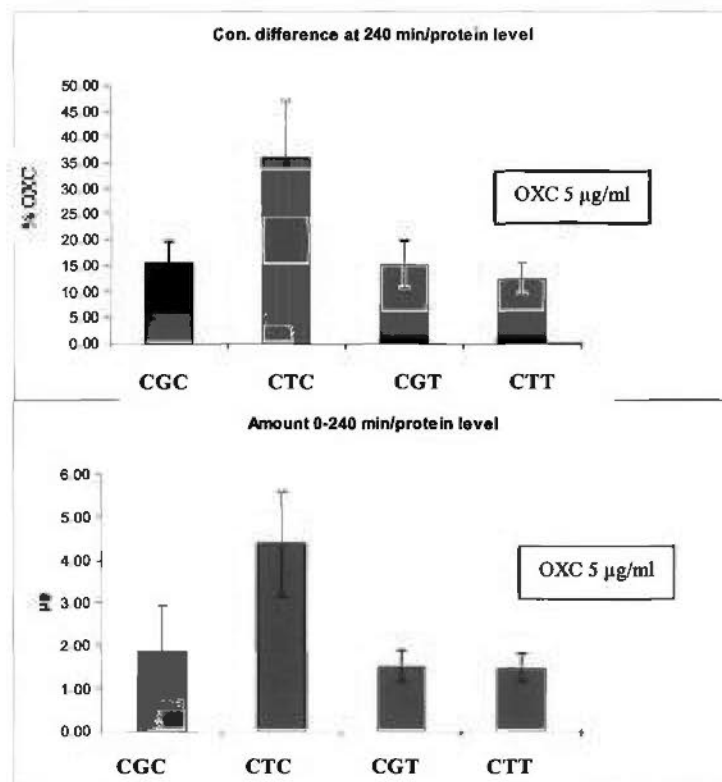
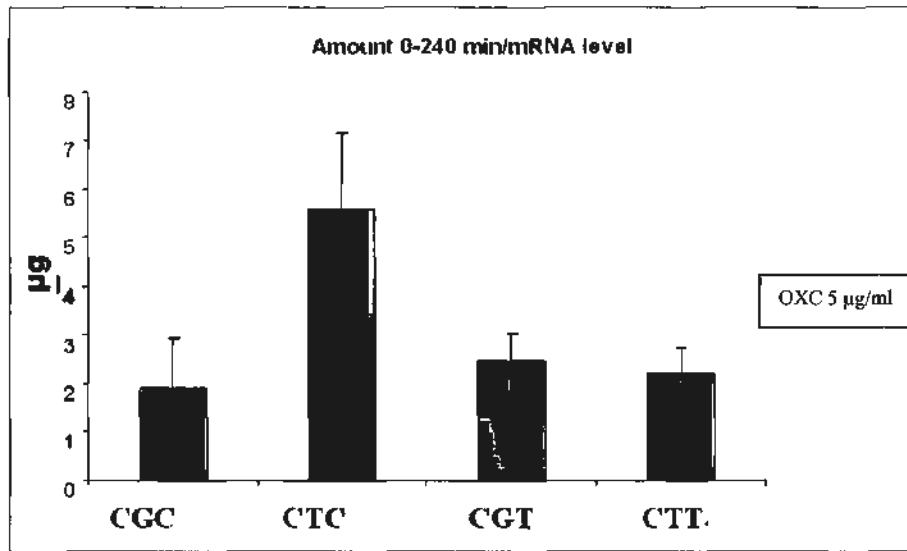Fig 7.6   The concentration difference between apical and basolateral sides at 240 min (Top) and the amount of drug transported by Pgp during 240 min divided (bottom) by the protein level of Pgp for MDR1-CGC (Ref-5), MDR1-CTC (CTC-5), MDR1-CGT (4-5), and MDR1-CTT (7-10). Data are given as the percentage of the initial drug concentration in either apical or basolateral chambers for the top figure. Experiments were performed in triplicate, and values are shown as mean ± SD.

153

7.3.4.1.2 Transport assay of ESL

The concentration equilibrium transport assay was also performed by using ESL for the above variants. At 10 µg/ml, ESL was transported from the basolateral to the apical side by all the variants, indicating that they all had Pgp function (Fig 7.7). The concentration difference between apical and basolateral sides at 240 min and the amount of drug transported by Pgp during 240 min were calculated and divided by Pgp protein expression level (Table 7.3 & Table 7.4) or MDR1 mRNA level (Table 7.3). All four values for MDR1-CTC cells were significantly higher than those for other variants (MDR1-CGC, MDR1-CTT, and MDR1-CGT), but there were no significant differences among MDR1-CGC, MDR1-CTT, and MDR1-CGT cell lines (Fig 7.8).

Fig 7.7   Concentration equilibrium transport assays of eslicarbazepine acetate (ESL) at 10 µg/ml for MDR1-CGC (Ref-5), MDR1-CTC (CTC-5), MDR1-CGT (4-5), and MDR1-CTT (7-10). Data are given as the percentage of the initial drug

concentration in either apical or basolateral chamber vs. time. Experiments were performed in triplicate, and values are shown as mean ± SD.

Table 7.3 The mRNA expression level and transport of ESL (at 10 µg/ml) by MDR1 variants.

|		L-REF-5 (MDR1-CGC)	L-CTC-5 (MDR1-CTC)	L-4-5 (MDR1-CGT)	L-7-10 (MDR1-CTT)
mRNA level		1.0	0.4	1.1	1.0
Con. difference at 240	Mean	38.8	49.9	57.3	48.5
min (%)	SD	2.2	6.3	2.4	0.3
Amount 0-240 min	Mean	4.6	5.7	5.9	6.3
(µg)	SD	0.5	0.8	0.7	1.0
Con. difference at 240	Mean	38.8	114.0	50.6	43.7
min / mRNA level	SD	2.2	14.4	2.1	0.3
Amount 0-240min /	Mean	4.6	13.0	5.2	5.7
mRNA level	SD	0.5	1.9	0.6	0.9
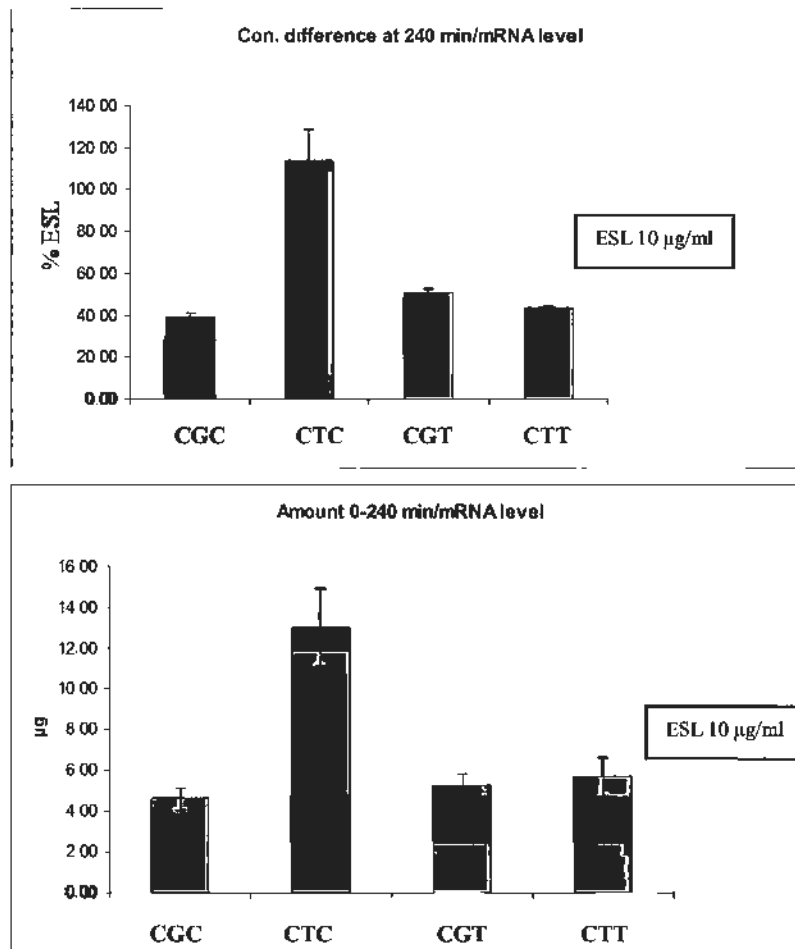
Fig 7.8   CETA for ESL at 10 µg/ml. The concentration difference between apical and basolateral sides at 240 min (Top) and the amount of drug transported by Pgp during 240 min divided (bottom) by the mRNA level of Pgp for MDR1-CGC (Ref-5), MDR1-CTC (CTC-5), MDR1-CGT (4-5), and MDR1-CTT (7-10). For the top figure, data are given as the percentage of the initial drug concentration in either apical or basolateral chambers. Experiments were performed in triplicate, and values are shown as mean ± SD.

The concentration difference at 240 min and amount of drug transported by Pgp during 240 min were divided by Pgp protein level (Table 7.4), resulting in the same relative pattern in the comparison of variants as seen for the values corrected by mRNA level.

156

The function of MDR1-CTC cells was highest and significantly higher than that of MDR1-CGC, MDR1-CTT, and MDR1-CGT. There was no significant difference among MDR1-CGC, MDR1-CTT, and MDR1-CGT cells (Fig 7.9).
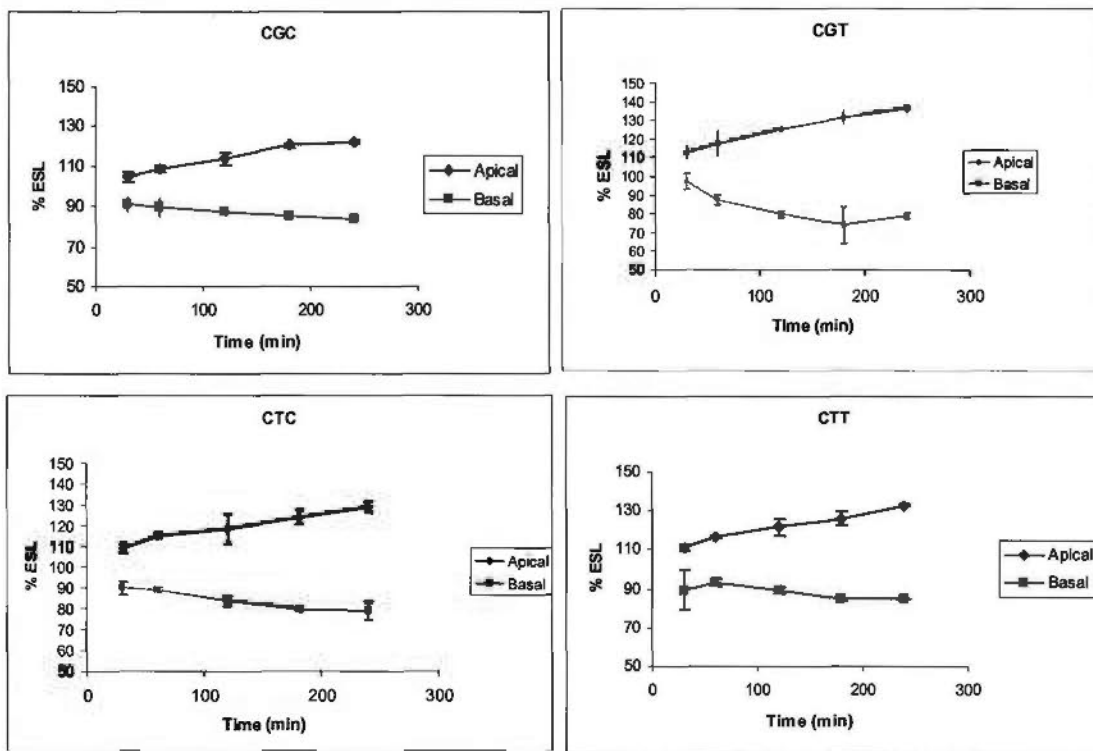
Table 7.4 The protein expression level and transport of ESL (at 10 µg/ml) by MDR1 variants.

|		L-REF-5 (MDR1-CGC)	L-CTC-5 (MDR1-CTC)	L-4-5 (MDR1-CGT)	L-7-10 (MDR1-CTT)
Protein level	Mean	1.0	0.6	1.8	1.7
	SD	0.0	0.1	0.2	0.5
Con. difference at 240 min (%)	Mean	38.8	49.9	57.3	48.5
	SD	2.2	6.3	2.4	0.3
Amount 0-240 min (µg)	Mean	4.6	5.7	5.9	6.3
	SD	0.5	0.8	0.7	1.0
Con. difference at 240min/protein level	Mean	38.8	89.1	31.5	29.0
	SD	2.2	11.2	1.3	0.2
Amount 0-240min/ protein level	Mean	4.6	10.2	3.3	3.8
	SD	0.5	1.5	0.4	0.6
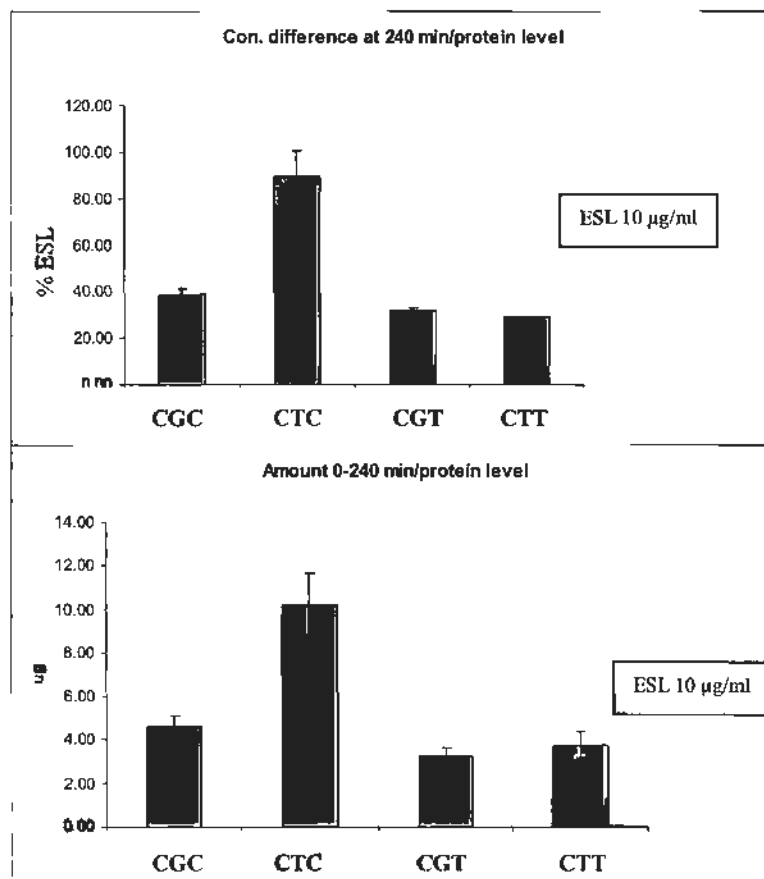
Fig 7.9   **CETA for ESL at 10 μg/ml. The concentration difference between apical and basolateral sides at 240 min (top) and the amount of drug transported by Pgp during 240 min (bottom) divided by the protein level of Pgp for MDR1-CGC (Ref-5), MDR1-CTC (CTC-5), MDR1-CGT (4-5), and MDR1-CTT (7-10). For the top figure, data are given as the percentage of the initial drug concentration in either apical or basolateral chambers. Experiments were performed in triplicate, and values are shown as mean ± SD.**

The clones were re-selected by a higher concentration of G418 in order to increase the Pgp expression level. MDR1-CGC, MDR1-CTC, MDR1-CGT, and MDR1-CTT were used. The mRNA and protein expression level were detected by real time PCR and western blotting. The expression level of Pgp is shown for each variant in Fig 7.10 and Table 7.5.
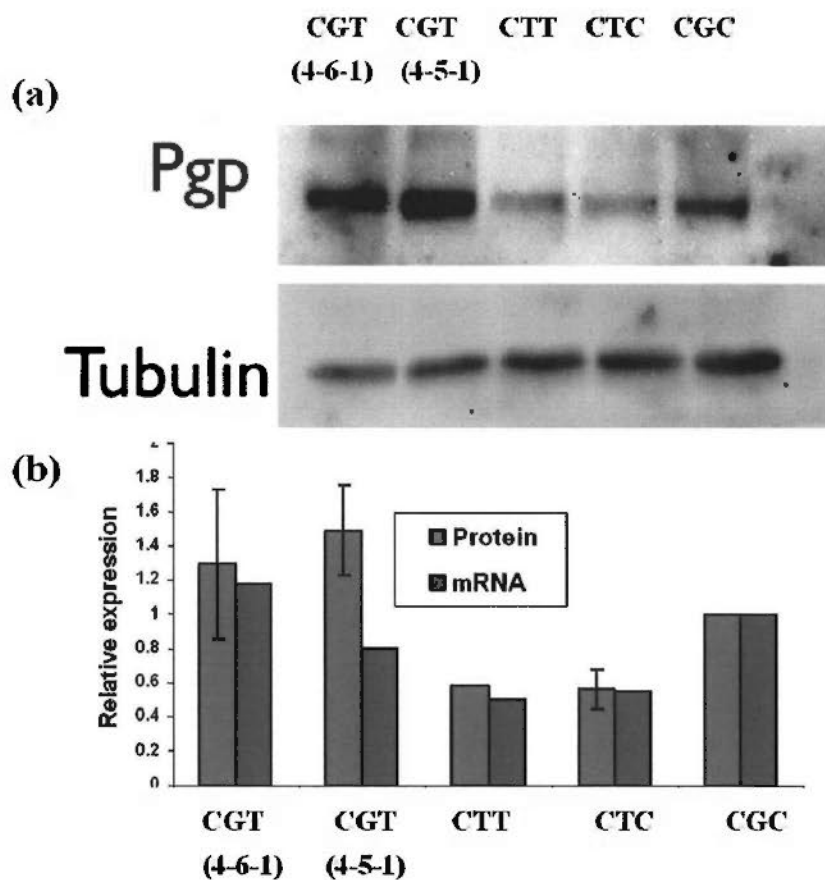
Fig 7.10   Expression of Pgp in MDR1-CGC (Ref-5-1), MDR1-CTC (CTC-5-1), MDR1-CGT
(4-5-1 and 4-6-1), and MDR1-CTT (7-10-1) cell lines: (a) western blotting of Pgp and
β-tubulin and (b) the relative expression level of protein (Pgp / β-tubulin) and
mRNA (MDR1 / β-actin).

Table 7.5 The mRNA expression level of MDR1 in variants.

Variant name	MDR1 Ct (Mean)	β-actin Ct (Mean)	Ratios (MDR1/ β-actin)
CGC	18.0	21.6	12.5
CTC	18.3	21.1	6.9
CTT	18.4	21.1	6.3
CGT (4-5-1)	17.9	21.2	10.0
CGT 4-6-1	17.2	21.1	14.7

The concentration equilibrium transport assay was performed by using 2 μg/ml ESL for these five clones. MDR1-CGC (Ref-5-1), MDR1-CTC (CTC-5-1), MDR1-CGT (4-5-1 and 4-6-1), and MDR1-CTT (7-10-1) all transported ESL from the basolateral to the apical side (Fig 7.11).

The concentration difference between apical and basolateral sides at 240 min was calculated for each clone, and the value was corrected by the mRNA level and protein level of Pgp (Table 7.6). The value of the concentration difference divided by the mRNA level in MDR1-CTC (CTC-5-1) was significantly higher than for MDR1-CGC (Ref-5-1), MDR1-CGT (4-5-1 and 4-6-1), and MDR1-CTT (7-10-1) variants. The con. difference at 240 min / mRNA value in MDR1-CGC (Ref-5-1) cells was significantly lower than in both clones of MDR1-CGT (clones: 4-5-1 & 4-6-1). There were no significant differences between MDR1-CGC and MDR1-CTT or between MDR1-CTT and MDR1-CGT (Fig 7.12). The concentration difference between apical and basal sides was also corrected by the Pgp protein level. The value for MDR1-CTC (CTC-5-1) was significantly higher than for MDR1-CGC (Ref-5-1), MDR1-CGT (4-5-1 and 4-6-1), and MDR1-CTT (7-10-1). There were no significant differences among other clones.
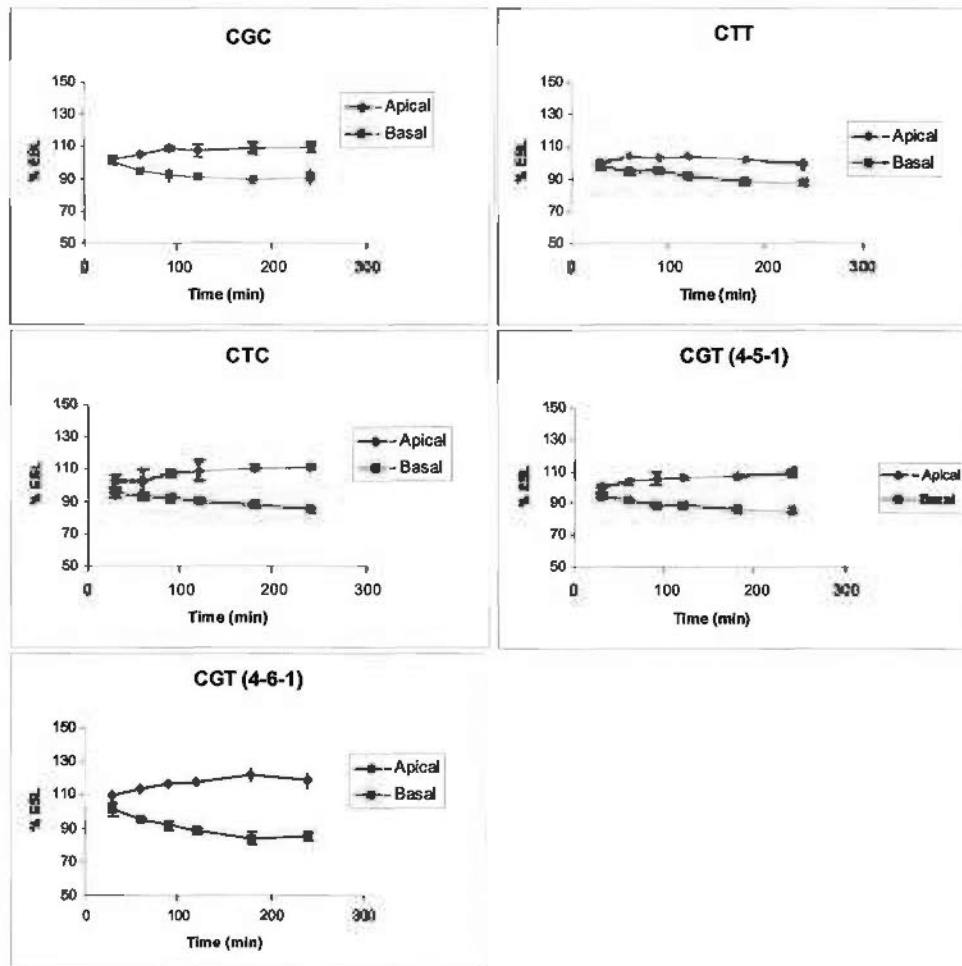
Fig 7.11   Concentration equilibrium transport assays of eslicarbazepine acetate (ESL) at 2 µg/ml for MDR1-CGC (Ref-5-1), MDR1-CTC (CTC-5-1), MDR1-CGT (4-5-1 and 4-6-1), and MDR1-CTT (7-10-1). Data are given as the percentage of the initial drug concentration in either apical or basolateral chamber vs. time. Experiments were performed in triplicate, and values are shown as mean ± SD.

Table 7.6 The protein and mRNA expression level and transport of ESL (at 2 µg/ml) by MDR1 variants.

		REF--5-1 (MDR1-CGC)	CTC-5-1 (MDR1-CTC)	L4--5-1 (MDR1-CGT)	L4--6-1 (MDR1-CGT)	7-10-1 (MDR1-CTT)
mRNA level		1.0	0.6	0.8	1.2	0.5
Protein level	Mean	1.0	0.6	1.5	1.3	0.6
	SE	0.0	0.1	0.3	0.4	0.0
Concentration difference at 240 min (%)	Mean	18.7	26.9	24.0	33.3	11.6
	SD	4.8	1.4	2.9	1.8	2.6
Concentration difference at 240min/mRNA level	Mean	18.7	48.6	30.0	28.2	22.7
	SD	4.8	2.5	3.6	1.5	5.1
Concentration difference at 240min/protein level	Mean	18.7	48.1	16.1	25.6	19.9
	SD	4.8	2.5	1.9	1.4	4.4
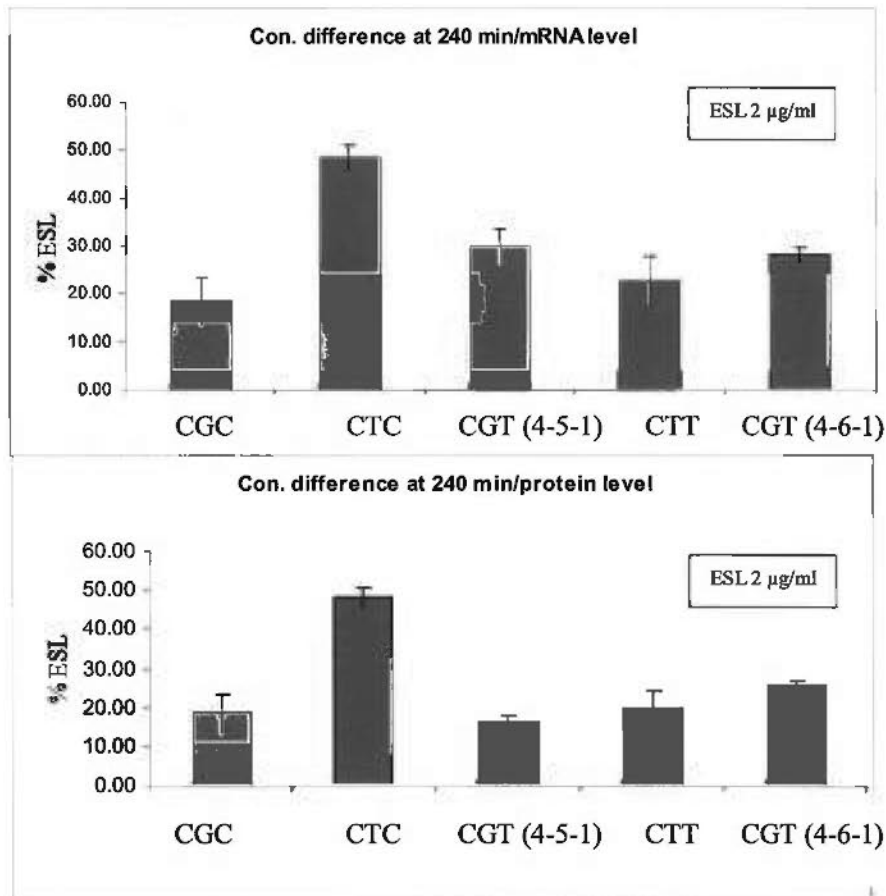
Fig 7.12 CETA for ESL at 2 µg/ml. The concentration difference between apical and basolateral sides at 240 min divided by the mRNA level (top) and protein level of Pgp (bottom) for MDR1-CGC (Ref-5-1), MDR1-CTC (CTC-5-1), MDR1-CGT (4-5-1 and 4-6-1), and MDR1-CTT (7-10-1). Data are given as the percentage of the initial drug concentration in either apical or basolateral chambers, and values are shown as mean ± SD.

7.3.4.2 Functional evaluation of clones selected by G418 and vincristine sulfate

7.3.4.2.1 Transport assay of OXC

The LLC cells transfected with plasmids of MDR1 variants were selected by G418 and vincristine sulfate in order to increase the expression of Pgp, which was measured by western blotting and real time PCR. The relative level of Pgp was calculated as Pgp / β-

tubulin for protein and MDR1 / β-actin for mRNA (Fig 7.13). The expression level of Pgp was increased by this method of clone selection (data not shown).
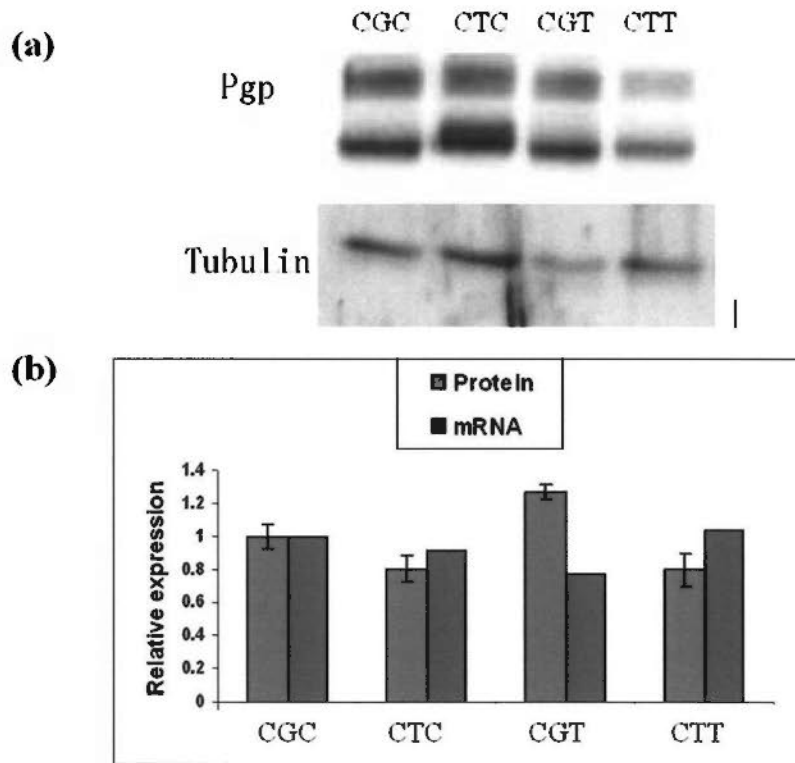
Fig 7.13   **Expression of Pgp in MDR1-CGC (LII-Ref-11), MDR1-CTC (LII-CTC-9), MDR1-CGT (LII-4-16), and MDR1-CTT (LII-7-7) by (a) western blotting and (b) western blotting (Pgp / β-tubulin) and real time PCR (MDR1 / β-actin).**

Concentration equilibrium transport assays were performed for OXC at 5 μg/ml. MDR1-CGC (LII-Ref-11), MDR1-CTC (LII-CTC-9), MDR1-CGT (LII-4-16), and MDR1-CTT (LII-7-7) all transported OXC from the basal to the apical side (Fig 7.14).

For each variant, the concentration difference between both sides at 240 min was calculated and the value corrected by the MDR1 mRNA level (con. difference at 240 min / mRNA level), revealing no significant difference among the variants (Fig 7.15). The

amount of OXC transported by Pgp was also calculated. After correction by mRNA level, there was no significant difference among the variants (Fig 7.15).

The concentration difference and amount of OXC transported were also corrected by the protein level (Fig 7.16). Perhaps because the protein expression level of MDR1-CGT (LII-4-16) was higher than for other clones (Fig 7.13), the two values (con. difference at 240 min / protein level and amount 0-240 min / protein level) for LII-4-16 were lower than for others (Fig 7.16).
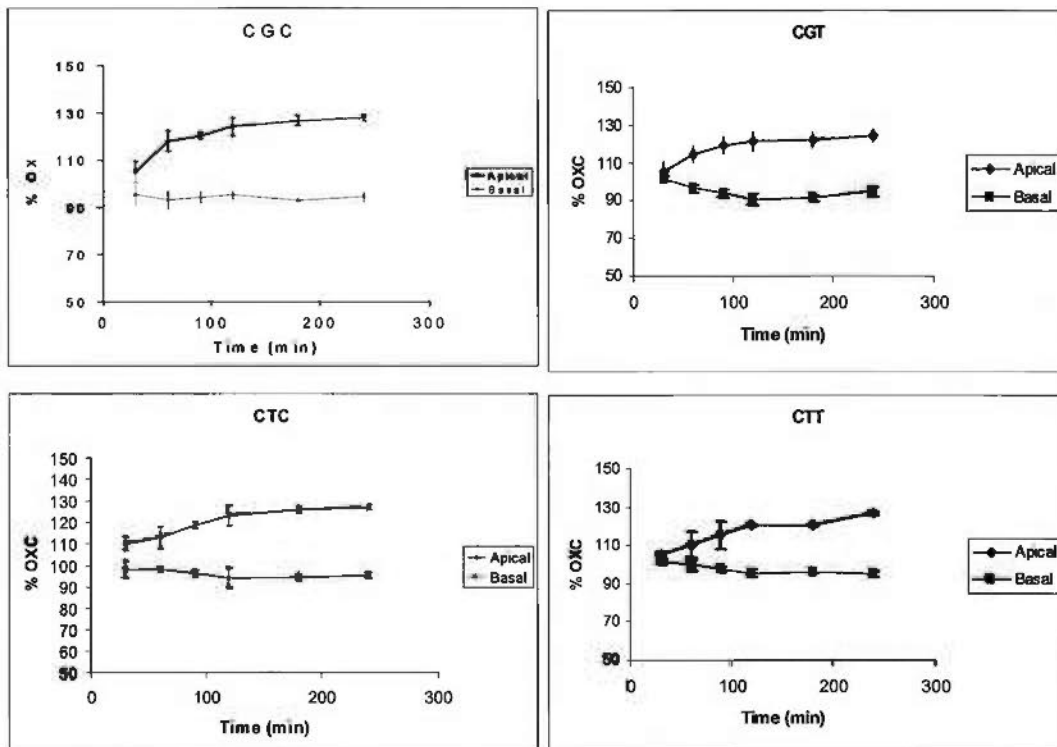
Fig 7.14 **Concentration equilibrium transport assays of oxcarbazepine for MDR1-CGC (LII-Ref-11), MDR1-CTC (LII-CTC-9), MDR1-CGT (LII-4-16), and MDR1-CTT (LII-7-7). Data are given as the percentage of the initial drug concentration in either apical or basolateral chamber vs. time. Experiments were performed in triplicate, and values are shown as mean ± SD.**

Fig 7.15 The concentration difference of OXC between apical and basolateral sides at 240 min (top) and the amount of OXC transported by Pgp during 240 min (bottom) divided by the mRNA level of MDR1 for MDR1-CGC (LII-Ref-11), MDR1-CTC (LII-CTC-9), MDR1-CGT (LII-4-16), and MDR1-CTT (LII-7-7). Data are given as the percentage of the initial drug concentration in either apical or basolateral chambers for the top figure. Experiments were performed in triplicate, and values are shown as mean ± SD.

Fig 7.16 The concentration difference of OXC between apical and basolateral sides at 240 min (top) and the amount of OXC transported by Pgp during 240 min (bottom) corrected by the protein level of Pgp for MDR1-CGC (LII-Ref-11), MDR1-CTC (LII-CTC-9), MDR1-CGT (LII-4-16), and MDR1-CTT (LII-7-7). Data are given as the percentage of the initial drug concentration in either apical or basolateral chambers for the top figure. Experiments were performed in triplicate, and values are shown as mean ± SD.

In order to confirm the results, we used other clones selected by G418 and vincristine— MDR1-CGC (LII-Ref-10), MDR1-CTC (LII-CTC-7), MDR1-CGT (LII-4-11), and MDR1-CTT (LII-7-8)—to measure expression levels (Fig 7.17) and transport of OXC at 5 µg/ml in the concentration equilibrium transport assay. These clones exhibited transport

values similar to those of each other and to those observed for the previous set of clones (Fig 7.18 and 7.19). The protein level of clone LII-4-11 was lower than others, which might be responsible for the transport of this clone being higher than others (Fig 7.20).

(a)   **(b)**
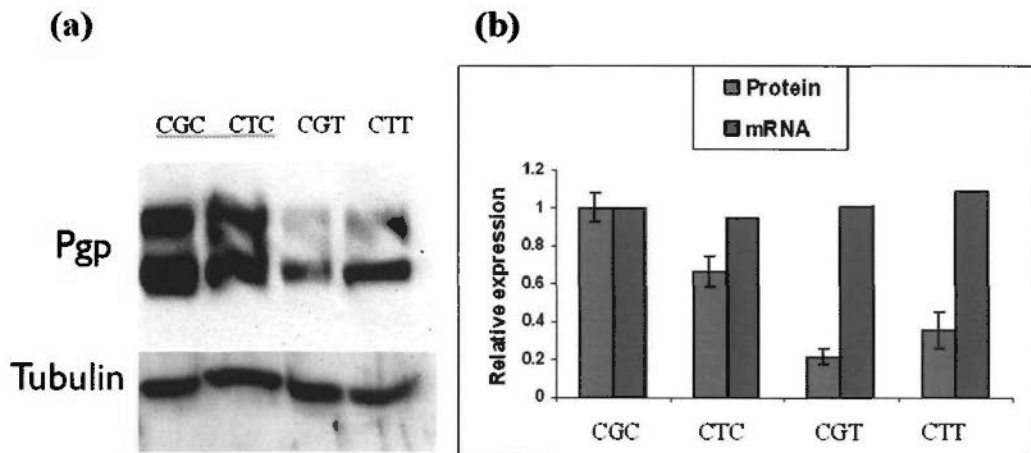
Fig 7.17   Western blotting and real time PCR to detect the expression level of Pgp and β-tubulin for MDR1-CGC (LII-Ref-10), MDR1-CTC (LII-CTC-7), MDR1-CGT (LII-4-11), and MDR1-CTT (LII-7-8). The left figure shows the result of western blotting, and the right figure shows the relative expression level of protein (Pgp/ β-tubulin) and mRNA (MDR1/ β-actin).
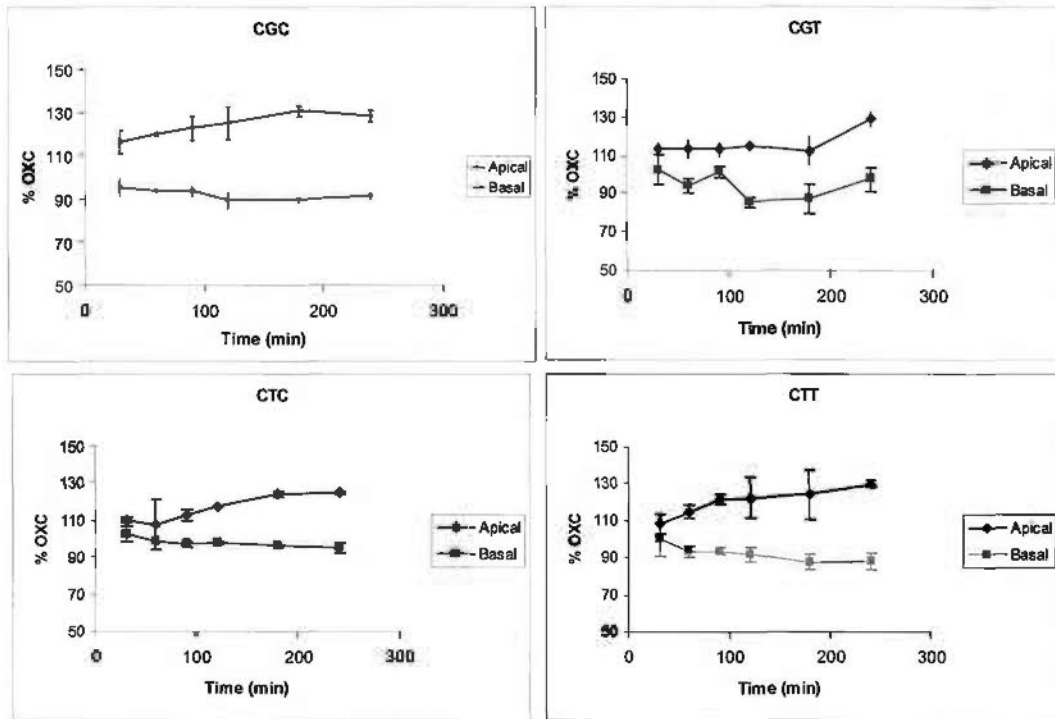
Fig 7.18   Concentration equilibrium transport assays of oxcarbazepine for MDR1-CGC (LII-Ref-10), MDR1-CTC (LII-CTC-7), MDR1-CGT (LII-4-11), and MDR1-CTT (LII-7-8). Data are given as the percentage of the initial drug concentration in either apical or basolateral chamber vs. time. Experiments were performed in triplicate, and values are shown as mean ± SD.
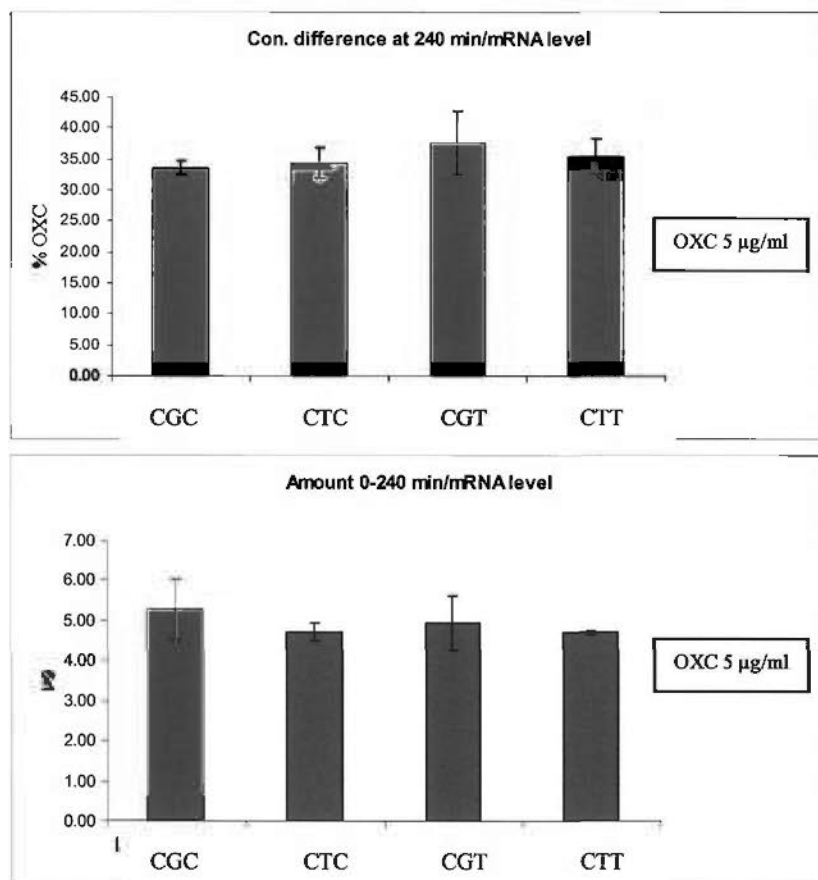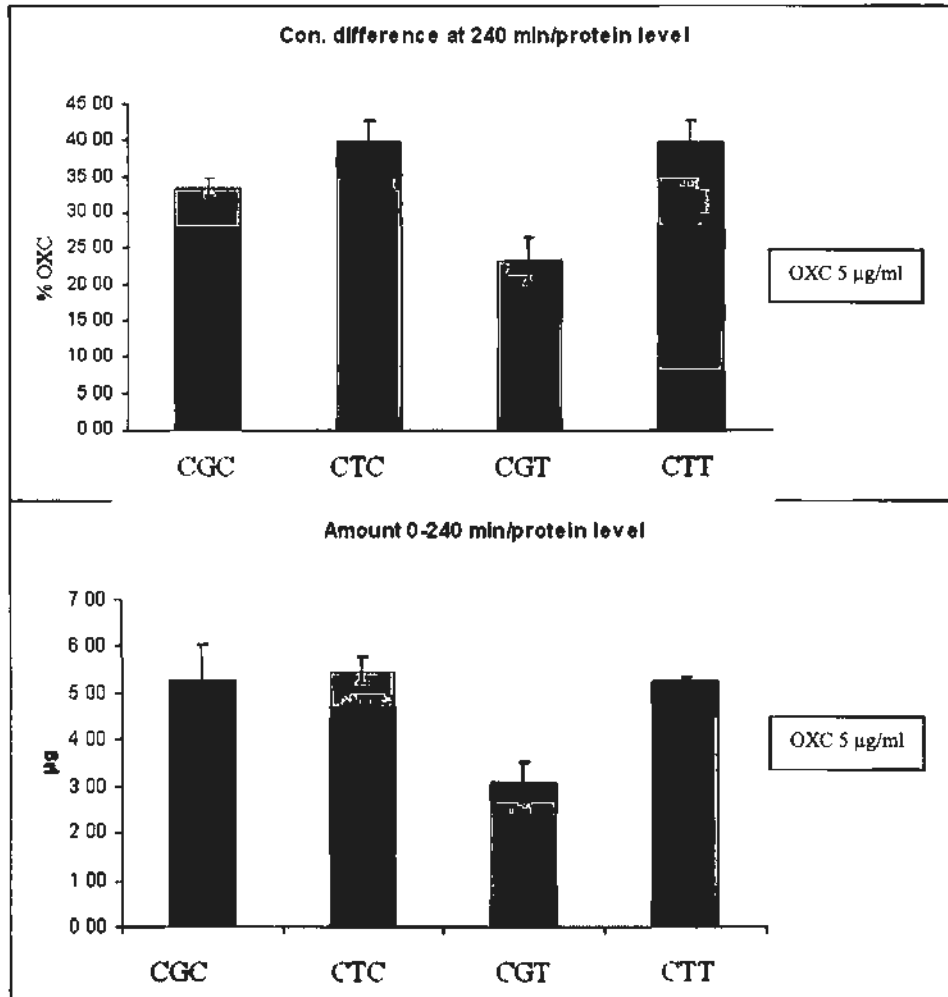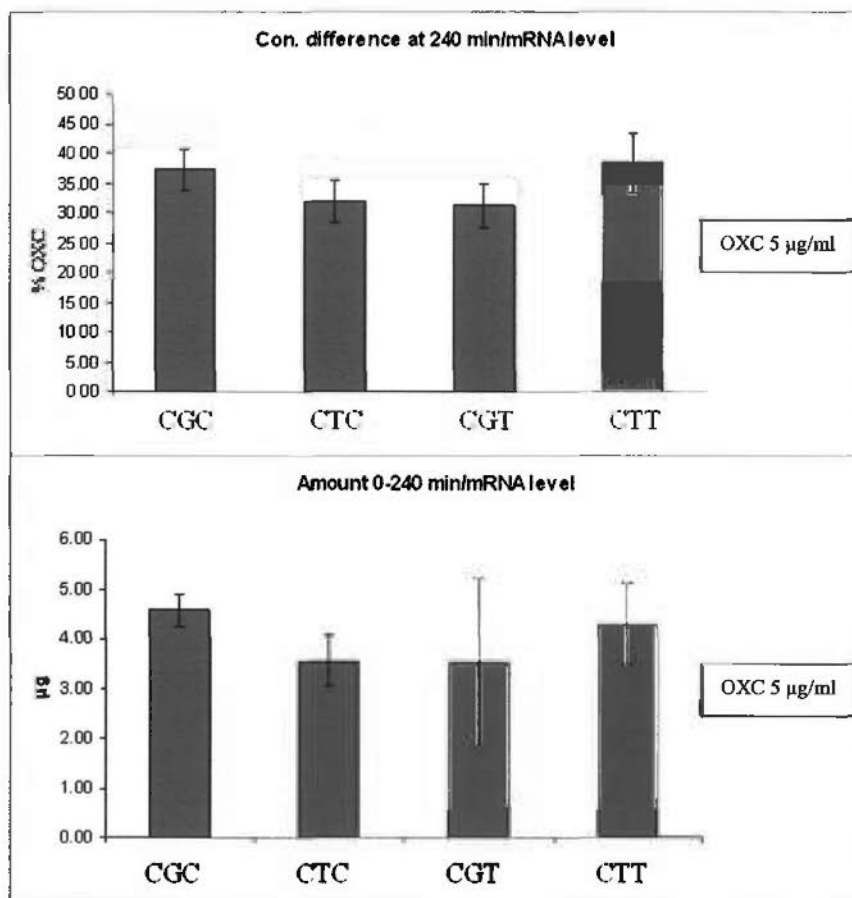
Fig 7.19 The concentration difference of OXC between apical and basolateral sides at 240 min (top) and the amount of OXC transported by Pgp during 240 min (bottom) divided by the mRNA level of MDR1 for MDR1-CGC (LII-Ref-10), MDR1-CTC (LII-CTC-7), MDR1-CGT (LII-4-11), and MDR1-CTT (LII-7-8). Data are given as the percentage of the initial drug concentration in either apical or basolateral chambers for the top figure. Experiments were performed in triplicate, and values are shown as mean ± SD.
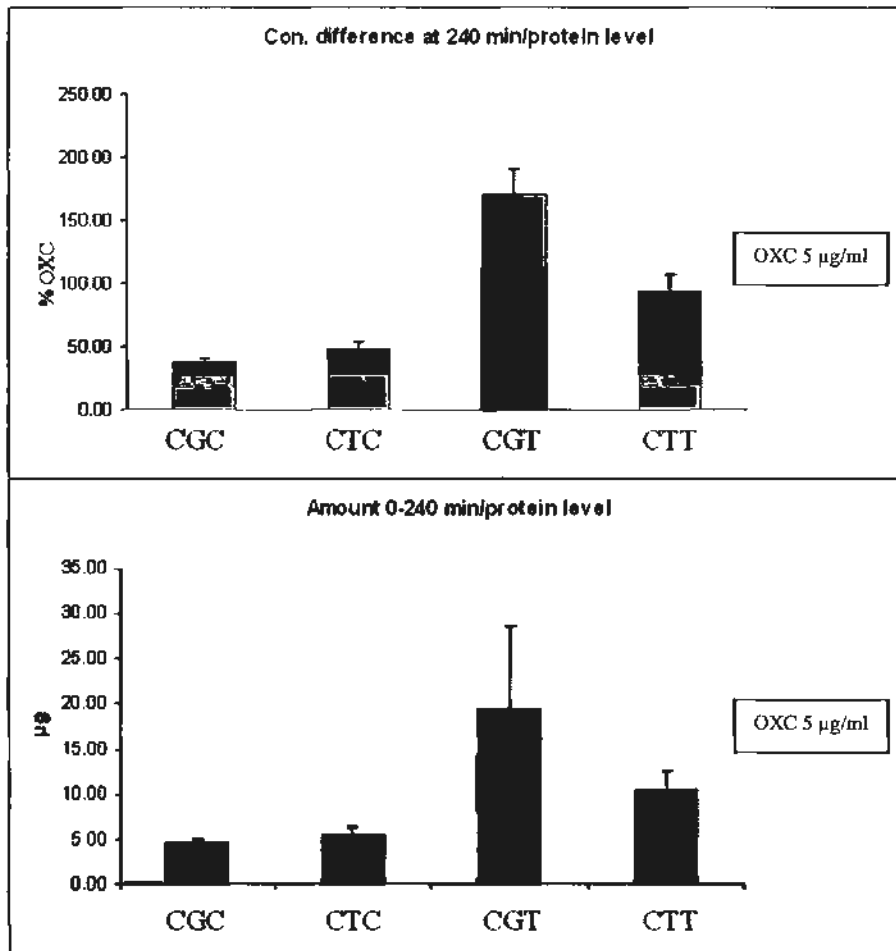
Fig 7.20 The concentration difference of OXC between apical and basolateral sides at 240 min (top) and the amount of OXC transported by Pgp during 240 min (bottom) corrected by the protein level of Pgp for MDR1-CGC (LII-Ref-10), MDR1-CTC (LII-CTC-7), MDR1-CGT (LII-4-11), and MDR1-CTT (LII-7-8). Data are given as the percentage of the initial drug concentration in either apical or basolateral chambers for the top figure. Experiments were performed in triplicate, and values are shown as mean ± SD.

7.3.4.2.2 Transport assay of ESL

The concentration equilibrium transport assay was performed by using ESL to evaluate the Pgp function of variants selected by vincristin sulfate. At 10 µg/ml, ESL was

transported by the clones with the variants, including MDR1-CGC (LII-Ref-11), MDR1-CTC (LII-CTC-9), MDR1-CGT (LII-4-16) (Fig 7.21).

Fig 7.21   **Concentration equilibrium transport assays of eslicarbazepine acetate (ESL) for MDR1-CGC (LII-Ref-11), MDR1-CTC (LII-CTC-9), MDR1-CGT (LII-4-16), and MDR1-CTT (LII-7-7). Data are given as the percentage of the initial drug concentration in either apical or basolateral chamber vs. time. Experiments were performed in triplicate, and values are shown as mean ± SD.**

ESL transport corrected by mRNA level was higher for MDR1-CGT (LII-4-16) and MDR1-CTC (LII-CTC-9) and lower for MDR1-CTT (LII-7-7) than MDR1-CGC (LII-Ref-11) (Fig 7.22). ESL transport corrected by Pgp protein level was higher for MDR1-CGT (LII-4-16) and lower for MDR1-CTC (LII-CTC-9) and MDR1-CTT (LII-7-7) than MDR1-CGC (LII-Ref-11) (Fig 7.23).

Fig 7.22 The concentration difference of ESL between apical and basolateral sides at 240 min (top) and the amount of ESL transported by Pgp during 240 min (bottom) divided by the mRNA level of Pgp for MDR1-CGC (LII-Ref-11), MDR1-CTC (LII-CTC-9), MDR1-CGT (LII-4-16), and MDR1-CTT (LII-7-7). Data are given as the percentage of the initial drug concentration in either apical or basolateral chambers for the top figure. Experiments were performed in triplicate, and values are shown as mean ± SD.

Fig 7.23   The concentration difference of ESL between apical and basolateral sides at 240 min (top) and the amount of ESL transported by Pgp during 240 min (bottom) divided by the protein level of Pgp for MDR1-CGC (LII-Ref-11), MDR1-CTC (LII-CTC-9), MDR1-CGT (LII-4-16), and MDR1-CTT (LII-7-7). Data are given as the percentage of the initial drug concentration in either apical or basolateral chambers for the top figure. Experiments were performed in triplicate, and values are shown as mean ± SD.

Concentration equilibrium transport assays were performed to evaluate the Pgp function for MDR1-CGC (LII-Ref-11), MDR1-TTC (LII-5-3), MDR1-TTT (LII-TTT-1), MDR1-TGT (LII-6-1), MDR1-CAC (LII-CAC-1), and MDR1-TGC (LII-3-9). The expression levels of these clones were detected by real time PCR and western blotting (Fig 7.24). ESL at 10 μg/ml was used in the experiment. All the variants had Pgp function and transported ESL from the basal to the apical side (Fig 7.25).

Fig 7.24   Expression of Pgp in MDR1-CGC (LII-Ref-11), MDR1-TTC (LII-5-3), MDR1-TTT (LII-TTT-1), MDR1-TGT (LII-6-1), MDR1-CAC (LII-CAC-1), and MDR1-TGC (LII-3-9) by (a) western blotting and (b) western blotting (Pgp / β-tubulin) and real time PCR (MDR1 / β-actin).
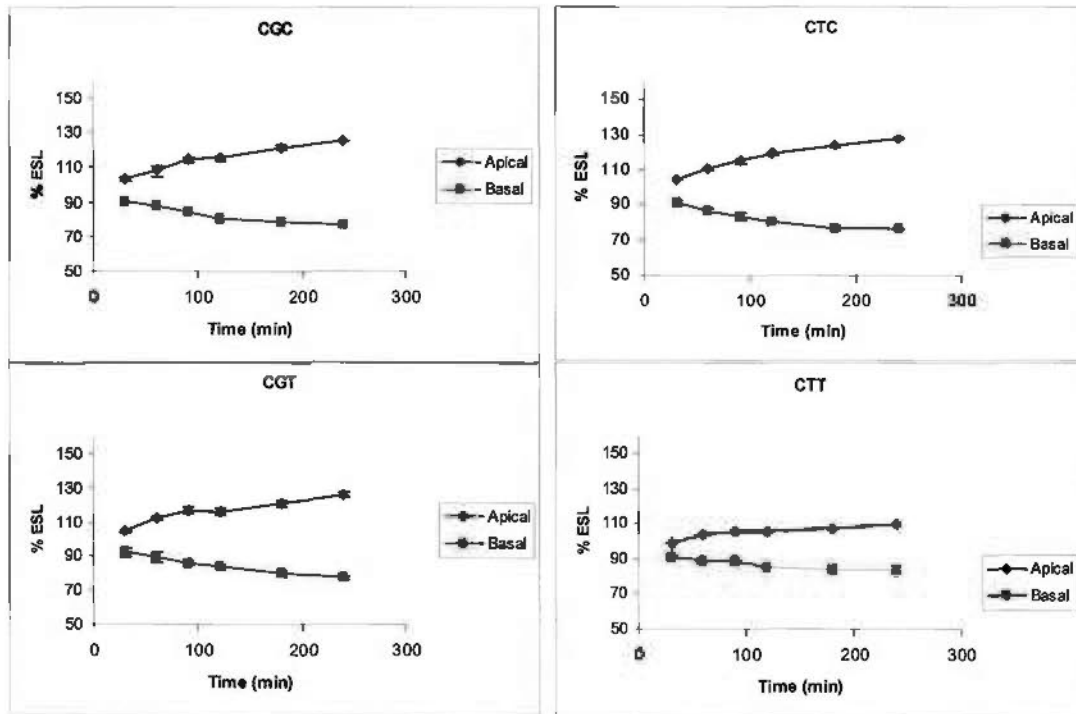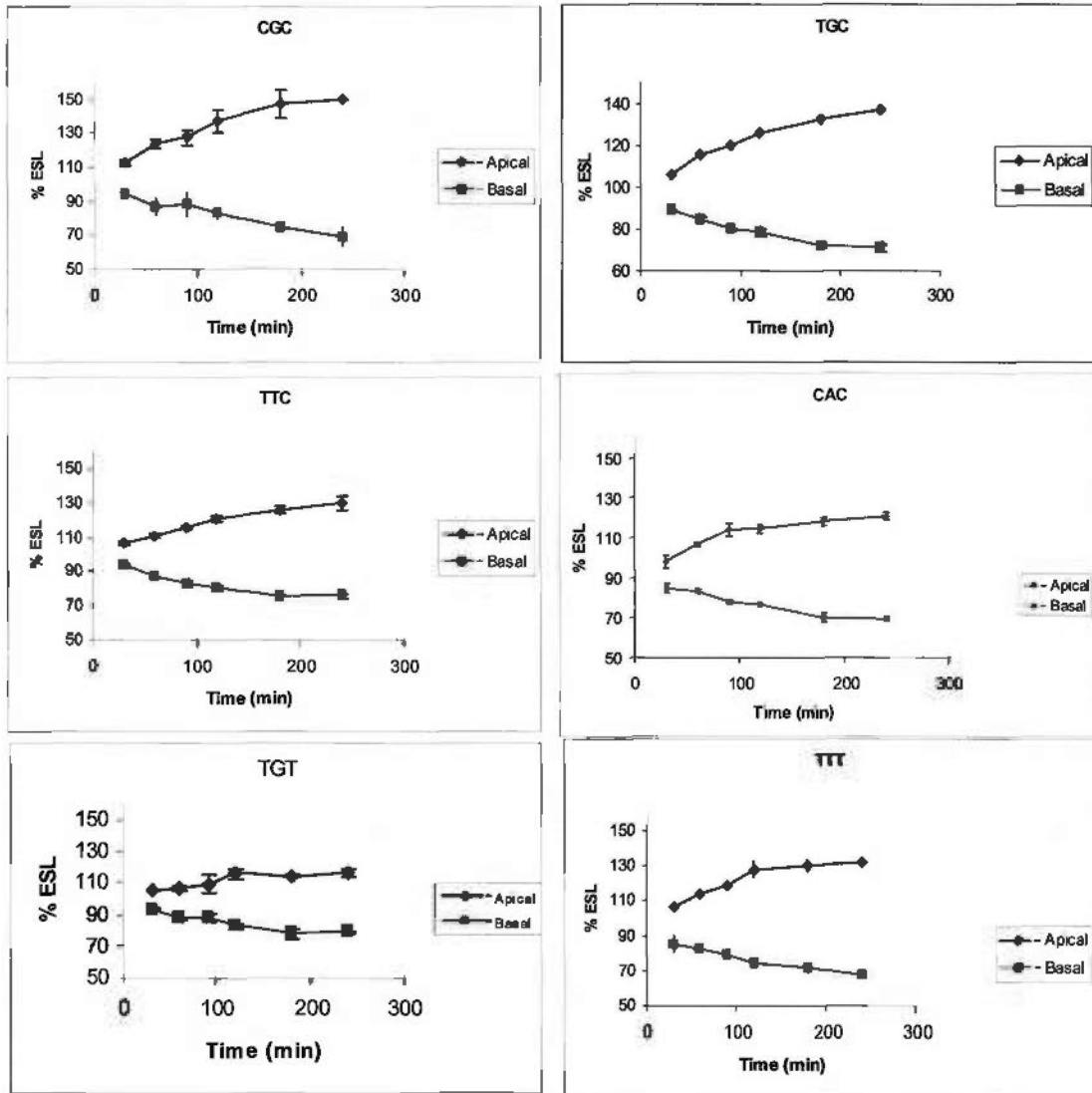
Fig 7.25   **Concentration equilibrium transport assays of eslicarbazepine acetate (ESL) for MDR1-CGC (LII-Ref-11), MDR1-TTC (LII-5-3), MDR1-TTT (LII-TTT-1), MDR1-TGT (LII-6-1), MDR1-CAC (LII-CAC-1), and MDR1-TGC (LII-3-9). Data are given as the percentage of the initial drug concentration in either apical or basolateral chamber vs. time. Experiments were performed in triplicate, and values are shown as mean ± SD.**

ESL transport corrected by MDR1 mRNA level was similar for all variants except MDR1-CGC (LII-Ref-11), which was higher than others (Fig 7.26). ESL transport corrected by Pgp protein level was similar for all variants (Fig 7.27). After correcting by

the mRNA level, MDR1-CTT had the lowest transport of ESL, followed by MDR1-TTT. Other variants, MDR1-TTC, MDR1-TGT, MDR1-CAC, MDR1-CTC, MDR1-CGT, and MDR1-TGC, were similar to the wild type (MDR1-CGC) (Fig 7.28).
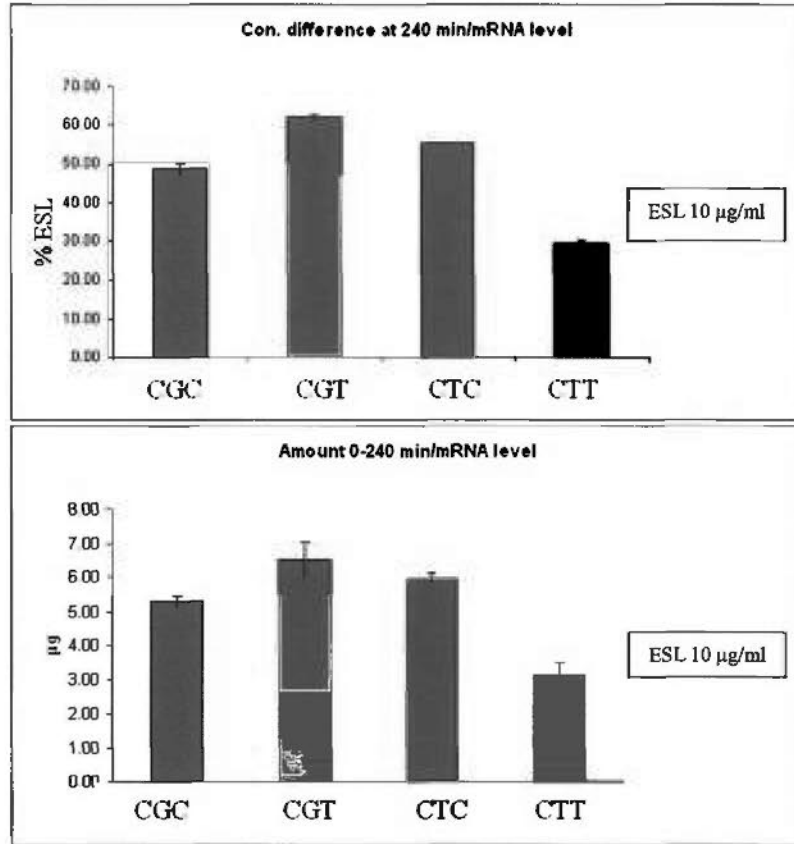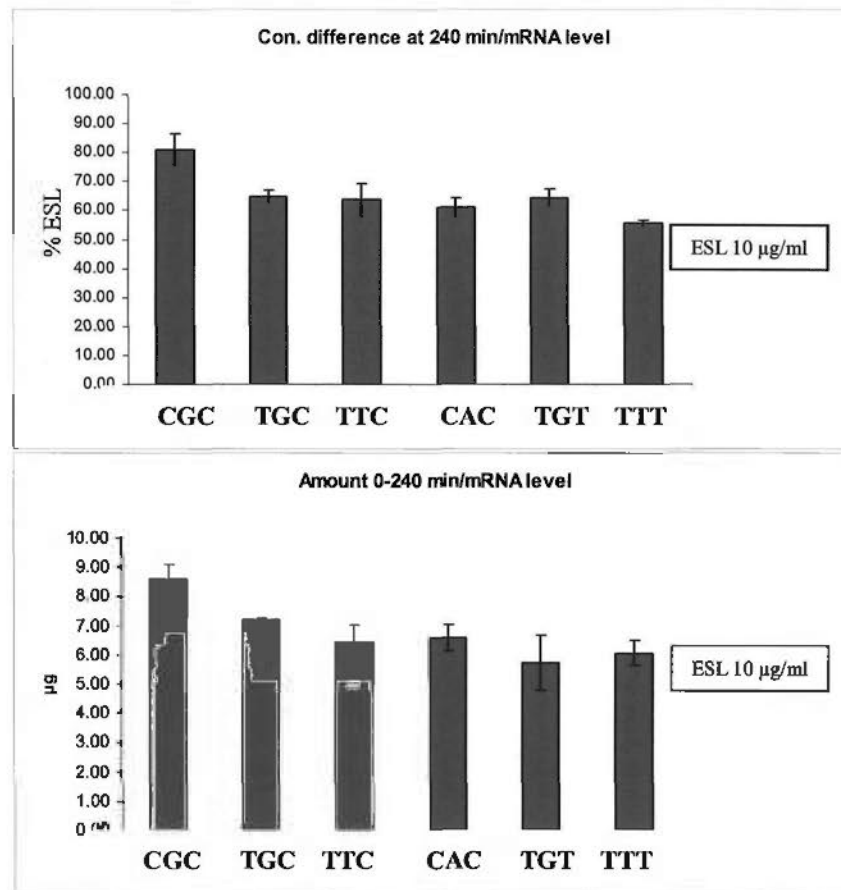

Fig 7.26 The concentration difference of ESL between apical and basolateral sides at 240 min (top) and the amount of ESL transported by Pgp during 240 min (bottom) divided by the mRNA level of MDR1 for MDR1-CGC (LII-Ref-11), MDR1-TTC (LII-5-3), MDR1-TTT (LII-TTT-1), MDR1-TGT (LII-6-1), MDR1-CAC (LII-CAC-1), and MDR1-TGC (LII-3-9). Data are given as the percentage of the initial drug concentration in either apical or basolateral chambers for the top figure. Experiments were performed in triplicate, and values are shown as mean ± SD.
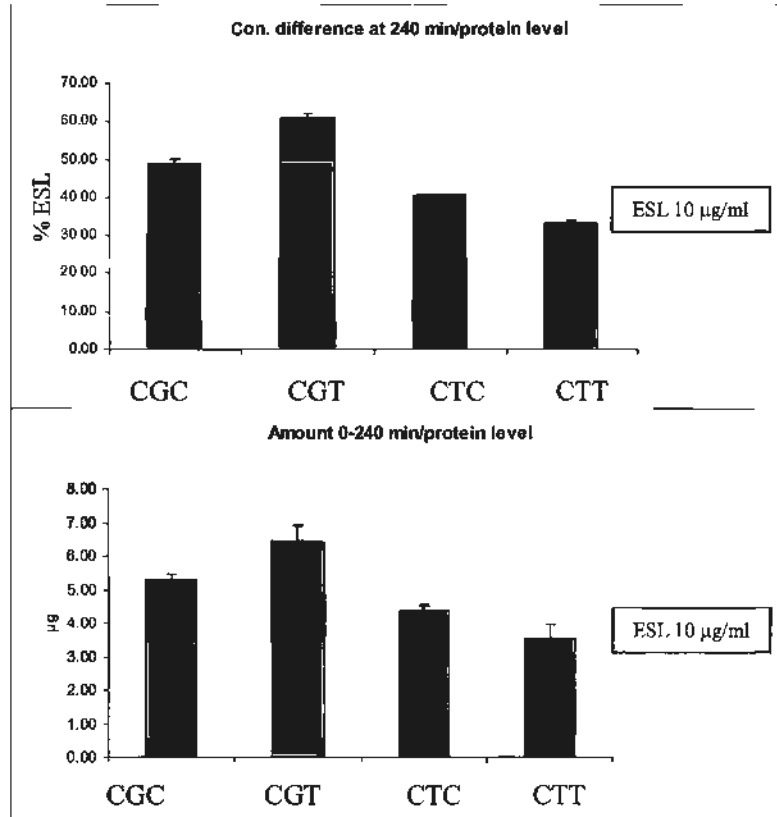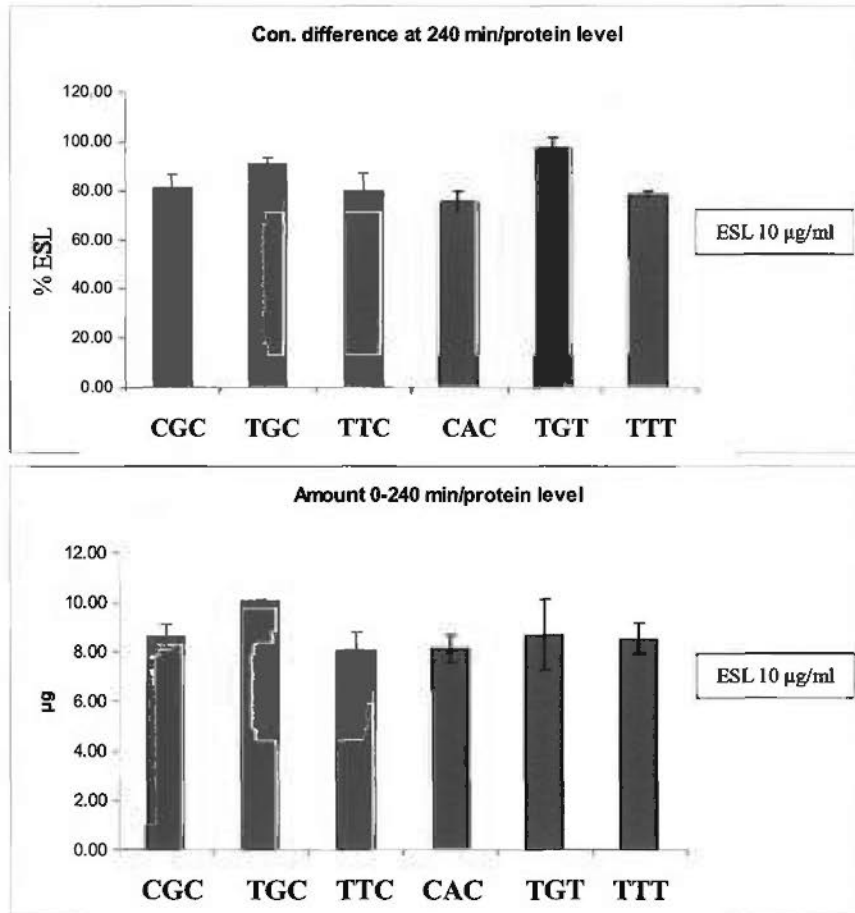
Fig 7.27   The concentration difference of ESL between apical and basolateral sides at 240 min (top) and the amount of ESL transported by Pgp d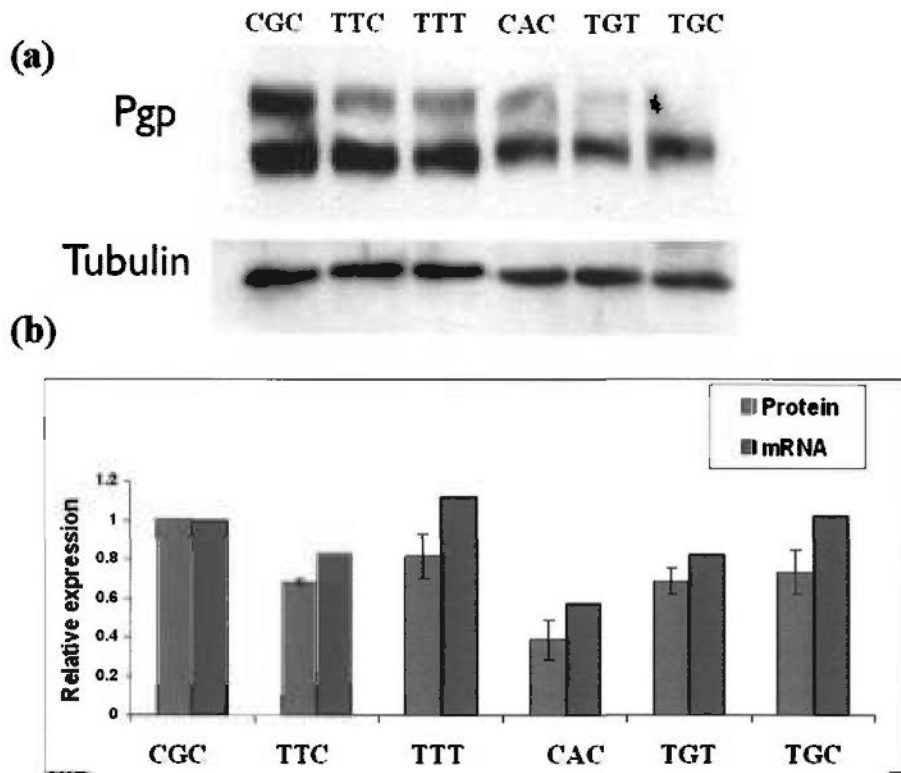uring 240 min (bottom) divided by the protein level of Pgp for MDR1-CGC (LII-Ref-11), MDR1-TTC (LII-5-3), MDR1-TTT (LII-TTT-1), MDR1-TGT (LII-6-1), MDR1-CAC (LII-CAC-1), and MDR1-TGC (LII-3-9). Data are given as the percentage of the initial drug concentration in either apical or basolateral chambers for the top figure. Experiments were performed in triplicate, and values are shown as mean ± SD.
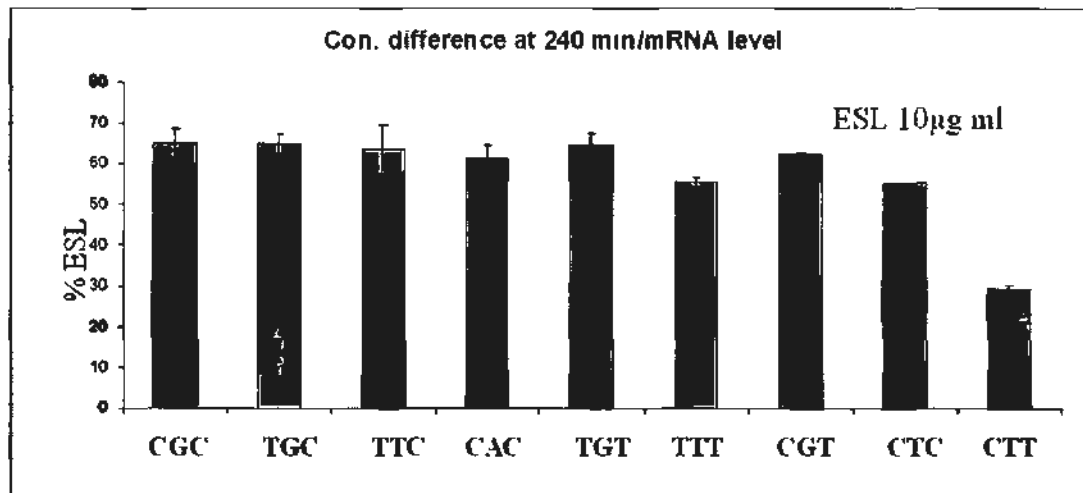
Fig 7.28 The concentration difference of ESL between apical and basolateral sides at 240 min divided by the mRNA level of MDR1 for MDR1-CGC (LII-Ref-11), MDR1-TTC (LII-5-3), MDR1-TTT (LII-TTT-1), MDR1-TGT (LII-6-1), MDR1-CAC (LII-CAC-1), MDR1-CTC (LII-CTC-9), MDR1-CGT (LII-4-16), MDR1-CTT (LII-7-7), and MDR1-TGC (LII-3-9).

7.3.5 Discussion

Single nucleotide polymorphisms (SNPs) in the *MDR1* gene were associated with drug resistance in epilepsy (Basic *et al.*, 2008; Kwan *et al.*, 2007a; Kwan *et al.*, 2000a; Kwan *et al.*, 2009; Seo *et al.*, 2006; Siddiqui *et al.*, 2003). Three common exonic SNPs, 1236C>T, 2677G>T, and 3435C>T, have been most frequently studied. In our experiments, we used cell monolayer models to evaluate the functional effects of these three SNPs. We established LLC-PK1 cell lines transfected with plasmids containing haplotypes at 1236, 2677, and 3435. We found that the haplotype CTC displayed higher Pgp function than other haplotypes among the clones selected by G418 alone. There were no significant differences in function among the variant clones selected by G418 and vincristine sulfate.

Several cell models were used in studying the variants. 293 cells with stable expression of MDR1 variants were used to detect the function of Pgp (Hung *et al.*, 2008). Uptake and efflux assays of Pgp substrates Rho123 and calcein were performed to evaluate the

function of MDR1 variants. Mammalian cells (HeLa, monkey, and CEM human cells) transiently transfected with MDR1 variants were also examined to detect the accumulation or efflux of fluorescent substrates of Pgp (Kimchi-Sarfaty *et al.*, 2007). LLC cells stably transfected with MDR1 variants were also used in the cell uptake model (Salama *et al.*, 2006). There has not been any report using the cell monolayer model with stable expression of MDR1 variants to evaluate functional effects of SNPs. The monolayer model mimics the blood brain barrier better than cell uptake models. Therefore we used clones stably expressing MDR1 to evaluate the effect of variants on transport function of Pgp. As described by previous chapters and reported results, the concentration equilibrium transport assay is more sensitive than the traditional bi-directional assay for evaluating Pgp function on the transport of AEDs (Luna-Tortos *et al.*, 2008c; Zhang *et al.*, 2010; Zhang *et al.*, 2011). We used the same system to evaluate the function of MDR1 variants.

Based on the previous results, oxcarbazepine and eslicarbazepine acetate are substrates of Pgp, and the fact that they exhibit relatively high transport is an advantage for their use in evaluating the effect of MDR1 variants on Pgp function. For all the clones selected, we tested the expression level of Pgp by real time PCR and western blotting. The clones that expressed a level of Pgp comparable to that of LLC-MDR1 wildtype cells were used to perform transport assays. Those clones having Pgp function were then used to conduct further experiments to determine the effects of variants on Pgp function.

As described in Chapter 6, the Pgp expression levels in clones selected by G418 were generally low. But a few clones demonstrated high levels and function of Pgp, and we chose those clones for transport studies. Four haplotypes were used, including MDR1-CGC (1236C, 2677G, and 3435C), MDR1-CTC (1236C, 2677T, and 3435C), MDR1-CGT (1236C, 2677G, and 3435T), and MDR1-CTT (1236C, 2677T, and 3435T). The amounts of OXC and ESL transported by different Pgp variants were measured and corrected by the mRNA or protein level of Pgp in order to compare the extent of transport among different variants. The haplotype MDR1-CTC demonstrated the greatest transport of ESL and OXC, suggesting that 2677T leads to increased Pgp function compared to

2677G. However, the MDR1-CTT haplotype did not transport more ESL and OXC than did MDR1-CGT, indicating that haplotypes rather than SNPs may be important in determining Pgp function. Two drugs (ESL and OXC) and two detection methods (real time PCR and western blotting) were used, and they were consistent with each other, lending support to the reliability of the transport assays.

To confirm our results, another clone (MDR1-CGT (4-6-1)) was selected, and the clones used above were re-selected by a higher concentration of G418 in order to improve the expression level of Pgp. Using the new clones, we tested the transport of ESL. In order to exclude the concentration-dependent effect on transport (detailed in Chapter 3), ESL at 2 μg/ml was used. As with previous results, CTC showed greater Pgp function than did other haplotypes. In membrane vesicles, 2677T increased the transport rates for vincristine about 50% compared to 2677G (Schaefer *et al.*, 2006). In 293 cells, 2677G>T did not affect Pgp protein expression but decreased the intracellular digoxin concentration, indicating it increased the function of Pgp (Kim *et al.*, 2001). In another report, 2677G>T did not affect the expression and function of Pgp (Kimchi-Sarfaty *et al.*, 2002). In placentas, 1236C>T, 2677G>T, and 3435C>T were associated with lower protein expression than wild type. But 2677G>T did not affect Pgp function (Hemauer *et al.*, 2010).

The haplotype MDR1-CTT had activity similar to that of MDR1-CGC and MDR1-CGT, indicating that these haplotypes did not affect Pgp function. However, the haplotype CTC can increase Pgp function compared to CGC. In the transient transfection of these variants into mammalian cells, they did not affect the accumulation and efflux of Rho123 (Kimchi-Sarfaty *et al.*, 2007). Variants at 2677 and 3435, when stably expressed in 293 and LLC-PK1 cells, also did not affect the uptake of Rho123 and verapamil (Hung *et al.*, 2008; Morita *et al.*, 2003). But in LLC-PK1 cells with stable expression of Pgp, these four variants significantly decreased the Rho123 efflux function of Pgp (Salama *et al.*, 2006). In placentas, the 1236C>T and 3435C>T polymorphisms decreased the Pgp protein level but increased Pgp transport of [H^3]-paclitaxel (Hemauer *et al.*, 2010). In LLC cells stably transfected with Pgp, the bi-directional transport assay was performed,

and there were no significant differences among the 2677 and 3435 variants (Morita *et al.*, 2003). The fact that the concentration equilibrium transport assay is more sensitive than the bi-directional transport assay might be the reason why we found a difference among variants while other groups did not. The lack of consistency among these studies may be caused by the different expression systems of Pgp, different substrates, and the different assay methods. Thus the establishment of a standard experimental system to evaluate the effect of variants on Pgp function is needed in further studies.

The clones selected by G418 and vincristine sulfate increased the expression level of Pgp. Vincristine sulfate can kill cells, but it is a substrate of Pgp, therefore cells with high Pgp expression will survive (Schinkel *et al.*, 1995). After selection, the clones were used to perform transport assays by using OXC and ESL. Four clones, MDR1-CGC, MDR1-CTC, MDR1-CGT, and MDR1-CTT, were used to performe the same experiments as the corresponding G418-selected clones. When using OXC as the substrate, we found no significant difference among them after correcting by the mRNA level (Fig 7.15). This result was confirmed by another batch of clones (Fig 7.19). When tested using ESL, MDR1-CTT transported less ESL than MDR1-CGC after correcting by mRNA levels (Fig 7.22). The difference between OXC and ESL results may be caused by the different substrate affinity for Pgp.

After correcting by the protein level for the clones selected by vincristine sulfate, the extent of transport by the haplotypes was not consistent with the transport values corrected by mRNA levels (Fig 7.16, Fig 7.20, and Fig 7.27). Some of the clones exhibited conflicting results. The reasons for these inconsistencies may include: first, quantification of western blotting results was imprecise. Second, the expression of protein and mRNA was not linear: the more protein was expressed, the more growth pressure on the cells.

The clones selected by vincristine sulfate did not show significant differences between MDR1-CTC and other variants; this conflicts with the results from the clones selected by G418 (Fig 7.8, Fig 7.15, and Fig 7.19). One possible explanation could be that vincristine

sulfate is a functional selection drug, thus its use may eliminate functional differences among the variants by killing clones with low Pgp activity. Thus, clones with similar (and high) function will tend to survive. Another possible explanation could be that vincristine sulfate induced other ABC transporters, which can also transport AEDs, and thus obscured differences among the variants.

Pgp inhibitors, including verapamil, cyclosporine A, and digoxin, were less effective against haplotypes CTT, TGT, and TTT than CGC (Gow *et al.*, 2008; Hung *et al.*, 2008; Kimchi-Sarfaty *et al.*, 2007; Schaefer *et al.*, 2006). The TTT haplotype had a lower MDR1 mRNA level than did CGC, which was mainly caused by 3435C>T, suggesting that 3435C>T decreases mRNA stability (Wang *et al.*, 2005). But in another study, the TTT did not affect the MDR1 mRNA and protein expression level. Rather, the haplotype may affect the time needed for cotranslational folding of Pgp, thus allowing Pgp to adopt alternate conformations, affecting the function (Kimchi-Sarfaty *et al.*, 2007).

The variants selected by G418 indicated that the CTC haplotype increased Pgp function. This finding may help explain the relations between genotype and drug resistance in epilepsy. The role of SNPs in treatment of epilepsy needs to be considered, which may help in developing genetic-based personal therapy and in demonstrating the importance of developing AEDs that are not substrates of Pgp.

7.4   Conclusion

LLC-PK1 cells transfected with MDR1 variants (1236C>T, 2677G>T/A, and 3435C>T) were established and validated. The cells were suitable for performing the concentration equilibrium transport assay. In the G418 selection condition, compared with reference haplotype CGC, the CTC haplotype increased Pgp activity to transport OXC and ESL while the CGT and CTT haplotypes did not significantly affect Pgp function. In the vincristine sulfate selection condition, compared with CGC, the haplotype CTT decreased Pgp activity, while other haplotypes, including CGC, CGT, CAC, CTC, TGC, TGT, TTT,

and TTC, did not affect function. Selection by vincristine sulfate may raise expression of Pgp and eliminate differences among the variants.

Overall conclusion

8.1   Conclusions

The association between drug resistance and Pgp in epilepsy patients has been suggested by a variety of previous results. In order to investigate the mechanisms underlying drug resistance, we used a cell monolayer model to detect the transport of antiepileptic drugs (AEDs) by Pgp. We used MDCK and LLC cells transfected with the human *MDR1* gene to investigate the Pgp substrate status of 12 AEDs, including first generation drugs, new generation drugs, and carbamazepine and its analogs/metabolites. We established LLC cell lines with stable expression of *MDR1* haplotypes at 1236C>T, 2677G>T/A, and 3435C>T sites. The effect of variants on Pgp transport was determined.

HPLC/UV or LC-MS/MS analysis methods were established to quantify drugs. The methods produced good inter-day and intra-day precision, linearity, and accuracy. The stability of drugs was measured in different conditions, reflecting those occurring in monolayer transport assays. The drugs were stable in the transport buffer and auto-sampler during experiments, indicating that the methods of drug analysis were suitable for our projects.

Using *MDR1*-transfected monolayer cell models, we detected the Pgp substrate status for first generation drugs phenytoin (PHT), phenobarbital (PB), and ethosuximide (ESM), which are still used widely in the clinic. We demonstrated that PHT and PB, but not ESM, are substrates of human Pgp, and that the transport of PHT and PB was affected by drug concentrations. A range of clinically relevant concentrations should be tested when evaluating whether an AED is transported by Pgp.

Carbamazepine (CBZ) and its structural analogs oxcarbazepine (OXC) and eslicarbazepine acetate (ESL) represent an important group of AEDs, sharing a common

185

molecular mechanism of action. They and their major stable active metabolites carbamazepine-10,11-epoxide (CBZ-E) and S-licarbazepine (S-LC) have similar structures, which makes it interesting to investigate their substrate status. Using monolayer models in concentration gradient and concentration equilibrium conditions, we demonstrated that CBE is not a substrate of Pgp, but, interestingly, its active metabolite CBZ-E is a substrate of Pgp. ESL, OXC, and their active metabolite S-LC are also substrates of Pgp.

Zonisamide (ZNS), pregabalin (PGB), rufinamide (RFM), and lacosamide (LCM) are new generation AEDs, approved in recent years. There is little evidence on their substrate status. In concentration equilibrium transport assays, we demonstrated that LCM is transported by Pgp, but PGB, RFM, and ZNS are not.

The concentration equilibrium transport assay (CETA) and conventional bi-directional transport assay were compared. The transport of PHT and PB by Pgp was significant in the CETA, but only minimal transport of PHT, and no transport of PB, was demonstrated in the bi-directional assay. When testing CBZ-E in the CETA, CBZ-E at 10 µg/ml was significantly transported in *MDR1*-transfected cells, indicating that CBZ-E is a substrate of Pgp. But in bi-directional transport, the cTR of CBZ-E by LLC-*MDR1* cells was 1.35, which was lower than the standard to define a Pgp substrate (standard value: 1.5). These confirm that the CETA is more sensitive than the bi-directional transport assay in detecting Pgp transport of AEDs with high passive permeability. Our findings strengthen the suggestion that the CETA should be used instead of the conventional bi-directional transport assay for study of compounds with high passive permeability across the BBB, particularly if they also have low transport efficiency.

We demonstrated that phenytoin, phenobarbital, oxcarbazepine, eslicarbazepine acetate, lacosamide, carbamazepine-10,11-epoxide, and S-licarbazepine are substrates of Pgp, while carbamazepine, ethosuximide, zonisamide, pregabalin, and rufinamide are not substrates of Pgp. Their structures and substrate status are listed in Table 8.1. CBZ and its analogs share an identical dibenzazepine nucleus but differ at the 10,11-position. Our

results showed that these compounds, with the exception of CBZ itself, are substrates for Pgp, which implies that groups at the 10,11-position (at least epoxide, acetate, hydroxyl, or ketone groups) could affect the substrate status of dibenzazepine compounds.
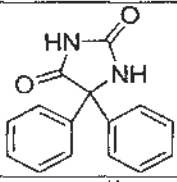
The pCl-neo plasmids containing *MDR1* SNPs at 1236, 2677, and 3435 sites were transfected into polarized LLC-PK1 cells. Stable clones were selected by two methods (G418 or G418/vincristine sulfate). The mRNA and protein level of Pgp were measured by real time PCR and western blotting. The expression level of Pgp in variants selected by G418/vincristine sulfate was higher than in variants selected by G418. The relative expression levels of mRNA and protein were consistent, indicating that SNPs do not affect the translation of *MDR1*. In the cell lines, exogenous Pgp was localized at the cell surface, indicating that the cell lines were suitable for monolayer assays. In the G418 selection condition, the CTC haplotype showed more Pgp transport of OXC and ESL than did reference haplotype CGC. But the CGT and CTT haplotypes did not significantly affect Pgp function, as compared with CGC. In the vincristine sulfate selection condition, the haplotype CTT decreased Pgp function compared with CGC, while other haplotypes, including CGC, CGT, CAC, CTC, TGC, TGT, TTT, and TTC, did not change Pgp function. The use of vincristine sulfate may lead to selection of clones with high Pgp activity, possibly reducing differences among the variants.

Our results identified the Pgp substrate status of a number of AEDs. This information may help explain why some patients are refractory to AEDs, given the overexpression of Pgp in the drug-resistant epilepsy brain. The substrate status of antiepileptic drugs may guide doctors in their choice of AEDs for epileptic patients. For monotherapy, the first choice among AEDs that are otherwise equivalent in desirability could be a drug which is not a Pgp substrate. Our results imply that more patients are resistant to Pgp substrate AEDs than to AEDs that are not Pgp substrates. Published studies have generally examined patients on a mix of AEDs, some of which are Pgp substrates and some of which are not. This mixing may obscure the association of resistance with Pgp substrate status, which might partly explain the conflicting results which appear in the literature. Furthermore, even among Pgp substrates, AEDs exhibit different degrees of transport by

Pgp. The different AEDs used, the different types of epilepsy, the different ethnicities of patients, and the different ages of patients may also contribute to inconsistencies among published studies.

Table 8.1 Structures and electron donor groups in AEDs.

Compounds	Structure	Aromatic rings	H-bond donors (>N-, -OH, =NH, -NH-)	H-bond acceptors (>N-, -OH, =O)	Substrate status
Phenytoin		2	2 –NH-	2 =O	Y
Phenobarbital		1	2 –NH-	3 =O	Y
Oxcarbazepine		2	1 >N-	2 =O	Y
Lacosamide		1	2 –NH-	1 =O	Y
Carbamazepine 10,11-epoxide		1	1 >N-	1 =O	Y
S-licarbazepine		2	1 >N-	1 =O 1 -OH	Y
Carbamazepine		2	1 >N-	1 =O	N
Ethosuximide		0	1 –NH-	2 =O	N
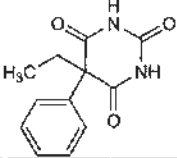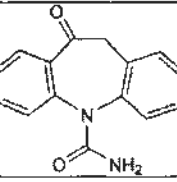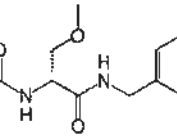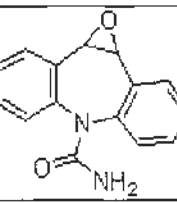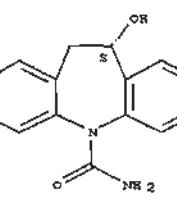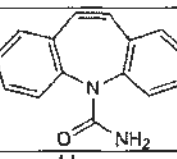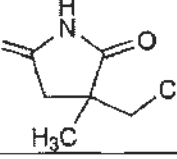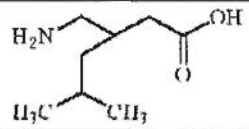
Pregabalin		0	0	1 =O 1 -OH	N
Rufinamide		1	1 >N-	1 =O	N
Zonisamide		1	1 >N-	2 =O 1 >N-	N
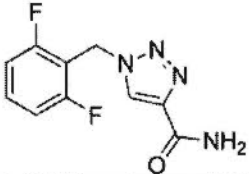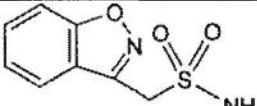
The frequencies of polymorphic alleles of *ABCB1* in drug-resistant epilepsy patients significantly differed, in some reports, from those in drug-responsive patients. The effects of *ABCB1* polymorphisms on AED transport may provide a molecular explanation of the reported associations, albeit inconsistent, between the polymorphisms and pharmacoresistance. This knowledge may help guide the design of genetic-based individualized therapy of epilepsy, and may lead to development of drugs to help treat the large number of patients who are refractory to all currently available AEDs.

8.2   Further studies

Our results suggest further studies:

I. We have identified some AEDs as substrates of Pgp, but we have not performed *in vivo* studies on these drugs. Determination of which AEDs are transported by Pgp will be vital in the appropriate design of clinical trials to overcome drug resistance in epilepsy. In future studies, we can perform *in vivo* experiments to investigate the effect of Pgp on drug concentrations in the brains of drug resistant animals or patients.

II. The functional effects of Pgp SNPs also need further study to determine the molecular mechanism. Electrophysiology is an important approach to understand the mechanisms of drug resistance in epilepsy. By experiments with whole cell currents and single channels, we can study the transport of AEDs by Pgp in LLC-PK1 cells transfected with MDR1

variants. These experiments should provide a mechanistic framework explaining how MDR1 polymorphisms might affect Pgp function, which may clarify associations between the polymorphisms and pharmacoresistance at a molecular level.

III. Some AEDs have similar structures but different substrate status. This may help us to seek the structure-activity relationship (SAR) of Pgp. We can determine the substrate status of structurally similar compounds and analyze their structures to learn more about the SAR of Pgp.

References

Aiken, SP, Brown, WM (2000). Treatment of epilepsy: existing therapies and future developments. *Front Biosci* **5**: E124-52.

Ak, H, Ay, B, Tanriverdi, T, Sanus, GZ, Is, M, Sar, M, Oz, B, Ozkara, C, Ozyurt, E, Uzan, M (2007). Expression and cellular distribution of multidrug resistance-related proteins in patients with focal cortical dysplasia. *Seizure* **16**: 493-503.

Almeida, L, Falcao, A, Maia, J, Mazur, D, Gellert, M, Soares-da-Silva, P (2005). Single-dose and steady-state pharmacokinetics of eslicarbazepine acetate (BIA 2-093) in healthy elderly and young subjects. *J Clin Pharmacol* **45**: 1062-6.

Alves, G, Figueiredo, I, Castel-Branco, M, Loureiro, A, Falcao, A, Caramona, M (2007a). Simultaneous and enantioselective liquid chromatographic determination of eslicarbazepine acetate, S-licarbazepine, R-licarbazepine and oxcarbazepine in mouse tissue samples using ultraviolet detection. *Anal Chim Acta* **596**: 132-40.

Alves, G, Figueiredo, I, Castel-Branco, M, Loureiro, A, Fortuna, A, Falcao, A, Caramona, M (2007b). Enantioselective HPLC-UV method for determination of eslicarbazepine acetate (BIA 2-093) and its metabolites in human plasma. *Biomed Chromatogr* **21**: 1127-34.

Ambudkar, SV, Kim, IW, Sauna, ZE (2006). The power of the pump: mechanisms of action of P-glycoprotein (ABCB1). *Eur J Pharm Sci* **27**: 392-400.

Ambudkar, SV, Kimchi-Sarfaty, C, Sauna, ZE, Gottesman, MM (2003). P-glycoprotein: from genomics to mechanism. *Oncogene* **22**: 7468-85.

Aronica, E, Gorter, JA, Jansen, GH, van Veelen, CW, van Rijen, PC, Leenstra, S, Ramkema, M, Scheffer, GL, Scheper, RJ, Troost, D (2003). Expression and cellular

distribution of multidrug transporter proteins in two major causes of medically intractable epilepsy: focal cortical dysplasia and glioneuronal tumors. *Neuroscience* **118**: 417-29.

Aronica, E, Gorter, JA, Ramkema, M, Redeker, S, Ozbas-Gerceker, F, van Vliet, EA, Scheffer, GL, Scheper, RJ, van der Valk, P, Baayen, JC, Troost, D (2004). Expression and cellular distribution of multidrug resistance-related proteins in the hippocampus of patients with mesial temporal lobe epilepsy. *Epilepsia* **45**: 441-51.

Aszalos, A (2007). Drug-drug interactions affected by the transporter protein, P-glycoprotein (ABCB1, MDR1) I. Preclinical aspects. *Drug Discov Today* **12**: 833-7.

Avendano, C, Menendez, JC (2002). Inhibitors of multidrug resistance to antitumor agents (MDR). *Curr Med Chem* **9**: 159-93.

Bakos, E, Evers, R, Szakacs, G, Tusnady, GE, Welker, E, Szabo, K, de Haas, M, van Deemter, L, Borst, P, Varadi, A, Sarkadi, B (1998). Functional multidrug resistance protein (MRP1) lacking the N-terminal transmembrane domain. *J Biol Chem* **273**: 32167-75.

Ballabh, P, Braun, A, Nedergaard, M (2004). The blood-brain barrier: an overview: structure, regulation, and clinical implications. *Neurobiol Dis* **16**: 1-13.

Baltes, S, Fedrowitz, M, Tortos, CL, Potschka, H, Loscher, W (2007a). Valproic acid is not a substrate for P-glycoprotein or multidrug resistance proteins 1 and 2 in a number of in vitro and in vivo transport assays. *J Pharmacol Exp Ther* **320**: 331-43.

Baltes, S, Gastens, AM, Fedrowitz, M, Potschka, H, Kaever, V, Loscher, W (2007b). Differences in the transport of the antiepileptic drugs phenytoin, levetiracetam and carbamazepine by human and mouse P-glycoprotein. *Neuropharmacology* **52**: 333-46.

References

Basic, S, Hajnsek, S, Bozina, N, Filipcic, I, Sporis, D, Mislov, D, Posavec, A (2008). The influence of C3435T polymorphism of ABCB1 gene on penetration of phenobarbital across the blood-brain barrier in patients with generalized epilepsy. *Seizure* **17**: 524-30.

Baulac, M, Leon, T, O'Brien, TJ, Whalen, E, Barrett, J (2010). A comparison of pregabalin, lamotrigine, and placebo as adjunctive therapy in patients with refractory partial-onset seizures. *Epilepsy Res* **91**: 10-9.

Beaulieu, E, Demeule, M, Ghitescu, L, Beliveau, R (1997). P-glycoprotein is strongly expressed in the luminal membranes of the endothelium of blood vessels in the brain. *Biochem J* **326 (Pt 2)**: 539-44.

Begley, DJ (2004). ABC transporters and the blood-brain barrier. *Curr Pharm Des* **10**: 1295-312.

Bendayan, R, Lee, G, Bendayan, M (2002). Functional expression and localization of P-glycoprotein at the blood brain barrier. *Microsc Res Tech* **57**: 365-80.

Berry, D, Millington, C (2005). Analysis of pregabalin at therapeutic concentrations in human plasma/serum by reversed-phase HPLC. *Ther Drug Monit* **27**: 451-6.

Berry, DJ (1990). Determination of zonisamide (3-sulphamoylmethyl-1,2-benzisoxazole) in plasma at therapeutic concentrations by high-performance liquid chromatography. *J Chromatogr* **534**: 173-81.

Bhatti, MM, Hanson, GD, Schultz, L (1998). Simultaneous determination of phenytoin, carbamazepine, and 10,11-carbamazepine epoxide in human plasma by high-performance liquid chromatography with ultraviolet detection. *J Pharm Biomed Anal* **16**: 1233-40.

Bialer, M, White, HS (2010). Key factors in the discovery and development of new antiepileptic drugs. *Nat Rev Drug Discov* **9**: 68-82.

194

Borst, P (1997). Multidrug resistant proteins. *Semin Cancer Biol* **8**: 131-4.

Brandt, C, Bethmann, K, Gastens, AM, Loscher, W (2006). The multidrug transporter hypothesis of drug resistance in epilepsy: Proof-of-principle in a rat model of temporal lobe epilepsy. *Neurobiol Dis* **24**: 202-11.

Brunner, M, Langer, O, Sunder-Plassmann, R, Dobrozemsky, G, Muller, U, Wadsak, W, Krcal, A, Karch, R, Mannhalter, C, Dudczak, R, Kletter, K, Steiner, I, Baumgartner, C, Muller, M (2005). Influence of functional haplotypes in the drug transporter gene ABCB1 on central nervous system drug distribution in humans. *Clin Pharmacol Ther* **78**: 182-90.

Callen, DF, Baker, E, Simmers, RN, Seshadri, R, Roninson, IB (1987). Localization of the human multiple drug resistance gene, MDR1, to 7q21.1. *Hum Genet* **77**: 142-4.

Cawello, W, Nickel, B, Eggert-Formella, A (2010). No pharmacokinetic interaction between lacosamide and carbamazepine in healthy volunteers. *J Clin Pharmacol* **50**: 459-71.

Chang, XB (2007). A molecular understanding of ATP-dependent solute transport by multidrug resistance-associated protein MRP1. *Cancer Metastasis Rev* **26**: 15-37.

Chen, CJ, Chin, JE, Ueda, K, Clark, DP, Pastan, I, Gottesman, MM, Roninson, IB (1986). Internal duplication and homology with bacterial transport proteins in the mdr1 (P-glycoprotein) gene from multidrug-resistant human cells. *Cell* **47**: 381-9.

Chen, SH, Wu, HL, Shen, MC, Kou, HS (1999). Trace analysis of ethosuximide in human plasma with a chemically removable derivatizing reagent and high-performance liquid chromatography. *J Chromatogr B Biomed Sci Appl* **729**: 111-7.

Chollet, DF (2002). Determination of antiepileptic drugs in biological material. *J Chromatogr B Analyt Technol Biomed Life Sci* **767**: 191-233.

Chowbay, B, Cumaraswamy, S, Cheung, YB, Zhou, Q, Lee, EJ (2003). Genetic polymorphisms in MDR1 and CYP3A4 genes in Asians and the influence of MDR1 haplotypes on cyclosporin disposition in heart transplant recipients. *Pharmacogenetics* **13**: 89-95.

Clinckers, R, Smolders, I, Meurs, A, Ebinger, G, Michotte, Y (2005). Quantitative in vivo microdialysis study on the influence of multidrug transporters on the blood-brain barrier passage of oxcarbazepine: concomitant use of hippocampal monoamines as pharmacodynamic markers for the anticonvulsant activity. *J Pharmacol Exp Ther* **314**: 725-31.

Contin, M, Mohamed, S, Candela, C, Albani, F, Riva, R, Baruzzi, A (2010) Simultaneous HPLC-UV analysis of rufinamide, zonisamide, lamotrigine, oxcarbazepine monohydroxy derivative and felbamate in deproteinized plasma of patients with epilepsy. *J Chromatogr B Analyt Technol Biomed Life Sci* **878**: 461-5.

Cordon-Cardo, C, O'Brien, JP, Boccia, J, Casals, D, Bertino, JR, Melamed, MR (1990). Expression of the multidrug resistance gene product (P-glycoprotein) in human normal and tumor tissues. *J Histochem Cytochem* **38**: 1277-87.

Cordon-Cardo, C, O'Brien, JP, Casals, D, Rittman-Grauer, L, Biedler, JL, Melamed, MR, Bertino, JR (1989). Multidrug-resistance gene (P-glycoprotein) is expressed by endothelial cells at blood-brain barrier sites. *Proc Natl Acad Sci U S A* **86**: 695-8.

Crespi, CL, Fox, L, Stocker, P, Hu, M, Steimel, DT (2000). Analysis of drug transport and metabolism in cell monolayer systems that have been modified by cytochrome P4503A4 cDNA-expression. *Eur J Pharm Sci* **12**: 63-8.

Cross, SA, Curran, MP (2009). Lacosamide: in partial-onset seizures. *Drugs* **69**: 449-59.

Crowe, A, Teoh, YK (2006). Limited P-glycoprotein mediated efflux for anti-epileptic drugs. *J Drug Target* **14**: 291-300.

Cucullo, L, Hossain, M, Rapp, E, Manders, T, Marchi, N, Janigro, D (2007). Development of a humanized in vitro blood-brain barrier model to screen for brain penetration of antiepileptic drugs. *Epilepsia* **48**: 505-16.

Dehouck, MP, Meresse, S, Delorme, P, Fruchart, JC, Cecchelli, R (1990). An easier, reproducible, and mass-production method to study the blood-brain barrier in vitro. *J Neurochem* **54**: 1798-801.

Delahoy, P, Thompson, S, Marschner, IC (2010). Pregabalin versus gabapentin in partial epilepsy: a meta-analysis of dose-response relationships. *BMC Neurol* **10**: 104.

Demeule, M, Regina, A, Jodoin, J, Laplante, A, Dagenais, C, Berthelet, F, Moghrabi, A, Beliveau, R (2002). Drug transport to the brain: key roles for the efflux pump P-glycoprotein in the blood-brain barrier. *Vascul Pharmacol* **38**: 339-48.

Di, L, Kerns, EH, Bezar, IF, Petusky, SL, Huang, Y (2009). Comparison of blood-brain barrier permeability assays: in situ brain perfusion, MDR1-MDCKII and PAMPA-BBB. *J Pharm Sci* **98**: 1980-91.

Dombrowski, SM, Desai, SY, Marroni, M, Cucullo, L, Goodrich, K, Bingaman, W, Mayberg, MR, Bengez, L, Janigro, D (2001). Overexpression of multiple drug resistance genes in endothelial cells from patients with refractory epilepsy. *Epilepsia* **42**: 1501-6.

Drescher, S, Schaeffeler, E, Hitzl, M, Hofmann, U, Schwab, M, Brinkmann, U, Eichelbaum, M, Fromm, MF (2002). MDR1 gene polymorphisms and disposition of the P-glycoprotein substrate fexofenadine. *Br J Clin Pharmacol* **53**: 526-34.

Ebid, AH, Ahmed, MM, Mohammed, SA (2007). Therapeutic drug monitoring and clinical outcomes in epileptic Egyptian patients: a gene polymorphism perspective study. *Ther Drug Monit* **29**: 305-12.

Eichelbaum, M, Fromm, MF, Schwab, M (2004). Clinical aspects of the MDR1 (ABCB1) gene polymorphism. *Ther Drug Monit* **26**: 180-5.

Everitt, AD, Sander, JW (1999). Classification of the epilepsies: time for a change? A critical review of the International Classification of the Epilepsies and Epileptic Syndromes (ICEES) and its usefulness in clinical practice and epidemiological studies of epilepsy. *Eur Neurol* **42**: 1-10.

Fellner, S, Bauer, B, Miller, DS, Schaffrik, M, Fankhanel, M, Spruss, T, Bernhardt, G, Graeff, C, Farber, L, Gschaidmeier, H, Buschauer, A, Fricker, G (2002). Transport of paclitaxel (Taxol) across the blood-brain barrier in vitro and in vivo. *J Clin Invest* **110**: 1309-18.

Feng, B, Mills, JB, Davidson, RE, Mireles, RJ, Janiszewski, JS, Troutman, MD, de Morais, SM (2008). In vitro P-glycoprotein assays to predict the in vivo interactions of P-glycoprotein with drugs in the central nervous system. *Drug Metab Dispos* **36**: 268-75.

Flesch, G, Francotte, E, Hell, F, Degen, PH (1992). Determination of the R-(-) and S-(+) enantiomers of the monohydroxylated metabolite of oxcarbazepine in human plasma by enantioselective high-performance liquid chromatography. *J Chromatogr* **581**: 147-51.

Fojo, AT, Ueda, K, Slamon, DJ, Poplack, DG, Gottesman, MM, Pastan, I (1987). Expression of a multidrug-resistance gene in human tumors and tissues. *Proc Natl Acad Sci U S A* **84**: 265-9.

Ford, JM, Hait, WN (1993). Pharmacologic circumvention of multidrug resistance. *Cytotechnology* **12**: 171-212.

Ford, JM, Yang, JM, Hait, WN (1996). P-glycoprotein-mediated multidrug resistance: experimental and clinical strategies for its reversal. *Cancer Treat Res* **87**: 3-38.

Frelet, A, Klein, M (2006). Insight in eukaryotic ABC transporter function by mutation analysis. *FEBS Lett* **580**: 1064-84.

Fung, KL, Gottesman, MM (2009). A synonymous polymorphism in a common MDR1 (ABCB1) haplotype shapes protein function. *Biochim Biophys Acta* **1794**: 860-71.

Gerlach, JH, Kartner, N, Bell, DR, Ling, V (1986). Multidrug resistance. *Cancer Surv* **5**: 25-46.

Ghose, AK, Viswanadhan, VN, Wendoloski, JJ (1999). A knowledge-based approach in designing combinatorial or medicinal chemistry libraries for drug discovery. 1. A qualitative and quantitative characterization of known drug databases. *J Comb Chem* **1**: 55-68.

Giacomini, KM, Huang, SM, Tweedie, DJ, Benet, LZ, Brouwer, KL, Chu, X, Dahlin, A, Evers, R, Fischer, V, Hillgren, KM, Hoffmaster, KA, Ishikawa, T, Keppler, D, Kim, RB, Lee, CA, Niemi, M, Polli, JW, Sugiyama, Y, Swaan, PW, Ware, JA, Wright, SH, Yee, SW, Zamek-Gliszczynski, MJ, Zhang, L (2010) Membrane transporters in drug development. *Nat Rev Drug Discov* **9**: 215-36.

Giavazzi, R, Kartner, N, Hart, IR (1984). Expression of cell surface P-glycoprotein by an adriamycin-resistant murine fibrosarcoma. *Cancer Chemother Pharmacol* **13**: 145-7.

Gidal, BE, Privitera, MD, Sheth, RD, Gilman, JT (1999). Vigabatrin: a novel therapy for seizure disorders. *Ann Pharmacother* **33**: 1277-86.

Gil-Nagel, A, Lopes-Lima, J, Almeida, L, Maia, J, Soares-da-Silva, P (2009). Efficacy and safety of 800 and 1200 mg eslicarbazepine acetate as adjunctive treatment in adults with refractory partial-onset seizures. *Acta Neurol Scand* **120**: 281-7.

Gitlin, M (2006). Treatment-resistant bipolar disorder. *Mol Psychiatry* **11**: 227-40.

Gottesman, MM, Pastan, I (1988). The multidrug transporter, a double-edged sword. *J Biol Chem* **263**: 12163-6.

Goulle, JP, Noyon, J, Layet, A, Rapoport, NF, Vaschalde, Y, Pignier, Y, Bouige, D, Jouen, F (1995). Phenobarbital in hair and drug monitoring. *Forensic Sci Int* **70**: 191-202.

Gow, JM, Hodges, LM, Chinn, LW, Kroetz, DL (2008). Substrate-dependent effects of human ABCB1 coding polymorphisms. *J Pharmacol Exp Ther* **325**: 435-42.

Gros, P, Croop, J, Housman, D (1986). Mammalian multidrug resistance gene: complete cDNA sequence indicates strong homology to bacterial transport proteins. *Cell* **47**: 371-80.

Hainzl, D, Parada, A, Soares-da-Silva, P (2001). Metabolism of two new antiepileptic drugs and their principal metabolites S(+)- and R(-)-10,11-dihydro-10-hydroxy carbamazepine. *Epilepsy Res* **44**: 197-206.

Hamandi, K, Sander, JW (2006). Pregabalin: a new antiepileptic drug for refractory epilepsy. *Seizure* **15**: 73-8.

Han, Y, Chin Tan, TM, Lim, LY (2008). In vitro and in vivo evaluation of the effects of piperine on P-gp function and expression. *Toxicol Appl Pharmacol* **230**: 283-9.

Hauser, WA, Annegers, JF, Kurland, LT (1993). Incidence of epilepsy and unprovoked seizures in Rochester, Minnesota: 1935-1984. *Epilepsia* **34**: 453-68.

Hemauer, SJ, Nanovskaya, TN, Abdel-Rahman, SZ, Patrikeeva, SL, Hankins, GD, Ahmed, MS (2010). Modulation of human placental P-glycoprotein expression and activity by MDR1 gene polymorphisms. *Biochem Pharmacol* **79**: 921-5.

Hennessy, M, Spiers, JP (2007). A primer on the mechanics of P-glycoprotein the multidrug transporter. *Pharmacol Res* **55**: 1-15.

Hirschfeld, RM, Kasper, S (2004). A review of the evidence for carbamazepine and oxcarbazepine in the treatment of bipolar disorder. *Int J Neuropsychopharmacol* **7**: 507-22.

Hitzl, M, Drescher, S, van der Kuip, H, Schaffeler, E, Fischer, J, Schwab, M, Eichelbaum, M, Fromm, MF (2001). The C3435T mutation in the human MDR1 gene is associated with altered efflux of the P-glycoprotein substrate rhodamine 123 from CD56+ natural killer cells. *Pharmacogenetics* **11**: 293-8.

Hoffmann, K, Loscher, W (2007). Upregulation of brain expression of P-glycoprotein in MRP2-deficient TR(-) rats resembles seizure-induced up-regulation of this drug efflux transporter in normal rats. *Epilepsia* **48**: 631-45.

Hoffmeyer, S, Burk, O, von Richter, O, Arnold, HP, Brockmoller, J, Johne, A, Cascorbi, I, Gerloff, T, Roots, I, Eichelbaum, M, Brinkmann, U (2000). Functional polymorphisms of the human multidrug-resistance gene: multiple sequence variations and correlation of one allele with P-glycoprotein expression and activity in vivo. *Proc Natl Acad Sci U S A* **97**: 3473-8.

Hosak, L, Libiger, J (2002). Antiepileptic drugs in schizophrenia: a review. *Eur Psychiatry* **17**: 371-8.

Hsiao, P, Bui, T, Ho, RJ, Unadkat, JD (2008). In vitro-to-in vivo prediction of P-glycoprotein-based drug interactions at the human and rodent blood-brain barrier. *Drug Metab Dispos* **36**: 481-4.

Huband, N, Ferriter, M, Nathan, R, Jones, H (2010) Antiepileptics for aggression and associated impulsivity. *Cochrane Database Syst Rev* **2**: CD003499.

Hung, CC, Chen, CC, Lin, CJ, Liou, HH (2008). Functional evaluation of polymorphisms in the human ABCB1 gene and the impact on clinical responses of antiepileptic drugs. *Pharmacogenet Genomics* **18**: 390-402.

Hussar, DA, Bilbow, C (2009). New drugs: Febuxostat, lacosamide, and rufinamide. *J Am Pharm Assoc (2003)* **49**: 460-3.

Jin, RF, Sun, RP, Xu, XP (2005). [Expression of multidrug resistance gene and topiramate affect expression of multidrug resistance gene in the hippocampus of spontaneous epileptic rats]. *Zhonghua Er Ke Za Zhi* **43**: 733-7.

Johannessen, SI, Tomson, T (2006). Pharmacokinetic variability of newer antiepileptic drugs: when is monitoring needed? *Clin Pharmacokinet* **45**: 1061-75.

Johne, A, Kopke, K, Gerloff, T, Mai, I, Rietbrock, S, Meisel, C, Hoffmeyer, S, Kerb, R, Fromm, MF, Brinkmann, U, Eichelbaum, M, Brockmoller, J, Cascorbi, I, Roots, I (2002). Modulation of steady-state kinetics of digoxin by haplotypes of the P-glycoprotein MDR1 gene. *Clin Pharmacol Ther* **72**: 584-94.

Jozwiak, S (2007). [Contemporary opinions on classification, pathogenesis and treatment of drug-resistant epilepsy]. *Wiad Lek* **60**: 258-64.

Juliano, RL, Ling, V (1976). A surface glycoprotein modulating drug permeability in Chinese hamster ovary cell mutants. *Biochim Biophys Acta* **455**: 152-62.

Juruena, MF, Ottoni, GL, Machado-Vieira, R, Carneiro, RM, Weingarthner, N, Marquardt, AR, Fleig, SS, Broilo, L, Busnello, EA (2009). Bipolar I and II disorder residual symptoms: oxcarbazepine and carbamazepine as add-on treatment to lithium in a double-blind, randomized trial. *Prog Neuropsychopharmacol Biol Psychiatry* **33**: 94-9.

Kato, M, Fukuda, T, Serretti, A, Wakeno, M, Okugawa, G, Ikenaga, Y, Hosoi, Y, Takekita, Y, Mandelli, L, Azuma, J, Kinoshita, T (2008). ABCB1 (MDR1) gene polymorphisms are associated with the clinical response to paroxetine in patients with major depressive disorder. *Prog Neuropsychopharmacol Biol Psychiatry* **32**: 398-404.

Kellinghaus, C (2009). Lacosamide as treatment for partial epilepsy: mechanisms of action, pharmacology, effects, and safety. *Ther Clin Risk Manag* **5**: 757-66.

Kemper, EM, van Zandbergen, AE, Cleypool, C, Mos, HA, Boogerd, W, Beijnen, JH, van Tellingen, O (2003). Increased penetration of paclitaxel into the brain by inhibition of P-Glycoprotein. *Clin Cancer Res* **9**: 2849-55.

Kemper, EM, Verheij, M, Boogerd, W, Beijnen, JH, van Tellingen, O (2004). Improved penetration of docetaxel into the brain by co-administration of inhibitors of P-glycoprotein. *Eur J Cancer* **40**: 1269-74.

Kerb, R, Hoffmeyer, S, Brinkmann, U (2001). ABC drug transporters: hereditary polymorphisms and pharmacological impact in MDR1, MRP1 and MRP2. *Pharmacogenomics* **2**: 51-64.

Kim, RB, Fromm, MF, Wandel, C, Leake, B, Wood, AJ, Roden, DM, Wilkinson, GR (1998). The drug transporter P-glycoprotein limits oral absorption and brain entry of HIV-1 protease inhibitors. *J Clin Invest* **101**: 289-94.

Kim, RB, Leake, BF, Choo, EF, Dresser, GK, Kubba, SV, Schwarz, UI, Taylor, A, Xie, HG, McKinsey, J, Zhou, S, Lan, LB, Schuetz, JD, Schuetz, EG, Wilkinson, GR (2001). Identification of functionally variant MDR1 alleles among European Americans and African Americans. *Clin Pharmacol Ther* **70:** 189-99.

Kimchi-Sarfaty, C, Gribar, JJ, Gottesman, MM (2002). Functional characterization of coding polymorphisms in the human MDR1 gene using a vaccinia virus expression system. *Mol Pharmacol* **62:** 1-6.

Kimchi-Sarfaty, C, Oh, JM, Kim, IW, Sauna, ZE, Calcagno, AM, Ambudkar, SV, Gottesman, MM (2007). A "silent" polymorphism in the MDR1 gene changes substrate specificity. *Science* **315:** 525-8.

Kimura, Y, Morita, SY, Matsuo, M, Ueda, K (2007). Mechanism of multidrug recognition by MDR1/ABCB1. *Cancer Sci* **98:** 1303-10.

Klotz, U (2007). The role of pharmacogenetics in the metabolism of antiepileptic drugs: pharmacokinetic and therapeutic implications. *Clin Pharmacokinet* **46:** 271-9.

Knight, JL, Weaver, DF (1998). A computational quantitative structure-activity relationship study of carbamate anticonvulsants using quantum pharmacological methods. *Seizure* **7:** 347-54.

Kothare, SV, Kaleyias, J (2008). Zonisamide: review of pharmacology, clinical efficacy, tolerability, and safety. *Expert Opin Drug Metab Toxicol* **4:** 493-506.

Krasowski, MD (2010). Therapeutic Drug Monitoring of the Newer Anti-Epilepsy Medications. *Pharmaceuticals (Basel)* **3:** 1909-1935.

Kroetz, DL, Pauli-Magnus, C, Hodges, LM, Huang, CC, Kawamoto, M, Johns, SJ, Stryke, D, Ferrin, TE, DeYoung, J, Taylor, T, Carlson, EJ, Herskowitz, I, Giacomini, KM, Clark, AG (2003). Sequence diversity and haplotype structure in the human ABCB1 (MDR1, multidrug resistance transporter) gene. *Pharmacogenetics* **13**: 481-94.

Kubota, H, Ishihara, H, Langmann, T, Schmitz, G, Stieger, B, Wieser, HG, Yonekawa, Y, Frei, K (2006). Distribution and functional activity of P-glycoprotein and multidrug resistance-associated proteins in human brain microvascular endothelial cells in hippocampal sclerosis. *Epilepsy Res* **68**: 213-28.

Kudriakova, TBSLAKEGGVA (1992). Possible relationships between carbamazepine metabolites levels and prophylactic efficacy. *Human Psychopharmacology* **7**: 135-138.

Kurata, Y, Ieiri, I, Kimura, M, Morita, T, Irie, S, Urae, A, Ohdo, S, Ohtani, H, Sawada, Y, Higuchi, S, Otsubo, K (2002). Role of human MDR1 gene polymorphism in bioavailability and interaction of digoxin, a substrate of P-glycoprotein. *Clin Pharmacol Ther* **72**: 209-19.

Kwan, P, Arzimanoglou, A, Berg, AT, Brodie, MJ, Allen Hauser, W, Mathern, G, Moshe, SL, Perucca, E, Wiebe, S, French, J (2010). Definition of drug resistant epilepsy: consensus proposal by the ad hoc Task Force of the ILAE Commission on Therapeutic Strategies. *Epilepsia* **51**: 1069-77.

Kwan, P, Baum, L, Wong, V, Ng, PW, Lui, CH, Sin, NC, Hui, AC, Yu, E, Wong, LK (2007a). Association between ABCB1 C3435T polymorphism and drug-resistant epilepsy in Han Chinese. *Epilepsy Behav* **11**: 112-7.

Kwan, P, Brodie, MJ (2000a). Early identification of refractory epilepsy. *N Engl J Med* **342**: 314-9.

Kwan, P, Brodie, MJ (2007b). Emerging drugs for epilepsy. *Expert Opin Emerg Drugs* **12**: 407-22.

Kwan, P, Brodie, MJ (2000b). Epilepsy after the first drug fails: substitution or add-on? *Seizure* **9**: 464-8.

Kwan, P, Brodie, MJ (2005). Potential role of drug transporters in the pathogenesis of medically intractable epilepsy. *Epilepsia* **46**: 224-35.

Kwan, P, Wong, V, Ng, PW, Lui, CH, Sin, NC, Poon, WS, Ng, HK, Wong, KS, Baum, L (2009). Gene-wide tagging study of association between ABCB1 polymorphisms and multidrug resistance in epilepsy in Han Chinese. *Pharmacogenomics* **10**: 723-32.

Lakhan, R, Misra, UK, Kalita, J, Pradhan, S, Gogtay, NJ, Singh, MK, Mittal, B (2009). No association of ABCB1 polymorphisms with drug-refractory epilepsy in a north Indian population. *Epilepsy Behav* **14**: 78-82.

Langer, O, Bauer, M, Hammers, A, Karch, R, Pataraia, E, Koepp, MJ, Abrahim, A, Luurtsema, G, Brunner, M, Sunder-Plassmann, R, Zimprich, F, Joukhadar, C, Gentzsch, S, Dudczak, R, Kletter, K, Muller, M, Baumgartner, C (2007). Pharmacoresistance in epilepsy: a pilot PET study with the P-glycoprotein substrate R-[(11)C]verapamil. *Epilepsia* **48**: 1774-84.

Lazarowski, A, Lubieniecki, F, Camarero, S, Pomata, H, Bartuluchi, M, Sevlever, G, Taratuto, AL (2004). Multidrug resistance proteins in tuberous sclerosis and refractory epilepsy. *Pediatr Neurol* **30**: 102-6.

Lazarowski, A, Sevlever, G, Taratuto, A, Massaro, M, Rabinowicz, A (1999). Tuberous sclerosis associated with MDR1 gene expression and drug-resistant epilepsy. *Pediatr Neurol* **21**: 731-4.

Lee, G, Dallas, S, Hong, M, Bendayan, R (2001). Drug transporters in the central nervous system: brain barriers and brain parenchyma considerations. *Pharmacol Rev* **53**: 569-96.

Lepper, ER, Nooter, K, Verweij, J, Acharya, MR, Figg, WD, Sparreboom, A (2005). Mechanisms of resistance to anticancer drugs: the role of the polymorphic ABC transporters ABCB1 and ABCG2. *Pharmacogenomics* **6**: 115-38.

Leschziner, GD, Andrew, T, Pirmohamed, M, Johnson, MR (2007). ABCB1 genotype and PGP expression, function and therapeutic drug response: a critical review and recommendations for future research. *Pharmacogenomics J* **7**: 154-79.

Liu, X, Yang, Z, Yang, J, Yang, H (2007). Increased P-glycoprotein expression and decreased phenobarbital distribution in the brain of pentylenetetrazole-kindled rats. *Neuropharmacology* **53**: 657-63.

Loscher, W (2007). Drug transporters in the epileptic brain. *Epilepsia* **48 Suppl 1**: 8-13.

Loscher, W, Potschka, H (2005). Drug resistance in brain diseases and the role of drug efflux transporters. *Nat Rev Neurosci* **6**: 591-602.

Loscher, W, Sills, GJ (2007). Drug resistance in epilepsy: why is a simple explanation not enough? *Epilepsia* **48**: 2370-2.

Lown, KS, Mayo, RR, Leichtman, AB, Hsiao, HL, Turgeon, DK, Schmiedlin-Ren, P, Brown, MB, Guo, W, Rossi, SJ, Benet, LZ, Watkins, PB (1997). Role of intestinal P-glycoprotein (mdr1) in interpatient variation in the oral bioavailability of cyclosporine. *Clin Pharmacol Ther* **62**: 248-60.

Luna-Tortos, C, Fedrowitz, M, Loscher, W (2008a). Several major antiepileptic drugs are substrates for human P-glycoprotein. *Neuropharmacology*.

Luna-Tortos, C, Fedrowitz, M, Loscher, W (2008b). Several major antiepileptic drugs are substrates for human P-glycoprotein. *Neuropharmacology* **55**: 1364-1375.

Luna-Tortos, C, Fedrowitz, M, Loscher, W (2008c). Several major antiepileptic drugs are substrates for human P-glycoprotein. *Neuropharmacology* **55**: 1364-75.

Luna-Tortos, C, Rambeck, B, Jurgens, UH, Loscher, W (2009). The Antiepileptic Drug Topiramate is a Substrate for Human P-glycoprotein but Not Multidrug Resistance Proteins. *Pharm Res.*

Mahar Doan, KM, Humphreys, JE, Webster, LO, Wring, SA, Shampine, LJ, Serabjit-Singh, CJ, Adkison, KK, Polli, JW (2002). Passive permeability and P-glycoprotein-mediated efflux differentiate central nervous system (CNS) and non-CNS marketed drugs. *J Pharmacol Exp Ther* **303**: 1029-37.

Maines, LW, Antonetti, DA, Wolpert, EB, Smith, CD (2005). Evaluation of the role of P-glycoprotein in the uptake of paroxetine, clozapine, phenytoin and carbamazapine by bovine retinal endothelial cells. *Neuropharmacology* **49**: 610-7.

Marchi, N, Guiso, G, Caccia, S, Rizzi, M, Gagliardi, B, Noe, F, Ravizza, T, Bassanini, S, Chimenti, S, Battaglia, G, Vezzani, A (2006). Determinants of drug brain uptake in a rat model of seizure-associated malformations of cortical development. *Neurobiol Dis* **24**: 429-42.

Marchi, N, Guiso, G, Rizzi, M, Pirker, S, Novak, K, Czech, T, Baumgartner, C, Janigro, D, Caccia, S, Vezzani, A (2005). A pilot study on brain-to-plasma partition of 10,11-dyhydro-10-hydroxy-5H-dibenzo(b,f)azepine-5-carboxamide and MDR1 brain expression in epilepsy patients not responding to oxcarbazepine. *Epilepsia* **46**: 1613-9.

Marchi, N, Hallene, KL, Kight, KM, Cucullo, L, Moddel, G, Bingaman, W, Dini, G, Vezzani, A, Janigro, D (2004). Significance of MDR1 and multiple drug resistance in refractory human epileptic brain. *BMC Med* **2:** 37.

Martin J Brodie, SCS, Patrick Kwan (ed) (2005). *Fast facts: Epilepsy.* Health Press Limited: Oxford.

Matsumoto, K, Miyazaki, H, Fujii, T, Kagemoto, A, Maeda, T, Hashimoto, M (1983). Absorption, distribution and excretion of 3-(sulfamoyl[14C]methyl)-1,2-benziosoxazole (AD-810) in Rats, Dogs and Monkeys and of AD-810 in Men. *Arzneimittelforschung* **33:** 961-8.

May, TW, Korn-Merker, E, Rambeck, B (2003). Clinical pharmacokinetics of oxcarbazepine. *Clin Pharmacokinet* **42:** 1023-42.

McCormack, PL, Robinson, DM (2009). Eslicarbazepine acetate. *CNS Drugs* **23:** 71-9.

Mihaljevic Peles, A, Bozina, N, Sagud, M, Rojnic Kuzman, M, Lovric, M (2008). MDR1 gene polymorphism: therapeutic response to paroxetine among patients with major depression. *Prog Neuropsychopharmacol Biol Psychiatry* **32:** 1439-44.

Miller, LK (1993). Baculoviruses: high-level expression in insect cells. *Curr Opin Genet Dev* **3:** 97-101.

Mizuno, N, Niwa, T, Yotsumoto, Y, Sugiyama, Y (2003). Impact of drug transporter studies on drug discovery and development. *Pharmacol Rev* **55:** 425-61.

Morinigo, A, Martin, J, Gonzalez, S, Mateo, I (1989). Treatment of resistant schizophrenia with valproate and neuroleptic drugs. *Hillside J Clin Psychiatry* **11:** 199-207.

Morita, N, Yasumori, T, Nakayama, K (2003). Human MDR1 polymorphism: G2677T/A and C3435T have no effect on MDR1 transport activities. *Biochem Pharmacol* **65**: 1843-52.

Moss, B (1991). Vaccinia virus: a tool for research and vaccine development. *Science* **252**: 1662-7.

Mosyagin, I, Runge, U, Schroeder, HW, Dazert, E, Vogelgesang, S, Siegmund, W, Warzok, RW, Cascorbi, I (2008). Association of ABCB1 genetic variants 3435C>T and 2677G>T to ABCB1 mRNA and protein expression in brain tissue from refractory epilepsy patients. *Epilepsia* **49**: 1555-61.

Nelson, MH, Birnbaum, AK, Nyhus, PJ, Remmel, RP (1998). A capillary GC-MS method for analysis of phenytoin and [13C3]-phenytoin from plasma obtained from pulse dose pharmacokinetic studies. *J Pharm Biomed Anal* **17**: 1311-23.

Nirogi, R, Kandikere, V, Mudigonda, K, Komarneni, P, Aleti, R (2009). Liquid chromatography atmospheric pressure chemical ionization tandem mass spectrometry method for the quantification of pregabalin in human plasma. *J Chromatogr B Analyt Technol Biomed Life Sci* **877**: 3899-906.

Oh, E, Ban, E, Woo, JS, Kim, CK (2006). Analysis of carbamazepine and its active metabolite, carbamazepine-10,11-epoxide, in human plasma using high-performance liquid chromatography. *Anal Bioanal Chem* **386**: 1931-6.

Owen, A, Pirmohamed, M, Tettey, JN, Morgan, P, Chadwick, D, Park, BK (2001). Carbamazepine is not a substrate for P-glycoprotein. *Br J Clin Pharmacol* **51**: 345-9.

Ozgon, GO, Bebek, N, Gul, G, Cine, N (2008). Association of MDR1 (C3435T) polymorphism and resistance to carbamazepine in epileptic patients from Turkey. *Eur Neurol* **59**: 67-70.

Palhagen, S, Canger, R, Henriksen, O, van Parys, JA, Riviere, ME, Karolchyk, MA (2001). Rufinamide: a double-blind, placebo-controlled proof of principle trial in patients with epilepsy. *Epilepsy Res* **43**: 115-24.

Pardridge, WM (2007). Blood-brain barrier delivery. *Drug Discov Today* **12**: 54-61.

Pardridge, WM, Golden, PL, Kang, YS, Bickel, U (1997). Brain microvascular and astrocyte localization of P-glycoprotein. *J Neurochem* **68**: 1278-85.

Pauli-Magnus, C, Kroetz, DL (2004). Functional implications of genetic polymorphisms in the multidrug resistance gene MDR1 (ABCB1). *Pharm Res* **21**: 904-13.

Pauli-Magnus, C, von Richter, O, Burk, O, Ziegler, A, Mettang, T, Eichelbaum, M, Fromm, MF (2000). Characterization of the major metabolites of verapamil as substrates and inhibitors of P-glycoprotein. *J Pharmacol Exp Ther* **293**: 376-82.

Perucca, E, Cloyd, J, Critchley, D, Fuseau, E (2008). Rufinamide: clinical pharmacokinetics and concentration-response relationships in patients with epilepsy. *Epilepsia* **49**: 1123-41.

Post, RM, Uhde, TW, Ballenger, JC, Chatterji, DC, Greene, RF, Bunney, WE, Jr. (1983). Carbamazepine and its -10,11-epoxide metabolite in plasma and CSF. Relationship to antidepressant response. *Arch Gen Psychiatry* **40**: 673-6.

Potschka, H, Baltes, S, Loscher, W (2004a). Inhibition of multidrug transporters by verapamil or probenecid does not alter blood-brain barrier penetration of levetiracetam in rats. *Epilepsy Res* **58**: 85-91.

Potschka, H, Fedrowitz, M, Loscher, W (2002). P-Glycoprotein-mediated efflux of phenobarbital, lamotrigine, and felbamate at the blood-brain barrier: evidence from microdialysis experiments in rats. *Neurosci Lett* **327**: 173-6.

Potschka, H, Fedrowitz, M, Loscher, W (2001a). P-glycoprotein and multidrug resistance-associated protein are involved in the regulation of extracellular levels of the major antiepileptic drug carbamazepine in the brain. *Neuroreport* **12**: 3557-60.

Potschka, H, Loscher, W (2001b). In vivo evidence for P-glycoprotein-mediated transport of phenytoin at the blood-brain barrier of rats. *Epilepsia* **42**: 1231-40.

Potschka, H, Volk, HA, Loscher, W (2004b). Pharmacoresistance and expression of multidrug transporter P-glycoprotein in kindled rats. *Neuroreport* **15**: 1657-61.

Ramachandra, M, Ambudkar, SV, Gottesman, MM, Pastan, I, Hrycyna, CA (1996). Functional characterization of a glycine 185-to-valine substitution in human P-glycoprotein by using a vaccinia-based transient expression system. *Mol Biol Cell* **7**: 1485-98.

Rambeck, B, Jurgens, UH, May, TW, Pannek, HW, Behne, F, Ebner, A, Gorji, A, Straub, H, Speckmann, EJ, Pohlmann-Eden, B, Loscher, W (2006). Comparison of brain extracellular fluid, brain tissue, cerebrospinal fluid, and serum concentrations of antiepileptic drugs measured intraoperatively in patients with intractable epilepsy. *Epilepsia* **47**: 681-94.

Raub, TJ (2006). P-glycoprotein recognition of substrates and circumvention through rational drug design. *Mol Pharm* **3**: 3-25.

Regesta, G, Tanganelli, P (1999). Clinical aspects and biological bases of drug-resistant epilepsies. *Epilepsy Res* **34**: 109-22.

Rivers, F, O'Brien, TJ, Callaghan, R (2008). Exploring the possible interaction between anti-epilepsy drugs and multidrug efflux pumps; in vitro observations. *Eur J Pharmacol* **598:** 1-8.

Rizzi, M, Caccia, S, Guiso, G, Richichi, C, Gorter, JA, Aronica, E, Aliprandi, M, Bagnati, R, Fanelli, R, D'Incalci, M, Samanin, R, Vezzani, A (2002). Limbic seizures induce P-glycoprotein in rodent brain: functional implications for pharmacoresistance. *J Neurosci* **22:** 5833-9.

Robey, RW, Lazarowski, A, Bates, SE (2008). P-glycoprotein--a clinical target in drug-refractory epilepsy? *Mol Pharmacol* **73:** 1343-6.

Rouan, MC, Souppart, C, Alif, L, Moes, D, Lecaillon, JB, Godbillon, J (1995). Automated analysis of a novel anti-epileptic compound, CGP 33,101, and its metabolite, CGP 47,292, in body fluids by high-performance liquid chromatography and liquid-solid extraction. *J Chromatogr B Biomed Appl* **667:** 307-13.

Ryvlin, P, Perucca, E, Rheims, S (2008). Pregabalin for the management of partial epilepsy. *Neuropsychiatr Dis Treat* **4:** 1211-24.

Sakaeda, T, Nakamura, T, Horinouchi, M, Kakumoto, M, Ohmoto, N, Sakai, T, Morita, Y, Tamura, T, Aoyama, N, Hirai, M, Kasuga, M, Okumura, K (2001). MDR1 genotype-related pharmacokinetics of digoxin after single oral administration in healthy Japanese subjects. *Pharm Res* **18:** 1400-4.

Sakaeda, T, Nakamura, T, Okumura, K (2003). Pharmacogenetics of MDR1 and its impact on the pharmacokinetics and pharmacodynamics of drugs. *Pharmacogenomics* **4:** 397-410.

Salama, NN, Yang, Z, Bui, T, Ho, RJ (2006). MDR1 haplotypes significantly minimize intracellular uptake and transcellular P-gp substrate transport in recombinant LLC-PK1 cells. *J Pharm Sci* **95**: 2293-308.

Schaefer, M, Roots, I, Gerloff, T (2006). In-vitro transport characteristics discriminate wild-type ABCB1 (MDR1) from ALA893SER and ALA893THR polymorphisms. *Pharmacogenet Genomics* **16**: 855-61.

Schaich, M, Kestel, L, Pfirrmann, M, Robel, K, Illmer, T, Kramer, M, Dill, C, Ehninger, G, Schackert, G, Krex, D (2009). A MDR1 (ABCB1) gene single nucleotide polymorphism predicts outcome of temozolomide treatment in glioblastoma patients. *Ann Oncol* **20**: 175-81.

Schinkel, AH (1997). The physiological function of drug-transporting P-glycoproteins. *Semin Cancer Biol* **8**: 161-70.

Schinkel, AH, Smit, JJ, van Tellingen, O, Beijnen, JH, Wagenaar, E, van Deemter, L, Mol, CA, van der Valk, MA, Robanus-Maandag, EC, te Riele, HP, et al. (1994). Disruption of the mouse mdr1a P-glycoprotein gene leads to a deficiency in the blood-brain barrier and to increased sensitivity to drugs. *Cell* **77**: 491-502.

Schinkel, AH, Wagenaar, E, Mol, CA, van Deemter, L (1996). P-glycoprotein in the blood-brain barrier of mice influences the brain penetration and pharmacological activity of many drugs. *J Clin Invest* **97**: 2517-24.

Schinkel, AH, Wagenaar, E, van Deemter, L, Mol, CA, Borst, P (1995). Absence of the mdr1a P-Glycoprotein in mice affects tissue distribution and pharmacokinetics of dexamethasone, digoxin, and cyclosporin A. *J Clin Invest* **96**: 1698-705.

Schmidt, D, Loscher, W (2005). Drug resistance in epilepsy: putative neurobiologic and clinical mechanisms. *Epilepsia* **46**: 858-77.

Schwab, M, Eichelbaum, M, Fromm, MF (2003). Genetic polymorphisms of the human MDR1 drug transporter. *Annu Rev Pharmacol Toxicol* **43:** 285-307.

Seegers, U, Potschka, H, Loscher, W (2002a). Expression of the multidrug transporter P-glycoprotein in brain capillary endothelial cells and brain parenchyma of amygdala-kindled rats. *Epilepsia* **43:** 675-84.

Seegers, U, Potschka, H, Loscher, W (2002b). Lack of effects of prolonged treatment with phenobarbital or phenytoin on the expression of P-glycoprotein in various rat brain regions. *Eur J Pharmacol* **451:** 149-55.

Seegers, U, Potschka, H, Loscher, W (2002c). Transient increase of P-glycoprotein expression in endothelium and parenchyma of limbic brain regions in the kainate model of temporal lobe epilepsy. *Epilepsy Res* **51:** 257-68.

Seelig, A (1998). A general pattern for substrate recognition by P-glycoprotein. *Eur J Biochem* **251:** 252-61.

Seo, T, Ishitsu, T, Ueda, N, Nakada, N, Yurube, K, Ueda, K, Nakagawa, K (2006). ABCB1 polymorphisms influence the response to antiepileptic drugs in Japanese epilepsy patients. *Pharmacogenomics* **7:** 551-61.

Shneker, BF, McAuley, JW (2005). Pregabalin: a new neuromodulator with broad therapeutic indications. *Ann Pharmacother* **39:** 2029-37.

Shorvon, SD (1990). Epidemiology, classification, natural history, and genetics of epilepsy. *Lancet* **336:** 93-6.

Siddiqui, A, Kerb, R, Weale, ME, Brinkmann, U, Smith, A, Goldstein, DB, Wood, NW, Sisodiya, SM (2003). Association of multidrug resistance in epilepsy with a polymorphism in the drug-transporter gene ABCB1. *N Engl J Med* **348:** 1442-8.

Sills, GJ, Kwan, P, Butler, E, de Lange, EC, van den Berg, DJ, Brodie, MJ (2002). P-glycoprotein-mediated efflux of antiepileptic drugs: preliminary studies in mdr1a knockout mice. *Epilepsy Behav* **3:** 427-432.

Silverman, JA (1999). Multidrug-resistance transporters. *Pharm Biotechnol* **12:** 353-86.

Sisodiya, SM, Heffernan, J, Squier, MV (1999). Over-expression of P-glycoprotein in malformations of cortical development. *Neuroreport* **10:** 3437-41.

Sisodiya, SM, Lin, WR, Harding, BN, Squier, MV, Thom, M (2002). Drug resistance in epilepsy: expression of drug resistance proteins in common causes of refractory epilepsy. *Brain* **125:** 22-31.

Sisodiya, SM, Lin, WR, Squier, MV, Thom, M (2001). Multidrug-resistance protein 1 in focal cortical dysplasia. *Lancet* **357:** 42-3.

Soldin, SJ, Hill, JG (1976). Rapid micromethod for measuring anticonvulsant drugs in serum by high-performance liquid chromatography. *Clin Chem* **22:** 856-9.

Stolker, AA, Niesing, W, Hogendoorn, EA, Versteegh, JF, Fuchs, R, Brinkman, UA (2004). Liquid chromatography with triple-quadrupole or quadrupole-time of flight mass spectrometry for screening and confirmation of residues of pharmaceuticals in water. *Anal Bioanal Chem* **378:** 955-63.

Stouch, TR, Gudmundsson, O (2002). Progress in understanding the structure-activity relationships of P-glycoprotein. *Adv Drug Deliv Rev* **54:** 315-28.

Sugawara, I, Kataoka, I, Morishita, Y, Hamada, H, Tsuruo, T, Itoyama, S, Mori, S (1988). Tissue distribution of P-glycoprotein encoded by a multidrug-resistant gene as revealed by a monoclonal antibody, MRK 16. *Cancer Res* **48**: 1926-9.

Szoeke, C, Sills, GJ, Kwan, P, Petrovski, S, Newton, M, Hitiris, N, Baum, L, Berkovic, SF, Brodie, MJ, Sheffield, LJ, O'Brien, TJ (2009). Multidrug-resistant genotype (ABCB1) and seizure recurrence in newly treated epilepsy: data from international pharmacogenetic cohorts. *Epilepsia* **50**: 1689-96.

Takano, A, Kusuhara, H, Suhara, T, Ieiri, I, Morimoto, T, Lee, YJ, Maeda, J, Ikoma, Y, Ito, H, Suzuki, K, Sugiyama, Y (2006). Evaluation of in vivo P-glycoprotein function at the blood-brain barrier among MDR1 gene polymorphisms by using 11C-verapamil. *J Nucl Med* **47**: 1427-33.

Tang-Wai, DF, Kajiji, S, DiCapua, F, de Graaf, D, Roninson, IB, Gros, P (1995). Human (MDR1) and mouse (mdr1, mdr3) P-glycoproteins can be distinguished by their respective drug resistance profiles and sensitivity to modulators. *Biochemistry* **34**: 32-9.

Tang, K, Ngoi, SM, Gwee, PC, Chua, JM, Lee, EJ, Chong, SS, Lee, CG (2002). Distinct haplotype profiles and strong linkage disequilibrium at the MDR1 multidrug transporter gene locus in three ethnic Asian populations. *Pharmacogenetics* **12**: 437-50.

Thiel-Demby, VE, Humphreys, JE, St John Williams, LA, Ellens, HM, Shah, N, Ayrton, AD, Polli, JW (2008). Biopharmaceutics Classification System: Validation and Learnings of an in Vitro Permeability Assay. *Mol Pharm*.

Tishler, DM, Weinberg, KI, Hinton, DR, Barbaro, N, Annett, GM, Raffel, C (1995). MDR1 gene expression in brain of patients with medically intractable epilepsy. *Epilepsia* **36**: 1-6.

Ueda, K, Taguchi, Y, Morishima, M (1997). How does P-glycoprotein recognize its substrates? *Semin Cancer Biol* **8**: 151-9.

Uhr, M, Steckler, T, Yassouridis, A, Holsboer, F (2000). Penetration of amitriptyline, but not of fluoxetine, into brain is enhanced in mice with blood-brain barrier deficiency due to mdr1a P-glycoprotein gene disruption. *Neuropsychopharmacology* **22**: 380-7.

Vahab, SA, Sen, S, Ravindran, N, Mony, S, Mathew, A, Vijayan, N, Nayak, G, Bhaskaranand, N, Banerjee, M, Satyamoorthy, K (2009). Analysis of genotype and haplotype effects of ABCB1 (MDR1) polymorphisms in the risk of medically refractory epilepsy in an Indian population. *Drug Metab Pharmacokinet* **24**: 255-60.

van Vliet, E, Aronica, E, Redeker, S, Marchi, N, Rizzi, M, Vezzani, A, Gorter, J (2004). Selective and persistent upregulation of mdr1b mRNA and P-glycoprotein in the parahippocampal cortex of chronic epileptic rats. *Epilepsy Res* **60**: 203-13.

van Vliet, EA, van Schaik, R, Edelbroek, PM, Redeker, S, Aronica, E, Wadman, WJ, Marchi, N, Vezzani, A, Gorter, JA (2006). Inhibition of the multidrug transporter P-glycoprotein improves seizure control in phenytoin-treated chronic epileptic rats. *Epilepsia* **47**: 672-80.

van Vliet, EA, van Schaik, R, Edelbroek, PM, Voskuyl, RA, Redeker, S, Aronica, E, Wadman, WJ, Gorter, JA (2007). Region-specific overexpression of P-glycoprotein at the blood-brain barrier affects brain uptake of phenytoin in epileptic rats. *J Pharmacol Exp Ther* **322**: 141-7.

Vermeij, TA, Edelbroek, PM (2007). Robust isocratic high performance liquid chromatographic method for simultaneous determination of seven antiepileptic drugs including lamotrigine, oxcarbazepine and zonisamide in serum after solid-phase extraction. *J Chromatogr B Analyt Technol Biomed Life Sci* **857**: 40-6.

Volk, H, Potschka, H, Loscher, W (2005a). Immunohistochemical localization of P-glycoprotein in rat brain and detection of its increased expression by seizures are sensitive to fixation and staining variables. *J Histochem Cytochem* **53**: 517-31.

Volk, HA, Burkhardt, K, Potschka, H, Chen, J, Becker, A, Loscher, W (2004). Neuronal expression of the drug efflux transporter P-glycoprotein in the rat hippocampus after limbic seizures. *Neuroscience* **123**: 751-9.

Volk, HA, Loscher, W (2005b). Multidrug resistance in epilepsy: rats with drug-resistant seizures exhibit enhanced brain expression of P-glycoprotein compared with rats with drug-responsive seizures. *Brain* **128**: 1358-68.

Volosov, A, Sintov, A, Bialer, M (1999). Stereoselective pharmacokinetic analysis of the antiepileptic 10-hydroxycarbazepine in dogs. *Ther Drug Monit* **21**: 219-23.

von Unruh, GE, Paar, WD (1986). Gas chromatographic/mass spectrometric assays for oxcarbazepine and its main metabolites, 10-hydroxy-carbazepine and carbazepine-10,11-trans-diol. *Biomed Environ Mass Spectrom* **13**: 651-6.

Wang, D, Johnson, AD, Papp, AC, Kroetz, DL, Sadee, W (2005). Multidrug resistance polypeptide 1 (MDR1, ABCB1) variant 3435C>T affects mRNA stability. *Pharmacogenet Genomics* **15**: 693-704.

Wang, Q, Strab, R, Kardos, P, Ferguson, C, Li, J, Owen, A, Hidalgo, IJ (2008). Application and limitation of inhibitors in drug-transporter interactions studies. *Int J Pharm* **356**: 12-8.

Wang, RB, Kuo, CL, Lien, LL, Lien, EJ (2003). Structure-activity relationship: analyses of p-glycoprotein substrates and inhibitors. *J Clin Pharm Ther* **28**: 203-28.

Weiss, J, Dormann, SM, Martin-Facklam, M, Kerpen, CJ, Ketabi-Kiyanvash, N, Haefeli, WE (2003a). Inhibition of P-glycoprotein by newer antidepressants. *J Pharmacol Exp Ther* **305**: 197-204.

Weiss, J, Kerpen, CJ, Lindenmaier, H, Dormann, SM, Haefeli, WE (2003b). Interaction of antiepileptic drugs with human P-glycoprotein in vitro. *J Pharmacol Exp Ther* **307**: 262-7.

West, CL, Mealey, KL (2007). Assessment of antiepileptic drugs as substrates for canine P-glycoprotein. *Am J Vet Res* **68**: 1106-10.

Winnicka, RI, Topacinski, B, Szymczak, WM, Szymanska, B (2002). Carbamazepine poisoning: elimination kinetics and quantitative relationship with carbamazepine 10,11-epoxide. *J Toxicol Clin Toxicol* **40**: 759-65.

Xiao, ZY, Yong; Wang, Xuefeng. (1999). Development of PHT-PB-resistant amygdala-kindled rats and expression of MDR1. *Zhonghua Shenjingke Zazhi* **32(6)**: 365-368.

Yamazaki, M, Neway, WE, Ohe, T, Chen, I, Rowe, JF, Hochman, JH, Chiba, M, Lin, JH (2001). In vitro substrate identification studies for p-glycoprotein-mediated transport: species difference and predictability of in vivo results. *J Pharmacol Exp Ther* **296**: 723-35.

Yang, ZH, Liu, XD (2008). P-glycoprotein-mediated efflux of phenobarbital at the blood-brain barrier evidence from transport experiments in vitro. *Epilepsy Res* **78**: 40-9.

Zhang, C, Kwan, P, Zuo, Z, Baum, L (2010). In vitro concentration dependent transport of phenytoin and phenobarbital, but not ethosuximide, by human P-glycoprotein. *Life Sci* **86**: 899-905.

Zhang, C, Zuo, Z, Kwan, P, Baum, L (2011). In vitro transport profile of carbamazepine, oxcarbazepine, eslicarbazepine acetate, and their active metabolites by human P-glycoprotein. *Epilepsia*.

Zhang, L, Lin, G, Kovacs, B, Jani, M, Krajcsi, P, Zuo, Z (2007). Mechanistic study on the intestinal absorption and disposition of baicalein. *Eur J Pharm Sci* **31**: 221-31.

Zhang, Y, Benet, LZ (2001). The gut as a barrier to drug absorption: combined role of cytochrome P450 3A and P-glycoprotein. *Clin Pharmacokinet* **40**: 159-68.